POLYAROMATIC ETHERS AND THIOETHERS COORDINATED TO CYCLOPENTADIENYLIRON COMPLEXES

BY

ERIN KATHLEEN TODD

A Thesis
Submitted to the Faculty of Graduate Studies
in Partial Fulfillment of the Requirements for the Degree of

DOCTOR OF PHILOSOPHY

Department of Chemistry
The University of Manitoba
Winnipeg, Manitoba

THE UNIVERSITY OF MANITOBA

FACULTY OF GRADUATE STUDIES

*****

COPYRIGHT PERMISSION PAGE

POLYAROMATIC ETHERS AND THIOETHERS COORDINATED TO CYCLOPENTADIENYLIRON COMPLEXES

BY

ERIN KATHLEEN TODD

A Thesis/Practicum submitted to the Faculty of Graduate Studies of The University of Manitoba in partial fulfillment of the requirements of the degree of

Doctor of Philosophy

Abstract

This research is focussed on the synthesis of polyaromatic ethers and thioethers using chloroarene complexes of cyclopentadienyliron. The first goal of this work was to establish that dichloroarene complexes could undergo nucleophilic aromatic substitution reactions with oxygen- and sulfur-based dinucleophiles to produce linear polyaromatic ethers and thioethers. These organometallic polymers were photolyzed, which allowed for the isolation of the corresponding organic polymers. A further examination of the reaction of trifunctional reagents with chloroarene complexes resulted in the production of star-shaped polyaromatic ethers. Polymers with ferrocenyl groups in their backbones and cyclopentadienyliron cations pendent to their backbones were prepared, and upon photolysis, ferrocene-based polymers were isolated. Reaction of chloroarene complexes functionalized with azobenzene groups with dinucleophiles allowed for the formation of highly colored polyaromatic ethers and thioethers. An investigation into the radical polymerization of methacrylate- and styrene-functionalized complexes of cyclopentadienyliron was undertaken. Polyaromatic ethers and thioethers containing methacrylate and styrene units in their side chains could also be isolated and the pendent olefinic groups were subsequently polymerized using a radical initiator to yield insoluble cross-linked polymers. It was concluded that η^6-arene-η^5-cyclopentadienyliron complexes are excellent precursors to aromatic polymers, and that these metallated polymers exhibit enhanced solubility compared to their organic analogues. The polymers displayed good thermal stability, and their glass transition temperatures were enhanced by the presence of the pendent cyclopentadienyliron cations. Electrochemical studies revealed that the iron centers in these polymers undergo reversible reduction processes.

Acknowledgements

I would like to thank my supervisor, Dr. Alaa Abd-El-Aziz for his support throughout the duration of my graduate studies. His dedication to research has inspired me to work hard and he has taught me a great deal. He has given me numerous opportunities to present my research at national and international conferences and has always been very encouraging. I would also like to thank the members of my Ph.D. advisory committee, Dr. Janzen, Dr. Dannefaer and Dr. Kroeker, for their helpful comments during the past few years, and Dr. Kunstatter and Dr. Gates for serving on my examining committee. I would also like to thank Manitoba Hydro for financial support.

I am also grateful to many of the present and past members of Dr. Abd-El-Aziz's research group who have made the past four years an enjoyable learning experience. I would like to thank Leslie May, Shelly Bernardin and Andrea Edel for helpful discussions and for making working in the lab fun. Other members of the research lab including Guozhang Ma, Rawda Okasha, Tarek Afifi, Chris Corkery and Sarrah Carruthers are also acknowledged. I would also like to thank my family and friends for understanding when I have been busy and for their continued support and encouragement.

Contents

List of Figures

List of Tables

Abbreviations

AIBN	2,2'-azobis(2-methylpropionitrile)
APT	Attached proton test
Cp	Cyclopentadienyl
$CpFe^+$	Cyclopentadienyliron
Cp*	Pentamethylcyclopentadienyl
CV	Cyclic voltammogram
DMF	*N,N*-Dimethylformamide
DMSO	Dimethyl sulfoxide
DSC	Differential scanning calorimetry
E_{pa}	Anodic peak potential
E_{pc}	Cathodic peak potential
$E_{½}$	Half-wave potential
e^-	Electron
GPC	Gel permeation chromatography
IR	Infrared
M_n	Number average molecular weight
M_w	Weight average molecular weight
NMR	Nuclear magnetic resonance
PDI	Polydispersity index
S_NAr	Nucleophilic aromatic substitution
T_c	Crystallization temperature
T_m	Melting temperature

TBAP	Tetrabutylammonium perchlorate
TGA	Thermogravimetric analysis
T_g	Glass transition temperature
THF	Tetrahydrofuran
UV	Ultraviolet
V	Volt
Vis	Visible

1.0 Introduction

1.1 Arenes Coordinated to Transition Metal Moieties

Over the past fifty years there has been a great deal of research directed towards the synthesis of organometallic complexes.[1-5] Transition metal coordinated arenes are one of the classes of organometallic complexes that have received considerable interest. In particular, arenes coordinated to $Cr(CO)_3$, $Mo(CO)_3$, $Mn^+(CO)_3$, $CpFe^+$ and Cp^*Ru^+ have been utilized in the design of novel molecules.[1-10] These complexes are of importance due to the electron-withdrawing power of the transition metal moieties, which allows for nucleophilic aromatic substitution and addition reactions.[9-18] The magnitude of the electron-withdrawing capacity of these metallic moieties has been shown to decrease in the order $Mn^+(CO)_3$ > $CpFe^+$ and Cp^*Ru^+ >> $Mo(CO)_3$ > $Cr(CO)_3$.[14-18] It has been reported that the chromium tricarbonyl moiety exerts the same magnitude of activation towards nucleophilic substitution reactions on haloarenes as a 4-nitro substituent, while the electron-withdrawing power of the cyclopentadienyliron cation on chlorobenzene is slightly lower than that of 2,4-dinitro substituents on arenes for certain nucleophiles.

Due to the ease of preparation of arene complexes and the wide range of reactions that they undergo, they represent an important class of materials in the design of monomers and polymers. While manganese tricarbonyl is the most electron-withdrawing fragment, difficulties involved in the preparation of its dihaloarene complexes has limited its use in polymer synthesis.[12] However, nucleophilic addition to arene-$Mn^+(CO)_3$ complexes has proven to be an effective method to functionalize aromatic rings.[10-12] Although it is the least electron-withdrawing system, the chromium tricarbonyl fragment

has often been used in organic synthesis to mediate nucleophilic reactions and is an important reagent in the design of enantiomerically pure compounds.[9-13,19,20] While the cyclopentadienyliron and ruthenium moieties exert similar electron-withdrawing properties, the preparation of the iron analogues is much more facile and inexpensive.[4,6-8] This thesis will focus on the use of arene cyclopentadienyliron complexes in the design of functionalized polyaromatic ethers and thioethers.

1.1.1 Synthesis of η^6-Arene-η^5-Cyclopentadienyliron Complexes

There have been many developments in the synthesis of η^6-arene-η^5-cyclopentadienyliron complexes over the past fifty years. The first cyclopentadienyliron coordinated arene was reported by Coffield and coworkers in 1957 via the reaction of refluxing mesitylene with cyclopentadienyliron dicarbonyl chloride in the presence of aluminum chloride.[2] Displacement of the carbonyl and chloride ligands by the aromatic ring resulted in the formation of the cyclopentadienyliron mesitylene iodide complex shown in Figure 1.1 following addition of potassium iodide. This reaction was limited by low yields and the inability of arenes containing electron-withdrawing groups to undergo ligand exchange reactions.

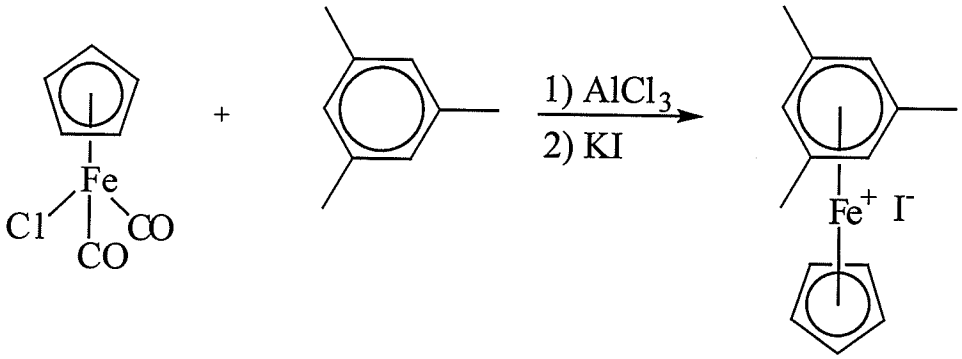

Figure 1.1: Synthesis of η^6-mesitylene-η^5-cyclopentadienyliron by Coffield

It was six years later in 1963 when Nesmeyanov and coworkers reported the synthesis of arene-cyclopentadienyliron complexes via displacement of one of the cyclopentadienyl rings of ferrocene with an arene in the presence of a Lewis acid and aluminum powder (Figure 1.2).[21,22] It was also demonstrated that the use of alkylated and acetylated ferrocenes can result in the formation of arene complexes containing substituted cyclopentadienyl ligands.[22-24] Bisarene dicationic complexes have also been prepared by reaction of substituted ferrocenes with alkylated arenes.[23,24]

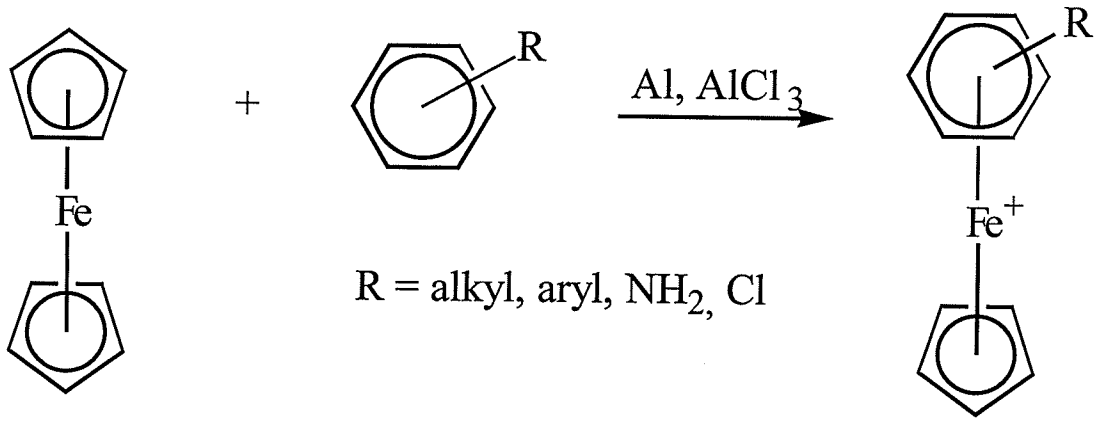

Figure 1.2: Synthesis of η^6-arene-η^5-cyclopentadienyliron complexes via reaction of ferrocene with substituted arenes

The most effective Lewis acid utilized to catalyze this ligand exchange reaction is aluminum chloride. The aluminum is added to the reaction to prevent oxidation of ferrocene to the ferrocenium ion.[22] The ligand exchange reaction is usually carried out at the boiling temperature of the arene used in the reaction, and can occur in the absence of a solvent, or in the presence of a solvent that will not undergo ligand exchange reaction

with ferrocene.[13] These reactions proceed for three to twenty-four hours, with a ferrocene/$AlCl_3$/Al ratio of 1/2/1, with an excess of arene being used. The yields of the ligand exchange reaction are highly dependent on the nature of the arene. Arenes functionalized with electron-donating groups undergo reaction much more readily than those containing electron-withdrawing groups. The yields of the reactions were also found to be highly dependent on the relative amount of aluminum chloride and ferrocene.[25] As the amount of ferrocene increases, the yields of these reactions decrease significantly. It has also been determined that the addition of a small amount of water or hydrochloric acid to the reaction medium can increase the yield of the ligand exchange reaction from about 40 to 90 %.[25] It was suggested based on these results that $HAlCl_4$ is the true catalyst in these reactions and that ligand exchange proceeds via protonation of the iron forming a $(C_5H_5)_2FeH^+$ complex. The mechanism of the ligand exchange reaction was examined by Astruc's and Sutherland's research groups.[7,23] The mechanism has been proposed to proceed via complexation of the Lewis acid to one of the electron-rich cyclopentadienyl rings of ferrocene as shown in Figure 1.3. This interaction results in a weakening of one of the iron-cyclopentadienyl bonds resulting in a cationic $CpFe^+$ intermediate that subsequently coordinates to the arene.

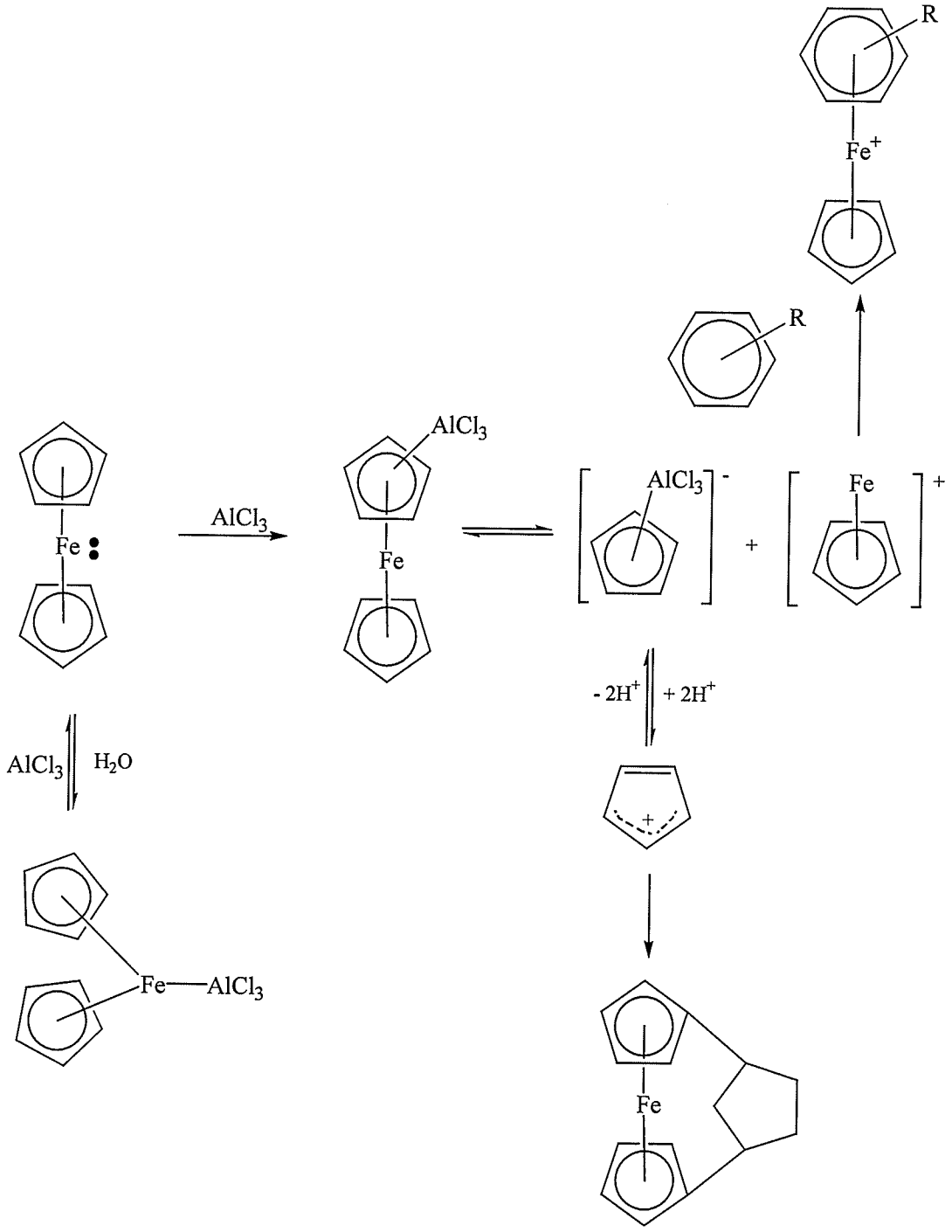

Figure 1.3: Proposed mechanism for ligand exchange reaction

A novel ligand exchange procedure involving microwave heating of the reagents was first described in 1993.[26] In addition to reducing reaction times to a few minutes, a number of arenes unable to undergo ligand exchange reactions using traditional methodologies could be isolated using microwave heating.[26-28] For example, the first synthesis of a complexed phenol by ligand exchange was reported.[27] The yields of these reactions ranged from very low to quite high, and the ratios of ferrocene/arene/$AlCl_3$/Al varied depending on the arene utilized. The disadvantage to this methodology is that these complexes were prepared on a small scale.

There have also been very good results obtained by the ligand exchange reactions of arene cyclopentadienyliron complexes with less acidic arene ligands. For example, a complex such as *p*-xylene cyclopentadienyliron is irradiated with visible light in a non-coordinating solvent in the presence of a more electron-rich arene to give the new π-coordinated arene complex.[29-34]

1.1.2 Photolytic Cleavage of Cyclopentadienyliron Cations

The ease of preparation of arene cyclopentadienyliron complexes and their high reactivity towards nucleophiles makes these materials important reagents in organic synthesis. It is important that these complexes are capable of being decomposed to give the modified arenes in high yield, which makes the metal-mediated methodologies valuable. Decomplexation studies of arene complexes have been conducted using a variety of techniques, the most common being photolysis, pyrolysis and electrolysis. Pyrolysis can be achieved by heating the arene complex in a high boiling point solvent such as dimethyl sulfoxide or by heating the complex under vacuum.[35-38] As an extension of their microwave dielectric heating synthesis of arene complexes, Roberts and coworkers have also described the decomplexation of arene complexes in a microwave.[28]

Electrolysis of cyclopentadienyliron arene complexes also allows for the isolation of free arenes.[38-43] These reactions have been found to result in the formation of ferrocene and zerovalent iron. The electrochemical reduction of cationic eighteen-electron complexes forms neutral nineteen-electron species which undergo coordination to solvent molecules resulting in the isolation of the free organic ligands.[39,40] Electrolysis in the presence of a phosphine ligand and a coordinating solvent increases the effectiveness of the decomplexation reactions. Yields for electrolysis are generally quite high and the absence of heat allows for the isolation of temperature sensitive aromatic compounds. The complexes are usually decomposed using potentials ranging from –1.5 to 2.0 V, however the potentials are dependent on the substituents on the arene.[43]

The most commonly applied method of decomplexation is photolysis. The advantage of photolysis is that heat- and electrochemically-sensitive arenes can be isolated. Nesmeyanov first reported the photolytic demetallation of arene cyclopentadienyliron complexes in 1970 and since that time many other researchers have investigated the conditions of this reaction and attempted to determine the mechanism of the demetallation process.[44] It has been established that coordinating solvents increase the rates of reaction and the yields of the reaction. Acetonitrile is usually used as the solvent or as a co-solvent in this reaction. In the absence of a coordinating solvent, it has also been found that the counterion of the cationic iron complex will affect the results of the photolytic reaction.[44-48] Pearson has reported that the addition of a sodium bicarbonate/sodium carbonate buffer solution to the acetonitrile increased the yields obtained by 30-40 %.[47] These photolytic reactions resulted in the formation of $Fe(OH)_3$ and carbon dioxide which helped drive these reactions to completion.

Nesmeyanov originally proposed that photolysis proceeded by a photodisproportionation reaction that was a result of a photo-induced electron transfer from the solvent molecules to the arene complex.[44] Schuster later reported an alternative mechanism for the photolytic demetallation of arene cyclopentadienyliron complexes.[48] It was proposed that initial irradiation of a complex resulted in its excitation to the triplet state, resulting in ring slippage from η^6 to η^4. Coordination of this unstable complex to the solvent eventually results in the formation of $[CpFe(NCCH_3)_3]^+$. This trisacetonitrile complex then decomposes to produce ferrocene and various iron salts. Figure 1.4 shows the general reaction that occurs during photolysis of arene complexes of cyclopentadienyliron.

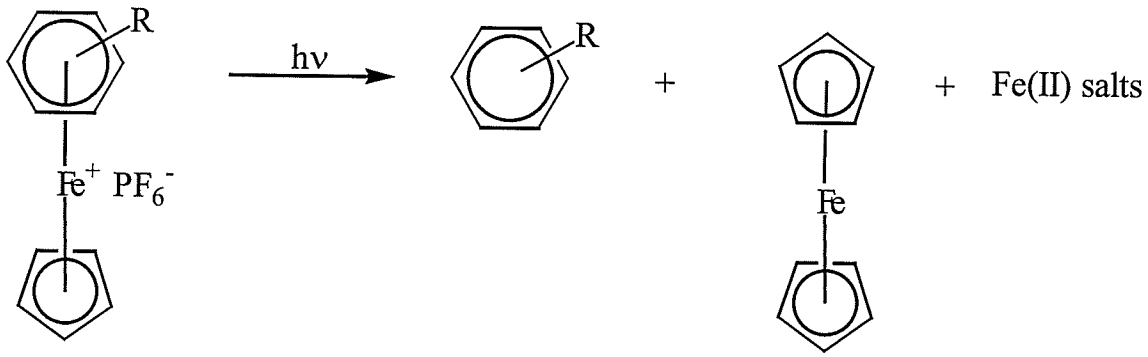

Figure 1.4: Photolytic demetallation of arene cyclopentadienyliron complexes

1.1.3 Electrochemical Properties of η^6-Arene-η^5-Cyclopentadienyliron Complexes

A number of studies have outlined the electrochemical properties of η^6-arene-η^5-cyclopentadienyliron complexes.[49-58] It has been established that this class of complex can be electrochemically reduced in two steps as shown in Figure 1.5. The first electrochemical reduction process converts the cationic eighteen-electron species to a neutral nineteen-electron complex, while the second electron transfer reaction results in the formation of an anionic twenty-electron complex. A twenty-one-electron dianionic naphthalene complex of cyclopentadienyliron has also been reported, however, this complex was very unstable.[59]

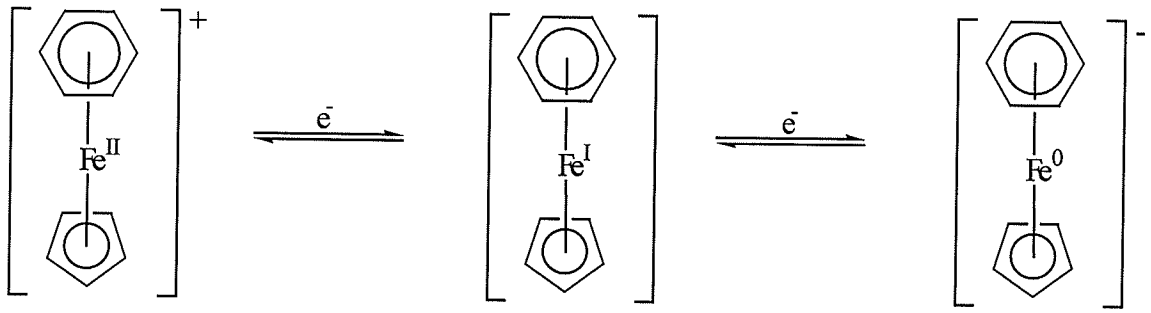

Figure 1.5: Reduction processes in η^6-arene-η^5-cyclopentadienyliron complexes

Astruc and coworkers have isolated the neutral nineteen-electron complexes formed from the electrochemical reduction of peralkylated arene complexes of cyclopentadienyliron.[6,49,60,61] It has been shown from X-ray studies that the iron-cyclopentadienyl bond is longer than those found in cationic cyclopentadienyliron arene complexes. The permethylated arene complex of cyclopentadienyliron can be reduced to

yield a stable nineteen-electron complex and it has been reported that these are the most electron-rich molecules that have been studied, making them useful as molecular electron reservoirs.[60-67] These nineteen-electron complexes are termed electron reservoirs because they have one electron in their antibonding orbital which makes them effective monoelectronic reducing agents.[49,62-67] Peralkylated arene complexes are useful electron reservoirs due to steric crowding which stabilizes the radicals. There are three areas where transition metal electron reservoir complexes may find applications: stoichiometric electron transfer, mediation or redox catalysis and initiation of electron-transfer chain catalysis.

It was reported by Astruc that varying the number of methyl groups on the arenes results in tailored electrocatalysts due to their different redox potentials.[62] For example, new iron, ruthenium and cobalt clusters were synthesized by the electron-transfer chain catalyzed reaction of $[M_3(CO)_{12}]$ (M = Fe, Ru) and $[CH_3CCo_3(CO)_9]$ with the nineteen-electron arene-cyclopentadienyliron complexes in which one or more of the carbonyl ligands were substituted with ferrocenyldiphenylphosphine (FDPP) ligands. While 1-10% of the hexamethylbenzene cyclopentadienyliron(I) complex was used as the catalyst in these studies, the benzene, toluene, *p*-xylene and mesitylene complexes were also examined with $[Ru_3(CO)_{12}]$. It was found that reaction of one equivalent of ferrocenyldiphenylphosphine with the ruthenium cluster in the presence of these catalysts gave the desired monosubstituted clusters, whereas reaction with three equivalents of ferrocenyldiphenylphosphine resulted in mixtures of products. The more methyl groups that were present on the arene, the higher the degree of conversion. Figure 1.6 shows the

electron-transfer chain catalyzed reactions of the metal clusters with the electron reservoir arene complexes.[62]

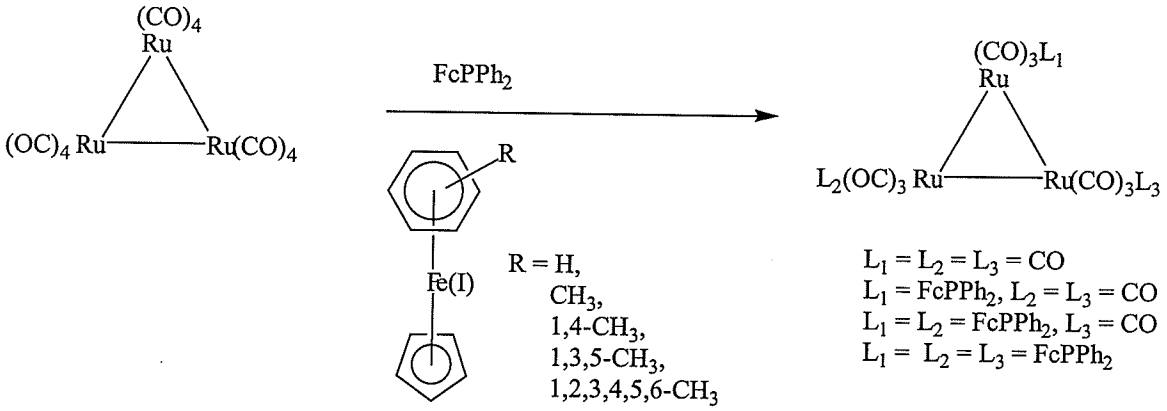

Figure 1.6: Electron-transfer chain catalyzed reactions of nineteen-electron arene complexes

The electrochemical stabilities of reduced arene cyclopentadienyliron complexes are dependent upon the arene and cyclopentadienyl ligands as well as the solvent and temperature of the solution.[52,55,61] In particular, it has been reported that the reversibility of the second reduction step is highly dependent upon the experimental conditions. The redox behaviour of a number of polycyclic arene complexes has been examined in acetonitrile, acetone, *N,N*-dimethylformamide, propylene carbonate and dimethyl sulfoxide using cyclic voltammetry.[52] It was found that the first reduction process was chemically reversible at 22 and –60 °C, while the second reduction process was chemically reversible only at –60 °C in DMF. The coordinating ability of these solvents was also an important factor in obtaining a reversible second reduction wave. The nineteen-electron complexes were the least stable in more highly coordinating solvents

such as acetonitrile and DMSO. The η^6-hexamethylbenzene- η^5-cyclopentadienyliron complex was recently suggested as a potential replacement of ferrocene as an internal reference in determining redox scales due to its excellent stability. It has been found that the redox potentials of this complex along with decamethylcobalticinium and decamethylferrocene do not vary with solvent or the supporting electrolyte while the potential of ferrocene is solvent-dependant.[68]

The electrochemical properties of oligomeric aryl ether complexes of cyclopentadienyliron have established that the iron centers behave as electronically isolated redox sites.[50,69] In contrast, bimetallic complexes containing aryl thioether spacers demonstrated a small degree of electrochemical communication between the iron centers.[50] The ability for the electrons to travel through the conjugated bridge between the complexed aromatic rings makes the second iron center slightly more difficult to reduce due to the increased electron density resulting from reduction of the first iron center. Thus, the second iron center gets reduced at a slightly more negative potential than the first iron center. It was also found that the thioether complexes were approximately five time more stable than their ether analogues. Figure 1.7 shows the cyclic voltammogram of a diiron complex containing aryl ether spacers obtained in DMF using a sweep rate of 40 V/s.[69]

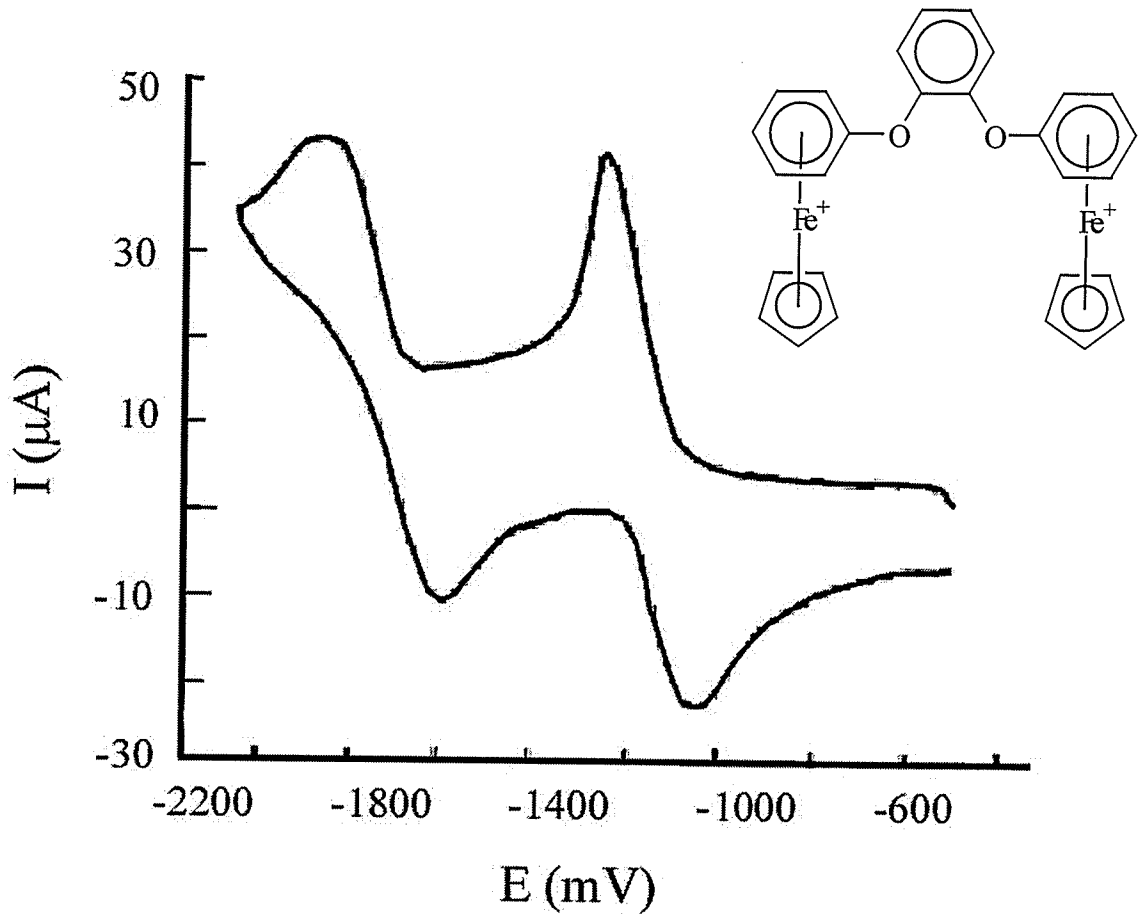

Figure 1.7: Cyclic voltammogram of diarylether complex[69]

In 1998, Astruc and coworkers reported that eighteen-electron arene cyclopentadienyliron complexes could undergo electrochemical oxidation in SO_2 to give seventeen-electron dicationic complexes.[70] It had previously been communicated by Solodovnikov and coworkers that arene complexes could be oxidized at low temperature using $SbCl_5$, however there was very little data provided to prove that the seventeen-electron complex was isolated.[71] For fully methylated sandwich complexes (arene and cyclopentadienyl), the oxidation processes were chemically and electrochemically reversible, however the reversibility decreased with decreasing the number of methyl substituents on the arenes. The oxidation potentials of these complexes occured between

0.9 and 1.7 V versus ferrocene.[64,70] The authors also found that they could oxidize the nineteen-electron neutral complex directly to the dicationic seventeen-electron complex. Therefore, in addition to being precursors to electron reservoirs, eighteen electron arene complexes of cyclopentadienyliron are also precursors to robust proton reservoirs. The applications of these complexes as proton reservoirs have been reviewed by Astruc.[64]

1.1.4 Reactions of η^6-Arene-η^5-Cyclopentadienyliron Complexes

1.1.4.1 Nucleophilic Addition

A number of studies have examined nucleophilic addition and substitution reactions of arene cyclopentadienyliron complexes. Nucleophilic addition to arene complexes has allowed for the design of a number of functionalized aromatic molecules.[72-83] It has been established that anions add exclusively to the arene and not to the cyclopentadienyl ring in accord with the rules outlined by Davies, Green and Mingos.[84] As well, hydride adds *meta* and *para* to electron-donating groups and *ortho* to electron-withdrawing substituents on the complexed arene.[73,74] With carbon nucleophiles, it has been found that addition generally occurs *ortho* and *para* to electron-withdrawing groups and *meta* to electron-donating substituents.[74] The bulk of the cyclopentadienyliron moieties directs the nucleophiles to add *exo* to the arene and the product of this reaction is an unstable neutral adduct.[85] This η^5-cyclohexadienyl undergoes demetallation in the presence of an oxidizing agent, thereby restoring the aromaticity to the six-membered rings.[72,73] While it has been shown that hydride can add to the rings, the most useful reactions involve the addition of carbanions to the electron-deficient complexed arenes. It has also been shown that nucleophilic addition to oligomeric aryl ether complexes could be achieved as shown in Figure 1.8.[86]

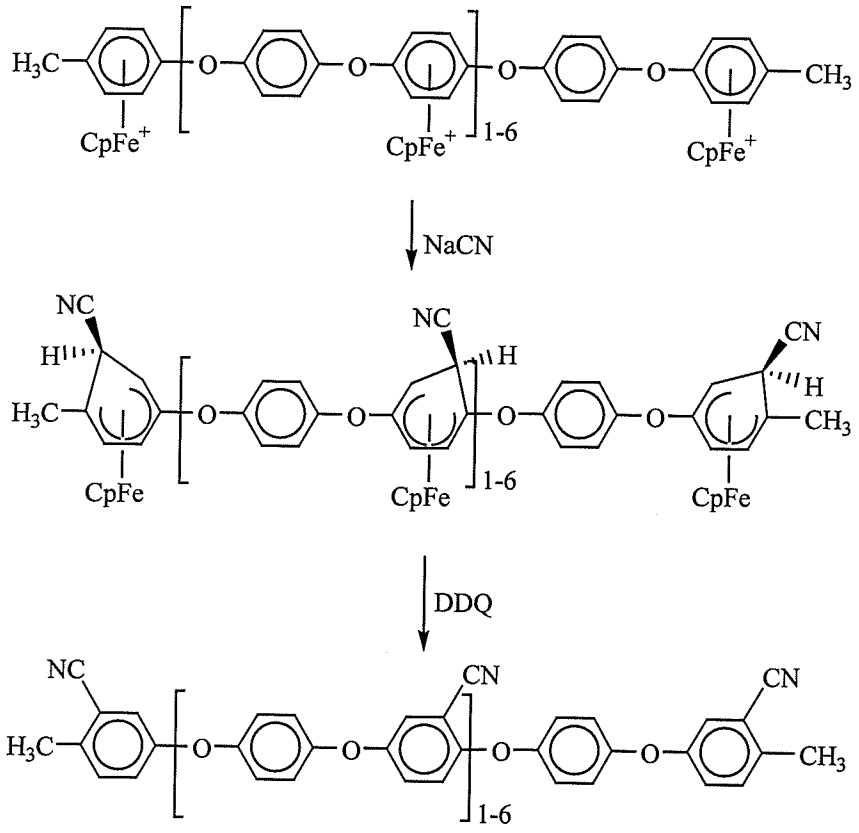

Figure 1.8: Addition of cyanide to complexed aromatic rings

1.1.4.2 Deprotonation

The protons on and vicinal to complexed aromatic rings exhibit enhanced acidity. It is possible to deprotonate heteroatoms as well as alkyl groups on these complexed arenes in the presence of a base.[13,87] Deprotonation of methyl substituents on complexed arenes provides an efficient route to prepare functionalized molecules.[88-100] In particular, Astruc and coworkers have utilized this chemistry to prepare multifunctional complexes used in the synthesis of star and dendritic polymers as shown in Figure 1.9.[91-100] Following deprotonation of the acidic benzylic C-H bonds, a zwitterionic complex is formed, which can also be found as a complex with an exocyclic double bond. It is possible for the exocyclic double bonds to react with a variety of electrophiles to generate highly functionalized materials.

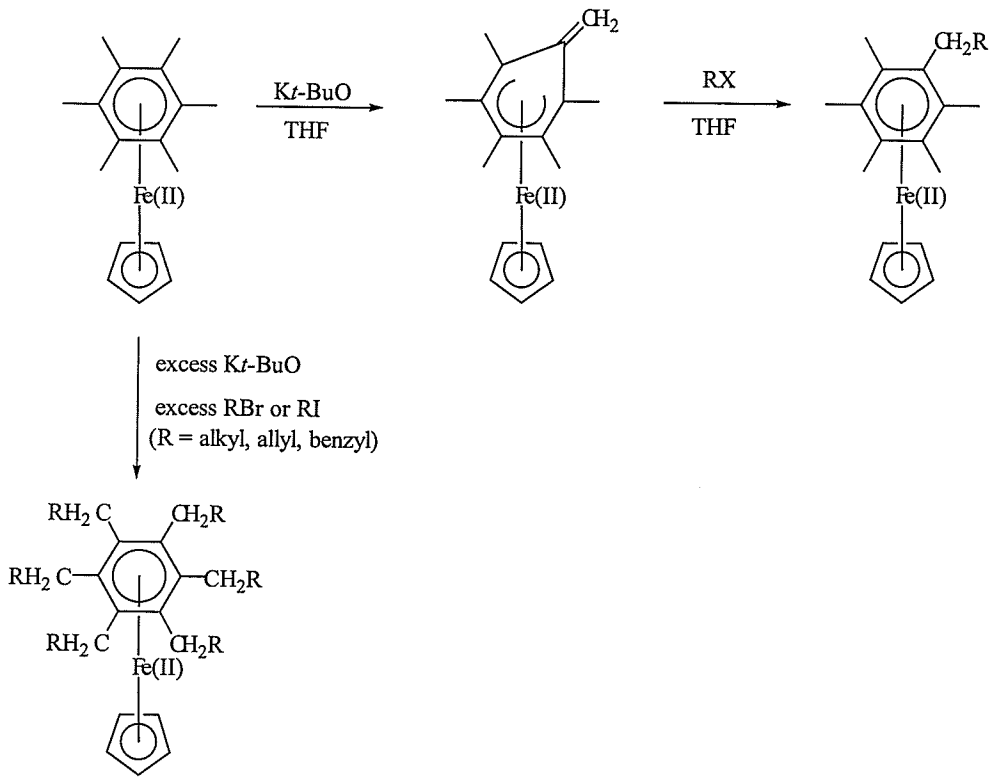

Figure 1.9: Deprotonation and functionalization of arene complexes

1.1.4.3 Nucleophilic Aromatic Substitution

In 1967, Nesmeyanov reported that chlorobenzene cyclopentadienyliron complexes undergo nucleophilic aromatic substitution reactions with a variety of nucleophiles.[101] Since that time, there have been many investigations into the design of novel aromatic complexes using this metal-mediated methodology. There have been a number of studies that have involved the reaction of oxygen- and sulfur-based nucleophiles to produce aryl ether and thioether bonds. These reactions are important because it is very difficult to conduct these types of reactions in the absence of strong-electron-withdrawing groups or metal catalysts.[102-115] Figure 1.10 shows the synthesis of mono- and di-iron complexes via reaction of *p*-dichlorobenzene cyclopentadienyliron with hydroquinone.[107]

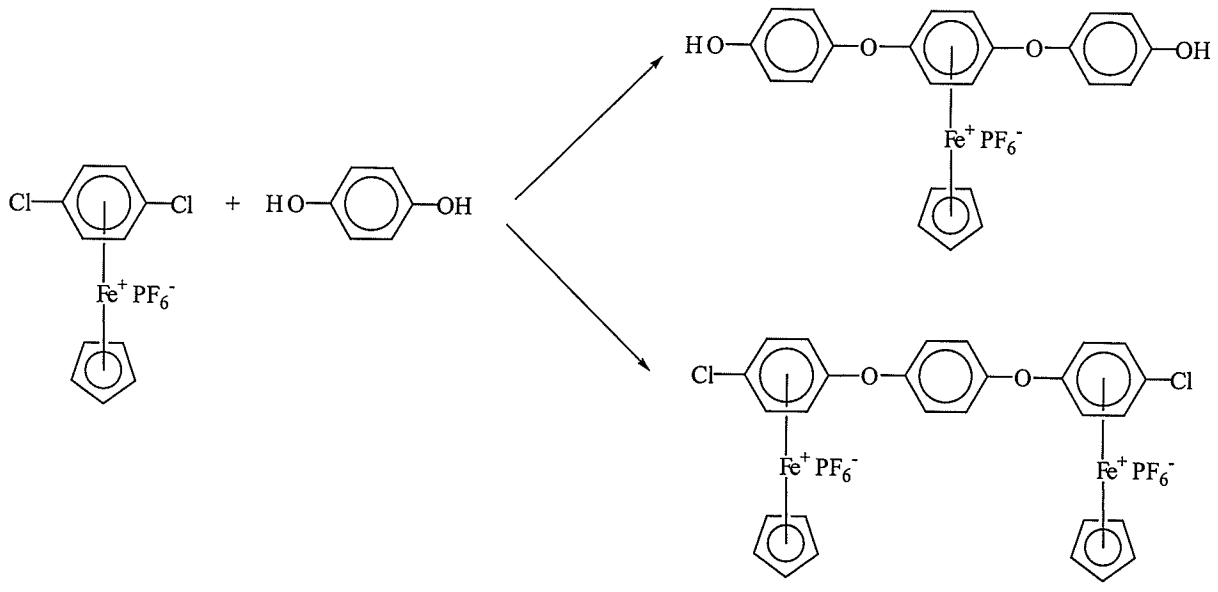

Figure 1.10: Formation of aryl ether complexes of cyclopentadienyliron

The synthesis of a number of amine complexes of cyclopentadienyliron have also been reported.[35-37,104,105,114-120] One of the interesting features of the reaction of primary amines with dichloroarenes is that upon substitution of the first chloro group, deprotonation of the amine results in the formation of a zwitterionic complex. This complex is electron rich and therefore the second chloro group will not substitute unless the reaction is conducted in the presence of glacial acetic acid.[114,115] Figure 1.11 shows the formation of a zwitterionic complex upon reaction of *p*-dichlorobenzene cyclopentadienyliron with a 1,6-hexanediamine.[114]

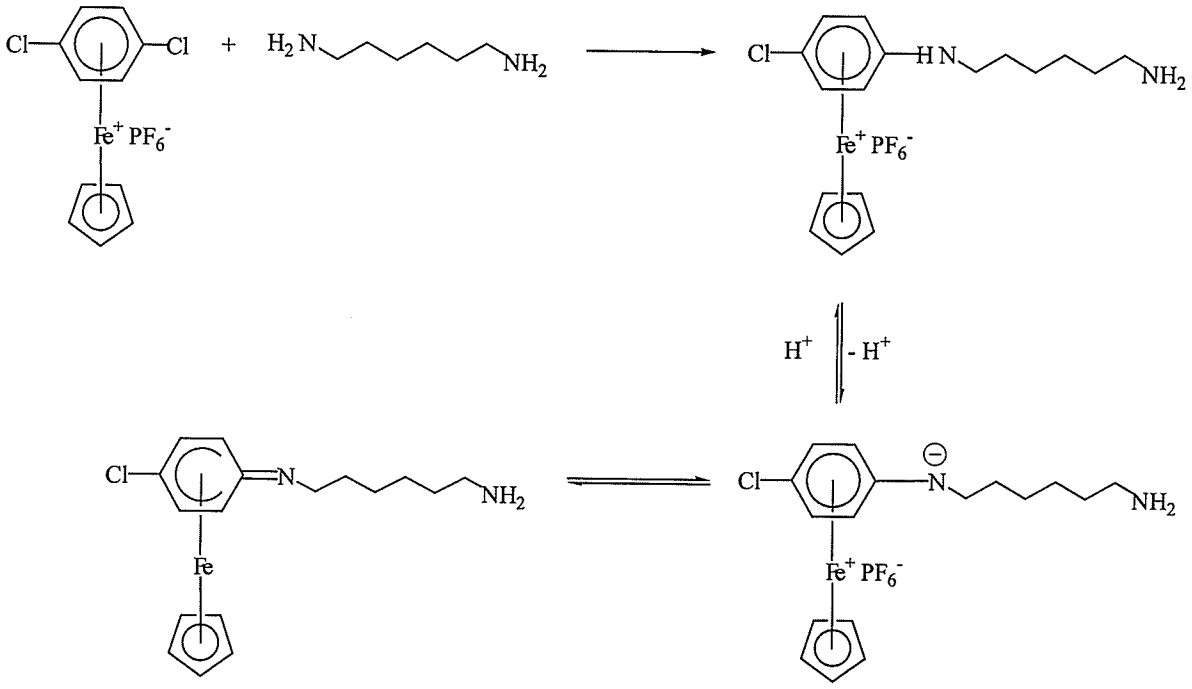

Figure 1.11: Formation of a zwitterionic complex of cyclopentadienyliron

There have also been a number of reports on the reaction of carbon nucleophiles with chloro- or nitro-benzene complexes of cyclopentadienyliron.[36,37,104,105,121-128] Similar to reaction with primary amines, reaction of dichloroarene complexes with primary or secondary carbanions leads to a monosubstituted complex due to zwitterion formation, however, the products formed from reaction with tertiary carbanions cannot be deprotonated and therefore, disubstituted arene complexes can result. Reaction of complexed arenes with carbon nucleophiles derived from 1,3-diketones, malonates, alkyl acetoacetates, cyanoacetates and arylphenylsulphonylacetonitriles has resulted in the isolation of a number of novel materials. Figure 1.12 shows the reaction of a nitroarene complex with phenylsulfonylacetonitrile.[128]

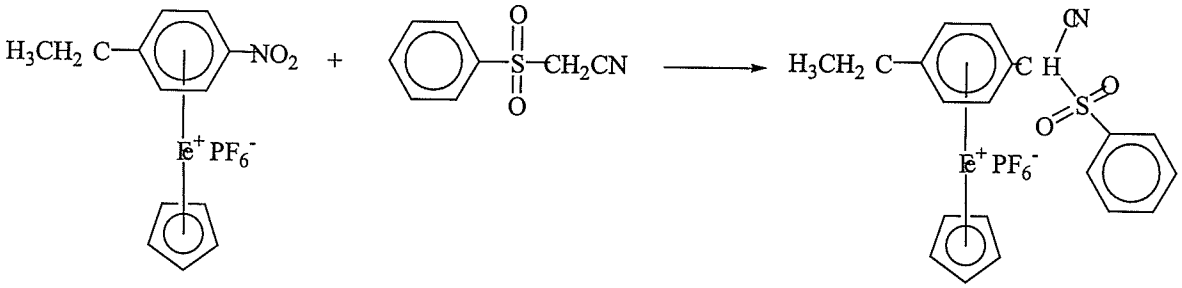

Figure 1.12: Reaction of a nitroarene complex with a carbon nucleophile

1.1.5 Transition Metal Coordinated Arenes in the Design of Monomers

Transition metal arene complexes have proven to be excellent precursors in the design of functionalized monomers. The mild reaction conditions associated with S_NAr reactions of chloroarene complexes allows for the design of aromatic ethers, which are often difficult to synthesize in a controlled manner. In 1993, Percec and Okita reported the synthesis of monomeric ethers prepared via $Cr(CO)_3$-mediated S_NAr reactions of the *p*-dichlorobenzene complex with mono and diphenolic compounds.[129] Although these reactions were facilitated by the electron-withdrawing capability of the chromium tricarbonyl moieties, they still required the addition of a phase transfer catalyst such as tetrabutylammonium hydrogen sulfate or 18-crown-6. This is because the chromium tricarbonyl moiety is the least electron-withdrawing of the arene transition metal complexes. However, demetallation of these complexes was easily achieved by the addition of iodine as shown in Figure 1.13. The resulting aryl ether monomer containing terminal chloro groups was subjected to Ni(0) catalyzed-polymerization to yield the corresponding polyaromatic ether with a number average molecular weight of 11 200.

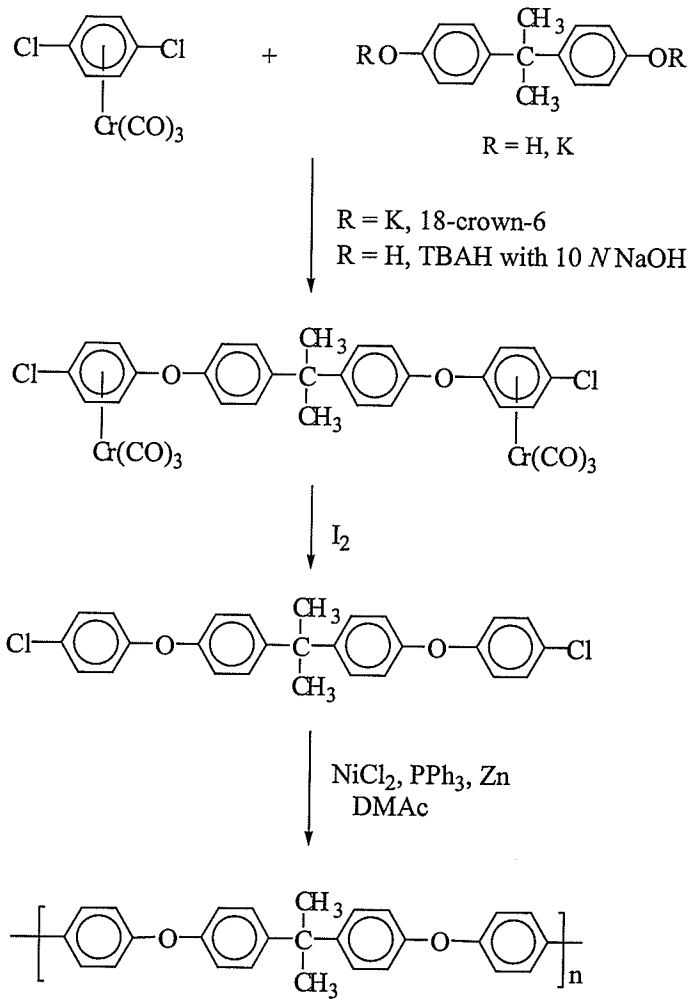

Figure 1.13: Synthesis of aryl ether monomers using chromium tricarbonyl complexes and their Ni-catalyzed polymerization

Pearson and coworkers have utilized chloroarene cyclopentadienyliron complexes in the synthesis of aromatic ether monomers.[47,130,131] These monomers, shown in Figure 1.14 were designed with phenolic and carboxylic acid groups. It was possible to prepare these complexes by taking advantage of the fact that the first chloro group on a dichloroarene complex of cyclopentadienyliron is slightly more easily displaced than the second. Following photolytic cleavage of the cyclopentadienyliron moieties,

polycondensation of these monomers produced polyaromatic ether esters that displayed liquid crystalline properties. It was also reported that the thermal properties of these polymers could be adjusted by altering the aromatic spacer and by changing the dichloroarene from *para* to *meta* substituted.

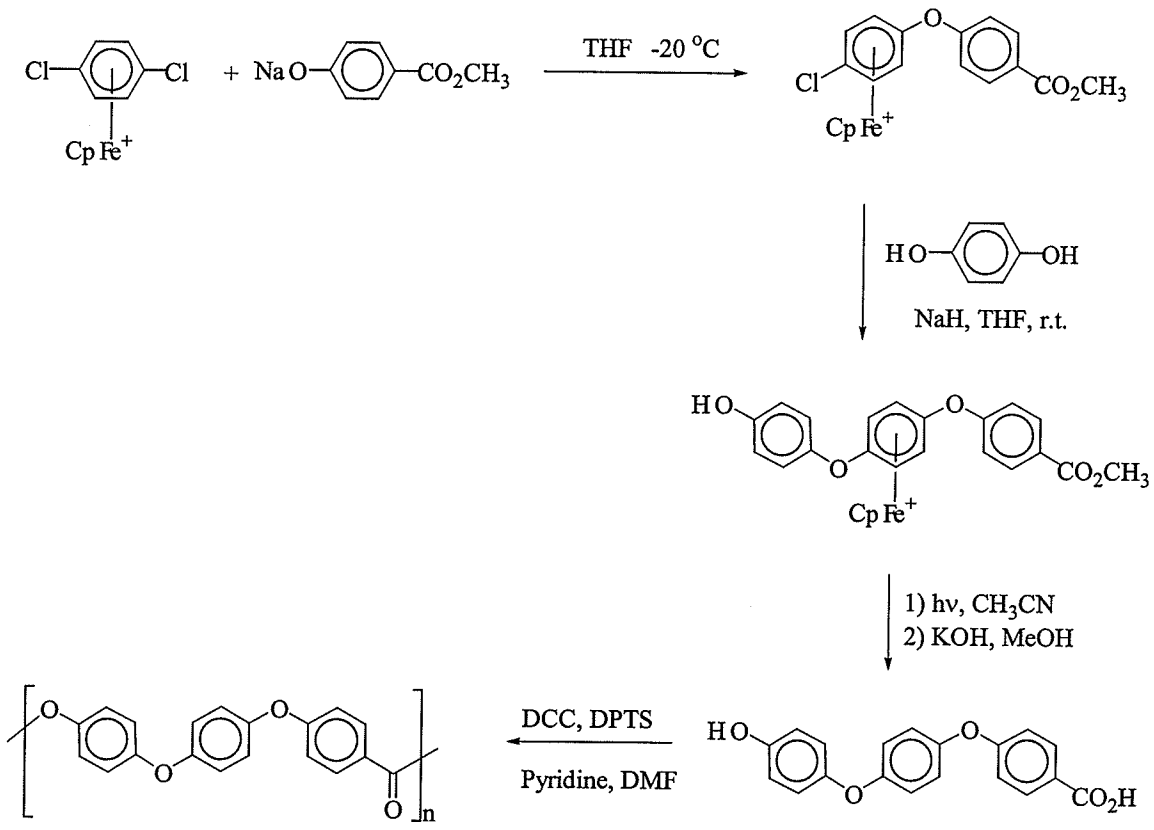

Figure 1.14: Synthesis of poly(aryl ether esters) using cyclopentadienyliron complexes to design novel monomers

Figure 1.15 shows another cyclopentadienyliron-mediated synthesis of aryl ether monomers.[132] Reaction of *p*-dichlorobenzene complexes with dinucleophiles yielded diiron complexes with terminal chloro groups. These complexes were then capped with naphthoxy groups, producing the organoiron-complexed aryl ether monomers that were subsequently demetallated photolytically. Reaction of these monomers with ferric chloride in nitrobenzene resulted in the isolation of thermally stable polyaromatic ethers. Polymerization of these monomers was achieved via the Scholl reaction, which proceeds via a radical-cation mechanism. The polyaromatic ethers had weight average molecular weights (M_w) as high as 124,000. The glass transition temperatures of these polymers ranged from 147 to 226 °C and thermogravimetric analysis showed that they were thermally stable until 458 to 575 °C depending on the spacers between the naphthyl rings.

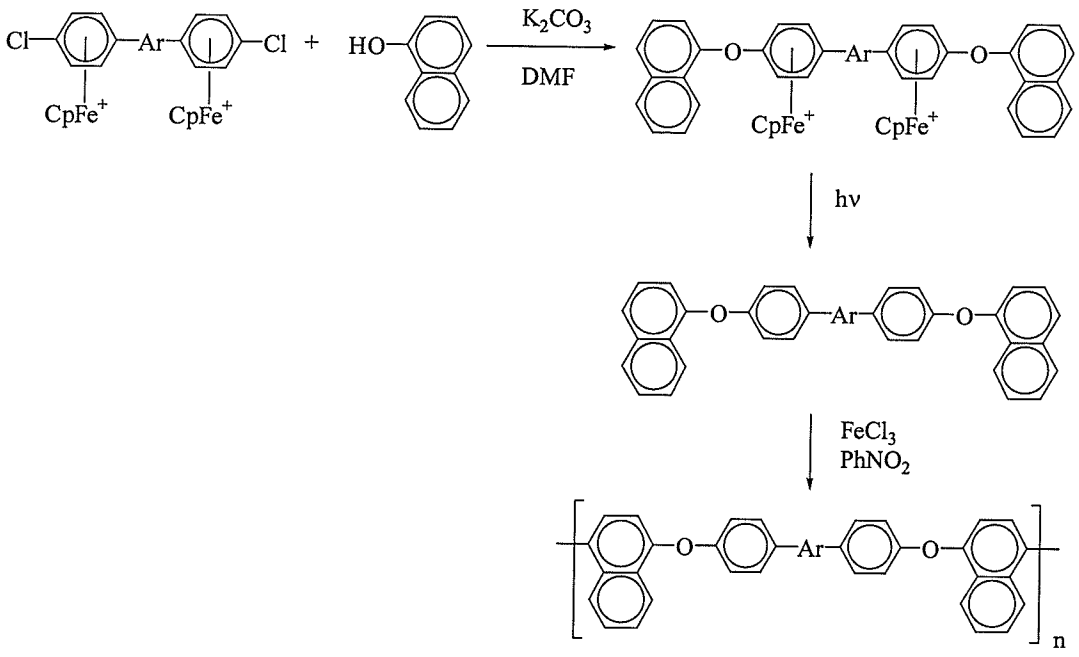

Figure 1.15: Synthesis of aromatic ether monomers using cyclopentadienyliron complexes and their metal-catalyzed polymerization reactions

Polymers containing ethers in their side chains have also benefited from metal mediated reactions.[133-135] It has been demonstrated that polynorbornenes containing aryl ether side chains possess enhanced thermal stability and glass transition temperatures relative to unsubstituted polynorbornene.[134,135] Figure 1.16 shows the methodology utilized to design monomers coordinated to cyclopentadienyliron cations. The incorporation of aliphatic ether spacers into the side chains of polynorbornenes has also been reported.[135] It was found that the thermal stability of these high molecular weight polymers (M_w = 397,000) increased with respect to polynorbornene, while their glass transition temperatures were much lower.

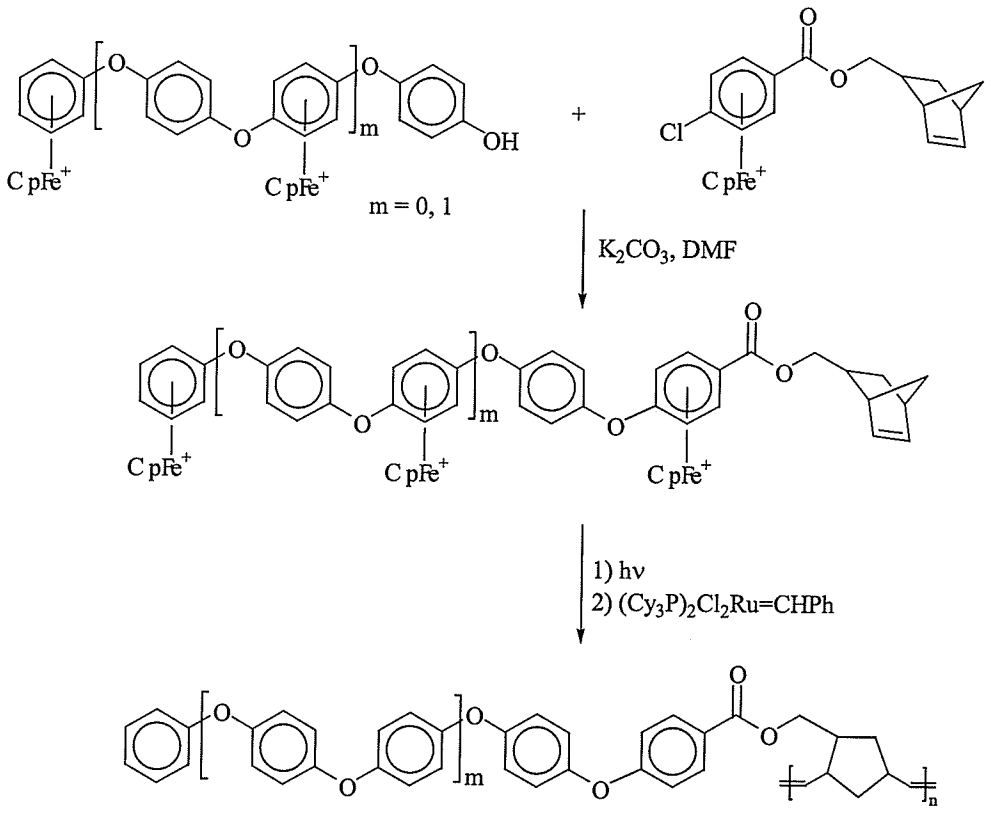

Figure 1.16: Polymerization of norbornene monomers prepared using cyclopentadienyliron complexes

1.2 Organometallic Polymers

Organometallic polymers have been the focus of many studies due to their promising catalytic, electrical, magnetic and optical properties.[136--155] While many of these materials include metals within their backbones, others incorporate the metallic moieties pendent to the macromolecule. In many organometallic polymers, the metallic moiety is an integral part of their structures, while in other cases, the metallic moieties are added to preformed polymers or may be cleaved from the polymeric material. Polymers with metal-carbon bonds in their backbones include heteroannular polymetallocenes, transition metal-acetylides and metallacyclopentadienes. Figure 1.17 gives examples of some of the most common classes of organometallic polymers.[156-160]

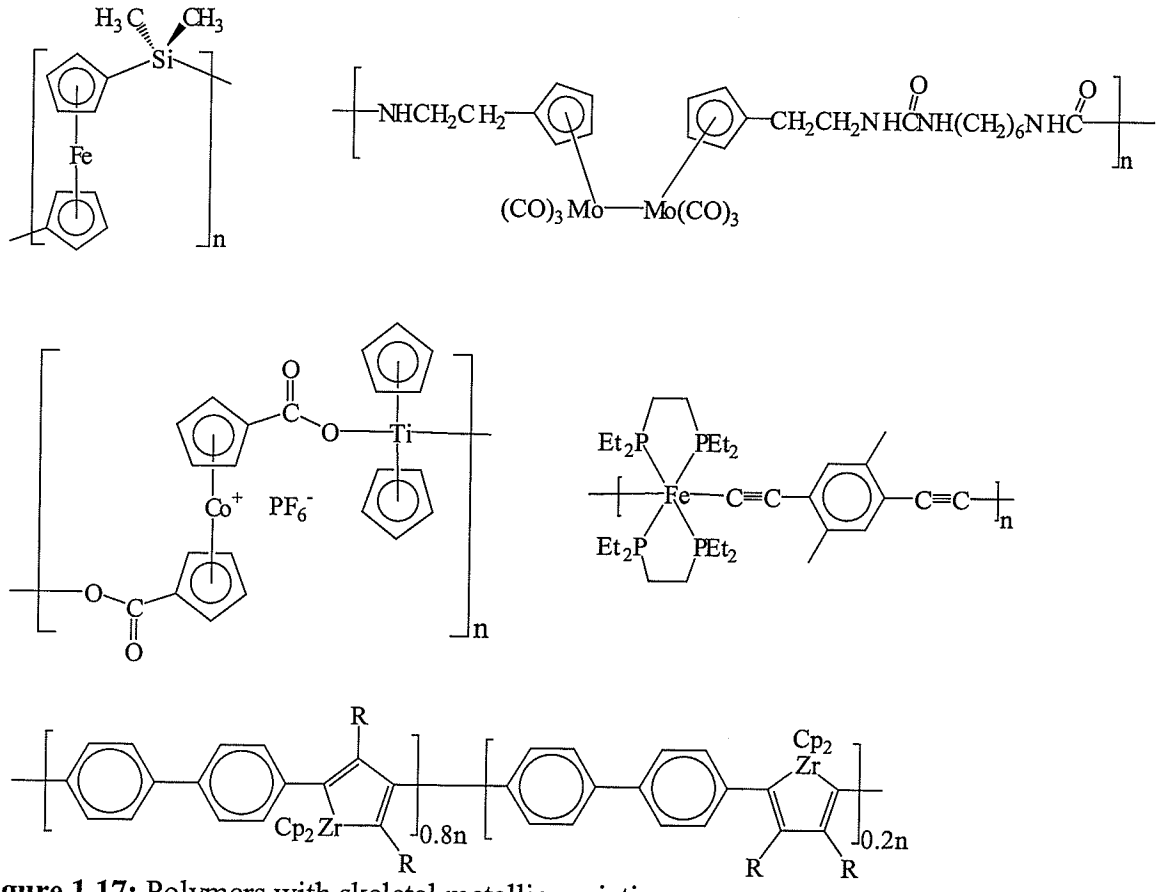

Figure 1.17: Polymers with skeletal metallic moieties

There are also a number of different classes of organometallic polymers in which the metallic moiety is pendent to the polymer backbone or pendent to the polymer side chains. Figure 1.18 gives examples of a homoannular polymetallocene, a polymer with pendent cyclopentadienylcobalt moieties and a polymer with a tungsten group in the polymer side chains.[161-163]

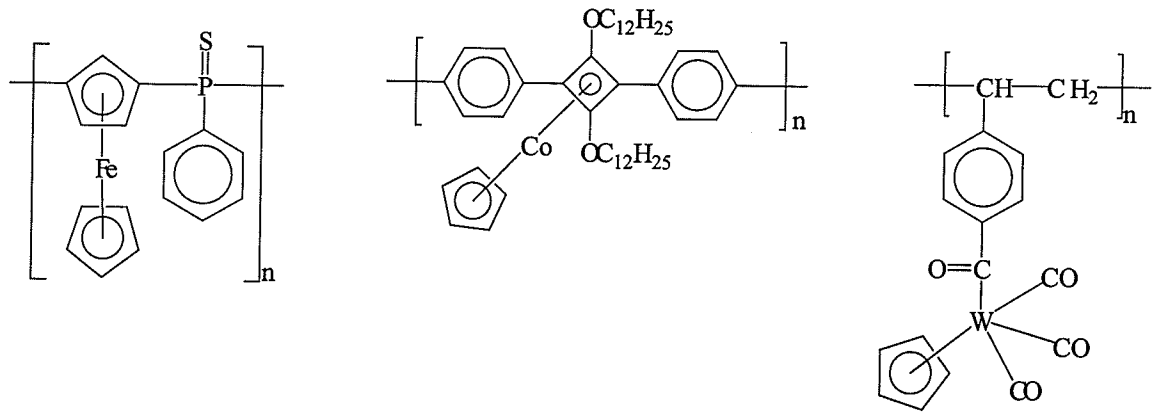

Figure 1.18: Polymers with pendent metallic moieties

1.2.1 Transition Metal Coordinated Arenes in the Design of Polymers

Polymers containing arene complexes of transition metals in their structures are an important class of organometallic polymers due to the interesting properties that these complexes possess. The enhanced reactivity of arene complexes towards nucleophiles has already been described, and this reactivity can lead to aromatic polymers using milder reaction conditions than those traditionally used to prepare these classes of materials. In addition, polymers containing arene complexes can be prepared using all the traditional methods utilized to prepare organic polymers. These include polycondensation, radical polymerization and ring-opening polymerization. Organic and inorganic polymers have also been functionalized with transition metal arene complexes in order to examine the properties of these materials. Within the past few years, there have also been reports on the supramolecular assembly of arene complexes to produce organometallic polymers. Interest in these materials stems from the properties that the metals introduce to the polymers, including electrochemical activity and catalytic activity. A number of these polymers were also found to possess other interesting properties such as liquid crystallinity and enhanced solubility. There have been numerous reports on the synthesis of polymers containing the organometallic moieties pendent to the polymer backbone and pendent to the polymer side chains. The synthesis and properties of these two classes of transition metal arene complexed polymers will be described.

1.2.1.1 Transition Metal Moieties Pendent to Arenes in the Polymer Backbone

In 1987, Jin and Kim reported the first examples of polyamides coordinated to chromium tricarbonyl moieties.[164] These polymers, which are shown in Figure 1.19, were prepared via condensation reactions of phenylenediamine-$Cr(CO)_3$ with organic acid chlorides. It was hoped that the presence of the organometallic moieties pendent to the polymer backbone would increase their solubility relative to organic aromatic polyamides. The desire to prepare these materials stemmed from the interesting properties associated with poly(*p*-phenylene terephthalamide) (PPTA), which is known to form a lyotropic liquid crystal in strong acids, and can be processed into high strength and modulus fibers. Polyamides with the same organic bridges were also prepared with phenylenediamine using similar reaction conditions in order to compare their solubilities to those of the metallated counterparts. While the organometallic polyamides remained in solution during the polymerization reactions, the organic polymers formed gels or precipitated out of solution during their preparation. Although the chromium tricarbonyl complexed polymers initially displayed good solubility, once they were dried, it became difficult to redissolve these polymers in polar organic solvents.[164]

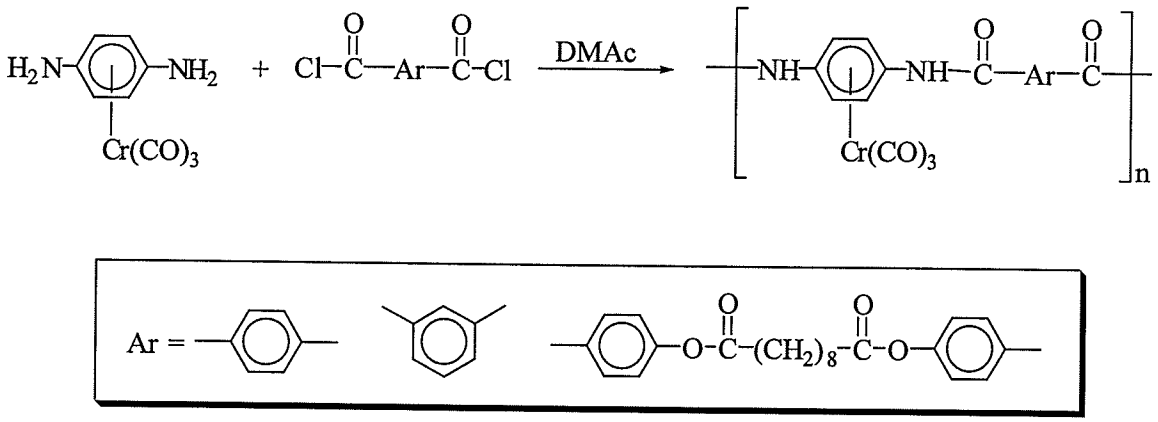

Figure 1.19: Synthesis of chromium tricarbonyl complexed polyamides

In 1993, Dembek and coworkers prepared high molecular weight PPTA in *N,N'*-dimethylacetamide coordinated to chromium complexes.[165,166] In addition to using the phenylenediamine complex of chromium tricarbonyl in the polymerization reactions, ligand exchange reactions were performed resulting in replacement of one of the carbonyl ligands for trimethylphosphine. All of the organometallic polymers exhibited nematic liquid crystallinity, although varying the ligands on chromium altered the concentration at which the nematic texture was observed. The lyotropic behavior of the organometallic polymers indicates that their rigid rod nature is retained even though their solubility is significantly enhanced by metal coordination. A copolymer, consisting of only half of the phenylenediamine rings coordinated to $Cr(CO)_3$ was prepared, and this polymer also displayed enhanced solubility and liquid crystalline behavior. The chromium-complexed polymers were subjected to oxidative demetallation with iodine to produce the insoluble organic polyamides. Figure 1.20 describes the synthesis of polyamides as reported by Dembek.[165,166]

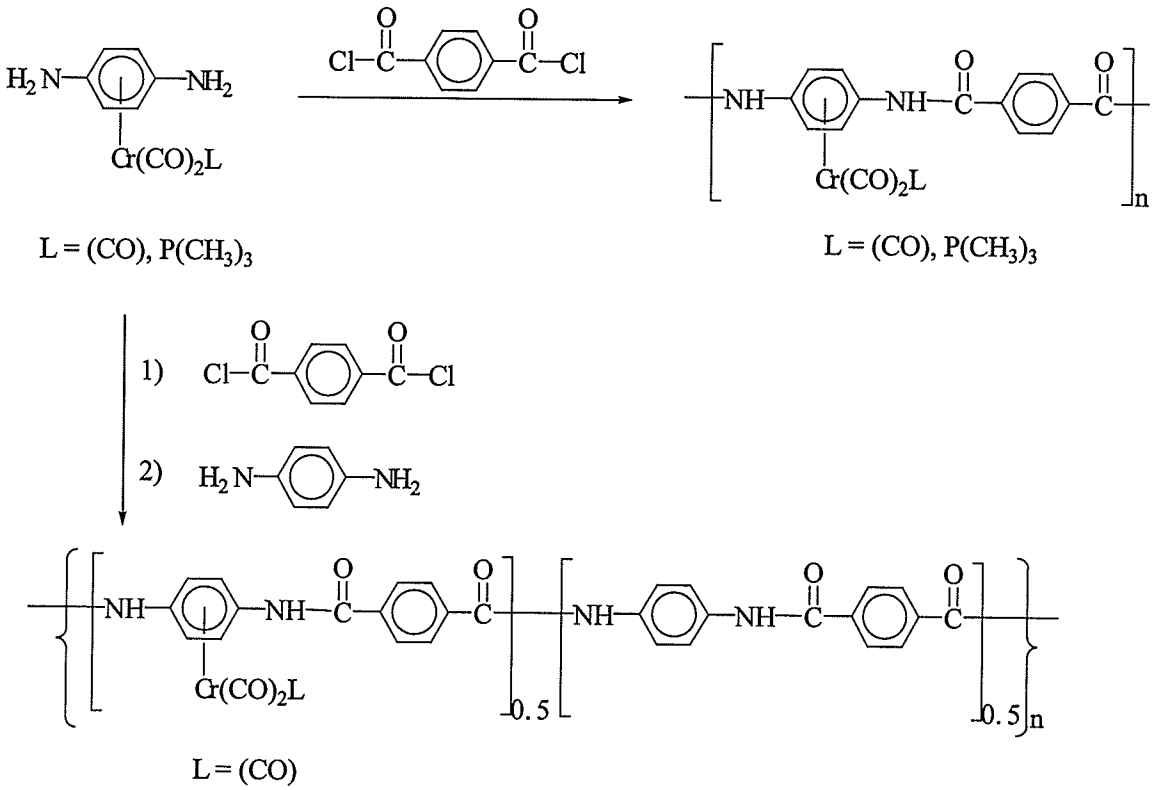

Figure 1.20: Synthesis of polyamides coordinated to chromium complexes

Wright later reported on the synthesis of different classes of conjugated polymers coordinated to chromium tricarbonyl moieties.[167-170] The first class of polymer was poly(phenyl acetylenes) coordinated to chromium tricarbonyl moieties.[167,168] These polymers were synthesized via a palladium catalyzed cross-coupling reaction of η^6-1,4-dichlorobenzene chromium tricarbonyl complexes with organostannane reagents. Figure 1.21 shows how these and copolymers prepared with 2,6-dibromopyridine were synthesized. In contrast to the studies of Jin[164] and Dembek,[165,166] it was found that these organometallic conjugated polymers displayed poor solubility in polar organic solvents. However, by using the η^6-1,3-dichlorobenzene complex, polymers with higher solubility

could be isolated.[168] Combustion analysis of the organometallic polymers indicated that their degree of polymerization was about 18, corresponding to molecular weights of about 7,800. Thermogravimetric analysis showed that $Cr(CO)_3$ units were lost from the polymers around 200 °C and then they were stable until about 380 °C under an argon atmosphere.[167] Combustion and IR analysis indicated that these materials underwent cross-linking reactions following loss of carbon monoxide from the metallic moieties.

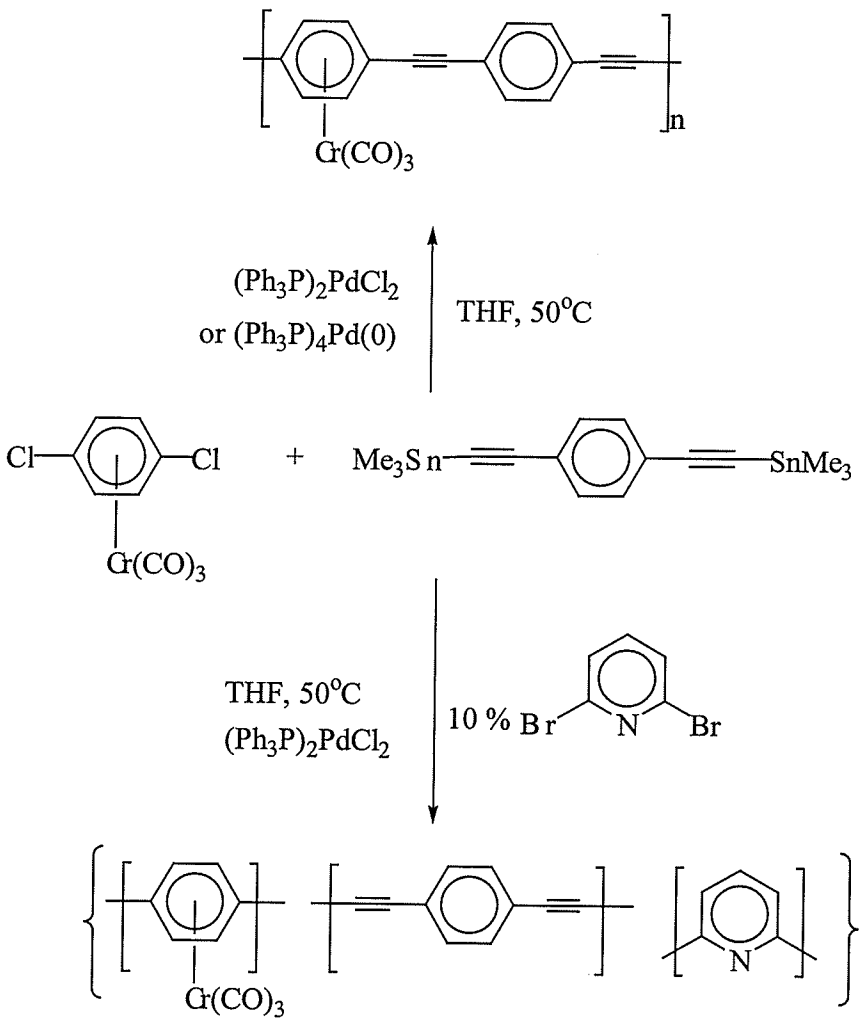

Figure 1.21: Synthesis of poly(phenyl acetylenes) coordinated to chromium tricarbonyl moieties

Reaction of a phosphine substituted arene complex with the rhodium complex shown in Figure 1.22 resulted in the isolation of a heterobimetallic coordination polymer.[169] The formation of these polymers could be monitored by the production of carbon monoxide. The molecular weights of these interesting polymers could not be obtained due to their thermal decomposition and air sensitivity. The solubility of these mixed metal polymers decreased over time, however, the chromium tricarbonyl coordinated polymer became completely insoluble, while the presence of a tributylphosphine group allowed for greater solubility.

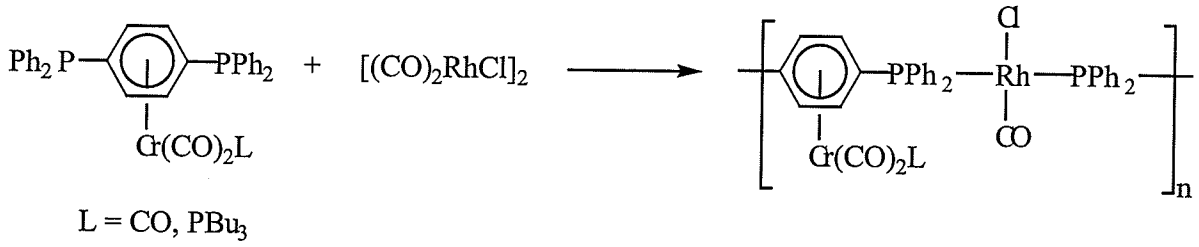

Figure 1.22: Synthesis of a heterobimetallic coordination polymer

Wright and Lowe-Ma have also reported one example of a conjugated polyimine coordinated to chromium tricarbonyl complexes via reaction of complexed η^6-terephthaldialdehyde with 1,3-phenylenediamine as shown in Figure 1.23.[170] The resulting conjugated polyimine precipitated from the reaction solution and was insoluble in common organic solvents.

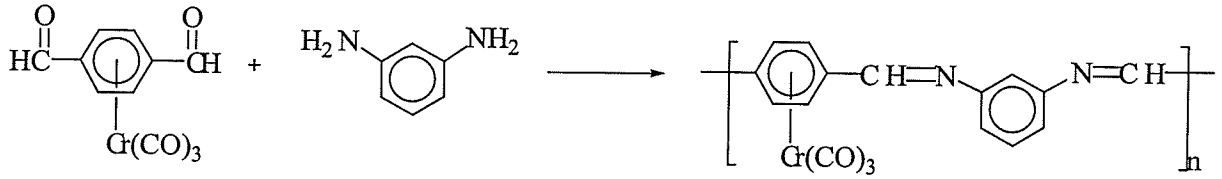

Figure 1.23: Synthesis of a conjugated polyimine coordinated to chromium tricarbonyl

The synthesis of polyether/imines coordinated to cyclopentadienyliron moieties has recently been communicated.[171] The organoiron polymers shown in Figure 1.24 were prepared by reaction of a dialdehyde complex of cyclopentadienyliron with aliphatic and aromatic diamines. These polycondensation reactions resulted in the isolation of the polyether/imines that displayed moderate solubility in polar organic solvents. However, upon removal of the cyclopentadienyliron cations pendent to the polymer backbones, the resulting organic polymers were insoluble.

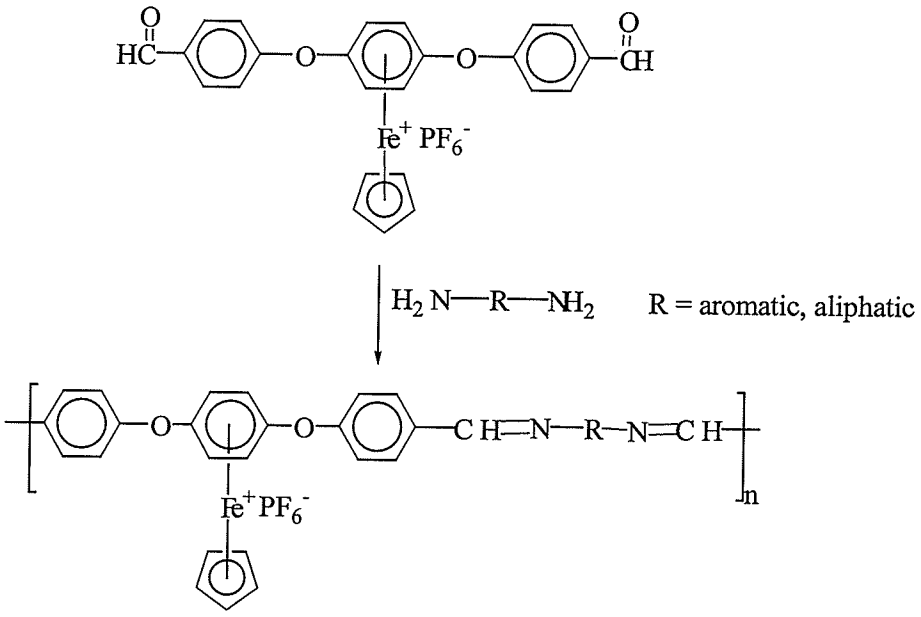

Figure 1.24: Synthesis of polyether/imines coordinated to cyclopentadienyliron cations

The importance of the electron-withdrawing capability of transition metals on arenes was demonstrated in 1985 when Segal reported the synthesis of polyaromatic ethers via cyclopentadienylruthenium ($CpRu^+$) mediated S_NAr reactions.[172] While there had been previous examples of the use of complexed arenes in the synthesis of small molecules, this was the first example utilizing these complexes to prepare macromolecules. These polyaromatic ethers exhibited the same enhanced solubility in polar organic solvents that the polyamides coordinated to chromium tricarbonyl possessed. However, these polymers were demetallated by thermolysis and the polyether polyether-ketone shown in Figure 1.25 was insoluble, while the polymer with an isopropylidene bridge in the backbone was soluble in organic solvents. The weight average molecular weight of the organic polyether was found to be 15,600 in 1,2-dichloroethane and the glass transition temperatures of the organic polyethers ranged from 115 to 144 °C.

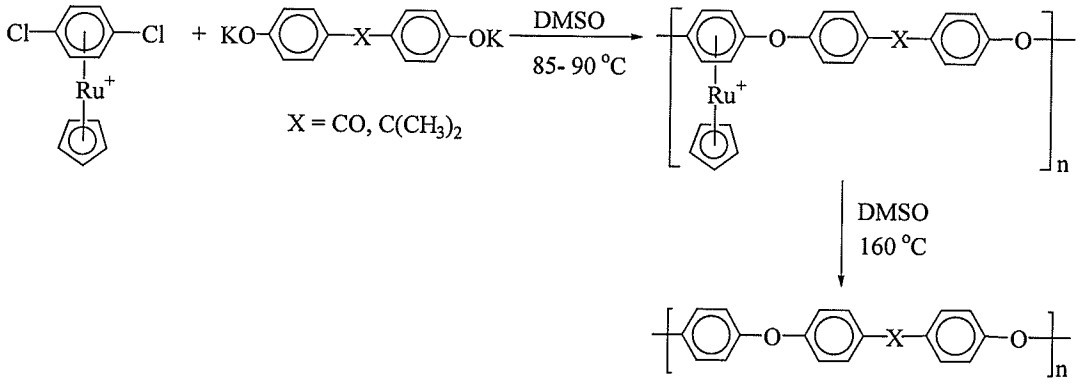

Figure 1.25: Synthesis of polyaromatic ethers coordinated to cyclopentadienylruthenium cations

In 1993, Dembek and coworkers reported the synthesis of poly(aromatic ethers and thioethers) with pendent pentamethylcyclopentadienylruthenium (Cp^*Ru^+) moieties.[173-175] One report of a cyclopentadienyliron coordinated polyphenylene sulfide was also reported in a patent.[175] The ruthenium-coordinated polymers shown in Figure 1.26 were prepared by reaction of aromatic oxygen- and sulfur-based dinucleophiles with the 1,4-η^6-dichlorobenzene complex.[173,174] The inherent viscosity of these metallated polymers ranged from 0.52 to 1.49 dL/g (0.5% in DMF, 30 °C). Reactions of tri- and tetra-chloro benzene complexes with phenol and thiophenol demonstrated that these complexes would be suitable for the preparation of highly branched polymers, however the polymers of these complexes were not reported.[174]

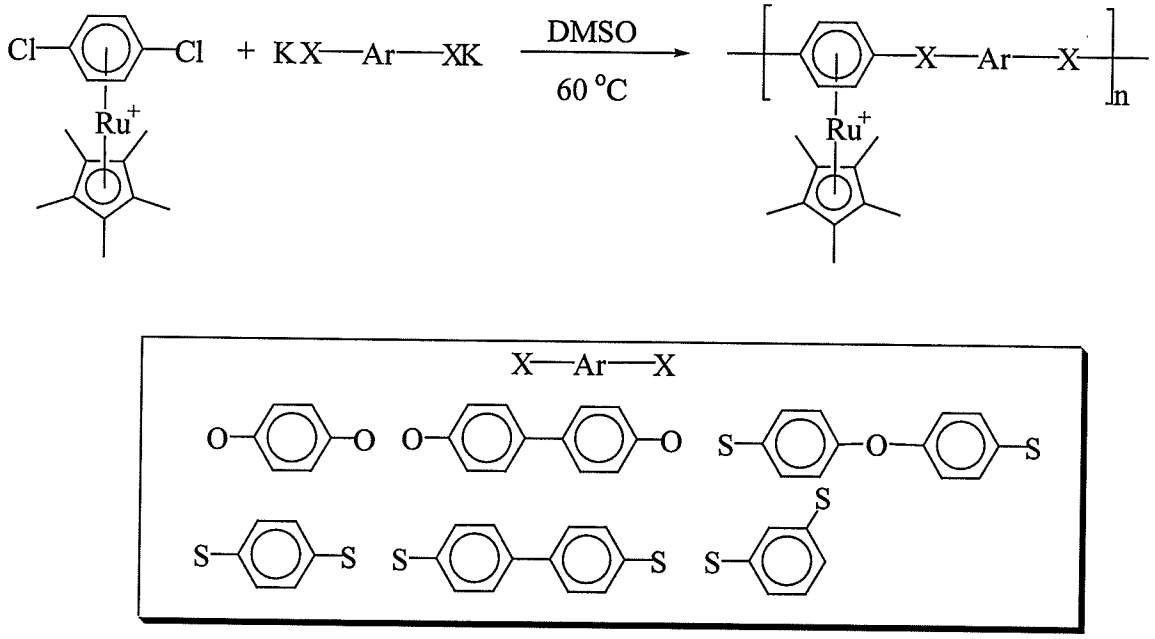

Figure 1.26: Synthesis of polyaromatic ethers and thioethers coordinated to pentamethylcyclopentadienylruthenium cations

It has been demonstrated that polyaromatic ethers with well-defined molecular weights can be prepared by sequential S_NAr reactions of chloroarene complexes of cyclopentadienyliron with hydroquinone.[106] This strategy has allowed for the isolation of aromatic ether complexes with as many as 35 metallic moieties pendent to their backbones.[51] Figure 1.27 shows the sequence of reactions that resulted in the production of these oligomeric and polymeric complexes.

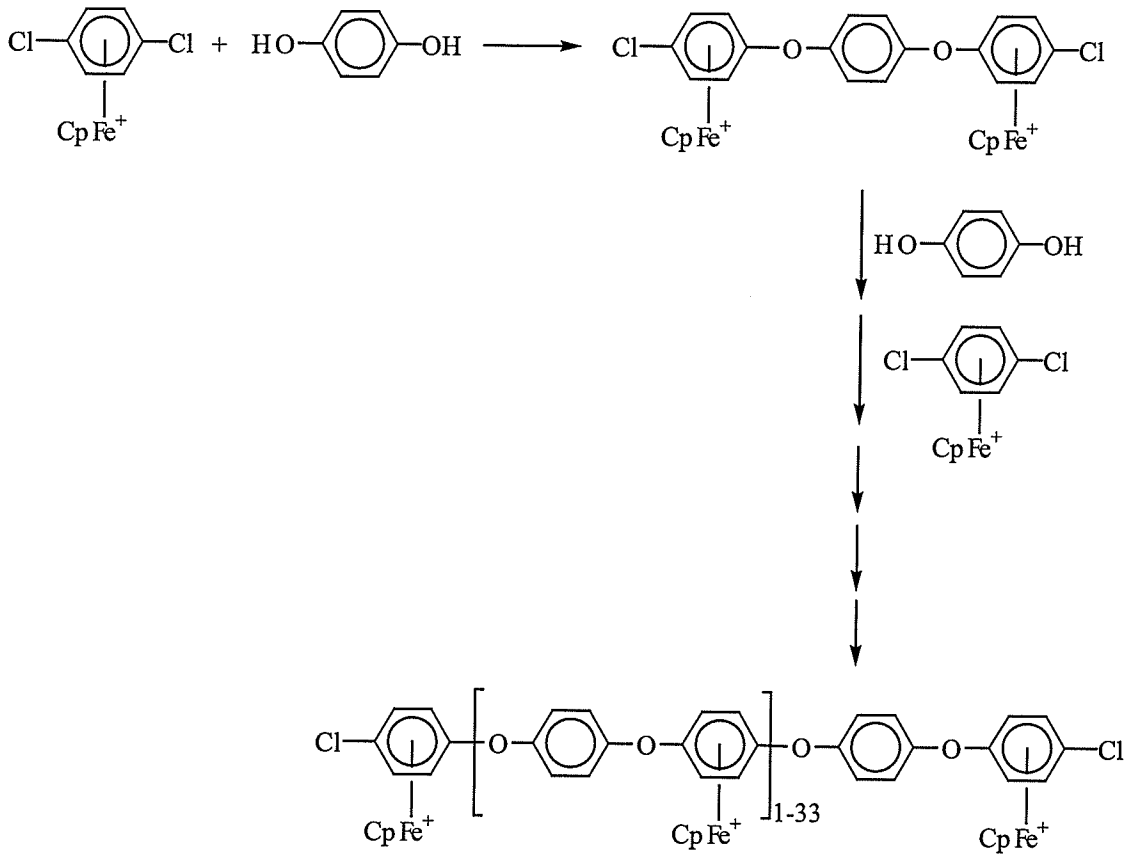

Figure 1.27: Step-wise synthesis of polyaromatic ethers and coordinated to cyclopentadienyliron cations

The first examples of aromatic polymers with transition metal moieties coordinated to their backbones were reported in 1984 by the coordination of preformed polyphenylenes with transition metal complexes.[176,177] Eyring and coworkers reported that 25 % of the aromatic rings in polyparaphenylene (PPP) were complexed to molybdenum tricarbonyl using this approach It was determined using infrared photoacoustic spectroscopy, that the organomolybdenum polymer and a potassium-doped PPP showed similar shifts in their spectra relative to the unmodified organic polymer.

In order to enhance the solubility of these polymers, Nishihara and coworkers reacted alkylated polyphenylenes with a variety of transition metal complexes.[178-180] Figure 1.28 shows the structures of some of the transition metal-coordinated polymers synthesized.

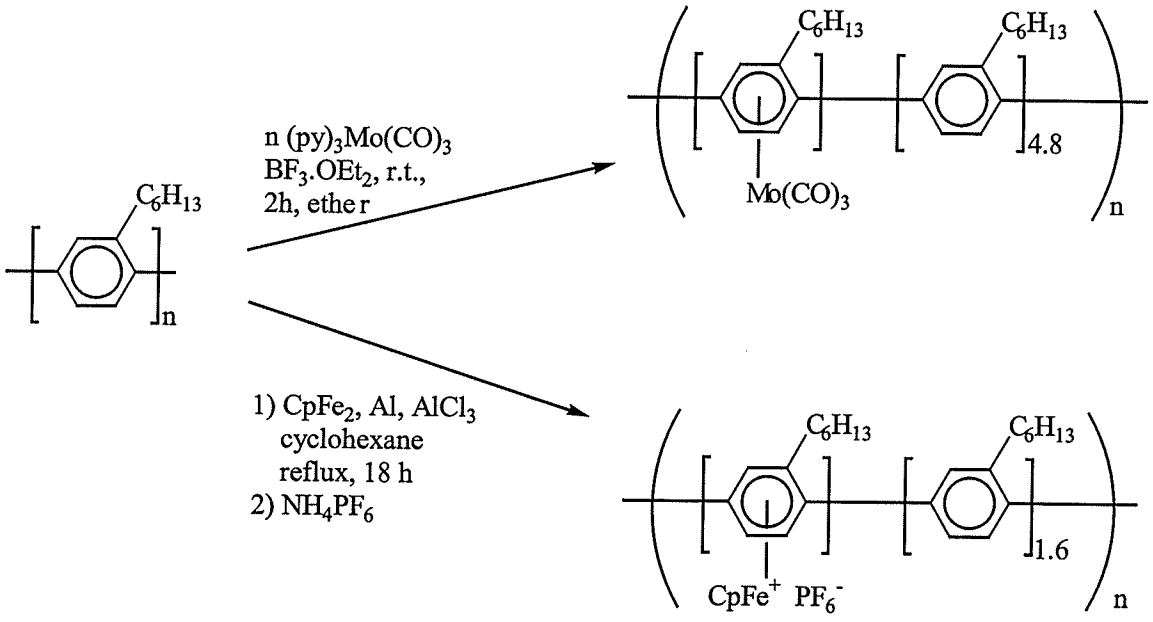

Figure 1.28: Coordination of transition metal complexes to preformed organic polymers

Nishihara found that when a molybdenum complex was utilized, approximately 1 in every 4.8 aromatic rings of the polymer was coordinated to $Mo(CO)_3$. The organic and organometallic polymers were analyzed using electrochemical and spectroscopic techniques as well as elemental analysis.[178-180] It was determined that the redox potential and conductivity of this polymer were affected by metal coordination, however, the band gap of the polymer did not change appreciably. A cyclopentadienyliron complex of PHP was also prepared, and it was determined that on average, 1 in every 1.6 aromatic rings was coordinated to a cyclopentadienyliron cation. Cyclic voltammetric studies of this polymer indicated that the iron centers were reduced around -1.7 V. It was also noted that there was an increase in ΔE_p with increasing sweep rate, which indicated that the heterogeneous electron transfer within the system was fairly slow. Spectroelectrochemical measurements of the organoiron polymer suggest that following reduction of the cationic iron centers, a network was formed between the aromatic rings of neighboring polymer chains. The results of Eyring and coworkers[176,177] and Nishihara and coworkers[178-180] showed that the π-coordination of metallic moieties to aromatic rings in conjugated aromatic polymers is an effective way to alter their electronic properties.

Within the past three years, a new class of supramolecular polymers containing arene complexes has emerged.[181-184] Brammer and coworkers have recently reported the use of arene chromium tricarbonyl complexes as building blocks in supramolecular assembly.[181,182] Carboxylate-functionalized arenes coordinated to chromium tricarbonyl moieties assembled via hydrogen bonds through the arene carboxylic acid substituents. Complexes containing one carboxylic acid group formed discrete dimers, however, di-

and tri-functionalized complexes formed extended supramolecular assemblies. In addition to hydrogen bonding via the carboxylic acid groups on the arenes, the three carbonyl oxygen atoms in the ligands on chromium also acted as hydrogen bond acceptors to C-H donors in the 2- and 5-positions on the arene rings. The C-H group in the 3- position of the arene also formed C——H– – –O hydrogen bonds to neighboring hydroxy oxygen atoms.

There have not been many reports on the synthesis of polymers containing arenes coordinated to manganese tricarbonyl moieties, even though this organometallic moiety is the most electron-withdrawing of the series. However, Sweigart and coworkers recently reported the self-assembly of deprotonated hydroquinone manganese tricarbonyl complexes to produce a novel class of organometallic supramolecular polymers.[183,184] Although the complexed arenes shifted from η^6 to η^4 or η^5 upon formation of the polymers, the precursors are arene complexes. As described earlier, the reason why the hydroquinone complex is so easy to deprotonate is due to the enhanced acidity caused by the electron-withdrawing manganese tricarbonyl group. Therefore, the chemistry of these polymers is dependent upon the same type of reactivity that governs other reactions of transition metal arene complexes. The oxygen atoms in the η^4-quinone complex were found to form σ-bonds with divalent metal ions in the presence of light or a basic solution of the metal ion.[183] Examples of polymers formed from the η^4 and η^5 complexes are shown in Figure 1.29.

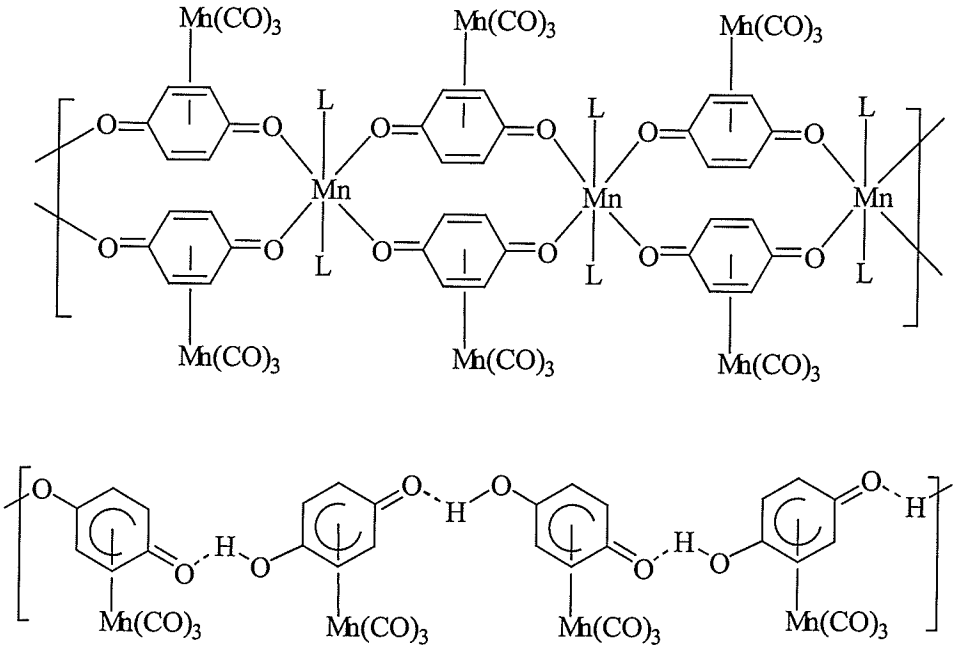

Figure 1.29: Supramolecular polymers formed from hydroquinone complexes

1.2.1.2 Transition Metal Moieties Pendent to Arenes in the Polymer Side Chains

In the 1970's, Pittman and coworkers reported the synthesis of polyacrylates, polymethacrylates and polystyrenes with side chains containing arenes coordinated to chromium tricarbonyl.[185-187] High molecular weight homo- and co-polymers were synthesized and a number of studies examined the reactivity of these organometallic monomers. Rausch and coworkers reported the synthesis of the styrene monomer coordinated to $Cr(CO)_3$ shown in Figure 1.30.[188] This organometallic monomer was subsequently co-polymerized with either styrene or methyl acrylate using azobisisobutyronitrile (AIBN).[187]

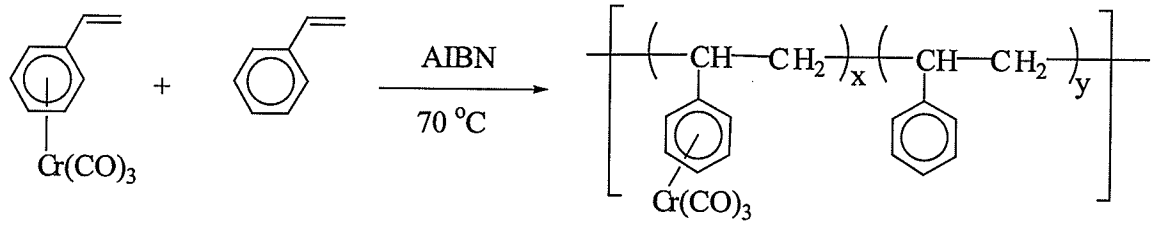

Figure 1.30: Polystyrenes containing arenes coordinated to chromium tricarbonyl

Interest in the use of transition metal containing polymers for catalysis prompted an investigation by Chaudret and coworkers in 1990.[189] They reported the isolation of a polystyrene in which some of the arene rings were coordinated to transition metal complexes, including the first example of a polymer-supported hydrido transition metal complex, which could display catalytic activity. Unlike the synthesis of organochromium polystyrenes by Pittman,[188] this work involved the coordination of the ruthenium

complexes to preformed polystyrene.[189] Figure 1.31 shows the structures of the polystyrenes containing pendent $Ru^{+}Cp^{*}$, $Ru^{+}C_8H_{11}$ or $Ru^{+}H(PCy_3)_2$. Depending on the bulkiness of the ligand attached to the ruthenium, anywhere from 25 to 100% of the aromatic rings in the polymer side chains became coordinated to ruthenium moieties.

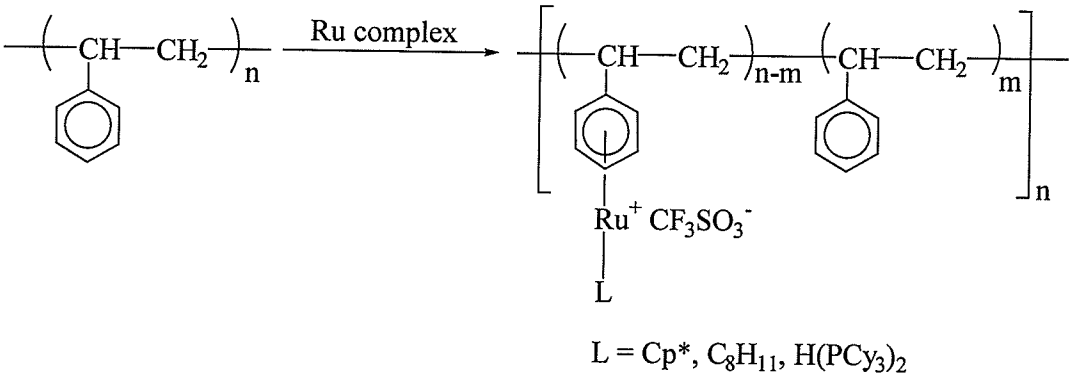

Figure 1.31: Polystyrenes containing arenes coordinated to ruthenium complexes

The polymerization of norbornene monomers functionalized with cationic cyclopentadienyliron complexes was recently reported.[190,191] The ring-opening metathesis polymerization of the metallated monomers was accomplished using Grubbs' catalyst, which is known to be tolerant to polar functional groups. While the cyclopentadienyliron-coordinated monomers were successfully polymerized using this ruthenium alkylidene catalyst, the molecular weights of the resulting polymers were lower than those obtained when analogous organic monomers were polymerized. The structures of some of these polymers are shown in Figure 1.32.

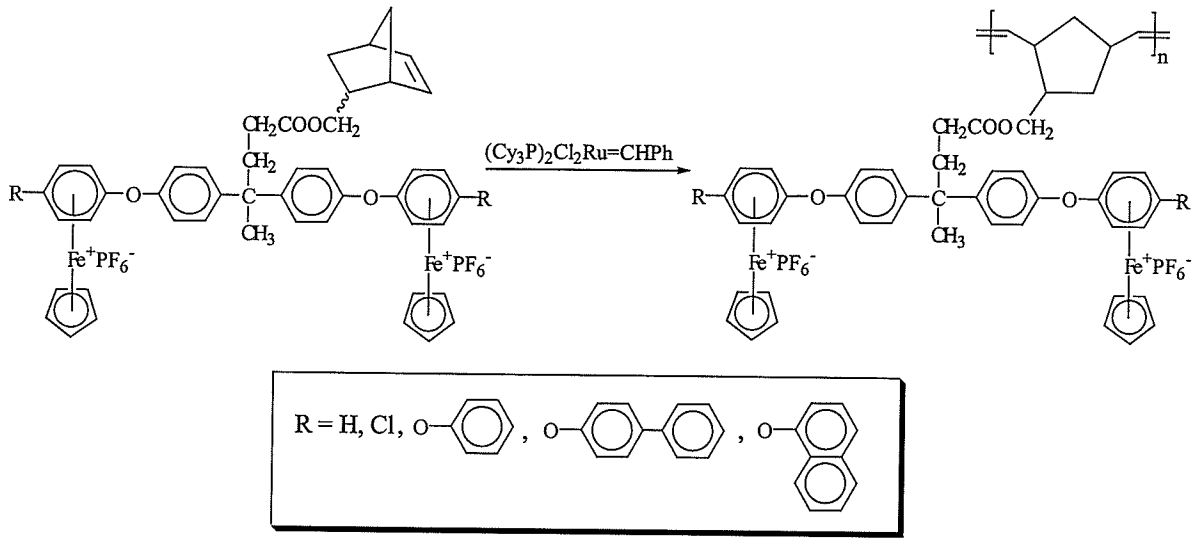

Figure 1.32: Polynorbornenes containing side chains with arenes coordinated to cyclopentadienyliron moieties

In 1991, Allcock and coworkers reported the synthesis of phosphazene monomers and polymers containing arenes coordinated to chromium tricarbonyl moieties.[192,193] Two approaches were taken in the production of the polymers, however, in both cases, the chromium tricarbonyl units were incorporated into the preformed polyphosphazenes.[193] The first, and more effective method involved the displacement of chloro groups of the polyphosphazene by aryloxy or arylalkoxy groups containing the $Cr(CO)_3$ fragment as shown in Figure 1.33. In order to effect complete displacement of the chloro groups by the organometallic nucleophiles, it was found that alkyl spacers were required in order to decrease the steric bulk surrounding the polymer backbone. Complete displacement of the chloro groups was important due to the instability of P-Cl bonds. A number of reactions were also performed in which these polymers were reacted

with organic molecules in order to ensure that all reactions went to completion. The second method utilized to prepare this class of polymer involved the reaction of an aryl-functionalized polyphosphazene with $Cr(CO)_6$. Differential scanning calorimetry showed that the glass transition temperatures of the chromium tricarbonyl functionalized polymers were higher than that of their organic analogues by approximately 50 °C.

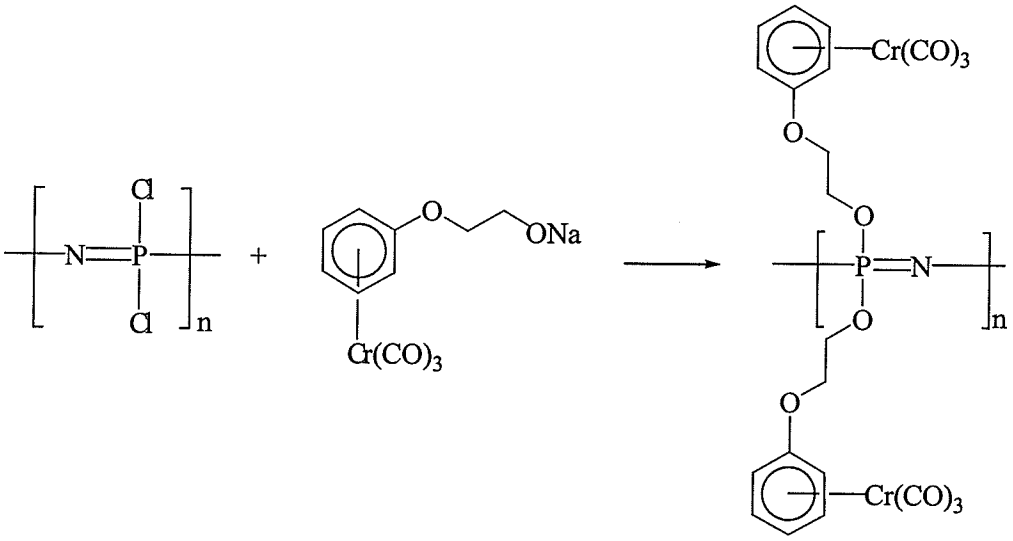

Figure 1.33: Polyphosphazene with side chains containing arenes coordinated to chromium tricarbonyl

1.2.2 Ferrocene-based Polymers

Ferrocene-based polymers have been extensively studied since the first report on the polymerization of vinylferrocene in 1955 by Arimoto and Haven.[194] There have been a number of routes investigated to prepare ferrocene-based polymers. These include step-growth, chain-growth and ring-opening polymerization. Early studies by Korshak and Nesmeyanov reported the synthesis of polyferrocenylenes (Figure 1.34) by reacting ferrocene with *t*-butyl hydroperoxide.[195,196] It was later reported by Neuse that these polymers consisted of homo-and hetero-annularly substituted polymers.[197] Conductive polyferrocenylenes (10^{-2} to 10^{-4} S/cm) were also isolated by reaction of dihaloferrocenes with magnesium.[198-200] The synthesis of poly(mercuriferrocenylene) was reported by Rausch in 1963,[201] and Neuse and Crossland later reported that reaction of this polymer with ferrocene at 245-260 °C allowed for the isolation of polyferrocenylene.[202] The molecular weights and solubilities of the early examples of polyferrocenylenes were quite low,[195-204] however, in 1996, Nishihara and coworkers synthesized a soluble 1,1'-dihexylferrocene based polymer by reaction of the dihexylfulvalene dianion with $[FeCl_2(THF)_2]$.[205] It was determined that the charge transfer complexes of this soluble polymer are p-type semiconductors.

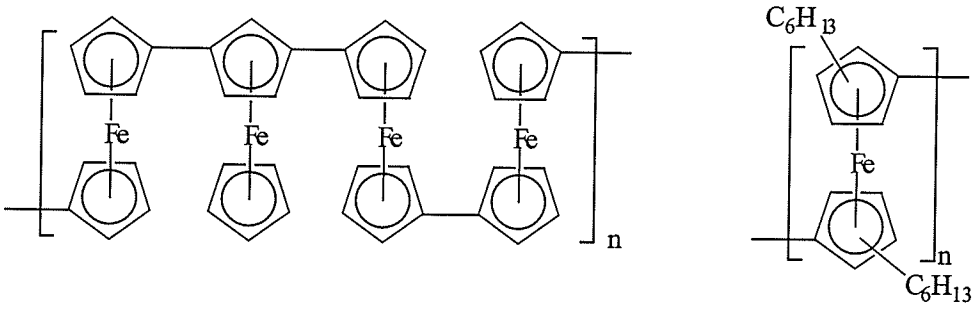

Figure 1.34: Homo- and hetero-annularly substituted poly(ferrocenylene) (left) and a soluble hexyl-substituted derivative (right)

The report by Arimoto and Haven outlining the homo- and co-polymerization of vinylferrocene prompted numerous investigations on the design of vinyl monomers functionalized with ferrocenyl groups. This class of polymer contains the ferrocenyl group as a side chain. Pittman and coworkers have described the synthesis and polymerization of a number of ferrocene based monomers containing acrylate and methacrylate functionalities.[206-215] The incorporation of ferrocene moieties into these classes of polymers resulted in materials with much higher glass transition temperatures than their organic analogues.[212] More recently, the polymerization of methacrylate monomers functionalized with ferrocene groups has resulted in the isolation of novel polymer containing liquid crystalline non-linear optical properties as shown in Figure 1.35.[216-219]

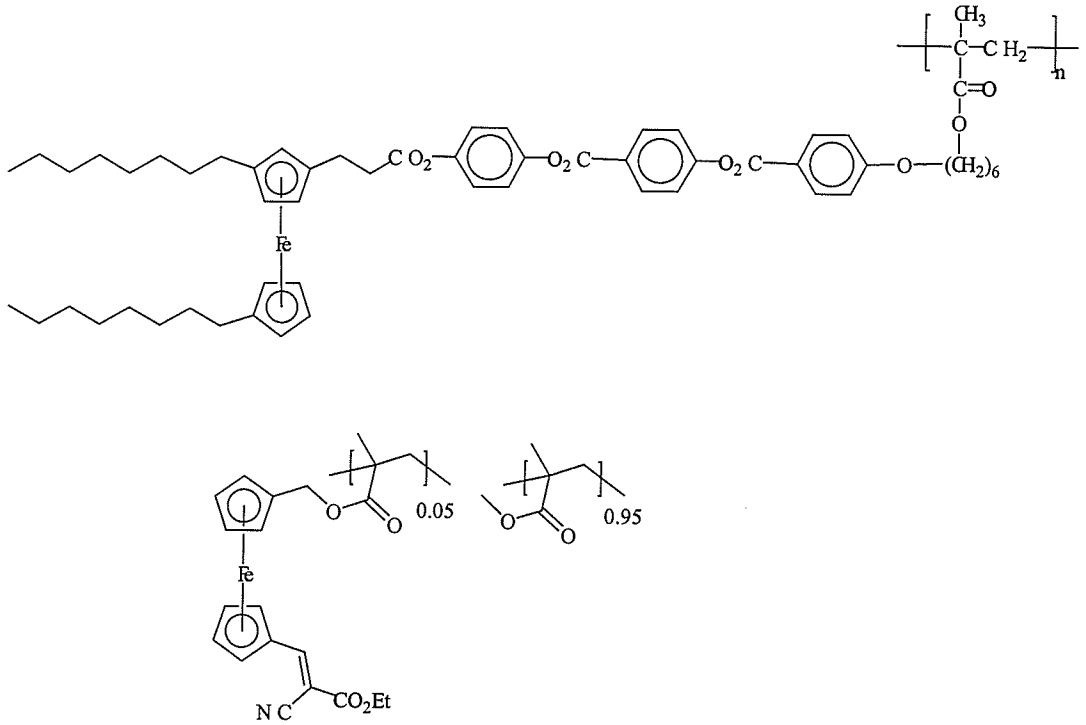

Figure 1.35: Ferrocene-bases polymers with liquid crystalline (top) and non-linear optical properties (bottom)

Polymers prepared via reaction of ferrocenes functionalized with carboxylic acids, acid chlorides, alcohols, amines and other functional groups have been utilized to synthesize condensation polymers containing ferrocenyl units in their backbones.[150,220-230] There is tremendous interest in this class of polymer due to the ease with which ferrocene derivatives can be prepared. Cuadrado has reported the synthesis of a polymer that was utilized to produce chemically modified electrodes as shown in Figure 1.36.[230]

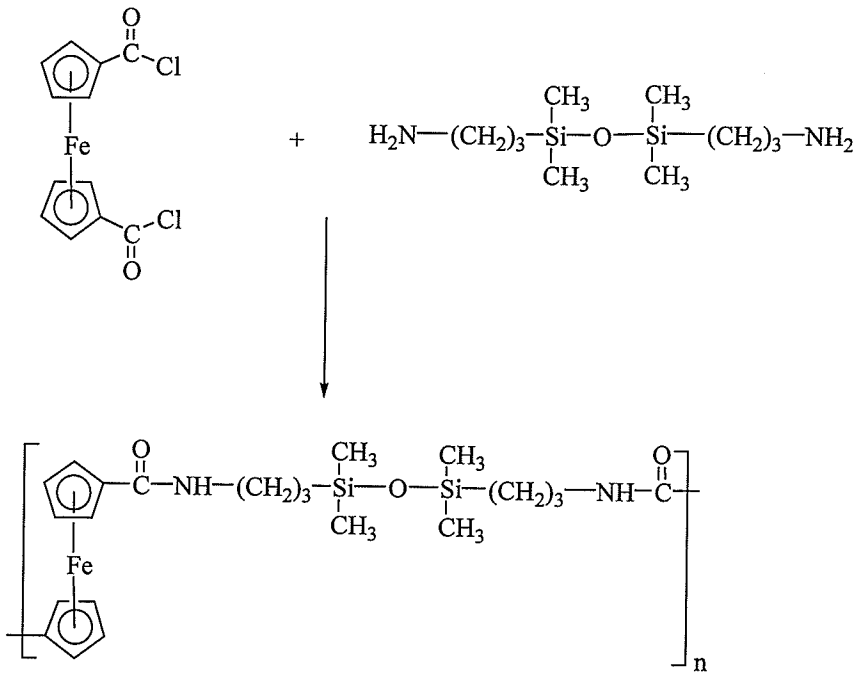

Figure 1.36: Polycondensation of ferrocene derivatives

Despite the successes that were obtained from the polycondensation of ferrocene derivatives, there were a few problems associated with these materials. They often possessed poor solubility, and their molecular weights were not usually very high. The new focus of research on polymers containing ferrocenyl units in their backbones is on

the ring-opening polymerization of ferrocenophanes. The synthesis and properties of poly(ferrocenylsilanes) have been extensively reviewed by Manners.[150,151,156] Thermal, anionic and transition metal catalyzed ring-opening polymerization (ROP) of [1]silaferrocenophanes has led to the production of polymers containing a variety of functional groups attached to the silicon atoms.[231-237] The anionic polymerization of a silicon-bridged [1]ferrocenophane has been found to lead to the preparation of living polymers which could be copolymerized with a number of different monomers.[238-245] Ferrocenophanes containing phosphorus,[246-251] tin,[252,253] germanium[254] and boron[255] bridges have also been polymerized. One interesting example reported by Manners was the copolymerization of a [1]chromarenophane with a [1]ferrocenophane by thermal ring-opening polymerization as shown in Figure 1.37.[256]

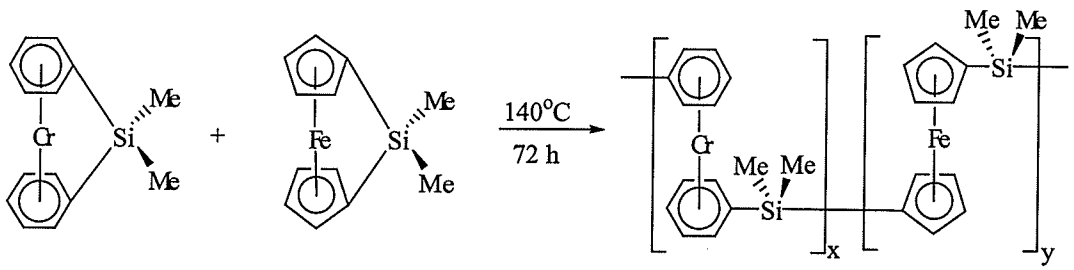

Figure 1.37: Copolymer containing chromium and iron groups in the polymer backbone

Rauchfuss has also reported the ring-opening and desulfurization of [3]-trithiaferrocenenes, which allowed for the preparation of ferrocene-based polymers containing disulfide linkages.[257-259] The ring-opening polymerization of [1]thia- and [1]selenaferrocenophanes has been accomplished thermally and in the presence of

of two reversible oxidation processes and it was found that these polymers possessed stronger Fe-Fe interactions than the analogous silicon-bridged materials.

Ring-opening metathesis polymerization (ROMP) of ferrocenophanes containing bridging olefinic groups has been examined in order to synthesize conjugated ferrocene-based polymers.[261-263] Lee and coworkers reported that the solubility of this class of polymer could be enhanced by incorporating substituents onto the bridging carbon chains.[263] Figure 1.38 shows the ROMP of the ferrocene-based monomer using a tungsten catalyst to produce a high molecular weight conjugated polymer.

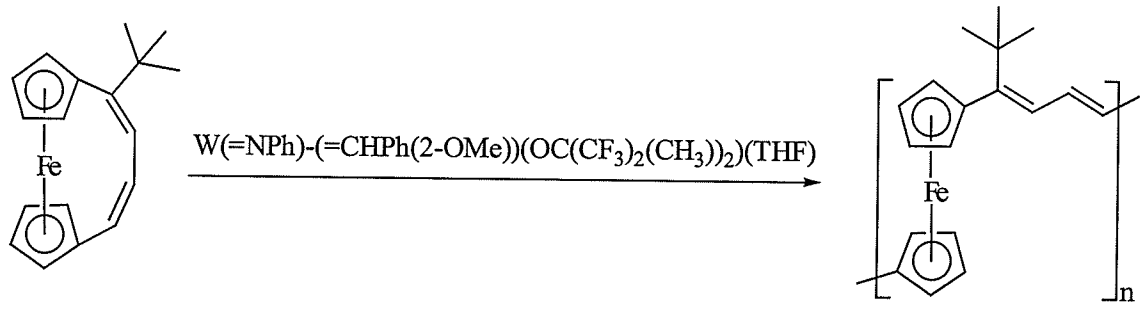

Figure 1.38: Ring-opening metathesis polymerization of a ferrocene monomer

1.3 Organometallic Star Polymers and Dendrimers

Organometallic star polymers and dendrimers have been the focus of numerous investigations in recent years.[264-274] The production of highly ordered, highly branched organometallic materials is of importance due to the catalytic, electronic, optical and biomedical applications that these materials find. Star polymers are macromolecules that have a multifunctional core but are not highly branched materials, while dendrimers are highly branched polymers with well-defined structures. Hyperbranched polymers are highly branched materials that possess properties and structural features similar to those of dendrimers, however, they are not as perfectly shaped. Astruc has reviewed the different applications that star polymers and dendrimers have found.[267] Due to the steric bulk found at the periphery of dendrimers, these molecules are highly suited for molecular recognition and sensing, while star polymers, are more suited for catalysis due to the low steric congestion at the polymeric periphery. Figures 1.39 and 1.40 show the structures of two ferrocene-functionalized polymers. The polymer in Figure 1.39 is more star-shaped than dendritic, while the polymer in Figure 1.40 is a dendrimer with 32 peripheral ferrocenyl moieties.[275,276]

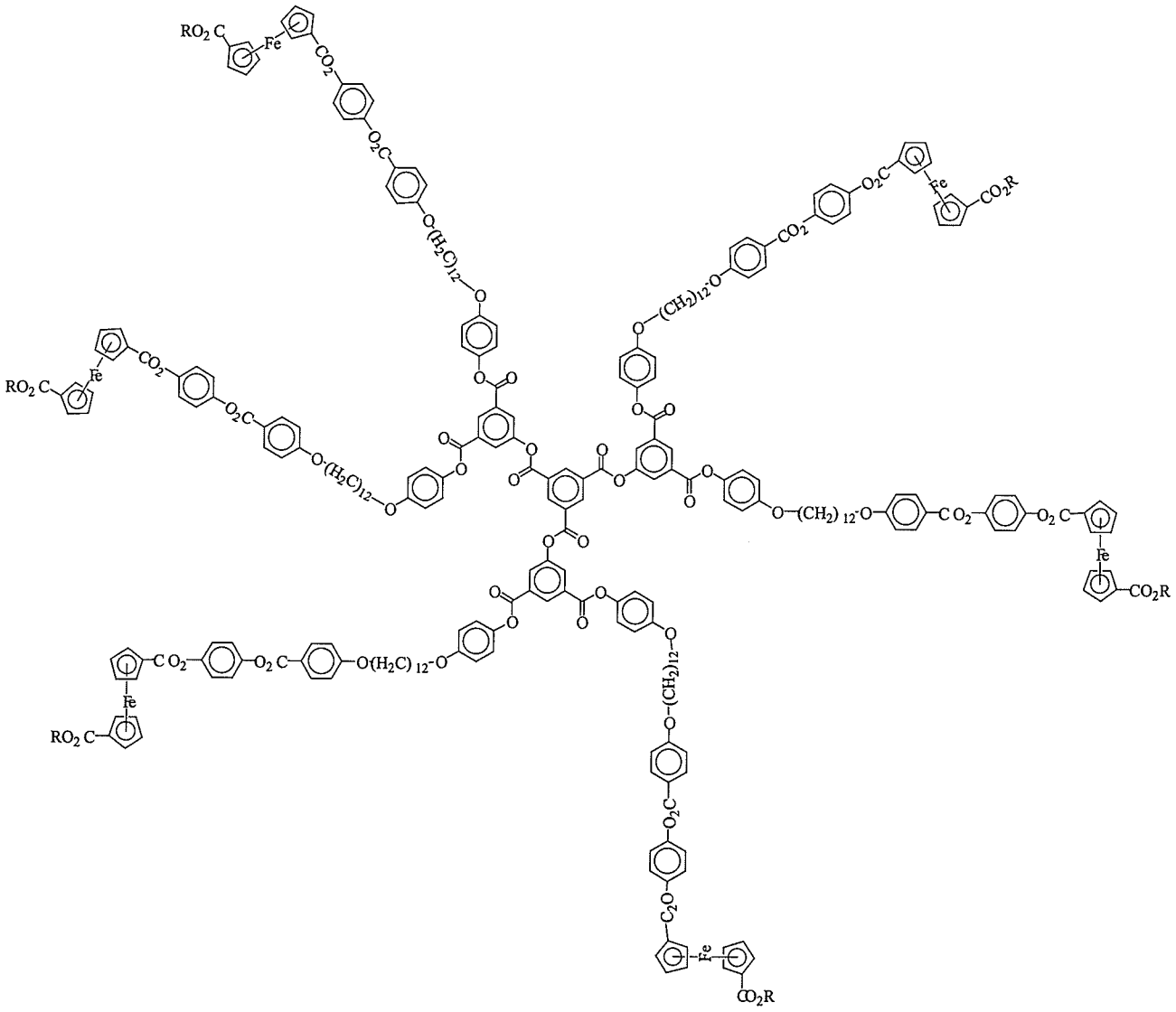

Figure 1.39: Structure of a star-shaped organometallic polymer[275]

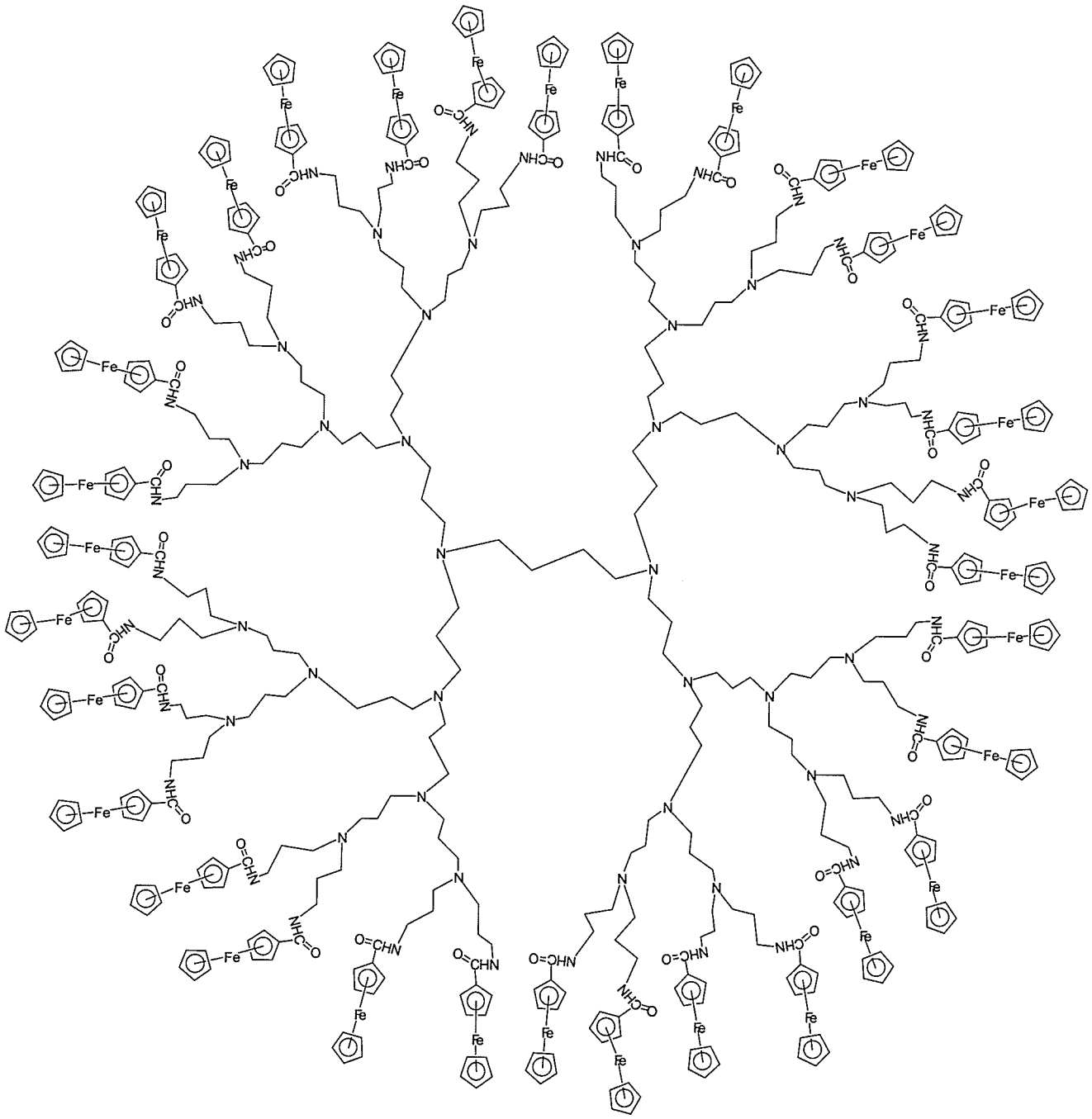

Figure 1.40: Structure of an organometallic dendrimer[276]

1.3.1 Transition Metal Coordinated Arenes in the Design of Star Polymers and Dendrimers

An efficient method for the design of star polymer and dendrimer cores was developed by Astruc using cyclopentadienyliron-mediated peralkylation, benzylation and allylation reactions of cationic tri-, tetra- and hexa-methylbenzene cyclopentadienyliron complexes.[91-100] Demetallation, followed by oxidation of an allyl-functionalized mesitylene complex gave rise to a branched compound containing nine terminal hydroxyl groups.[98] This compound was then reacted with nine equivalents of η^6-*p*-fluorotoluene-η^5-cyclopentadienyliron hexafluorophosphate to yield the nonairon complex shown in Figure 1.41. Cyclic voltammetry of this complex showed that the cationic organometallic dendrimer underwent nine reversible quasi-equivalent reduction processes at –1.37 V vs. SCE.

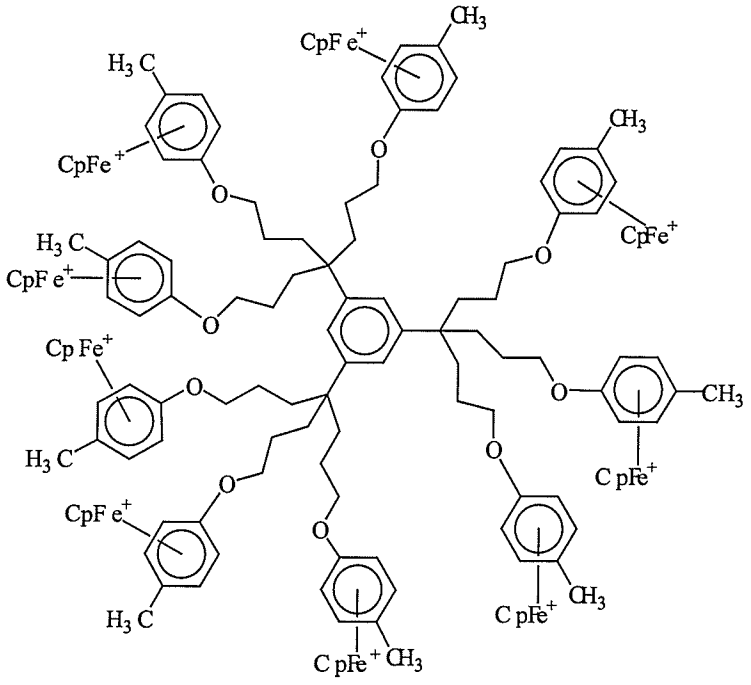

Figure 1.41: Dendrimer with nine peripheral cyclopentadienyliron moieties

The synthesis of a water-soluble organometallic complex containing six peripheral cationic cyclopentadienyliron moieties has also been reported by Astruc.[277] In contrast to most studies of arene cyclopentadienyliron complexes, the functionalization of these materials was accomplished via the Cp rings rather than the arene rings. This star-shaped organoiron complex was studied as a redox catalyst for the cathodic reduction of nitrates and nitrites to ammonia (Figure 1.42).[277]

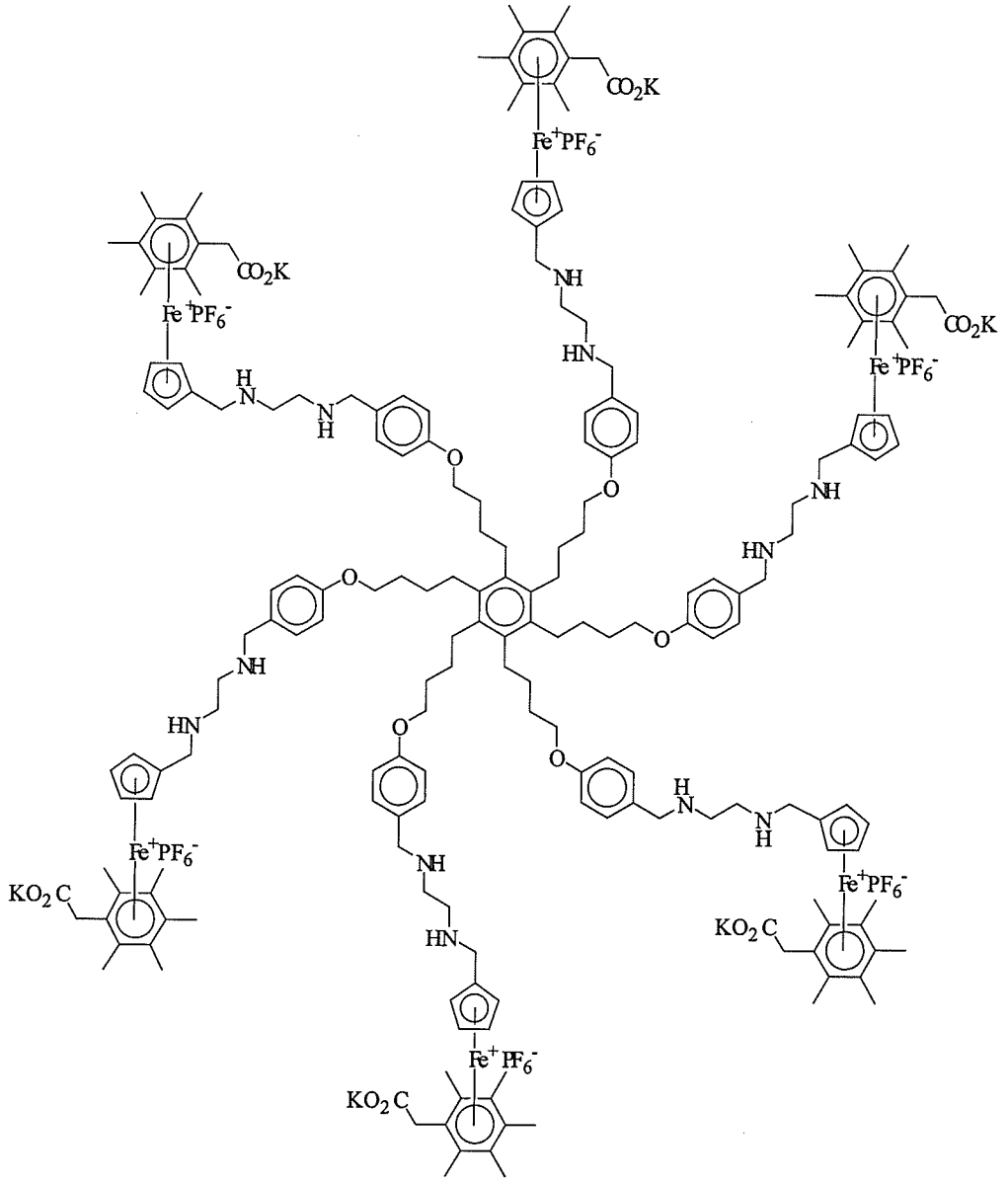

Figure 1.42: Water-soluble star-shaped polymer

Tilley and coworkers have reported the synthesis of organosilane dendrimers that were reacted with a ruthenium complex to produce organometallic dendrimers with 12, 24, 36 and 72 pentamethylcyclopentadienylruthenium cations.[278] These polycationic dendrimers were designed to be combined with polyanions to form superlattices. Figure 1.43 shows the synthesis of the dendrimer coordinated to 72 positively charged ruthenium. Mass spectrometry of this highly branched complex indicated that although the desired complex was present in the sample, incomplete coordination of the aromatic rings was observed due to steric crowding.

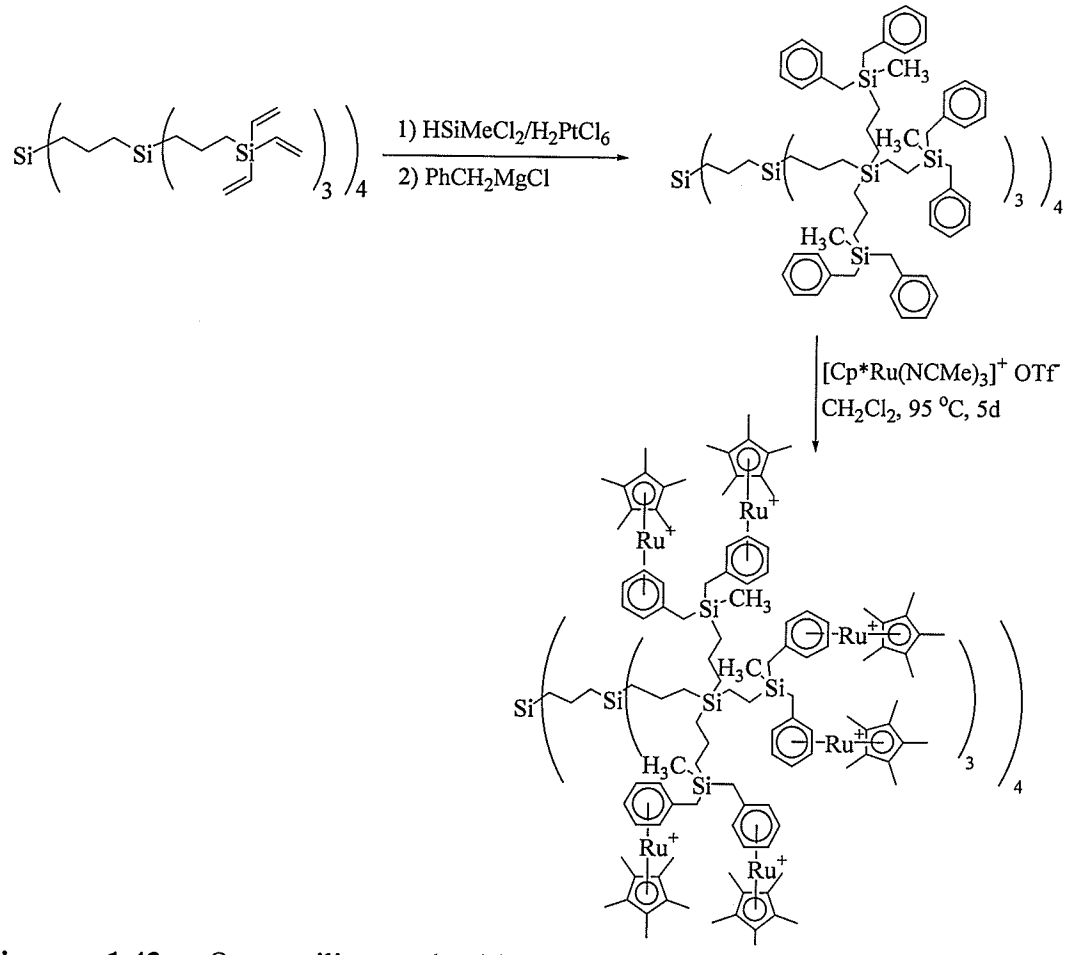

Figure 1.43: Organosilicon dendrimer functionalized with 72 pentamethyl-cyclopentadienylruthenium complexes

Cuadrado and coworkers have described the synthesis of low generation organosilicon dendrimers containing arenes coordinated to chromium tricarbonyl moieties.[279,280] These organosilicon dendrimers were reacted with a chromium complex to produce the dendrimer shown in Figure 1.44.[279] Although there were eight possible sites where coordination of the $Cr(CO)_3$ moieties could have occurred, the harsh conditions required to coordinate the other four aromatic rings resulted in decomposition of the dendrimers. Cyclic voltammetry of these materials showed that oxidation of the chromium atoms occurred reversibly in the absence of nucleophilic species, and that the chromium tricarbonyl units behaved as isolated redox centers.

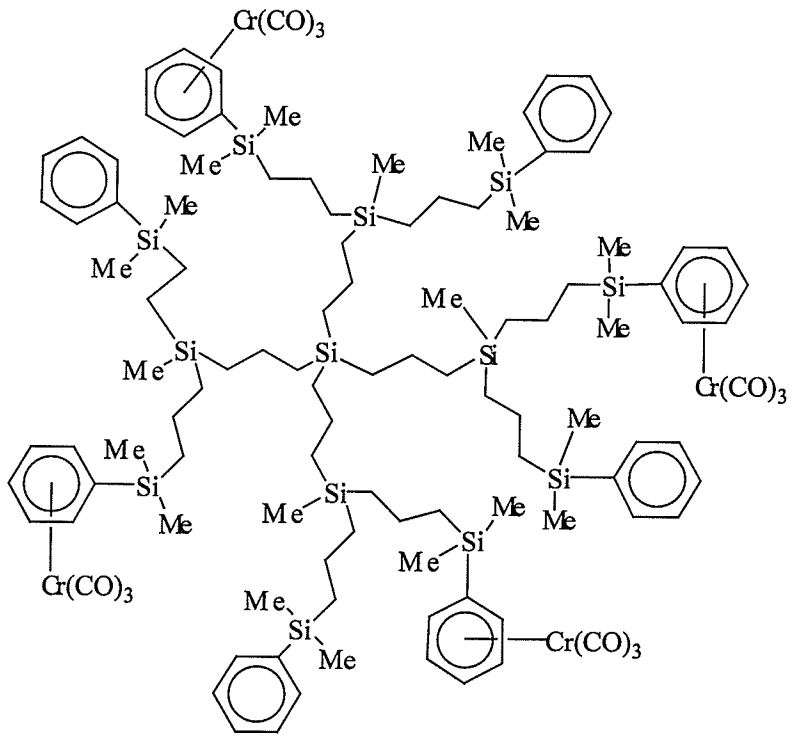

Figure 1.44: Organosilicon dendrimer functionalized with chromium tricarbonyl moieties

1.4 Polyaromatic Ethers and Thioethers

Polyaromatic ethers and thioethers are two classes of polymers that have generated a great deal of interest due to their high performance properties.[281-287] These include excellent thermal and chemical stabilities which makes these materials suitable for high temperature applications. Aromatic polymers are being designed to replace metal parts, which would result in lower weight and lower cost materials.[284] In addition, a high temperature polymer must possess good physical properties related to its mechanical strength and modulus, as well as dimensional stability at high temperatures. Rigid polymers, particularly aromatic polymers, are desirable for high temperature applications since they possess high bond strengths, and the introduction of heteroatoms and other carbon chains between the aromatic rings lowers their thermal stability. Aromatic polymers are termed stiff polymers because their rigidity reduces their tendency to deform and soften upon heating.[284-286] By introducing cross-linking and ensuring that the polymers are high molecular weight, their rigidity, and therefore, their thermal stability should be further enhanced. Polymers with secondary attractive forces increase thermal stability by inducing interactions between polymer chains, while branching reduces thermal stability by preventing the polymer chains from stacking. Although it is desirable to maximize the rigidity of a polymer in order to enhance its thermal stability, the more rigid the polymer, the more difficult it is to synthesize and process. Polyaromatic ethers and thioethers possess excellent resistance to organic and aqueous solvents, acids and bases. Polyaromatic thioethers display excellent fire retardant properties but are more susceptible to oxidation than polyaromatic ethers.[283,284]

1.4.1 Synthesis of Polyaromatic Ethers

There are many routes available for the synthesis of polyaromatic ethers. While many of these methodologies involve the reaction of monomers containing aryl ether linkages, there are only a few routes that allow for the direct formation of an aryl ether bond. The most commonly utilized method is via nucleophilic aromatic substitution (S_NAr). Polyetherketones and polyethersulfones are the most common classes of polymers prepared via S_NAr reactions.[281-286,288-305] These polymers are generally prepared by reaction of bisphenolate salts with aromatic dihalides containing a sulfonyl or carbonyl group in the *para* position. The reason why these monomers are utilized is that the sulfonyl and carbonyl groups are electron-withdrawing and therefore facilitate the displacement of the halogens. These reactions are performed in polar aprotic solvents, which increase the nucleophilicity of the phenoxide anion by preferentially solvating cations. These reactions are generally carried out at high temperature (>160 °C) to increase the solubility of the bisphenolate and the polymer as it is forming. Dry solvents are required to obtain high molecular weight polymers. Phase transfer catalysts have also been used to help promote the generation of high molecular weight polymers.[305] These catalysts are especially important when using the less reactive chloroarenes rather than the more reactive fluoro derivatives. Phase transfer catalysts increase the nucleophilicity and the solubility of the phenolate, thereby allowing higher molecular weight species to be generated. Polyether ketones have been rated for continuous use at temperatures between 150 and 200 °C, while polyether sulfones have been rated for continuous service between 240 and 280 °C.[284] Figure 1.45 shows the synthesis of polyether ketones via nucleophilic aromatic substitution.[300]

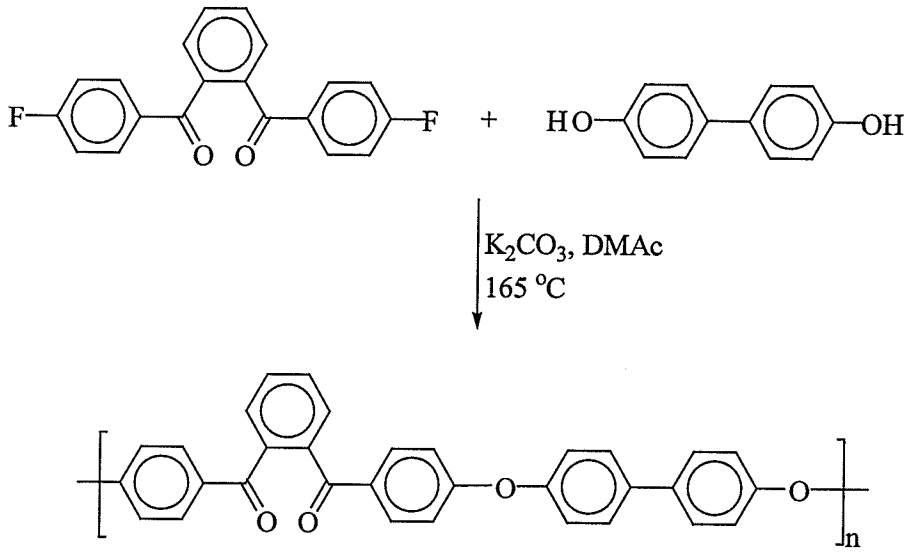

Figure 1.45: Polyaromatic ethers via nucleophilic aromatic substitution

The commercial production of poly(*p*-phenylene oxide) (PPO) is achieved by oxidative coupling of 2,6-disubstituted phenols as shown in Figure 1.46.[283,284] This reaction involves bubbling oxygen through a solution of the phenol containing a catalyst generated from the reaction of a cuprous salt with an amine. When the substituents are small, polymerization proceeds rapidly at temperatures ranging from 25 to 50 °C, however, bulky substituents result in the formation of dimers. PPO (R = CH_3) has a very high melt viscosity which impedes its commercial use, however, there are a number of polymer blends that incorporate this polymer.

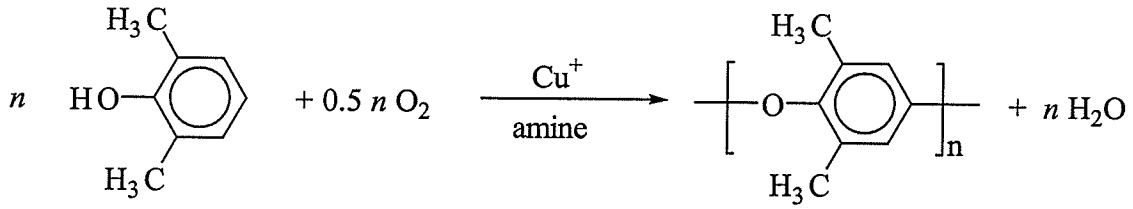

Figure 1.46: Polyaromatic ethers via oxidative coupling

Another method that has been utilized to synthesize aryl ether bonds is the Ullmann condensation reaction.[306-310] This is a copper-catalyzed reaction between aromatic halides and alkali metal phenoxides. The drawbacks to this reaction include harsh reaction conditions, low yields, and side products. These reactions have not been widely used in polymer synthesis.[310]

There are also a number of indirect routes to producing polyaromatic ethers. These reactions include electrophilic aromatic substitution, metal-catalyzed coupling reactions and ring-opening of cyclic aryl ethers. Electrophilic aromatic substitution of diphenyl ethers allows for the synthesis of poly(aryl ethers) that incorporate sulfonyl or carbonyl groups into the backbone of polymeric chains through a Friedel-Crafts mechanism.[288,311-313] The disadvantage to this methodology is the number of substitution patterns that can take place. In a study by Cudby and coworkers, it was found that either *para* or a mixture of *ortho* and *para* substituted polymers were isolated.[311] These reactions are shown in Figure 1.47 where the reaction on the bottom gives about 20 % of the *ortho* product.

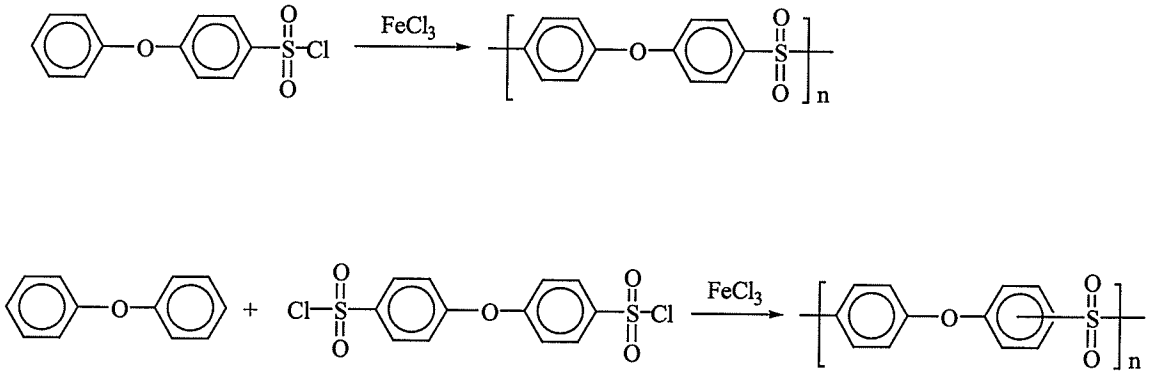

Figure 1.47: Electrophilic aromatic substitution

Another route to the synthesis of poly(aryl ethers) is through coupling reactions catalyzed by metal salts.[129,314-323] These reactions proceed with monomers that contain aryl ether linkages already present in their structures. The palladium-catalyzed cross-coupling of an aromatic diacid chloride with a bis(trimethylstannane) monomer is shown in Figure 1.48.[315]

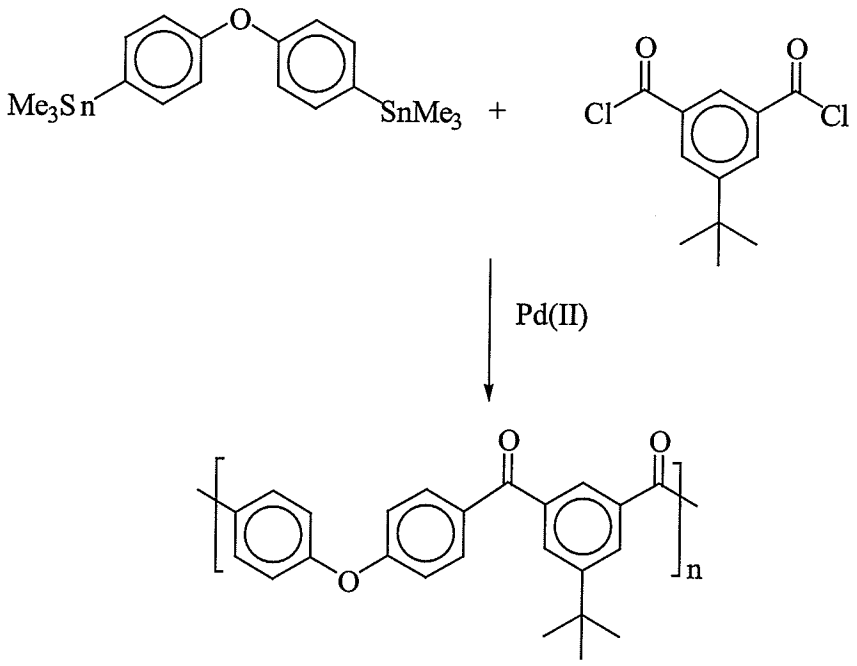

Figure 1.48: Palladium-catalyzed cross-coupling reaction

A newer development in the synthesis of high molecular weight polyaromatic ethers is via ring-opening polymerization of cyclic aryl ethers.[324-326] The macrocylic monomers are heated in the presence of a base to produce the ring-opened polyaromatic ethers.

1.4.2 Synthesis of Polyaromatic Thioethers

The synthesis of polyphenylene sulfide (PPS) has been examined using a number of different approaches.[283,284,287,327-341] The first report on the synthesis of this polymer was in 1897 by the reaction of benzene with sulfur in the presence of aluminum chloride.[327] Commercial preparation of this polymer is via reaction of 1,4-dichlorobenzene with sodium sulfide in a polar solvent such as 1-methyl-2-pyrrolidone (NMP) as shown in Figure 1.49.[283,284,287] This reaction requires temperatures of about 250 °C and 160 psi to obtain high molecular weights. It is believed that this reaction does not proceed via a simple nucleophilic aromatic substitution mechanism, however, the exact mechanism is not fully understood. Polyphenylene sulfide is approximately 60-65 % crystalline and has been rated for continuous service between 200 and 240 °C.[284] This polymer is easily processed into films and fibers. When this polymer is heated between 315 and 425 °C, oxidation of the sulfur, cross-linking and other reactions occur.[283,287]

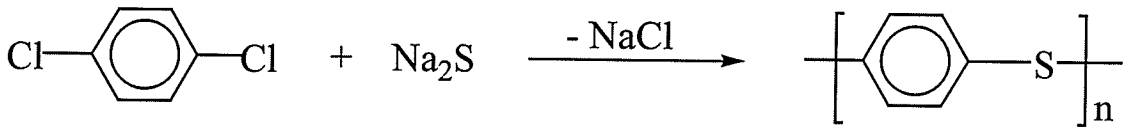

Figure 1.49: Synthesis of polyphenylene sulfide

Polyphenylene sulfide becomes a conductive polymer upon oxidation with AsF_5, SbF_5 and SO_3.[284,287] This polymer has advantages over other organic conductive polymers because it can be melt processed, while polymers such as polyacetylene, polypyrrole and poly(*p*-phenylene) are infusible and intractable.[287] It is believed that the

conductivity arises from the conjugated resonance form of the polymer. The conductivity of doped *p*-PPS has been measured to be 2.7 S/cm, while a *m*-substituted polymer does not exhibit the same capability of electron delocalization and its conductivity is therefore lower (0.08 S/cm).[287] The sulfur p-orbitals overlap with the aromatic π-orbitals which contributes to the electron delocalization in doped PPS.[287] It has also been reported that the AsF_5 actually forms bonds with the carbon atoms *ortho* to the sulfide linkages.[284] There is evidence that this doped polyphenylene sulfide eventually forms a polybenzothiophene type structure.[287]

There have been a number of new synthetic methodologies developed in the past ten years that have allowed for a more controlled and facile synthesis of polyphenylene sulfide.[334-336] The use of disulfide monomers or catalysts has allowed for the production of high molecular weight polyphenylene sulfide. The reaction developed by Wang and Hay is shown in Figure 1.50.[334] The use of temperatures of up to 270 °C are required to obtain high molecular weight materials. 4-Bromobenzenethiol could also be polymerized thermally with the addition of a disulfide monomer to promote free radical initiation.[336]

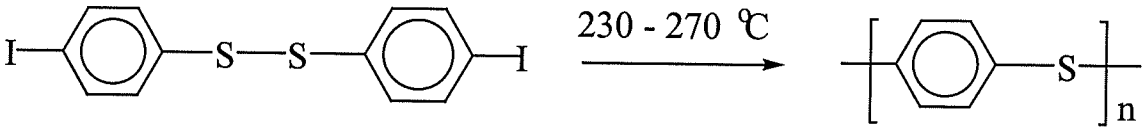

Figure 1.50: Synthesis of polyphenylene sulfide using a disulfide monomer

In 1996, Hay reported the ring-opening polymerization of cyclic disulfide monomers to produce polyphenylene sulfides.[339] The disulfide monomers were reacted with 1,4-diiodo- or 1,4-dibromobenzene in phenyl ether at 270 °C for ten hours under a nitrogen atmosphere. Cyclic phenylene sulfide monomers with 1,4- and 1,3-linkages were also polymerized in the presence of 1 mol % sulfur at 300 °C for thirty minutes to produce the corresponding polyphenylene sulfides via a free radical mechanism.[340] The *meta* substituted polymer possessed good solubility, while the *para* derivative was insoluble. The synthesis of a cyclic monomer and its ring-opening polymerization is shown in Figure 1.51.[341]

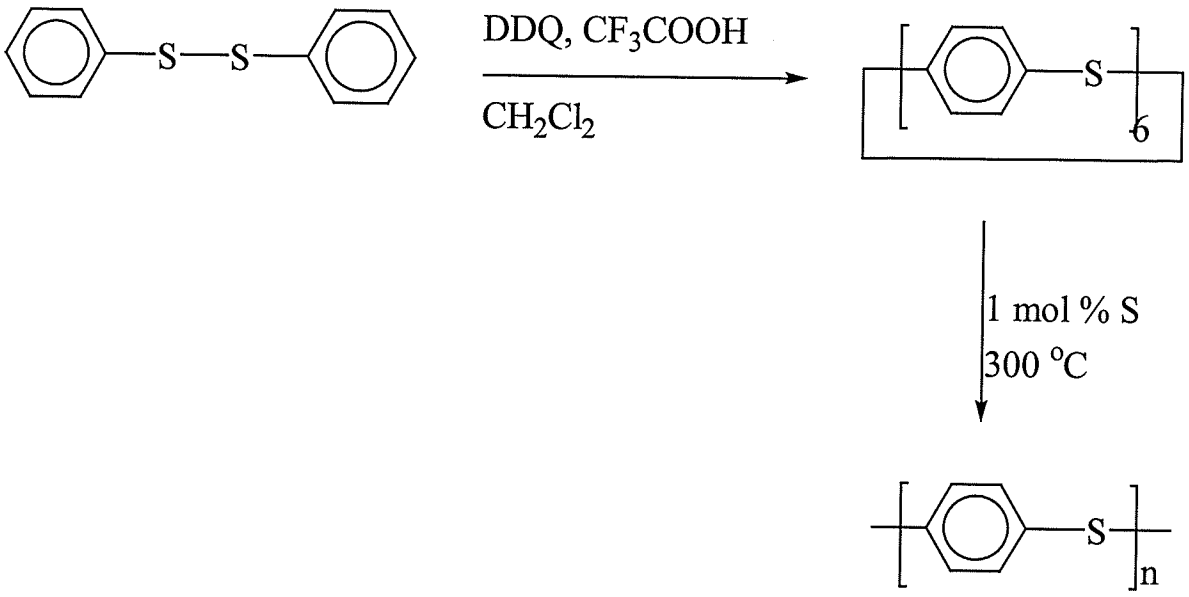

Figure 1.51: Ring-opening polymerization of cyclic sulfide monomers

1.4.3 Synthesis of Polyaromatic Ether-Thioethers

There have also been many reports on the synthesis of polymers containing aromatic ether and thioether linkages.[339-346] Interest in these materials stems from the properties that arise from combining aryl ether and thioether spacers together in the same polymer. These polymers are generally prepared using the same methodologies applied to the synthesis of the polyaromatic ethers and thioethers already described. There has been increasing interest in the design of this class of material. A very common method used in the production of these materials is via ring-opening polymerization.[339-343] This can be achieved via ring-opening of a cyclic monomer containing ether and thioether linkages, or via copolymerization of a monomer containing thioether linkages with an aryl ether monomer. Figure 1.52 shows the synthesis of high molecular weight polymers which was accomplished in the melt with a catalytic amount of 2,2'-dithiobis(benzothiazole) (DTB) disulfide.[342,343]

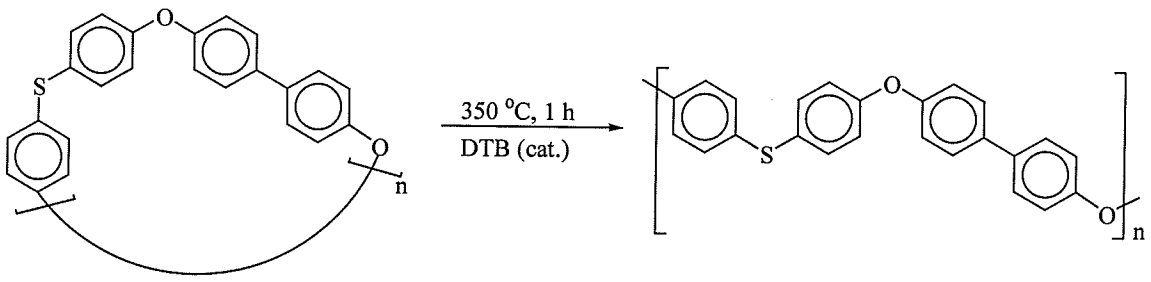

Figure 1.52: Synthesis of polymers with aromatic ether and thioether spacers

2.0 Synthesis of Polyaromatic Ethers, Thioethers and Amines Coordinated to Cationic Cyclopentadienyliron Moieties

2.1 Introduction

Over the past few decades, there has been tremendous interest in the production of thermally stable polymers as replacements for metals and ceramics in the aerospace and automotive industries.[281-287] Polyaromatic ethers and thioethers are two classes of thermally stable polymers that are able to withstand temperatures in excess of 200 °C and exhibit excellent resistance to acids, bases, and organic solvents. The limited solubilities of these classes of polymers in organic solvents at room temperature, and their high melting points decreases their processability.

There are a limited number of methodological approaches to the synthesis of polyaromatic ethers and thioethers, and many of these routes limit the molecular weights that are obtained due to the low solubility of these classes of polymer.[281-287] Electrophilic aromatic sulfonylation or acylation reactions, metal-catalyzed coupling reactions, and nucleophilic aromatic substitution are the most widely used routes used to prepare these materials. Of these methodologies, the most common synthetic route that allows for the direct incorporation of an etheric or thioetheric bond into the backbone of a polymer chain is nucleophilic aromatic substitution.[288-305]

It has been demonstrated that nucleophilic aromatic substitution of haloarenes complexed to transition metal moieties with oxygen-, sulfur-, and nitrogen-containing nucleophiles allows for the synthesis of a wide variety of aryl ethers, thioethers, and amines.[101-115] These metal-mediated reactions proceed under very mild conditions and allow for the incorporation of a number of different functional groups. Nucleophilic

substitution reactions of chloroarenes complexed to the cyclopentadienyliron moiety have been the focus of many studies directed towards the design of functionalized monomers.[129-135]

There have been only a few reports on the synthesis of polymers containing transition metal moieties π-coordinated to phenylene units in the polymer backbones. The metallic groups have included chromium tricarbonyl,[164-170,178,181,182] molybdenum tricarbonyl,[176-179] manganese tricarbonyl,[183,184] cyclopentadienyliron,[106,171,173,180] cyclopentadienylruthenium[172] and pentamethylcyclopentadienylruthenium.[173-175] These organometallic polymers have exhibited interesting electrochemical and liquid crystalline properties. A number of studies have indicated that the incorporation of metallic moieties pendent to polymeric materials resulted in enhanced solubilities of the organometallic polymers.[164-166,172-175] Various approaches to the synthesis of this class of polymer have been used; one approach involves the coordination of a metallic moiety to an organic polymer via a ligand exchange reaction.[176-180] This methodology has been utilized in the production of polymers with $Cr(CO)_3$, $Mo(CO)_3$ and $CpFe^+$ moieties pendent to aromatic rings in the polymer backbone. Another method that has been implemented in the synthesis of η^6-complexed organometallic polymers involves polycondensation reactions of π-coordinated organometallic monomers.[164-171] The supramolecular assembly of arene complexes has also recently been decribed.[181-184] The final approach is via nucleophilc aromatic substitution reactions mediated by the transition metal moiety. This work describes the synthesis and characterization of polyaromatic ethers, thioethers and copolymers containing ether/thioether and amine/thioether bridges coordinated to cyclopentadienyliron cations via nucleophilic aromatic substitution reactions.

2.2 Results and Discussion

2.2.1 Synthesis of Polyaromatic Ethers

2.2.1.1 Synthesis of Polyaromatic Ethers Coordinated to Cationic Cyclopentadienyliron Moieties

It is well known that the type of aromatic linkages incorporated into polyaromatic ethers has a strong influence on the thermal and physical properties of these materials. Therefore, it was desired to include a wide range of aromatic spacers into the polymers under investigation in this study. The organoiron polymers shown in Scheme 2.1 were prepared by the reaction of *p*-dichlorobenzene complex (**2.1**) with a number of compounds containing terminal phenolic groups (**2.2-2.9**). These reactions allowed for the formation of polyaromatic ethers containing pendent cyclopentadienyliron moieties (**2.10-2.17**) in yields ranging from 89-99%. Traditionally, this class of polymer is synthesized at high temperatures and in the presence of strong electron-withdrawing groups. However, the presence of the electron-withdrawing cyclopentadienyliron moiety pendent to the dichloroarene allowed these polymerization reactions to occur at 60 °C over a period of 6 to 12 hours. In addition, it was not necessary to distill the DMF prior to reaction or to use a mixed solvent system. The ability to prepare polyaromatic ethers at moderate temperatures makes the cyclopentadienyliron-mediated methodology quite valuable.

All of the organoiron polymers were soluble in polar aprotic solvents such as DMAc, DMF and DMSO and had varying degrees of solubility in solvents such as acetone, dichloromethane and acetonitrile. The solubilities of all the organoiron-coordinated polyethers can be found in Table 2.1. Polymer **2.12**, with pendent carboxylic

acid groups was also soluble in a water solution containing sodium hydroxide. The polymers with alkyl functionalities (**2.12-2.17**) were synthesized to determine the effect of these groups on the solubility of the organoiron and their corresponding organic polymers. These alkyl-functionalized polymers displayed much higher solubility than the unalkylated polymers. It is known that the inherent poor solubility of rigid aromatic molecules, even at low molecular weights, decreases the ability to prepare these types of polymers.[281-286] However, this insolubility makes polyaromatic ethers valuable for certain applications where these materials need to maintain their chemical resistance over long periods of time.

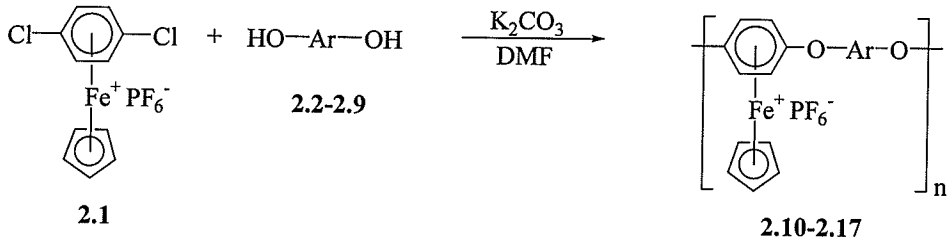

2.1 **2.2-2.9** **2.10-2.17**

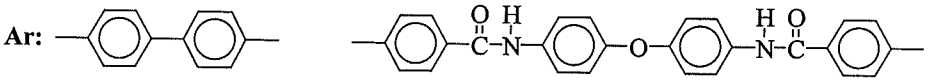

2.2 **2.3**

2.4

2.5

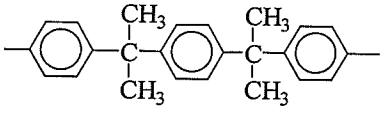

2.6

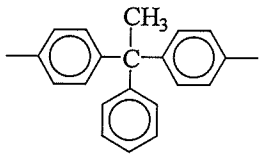

2.7

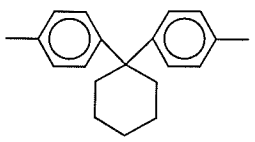

2.8

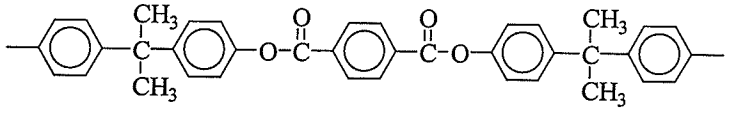

2.9

Scheme 2.1

Table 2.1: Solubility of Organoiron Polymers[a]

	Solvent					
Polymer	**CH_2Cl_2**	**Acetone**	**CH_3CN**	**DMAc**	**DMF**	**DMSO**
2.10	I	I	PS	PS	PS	PS
2.11	I	I	I	S	S	S
2.12	I	PS	PS	PS	S	S
2.13	PS	S	S	S	S	S
2.14	PS	S	S	S	S	S
2.15	I	I	PS	S	S	S
2.16	I	PS	PS	S	S	S
2.17	I	I	PS	S	PS	S

[a]Solubility at room temperature: (S), soluble; (PS), partially soluble; (I), insoluble.

It was also of interest to incorporate amide and ester linkages into these polymers in order to examine the influence of these functional groups on the thermal properties of the polymers. Nucleophiles **2.3** and **2.9** were synthesized by condensation reactions, and their analytical and spectroscopic data are given in Tables 2.2 and 2.3. Table 2.2 provides the % yield, melting point ranges and ^{1}H NMR analysis of compounds **2.3** and **2.9**, while Table 2.3 provides their CH, IR and ^{13}C NMR analysis. It is important to note that the ^{1}H NMR analysis of **2.3** shows the presence of OH and NH peaks at 10.04 and 10.16 ppm, respectively, while the spectrum of **2.4** shows an OH resonance at 9.21 ppm. Following polymerization, these OH peaks were no longer observed in polymers **2.11** and **2.17**.

Table 2.2: % Yield, Melting Point and ^{1}H NMR Analysis of Dinucleophiles **2b, 2h** in DMSO-d_6

Compound	% Yield	m.p. (°C)	Other	Ar
2.3	92	263-265	10.04 (s, 1H, OH), 10.16 (s, 1H, NH)	6.87 (d, *J*=8.67 Hz, 2H), 7.00 (d, *J*=8.91 Hz, 2H), 7.76 (d, *J*=8.99 Hz, 2H), 7.86 (d, *J*=8.71 Hz, 2H)
2.9	65	199-201	1.61 (s, 6H, CH_3), 9.21 (s, 1H, OH)	6.67 (d, *J*=8.22 Hz, 2H), 7.04 (d, *J*=7.98 Hz, 2H), 7.20 (d, *J*=8.51 Hz, 2H), 7.29 (d, *J*=8.14 Hz, 2H), 8.30 (s, 2H)

Table 2.3: CH, IR and ^{13}C NMR Analysis of Dinucleophiles **2b, 2h** in DMSO-d_6

Compound	CH analysis	IR (cm^{-1})	Other	Complexed Ar
2.3	$C_{26}H_{20}N_2O_5$: Found: C, 70.72; H, 4.67, N, 6.22. Calculated: C, 70.90; H, 4.58; N, 6.36	1642 (CO), 3317 (NH)	165.02 (CO)	114.98, 118.59, 122.03, 125.45*, 129.73, 135.02*, 152.71*, 160.58*
2.9	$C_{38}H_{34}O_6$: Found: C, 78.01; H, 5.79. Calculated: C, 77.80; H, 5.84	1738 (CO)	30.74 (CH_3), 40.38 (C), 162.10 (CO)	114.81, 121.16, 127.46, 127.67, 130.28, 133.52*, 140.29*, 148.16*, 148.86*, 155.26*

*Denotes quaternary carbons

^{1}H and ^{13}C NMR analysis of the cyclopentadienyliron-coordinated polyaromatic ethers was a very useful technique to determine the success of the polymerization reactions. The ^{1}H NMR spectrum of the *p*-dichlorobenzene complex (**2.1**) is very simple, with the cyclopentadienyl resonance appearing as a singlet at 5.45 ppm, and the complexed aromatic protons resonating as a singlet at 6.99 ppm. Upon polymerization, the resonances corresponding to both of these peaks underwent quite noticeable upfield shifts. The appearance of one singlet representing the cyclopentadienyl protons in the polymers' spectra from 5.0-5.3 ppm indicated that there was no starting complex remaining. As well, the complexed aromatic protons were shifted upfield in polymers **2.10-2.17** to 6.2-6.6 ppm. The ^{13}C NMR spectra of the organoiron polymers were also important in evaluating the polymerization reactions. In particular, the presence of one Cp resonance from 77-78 ppm for polymers **2.10-2.17** with etheric bridges indicated successful polymer formation. Additionally, the presence of one complexed aromatic resonance (CH) from 74-77 ppm for polymers **2.10-2.17** demonstrated the equivalence of the complexed aromatic CH carbons.

Figure 2.1 shows the ^{1}H NMR spectrum of polymer **2.14**. The twelve protons of the isopropylidene groups appear as a singlet at 1.65 ppm, and the protons corresponding to the bridging aromatic rings appear as a multiplet integrating for eight protons at 7.18 ppm and a doublet integrating for four protons at 7.36 ppm. It can be seen that the five cyclopentadienyl protons are resonating as a single peak at 5.20 ppm, and the four complexed aromatic protons have shifted upfield, and appear as a singlet at 6.23 ppm.

The ^{13}C NMR spectrum of polymer **2.14** is given in Figure 2.2. This spectrum shows the methyl carbons appearing as a downward peak at 30.39 ppm, and the

quaternary carbon of the isopropylidene group appears pointing upwards at 41.83 ppm. The cyclopentadienyl resonance appears at 77.74 ppm as an intense peak pointing down. The complexed aromatic CH carbons appear at 74.76 ppm, while the quaternary complexed aromatic carbons appear at 130.07 ppm. The uncomplexed aromatic peaks appear further downfield at 119.77, 126.12 and 128.62 ppm and the quaternary carbons were at 146.98, 147.99 and 151.09 ppm. The ^{1}H NMR and % yields of polymers **2.10-2.17** are given in Table 2.4, while their IR and ^{13}C NMR are given in Table 2.5.

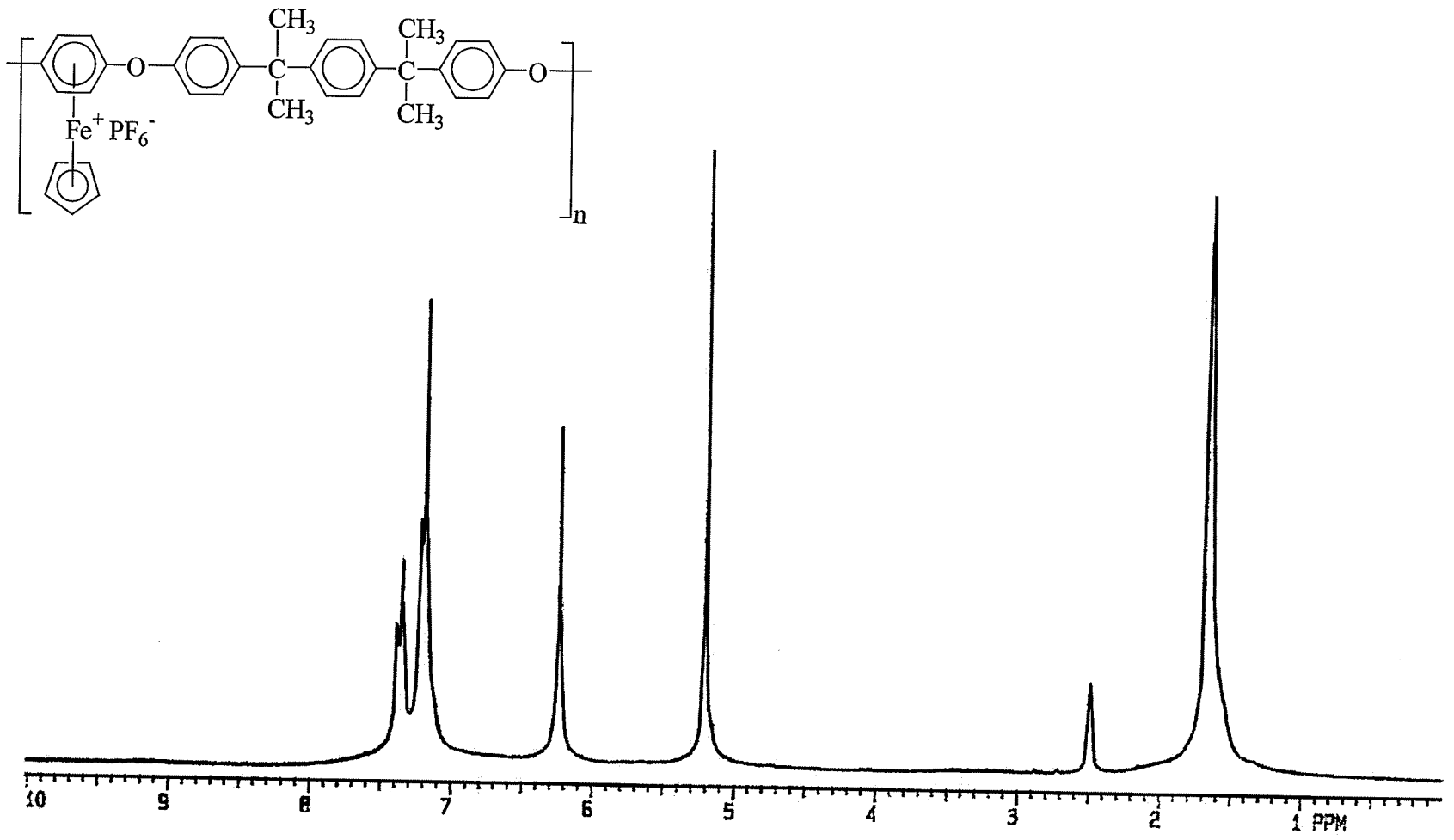

Figure 2.1: ^{1}H NMR spectrum of polymer **2.14** in DMSO-d_6

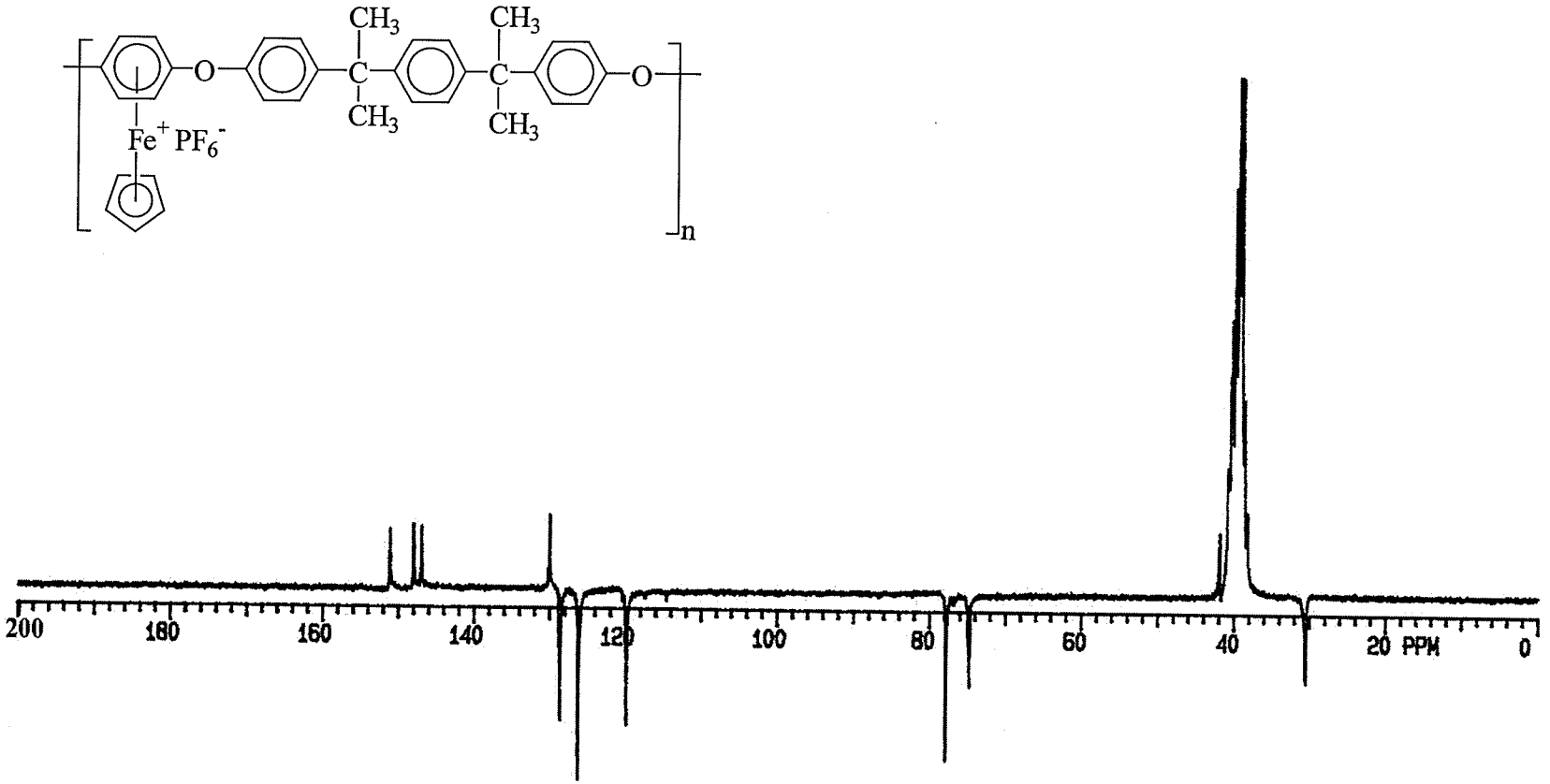

Figure 2.2: ^{13}C NMR spectrum of polymer **2.14** in DMSO-d_6

Table 2.4: % Yield and ^{1}H NMR Analysis of Polymers **2.10-2.17** in DMSO-d_6

Polymer	% Yield	Other	Cp	Complexed ArH	ArH
2.10	89		5.37 (s, 5H)	6.37 (s, 4H)	7.41 (d, *J*=7.09 Hz, 4H), 7.87 (d, *J*=7.09 Hz, 4H)
2.11	92	10.39 (s, 2H, NH)	5.29 (s, 5H)	6.44 (s, 4H)	7.04 (d, *J*=8.51 Hz, 4H), 7.46 (d, *J*=7.90 Hz, 4H), 7.81 (d, *J*=8.51 Hz, 4H), 8.17 (d, *J*=8.05 Hz, 4H)
2.12	92	1.65 (br. s, 3H, CH_3), 2.01 (br. s, 2H, CH_2), 2.37 (br. s, 2H, CH_2)	5.21 (s, 5H	6.27 (s, 4H)	7.24 (d, *J*=8.51 Hz, 4H), 7.36 (d, *J*=8.42 Hz, 4H)
2.13	89	1.70 (s, 6H, CH_3)	5.20 (s, 5H)	6.25 (s, 4H)	7.22 (d, *J*=8.14 Hz, 4H), 7.40 (d, *J*=8.02 Hz, 4H)
2.14	98	1.65 (s, 12H, CH_3)	5.20 (s, 5H)	6.23 (s, 4H)	7.18 (m, 8H), 7.36 (d, *J*=8.14 Hz, 4H)
2.15	99	2.19 (s, 3H, CH_3)	5.21 (s, 5H)	6.30 (s, 4H)	7.22 (br. s, 13H)
2.16	94	1.50 (br. s, 6H, CH_2), 2.31 (br. s, 4H, CH_2)	5.19 (s, 5H)	6.23 (s, 4H)	7.21 (d, *J*=7.53 Hz, 4H), 7.47 (d, *J*=7.77 Hz, 4H)
2.17	96	1.71 (s, 12H, CH_3)	5.21 (s, 5H)	6.25 (s, 4H)	7.23 (d, *J*=6.88 Hz, 8H), 7.40 (d, *J*=6.23 Hz, 8H), 8.31 (s, 4H)

Table 2.5: IR and ^{13}C NMR Analysis of Polymers **2.10-2.17** in DMSO-d_6

Polymer	IR (cm^{-1})	Other	Cp	Complexed Ar	Ar
2.10			78.01	75.36, 130.00*	120.94, 128.97, 136.91*, 153.31*
2.11	1664 (CO), 3405 (NH)	164.24 (CO)	78.24	76.11, 129.41*	118.66, 119.86, 122.28, 130.41, 132.67*, 134.56*, 152.96*, 156.27*
2.12	1704 (CO), 3420 (OH)	27.05 (CH_3), 29.97 (CH_2), 38.03 (CH_2), 45.01 (C), 174.60 (CO)	77.89	75.11, 130.07*	119.98, 129.24, 146.17*, 151.52*
2.13		30.62 (CH_3), 42.25 (C)	77.93	75.00, 130.19*	120.01, 128.83, 147.80*, 151.45*
2.14		30.39 (CH_3), 41.83 C)	77.74	74.76, 130.07*	119.77, 126.12, 128.62, 146.98*, 147.99*, 151.09*
2.15		30.20 (CH_3), 51.59 (C)	77.84	75.03, 129.91*	119.71, 126.30, 128.16, 130.42, 146.22*, 148.10*, 151.60*
2.16		22.39, 36.22, 45.16 (C, CH_2)	77.73	74.95, 129.91*	119.91, 128.95, 145.62*, 151.09*
2.17	1739 (CO)	30.51 (CH_3), 38.28 (C), 163.87 (CO)	77.84	74.93, 130.13*	119.91, 121.34, 127.70, 128.72, 130.22, 133.42*, 147.75*, 147.92*, 148.36*, 151.32*

*Denotes quaternary carbons

2.2.1.2 Isolation of the Organic Polyaromatic Ethers

Removal of the cyclopentadienyliron moieties pendent to the polymer backbones was accomplished by irradiating **2.10-2.17** with ultraviolet light for four to eight hours as shown in Scheme 2.2. The demetallations were accomplished by dissolving the polymers in acetonitrile/dichloromethane, acetonitrile/dimethylformamide or dimethylformamide solutions, depending on their solubilities in these solvent systems to give polymers **2.18-2.25**. The organic polymers were isolated in yields ranging from 70-97%.

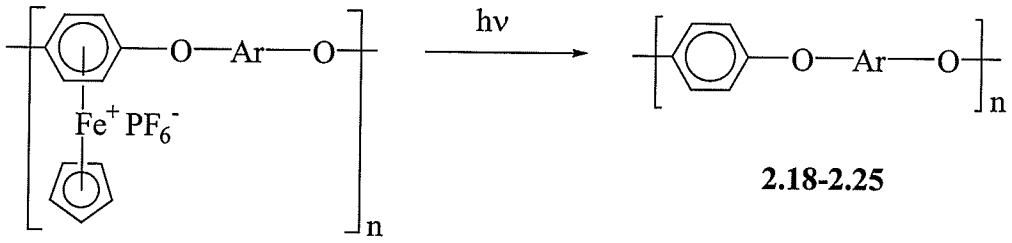

2.10-2.17 **2.18-2.25**

Scheme 2.2

While all of the cyclopentadienyliron-coordinated polyaromatic ethers were soluble in polar organic solvents, their demetallated analogues (**2.18-2.25**) displayed varying degrees of solubility. This became apparent during the attempted isolation of the polyaromatic ethers following photolysis. Polymers **2.21-2.25** demonstrated much higher solubility than polymers **2.18-2.20** following cleavage of the cyclopentadienyliron moieties. For example, polymer **2.18** was completely insoluble in a number of chlorinated and non-chlorinated organic solvents. Polymer **2.20** with the pendent carboxylic acid groups had limited solubility in both organic and aqueous solvents. Polyaromatic ethers with flexible alkyl groups in their backbones (**2.21-2.25**) were

extracted with chloroform following photolysis. These polymers exhibited good solubility in chloroform, dichloromethane and THF, had very limited solubility in DMF, DMSO and DMAc and were insoluble in acetone and acetonitrile. The polymers that were insoluble in chloroform (**2.18-2.20**) were dried and the solid residue that remained was collected in a crucible and washed with water repeatedly to remove iron salts formed during the demetallation process. The off-white material was then washed with hexane to remove ferrocene.

NMR analysis of the demetallated polymers was also valuable for the characterization of these materials. Following photolytic demetallation, the most noticeable difference in the spectra was the absence of the cyclopentadienyl resonances. Further evidence of successful demetallation was a downfield shift of the complexed aromatic resonances to about 7-7.5 ppm in the ^{1}H spectra and to about 120-130 ppm in the ^{13}C spectra of the organic polymers. Figures 2.3 and 2.4 show the ^{1}H and ^{13}C NMR spectra of polymer **2.22**, which is the organic analogue of polymer **2.14**. The ^{1}H NMR spectrum shows a singlet at 1.62 ppm, corresponding to the twelve methyl protons, two broad singlets at 6.87 and 6.95 ppm corresponding to eight aromatic protons, and another broad singlet at 7.10 ppm, which was assigned to the remaining eight aromatic protons of this polymer. The ^{13}C NMR spectrum also shows the absence of a cyclopentadienyl resonance, and the complexed aromatic CH carbons have shifted downfield to 117.53, 120.33, 126.25 and 128.03, and the quaternary carbons appear at 145.33, 147.67, 152.65 and 155.49. The methyl appears at 30.88 and the quaternary isopropylidene carbon appears at 42.05 ppm. Full spectroscopic analysis of polymers **2.18-2.25** can be found in Tables 2.6 and 2.7.

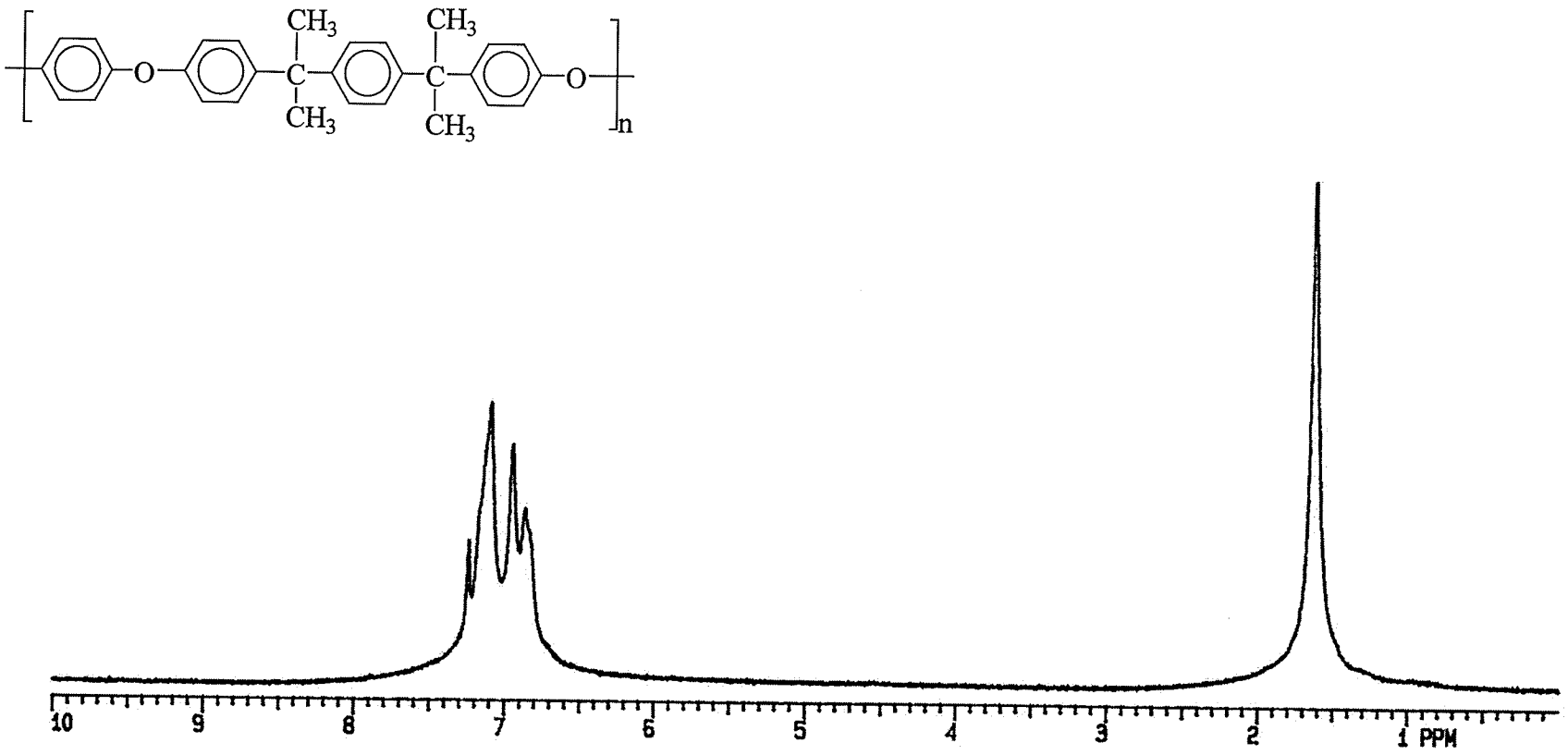

Figure 2.3: ^{1}H NMR spectrum of polymer **2.22** in $CDCl_3$

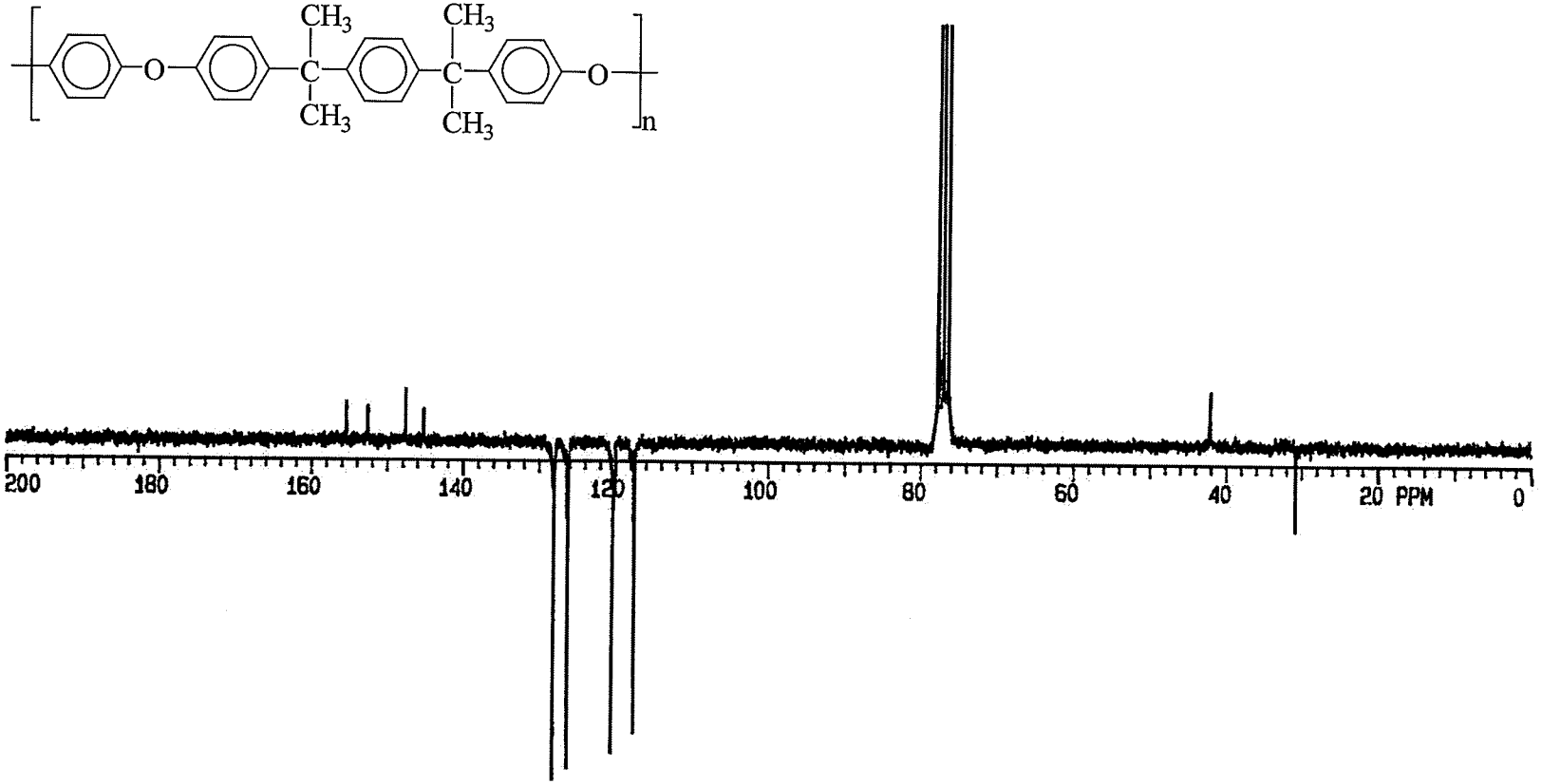

Figure 2.4: ^{13}C NMR spectrum of polymer **2.22** in $CDCl_3$

Table 2.6: % Yield and ^{1}H NMR Analysis of Polymers **2.18-2.25** in $CDCl_3$

Polymer	**% Yield**	CH_3	CH_2	**ArH**
2.18	86	-----	-----	-----
2.19	87	-----	-----	-----
2.20	97	-----	-----	-----
2.21	71	1.66 (s, 6H)		6.88 (d, *J*=8.14 Hz, 4H), 6.97 (s, 4H), 7.17 (d, *J*=8.34 Hz, 4H)
2.22	89	1.62 (s, 12H)		6.87 (br. s., 4H), 6.95 (br. s, 4H), 7.10 (br. s., 8H)
2.23	84	2.13 (s, 3H)		6.84 (d, *J*=7.97 Hz, 4H), 6.98 (s, 4H), 7.03 (br. s, 2H), 7.07 (d, *J*=7.41Hz, 4H), 7.20 (br. s, 3H)
2.24	91		1.50 (s, 6H), 2.21 (s, 4H)	6.85 (d, *J*=8.26 Hz, 4H), 6.93 (s, 4H), 7.18 (d, *J*=8.26 Hz, 4H)
2.25	70	1.69 (s, 12H)		6.98 (s, 4H), 7.17 (s, 8H), 7.29 (s, 4H), 8.30 (s, 4H)

Table 2.7: IR and ^{13}C NMR Analysis of Polyethers **2.18-2.25** in $CDCl_3$

Polymer	IR (cm^{-1})	C, CO	CH_3	CH_2	Ar
2.18		-----	-----	-----	-----
2.19	1660 (CO), 3407 (NH)	-----	-----	-----	-----
2.20	1707 (CO), 3420 (OH)	-----	-----	-----	-----
2.21		42.55 (C)	31.52		118.14, 120.86, 128.49, 145.77*, 153.18*, 156.09*
2.22		42.05 (C)	30.88		117.53, 120.33, 126.25, 128.03, 145.33*, 147.67*, 152.65*, 155.49*
2.23		51.54 (C)	30.67		117.30, 120.56, 126.03, 127.90, 128.56, 129.91, 143.64*, 149.03*, 152.54*, 155.91*
2.24		37.40 (C)		22.89, 26.38, 37.40	117.76, 120.43, 128.36, 143.21*, 152.61*, 155.36*
2.25	1737 (CO)	42.32 (C), 164.39 (CO)	30.96		117.69, 120.39, 120.99, 127.95, 128.05, 130.26, 133.93*, 144.93*, 148.60*, 152.66*, 155.68*

*Denotes quaternary carbons

The molecular weights of the organic polymers were determined using gel permeation chromatography (GPC), with chloroform as the eluent (Table 2.8). Although the solubility of the organic materials was often much lower than that of their organoiron analogues, the molecular weights of the metallated polymers could not be determined by GPC due to interactions of cationic organometallic moieties with GPC columns.[20] However, the molecular weights of the demetallated polymers allowed for the determination of the approximate molecular weights of the organoiron polymers. For example, polymer **2.21** had a weight average molecular weight (M_w) of 18,100, which corresponds to a degree of polymerization of about 60. The M_w of the corresponding organoiron polymer was calculated to be approximately 34,000. It is important to note that the molecular weights of the organic polymers represented their soluble portions, and were not necessarily indicative of the true molecular weights of these materials.

Table 2.8: Molecular weight Analysis of Polyethers **2.18-2.25**

Polymer	$\mathbf{M_w}$	$\mathbf{M_n}$	$\mathbf{M_w/M_n}$
2.18	insoluble		
2.19	insoluble		
2.20	insoluble		
2.21	18 100	8 800	2.1
2.22	21 400	9 900	2.2
2.23	7 300	3 500	2.1
2.24	8 800	3 700	2.4
2.25	16 100	7 400	2.2

2.2.1.3 Thermal Properties of Polyaromatic Ethers

The thermal properties of the metallated and demetallated polymers were investigated using thermogravimetric analysis (TGA). The TGA thermograms provide information about the thermal stability of these materials by measuring their weight losses when they are heated. All of the metallated polymers (**2.10-2.18**) exhibited a 17 to 27% weight loss between 219 and 296 °C, corresponding to the cleavage of the cyclopentadienyliron hexafluorophosphate moieties. Following this initial weight loss, the polymers experienced second weight losses that were dependent upon the aromatic linkages in their backbones. For example, the polymers lost anywhere between 20 and 39% of their weight starting at 417 to 521 °C. Polymer **2.10** experienced only a 20 % weight loss starting at 521 °C, which is consistent with its rigid aromatic backbone. Following photolytic demetallation, the thermal stabilities of polymers **2.18-2.25** were examined. It was noted that there was only one weight loss experienced and it corresponded to decomposition of the polymer backbones. These results indicated that the presence of organoiron moieties did not significantly influence the thermal stability of the polymer backbones. TGA also confirmed that the metallic moieties were no longer present in polymers **2.18-2.20**, since these polymers were insoluble and could not be analyzed using NMR spectroscopy. The TGA thermograms of organoiron polymer **2.13** and its corresponding organic polymer **2.21** can be seen in Figure 2.5. It can be seen that polymer **2.13** displayed a weight loss of 34% beginning at 517 °C and ending at 554 °C. Following demetallation, polymer **2.21** had a 62% weight loss that began at 533 °C and continued until 562 °C. The TGA analysis for polymers **2.10-2.17** and **2.18-2.25** are given in Tables 2.9 and 2.10, respectively.

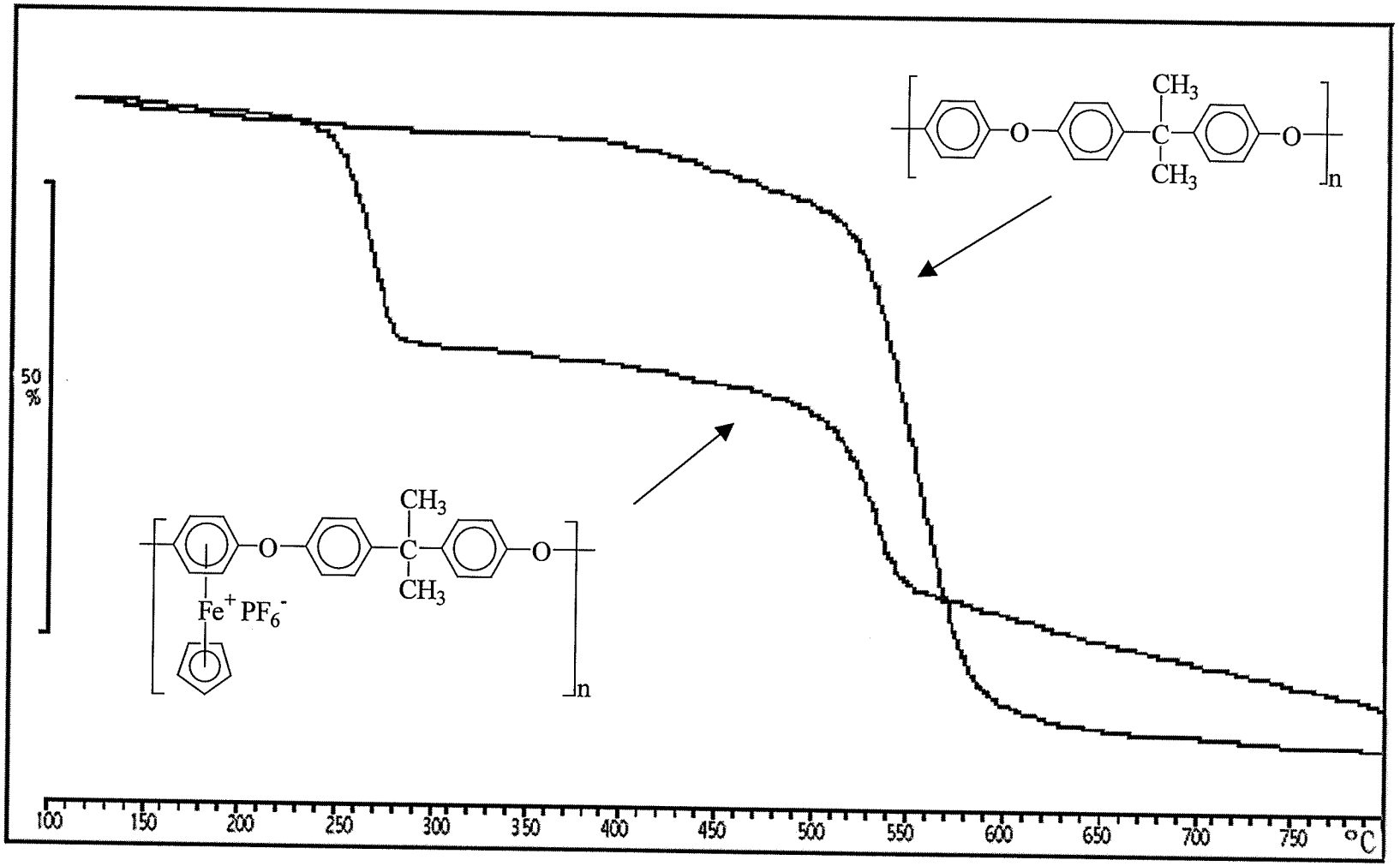

Figure 2.5: TGA thermograms of polymers **2.13** and **2.21**

Table 2.9: TGA Results for Organometallic Polyethers **2.10-2.17**

Polymer	Weight loss (%)	T_{onset} (°C)	$T_{midpoint}$ (°C)	T_{endset} (°C)
2.10	23	260	274	289
	20	521	555	586
2.11	17	219	236	255
	27	447	494	531
2.12	19	238	254	272
	25	441	481	524
2.13	23	247	259	272
	34	517	533	554
2.14	17	246	261	278
	23	514	534	554
2.15	23	271	283	296
	21	502	527	550
2.16	27	261	277	293
	35	518	536	557
2.17	13	238	252	266
	39	417	481	517

Table 2.10: TGA Results for Demetallated Polyethers **2.18-2.25**

Polymer	Weight loss (%)	T_{onset} (°C)	$T_{midpoint}$ (°C)	T_{endset} (°C)
2.18	23	541	576	589
2.19	35	440	494	530
2.20	29	456	503	534
2.21	62	533	546	562
2.22	56	519	567	573
2.23	48	489	530	548
2.24	74	507	530	554
2.25	77	473	634	734

The thermal properties of the organic polyethers were also examined using differential scanning calorimetry (DSC). DSC indicated that the glass transition temperatures (T_g) of the polyaromatic ethers ranged from 113 to 165 °C (Table 2.11). The glass transition temperatures of the cyclopentadienyliron-coordinated polymers were investigated, however, they were determined to be above their decomposition temperatures. Figure 2.6 shows the DSC thermograms for polymers **2.21-2.23**. It can be seen that polymer **2.23**, with the aromatic groups pendent to the polymer backbone has the highest glass transition temperature of this series, while polymer **2.21**, with only one isopropylidene group in its backbone has the lowest T_g. As expected, polymers with polar groups in their structures possessed higher T_gs. For example, polymer **2.20** had the highest T_g (165 °C) due to the presence of the carboxylic acid group pendent to its backbone.

Table 2.11: DSC Results for Polyethers **2.18-2.25**

Polymer	T_g Onset (°C)
2.18	150
2.19	146
2.20	165
2.21	119
2.22	130
2.23	142
2.24	113
2.25	144

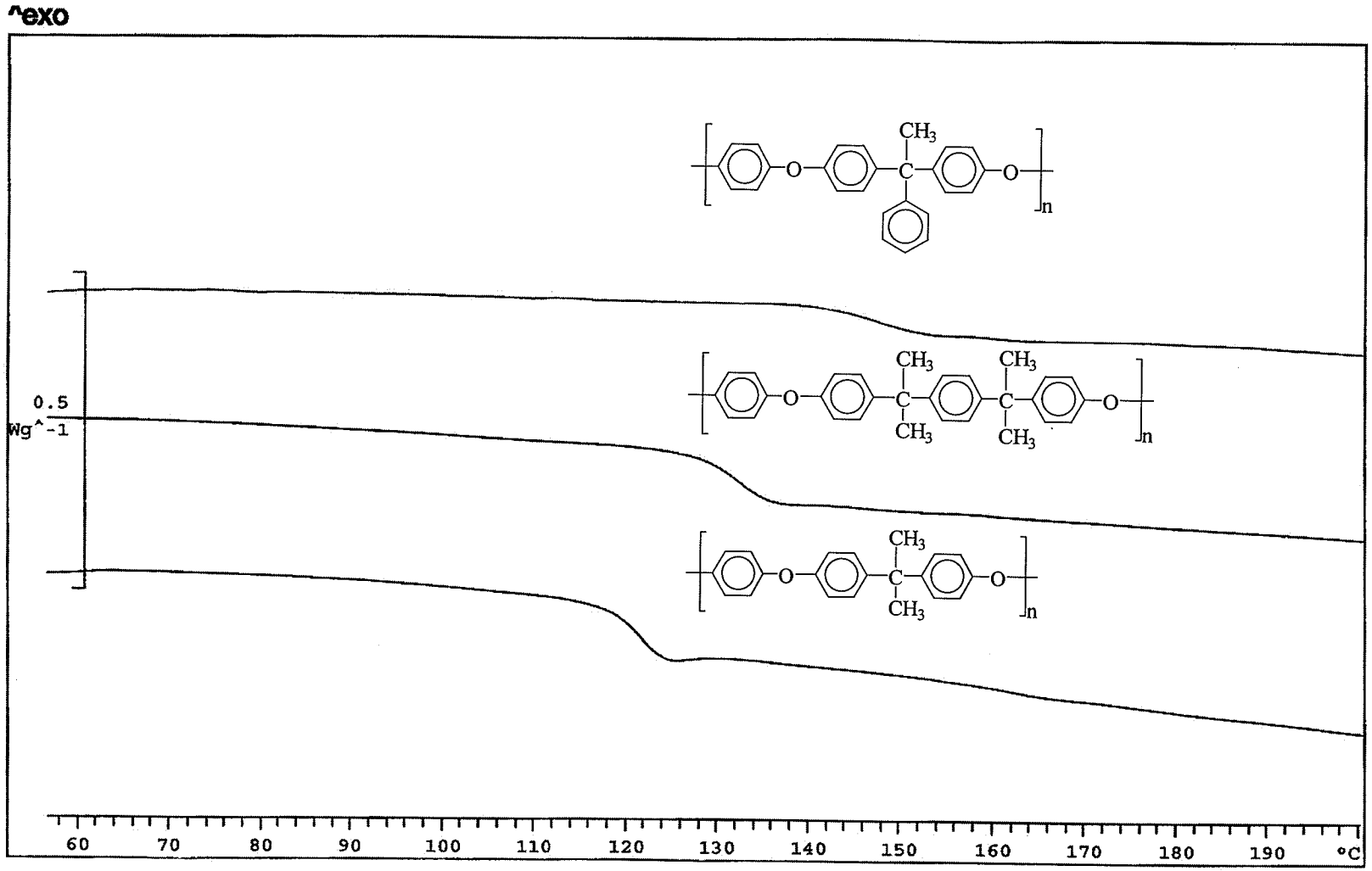

Figure 2.6: DSC traces of polymers **2.21-2.23**

2.2.2 Synthesis of Polythioethers Containing Aliphatic Spacers

2.2.2.1 Synthesis of Polythioethers Containing Aliphatic Spacers Coordinated to Cationic Cyclopentadienyliron Moieties

In order to examine the influence of aliphatic bridges on the properties of the organoiron polymers, reactions of 1,4-butanedithiol (**2.26**), 1,6-hexanedithiol (**2.27**) and 1,8-octanedithiol (**2.28**) with *p*-dichlorobenzene complex (**2.1**) were also studied. Scheme 2.3 shows the isolation of the resulting cyclopentadienyliron-coordinated polythioethers **2.29-2.31**. It was found that the length of the aliphatic bridge had a tremendous affect on the success of the polymerization reaction, as well as the solubilities and molecular weights of the resulting polymers. Polymers prepared with 1,4-butanedithiol were much more difficult to produce than those prepared with 1,6-hexanedithiol or 1,8-octanedithiol, as the resulting polymers precipitated out of the reaction solution more readily than those prepared with the nucleophiles containing longer alkyl bridges. Polymers **2.29-2.31** were isolated in 88-91% yield as beige or brown solids. Polymers **2.30** and **2.31** were often elastomeric in nature and formed sticky solids, while polymer **2.29** always formed a precipitate.

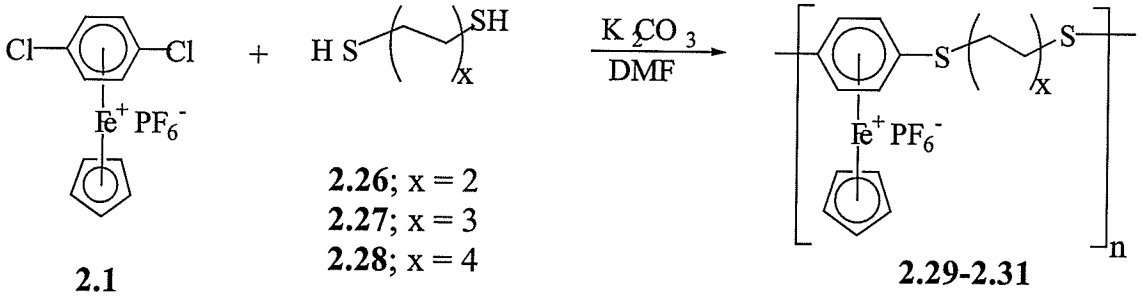

2.1

2.26; x = 2
2.27; x = 3
2.28; x = 4

2.29-2.31

Scheme 2.3

It was noted that the greater the number of methylene units in the dithiol, the higher the solubility of the resulting polythioether. For example, polymers prepared with 1,8-octanedithiol as the nucleophile were formed more rapidly, were more soluble and yielded higher molecular weight materials. As well, the hexamethylene (**2.30**) and octamethylene (**2.31**) bridged polymers were much more stable at high temperatures during the polymerization reactions than the tetramethylene (**2.29**) bridged polymers. The results of the solubility study of polymers **2.29-2.31** in polar organic solvents are given in Table 2.12.

Table 2.12: Solubility of Organoiron Polymers[a]

	Solvent					
Polymer	**CH_2Cl_2**	**Acetone**	**CH_3CN**	**DMAc**	**DMF**	**DMSO**
2.29	I	PS	PS	PS	PS	PS
2.30	PS	PS	PS	PS	S	S
2.31	PS	S	S	S	S	S

[a] Solubility at room temperature: (S), soluble; (PS), partially soluble; (I), insoluble.

NMR analysis of polymers **2.29-2.31** was utilized to evaluate the polymerization reactions with the aliphatic dithiols. The ^1H NMR spectra showed one cyclopentadienyl resonance between 5.01 and 5.04 ppm, and a singlet corresponding to the complexed aromatic protons between 6.41 and 6.47 ppm. The methylene bridges in the backbones of these polymers resonated between 1.22 and 3.26 ppm. The most downfield of these resonances integrated for four protons, and correspond to the methylene groups alpha to

the sulfur atoms. The ^{1}H NMR spectrum of polymer **2.30** is given in Figure 2.7. It can be seen that there are three resonances corresponding to the methylene peaks in the polymer backbone at 1.42, 1.71, and 3.26 ppm. Each of these peaks integrated for four protons, demonstrating the symmetry within the hexamethylene bridges. The cyclopentadienyl protons appeared as one singlet integrating for five protons at 5.01 ppm, while the complexed aromatic protons appear as a singlet integrating for four protons at 6.41 ppm.

The ^{13}C NMR spectra of these polymers also indicated that the polymerization reactions had been successful. In particular, the presence of one Cp resonance from 78.93-79.56 ppm for polymers **2.29-2.31** was an important feature of these spectra. Additionally, the presence of one complexed aromatic resonance (CH) from 83.00 to 83.19 ppm for polymers **2.29-2.31** demonstrated the equivalence of the complexed aromatic CH carbons. The quaternary aromatic carbon peaks appeared between 106.39 and 107.08 ppm for these complexed polymers. The CH_2 peaks showed two, three and four peaks for the tetramethylene, hexamethylene and octamethylene bridged polymers, respectively. The ^{13}C NMR spectrum of polymer **2.30** is shown in Figure 2.8. The methylene resonances appear as three upward peaks at 28.01, 29.32 and 31.06 ppm. The cyclopentadienyl resonance appears as a strong peak at 79.56 ppm, while the complexed aromatic carbons (CH and C) appear at 83.14 and 107.08 ppm, respectively.

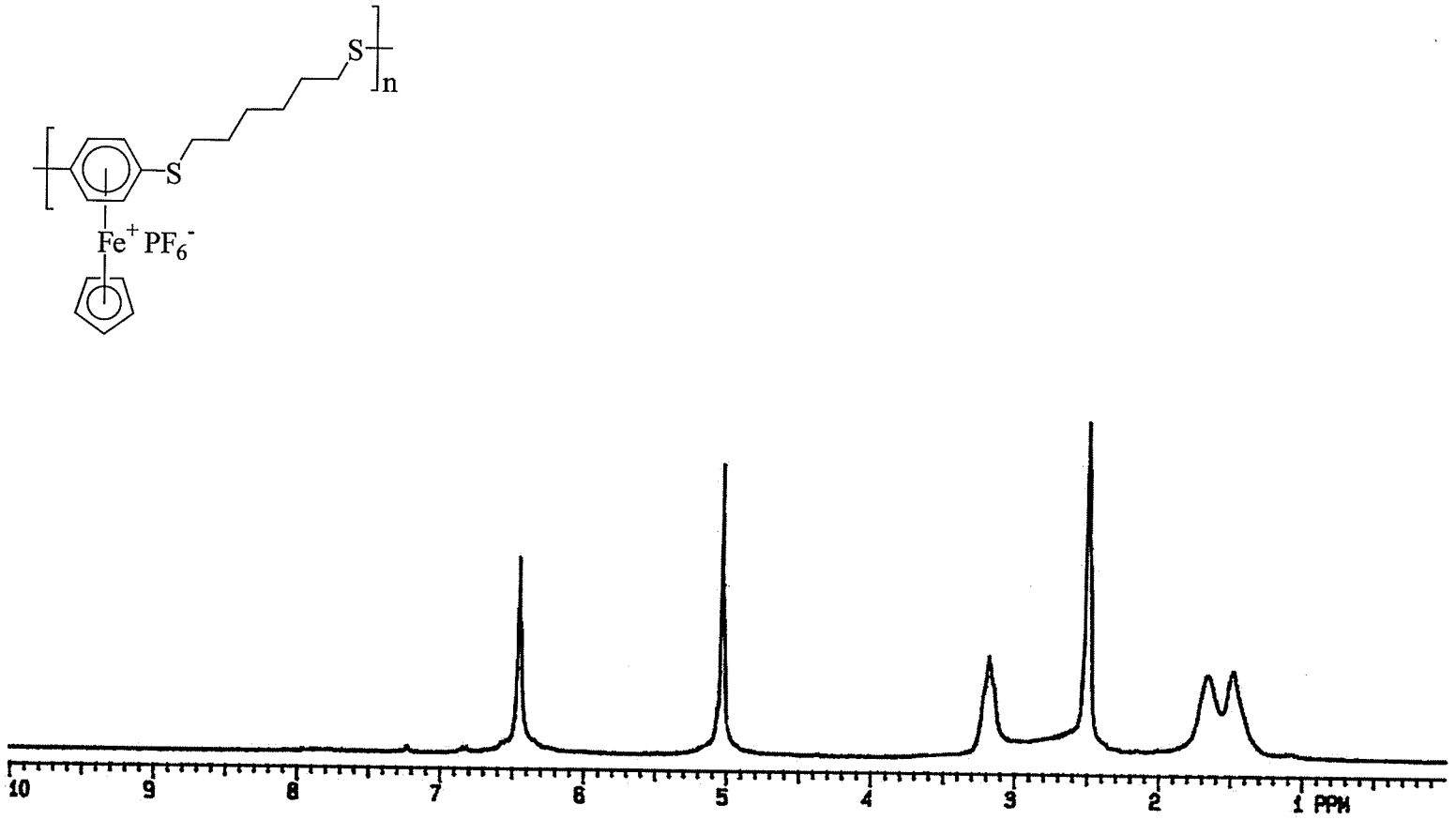

Figure 2.7: ^{1}H NMR spectrum of polymer **2.30** in DMSO-d_6

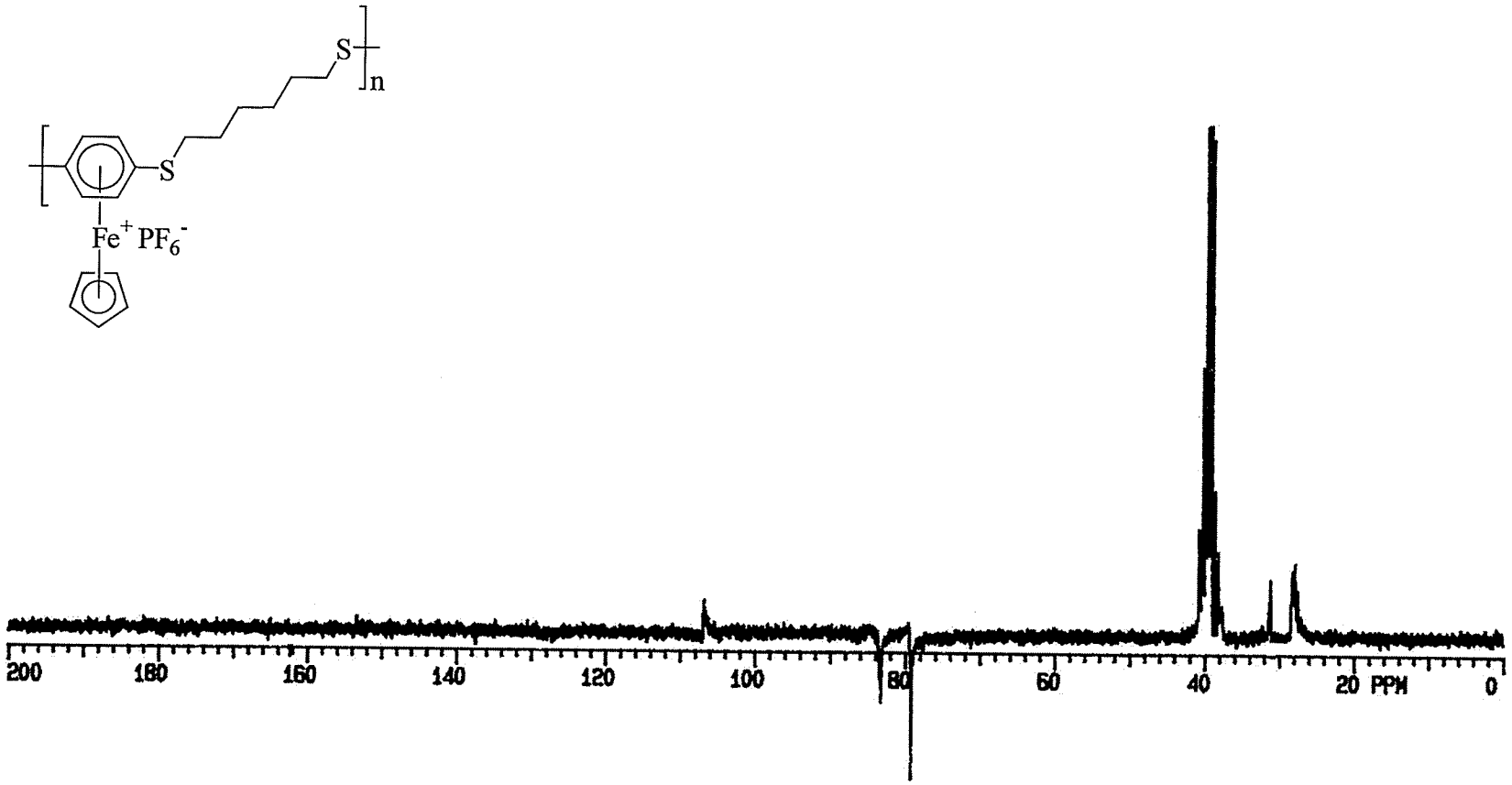

Figure 2.8: ^{13}C NMR spectrum of polymer **2.30** in DMSO-d_6

Table 2.13: % Yield and ^{1}H NMR Analysis of Polymers **6a-c** in DMSO-d_6

Polymer	% Yield	CH_2	Cp	Complexed Ar
2.29	91	1.22 (br. s, 4H), 3.24 (br. s, 4H)	5.04 (s, 5H)	6.47 (s, 4H)
2.30	88	1.42 (br. s, 4H), 1.71 (br. s, 4H), 3.26 (br. s, 4H)	5.01 (s, 5H)	6.41 (s, 4H)
2.31	89	1.28 (br. s., 4H), 1.59 (br. s., 4H), 2.66 (br. s., 4H), 3.15 (br. trip., 4H)	5.02 (s, 5H)	6.44 (s, 4H)

Table 2.14: ^{13}C NMR Analysis of Polymers **6a-c** in DMSO-d_6

Polymer	CH_2	Cp	Complexed Ar
2.29	26.87, 30.33	78.93	83.00, 106.39*
2.30	28.01, 29.32, 31.06	79.56	83.14, 107.08*
2.31	27.96, 28.29, 28.36, 31.15	79.06	83.19, 106.75*

*Denotes quaternary carbons

2.2.2.2 Isolation of the Organic Polythioethers with Aliphatic Spacers

Scheme 2.4 shows the photolysis of polymers **2.29-2.31**, allowing for the isolation of polymers **2.32-2.34**. While polymers **2.33** and **2.34** displayed good solubility in polar organic solvents such as chloroform, polymer **2.32** was insoluble in all solvents tested. As well, the solubility of polymers **2.33** and **2.34** decreased over time, and analysis of these materials needed to be accomplished within a few days of their work-up.

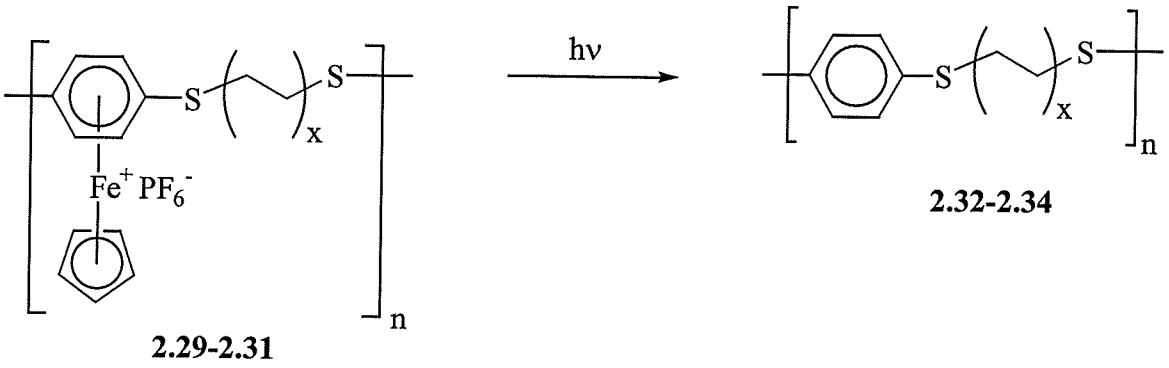

Scheme 2.4

Figures 2.9 and 2.10 show the ^{1}H and ^{13}C NMR spectra of polymer **2.33**, obtained in deuterated chloroform. It can be seen that the cyclopentadienyl resonance is no longer present in the spectra and that the complexed aromatic peaks have shifted downfield to the uncomplexed aromatic region. For example, the protons on the aromatic ring in the polymer backbone appear as a singlet at 7.20 ppm in the ^{1}H NMR spectrum, while the ^{13}C NMR spectrum shows the aromatic CH carbons at 129.67 ppm and the quaternary carbon at 134.31 ppm. This is in contrast to their appearances at 6.41 ppm in the ^{1}H NMR spectrum of the metallated analogue (**2.30**) and at 83.14 and 107.08 ppm, respectively in the ^{13}C NMR spectrum of **2.30**.

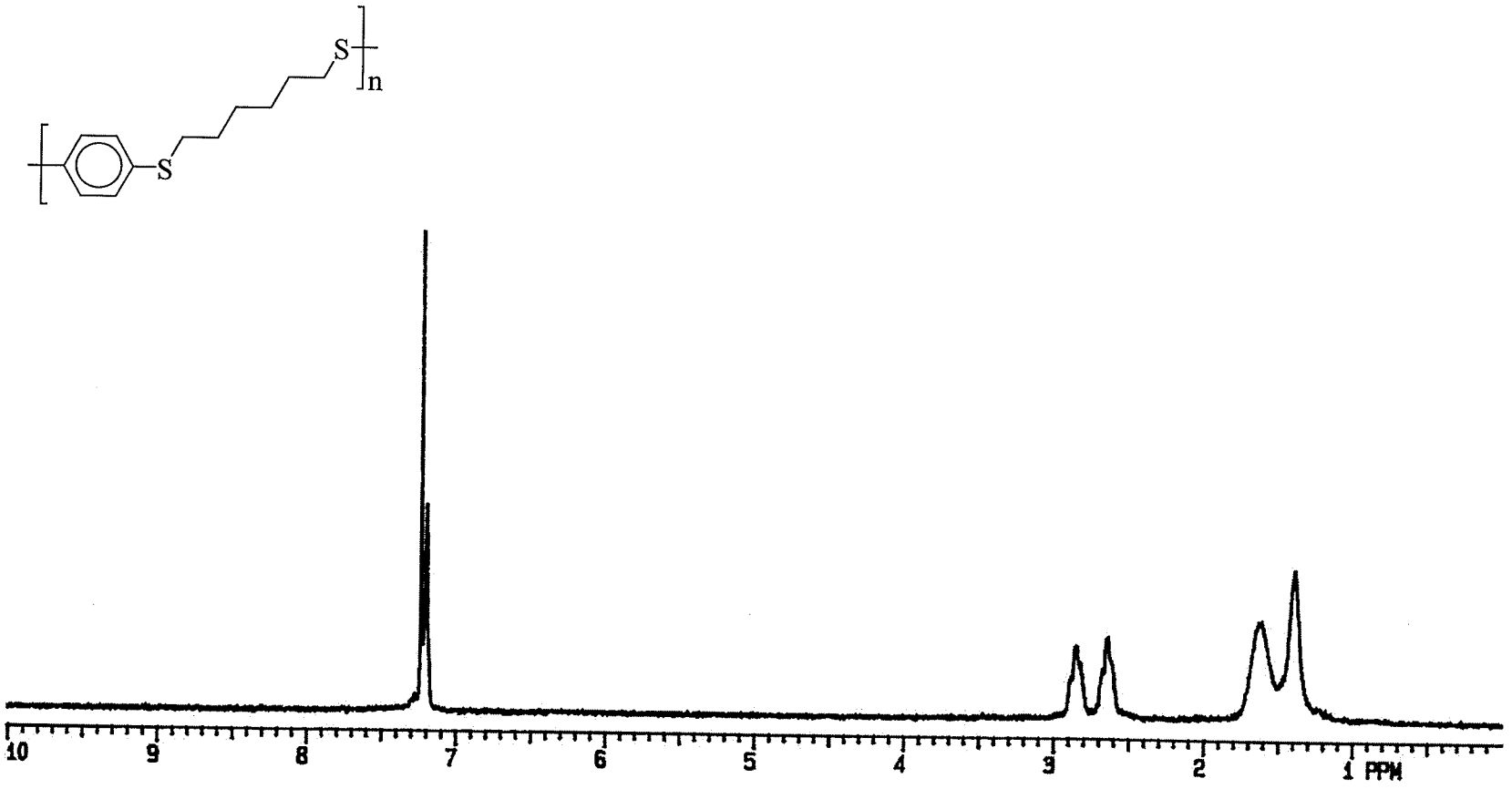

Figure 2.9: ^{1}H NMR spectrum of polymer **2.33** in $CDCl_3$

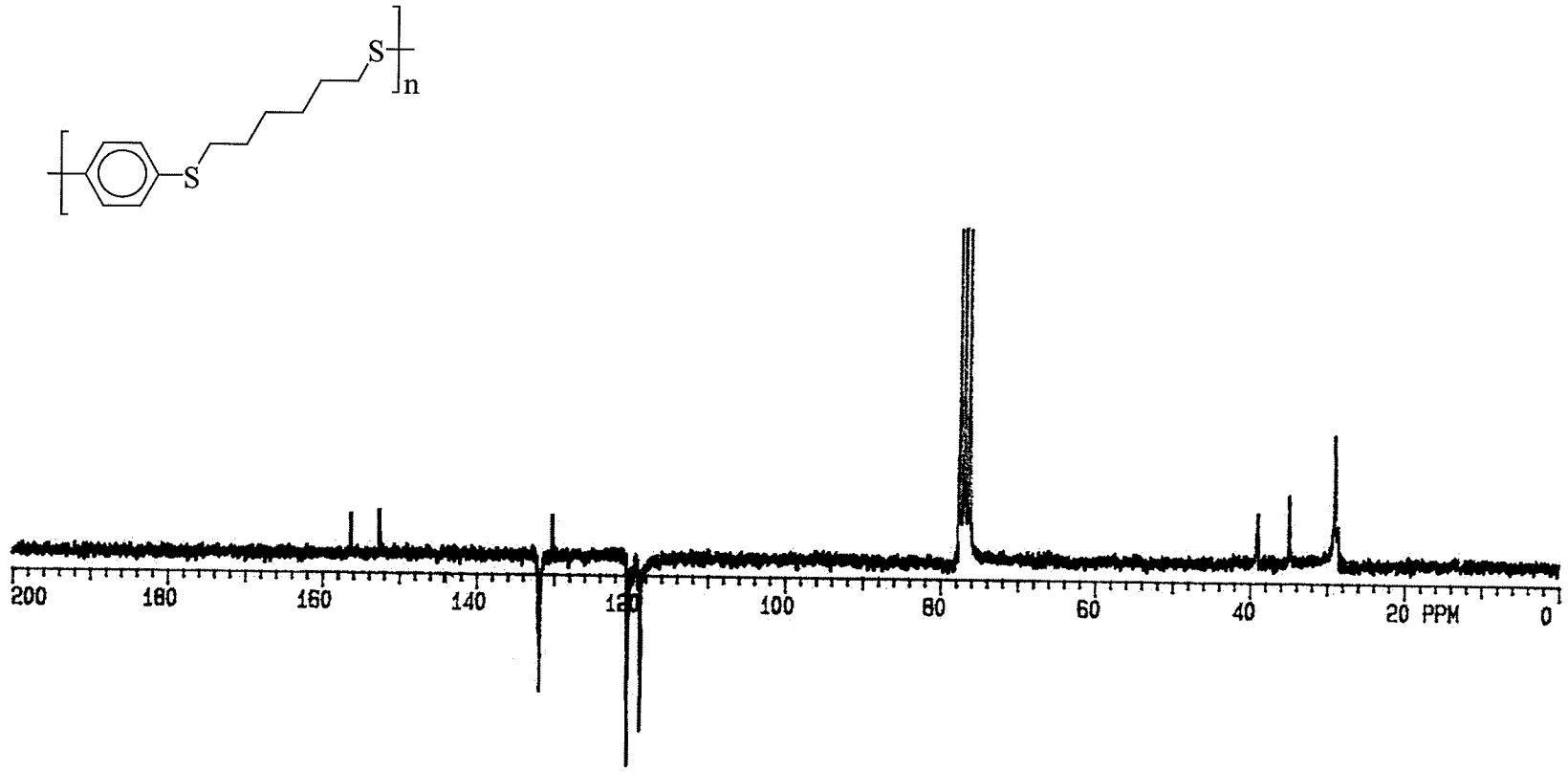

Figure 2.10: ^{13}C NMR spectrum of polymer **2.33** in $CDCl_3$

Table 2.15 provides the % yields of polymers **2.32-2.34** and the ^{1}H NMR data for polymers **2.33** and **2.34**. The ^{13}C NMR data for polymers **2.33** and **2.34** are given in Table 2.16.

Table 2.15: % Yield and ^{1}H NMR Analysis of **2.32-2.34** in $CDCl_3$

Polymer	% Yield	CH_2	Aromatics
2.32	91	insoluble	
2.33	83	1.40 (br. s, 4H), 2.66 (br. s, 4H), 2.88 (br. s, 4H)	7.20 (s, 4H)
2.34	74	1.27 (br. s, 4H), 1.30 (br. s, 4H), 2.63 (br. s, 4H), 2.69 (br. t, 4H)	7.21 (s, 4H)

Table 2.16: ^{13}C NMR Analysis of **2.32-2.34** in $CDCl_3$

Polymer	CH_2	Aromatics
2.32	insoluble	
2.33	28.95, 33.83, 38.92	129.67, 134.31*
2.34	28.94, 29.03, 33.87, 39.05	129.56, 134.31*

*Denotes quaternary carbons

As previously mentioned, depending on the nature of the polymer backbones, the solubilities of these materials varied quite dramatically. For example, the short length of the aliphatic bridge in polymer **2.32** made this polymer insoluble, while the solubility of **2.33** was slightly less than observed for **2.34**. As the solubility of the polymers increased, there was an observed increase in their molecular weights, and the weight average molecular weight of **2.33** was determined to be 13 500, while the M_w of **2.34** was 21 400.

Table 2.17: Molecular weights of Organic Polymers **2.32-2.34***

Polymer	$\mathbf{M_w}$	$\mathbf{M_n}$	$\mathbf{M_w/M_n}$
2.32	insoluble		
2.33	13 500	5 900	2.3
2.34	21 400	6 300	3.4

*Soluble Portions

2.2.2.3 Thermal Properties of the Polythioethers with Aliphatic Spacers

The thermal stability of the metallated polymers was investigated using thermogravimetric analysis, and it was found that polymers **2.29-2.31** possessed similar thermograms to the metallated polyaromatic ethers discussed in the previous section. However, the thermal stability of the polythioethers was much lower than the polyaromatic ethers. Following the initial weight loss corresponding to the loss of the metallic moieties pendent to the polymer backbones, second weight losses of 41-46% were observed starting from 347 to 402 °C. In contrast, the lowest onset for weight loss in polymers **2.10-2.17** occurred at 417 °C, and the % weight losses corresponding to degradation of the polymer backbones were generally in the 25% range.

Figure 2.11 shows the TGA thermograms of the cyclopentadienyliron-coordinated polythioethers (**2.29-2.31**). It can be seen that an initial weight loss of 17 to 25 % occurred between 200 and 250 °C, due to loss of the cyclopentadienyliron moieties. Thereafter, the organic portions of these polymers began to decompose at around 350 °C. Figure 2.12 shows the TGA thermograms of the organic polythioethers **2.32-2.34**. From these thermograms, it is apparent that there is no longer a weight loss in the region of 200-250 °C corresponding to loss of the organoiron groups. These organic polymers lost between 48 and 66 % of their weight between 345 and 450 °C. Tables 2.18 and 2.19 provide the % weight loss, onset, midpoint and endset temperatures determined for polymers **2.29-2.31** and **2.32-2.34**, respectively.

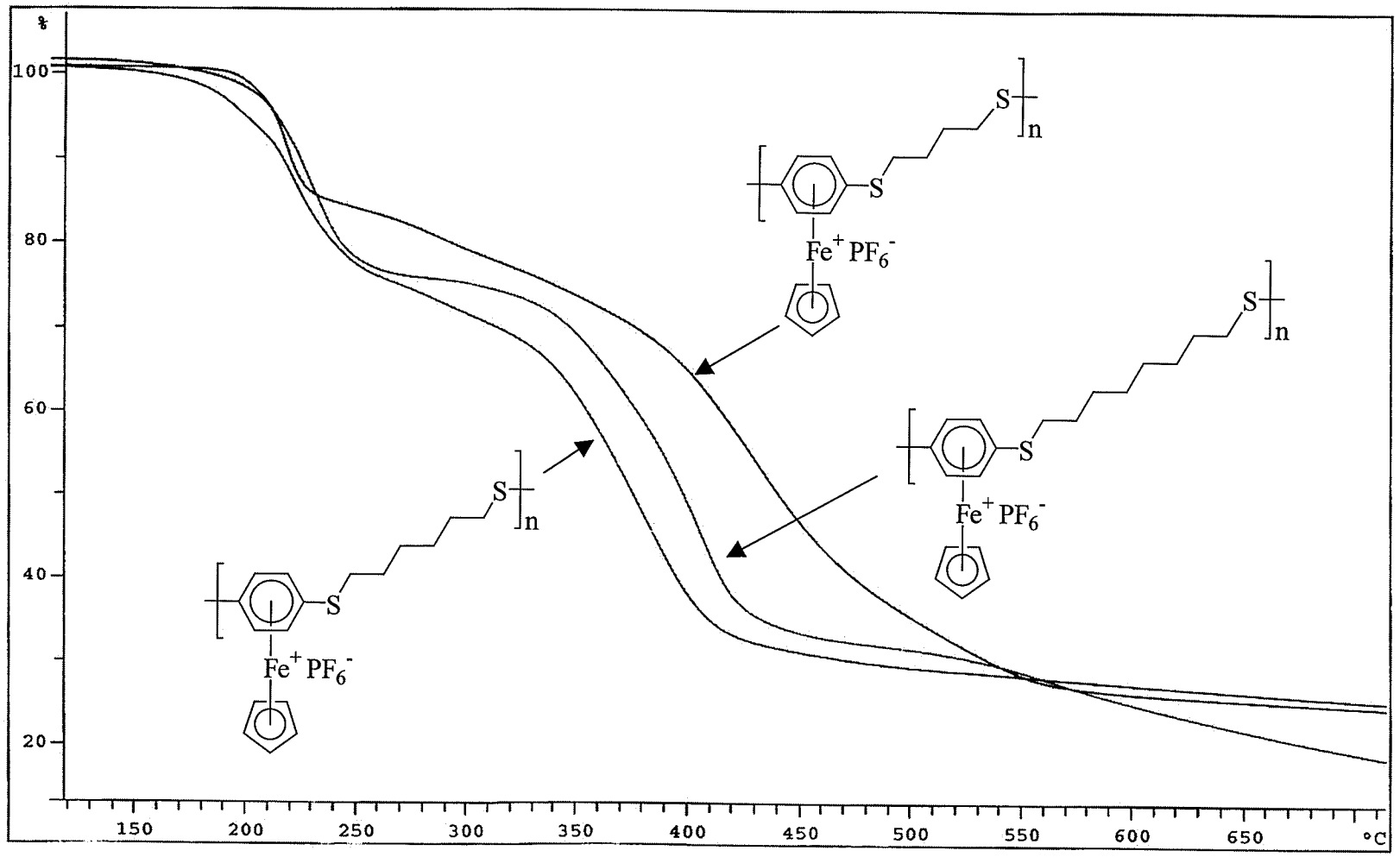

Figure 2.11: TGA thermogram of polymers **2.29-2.31**

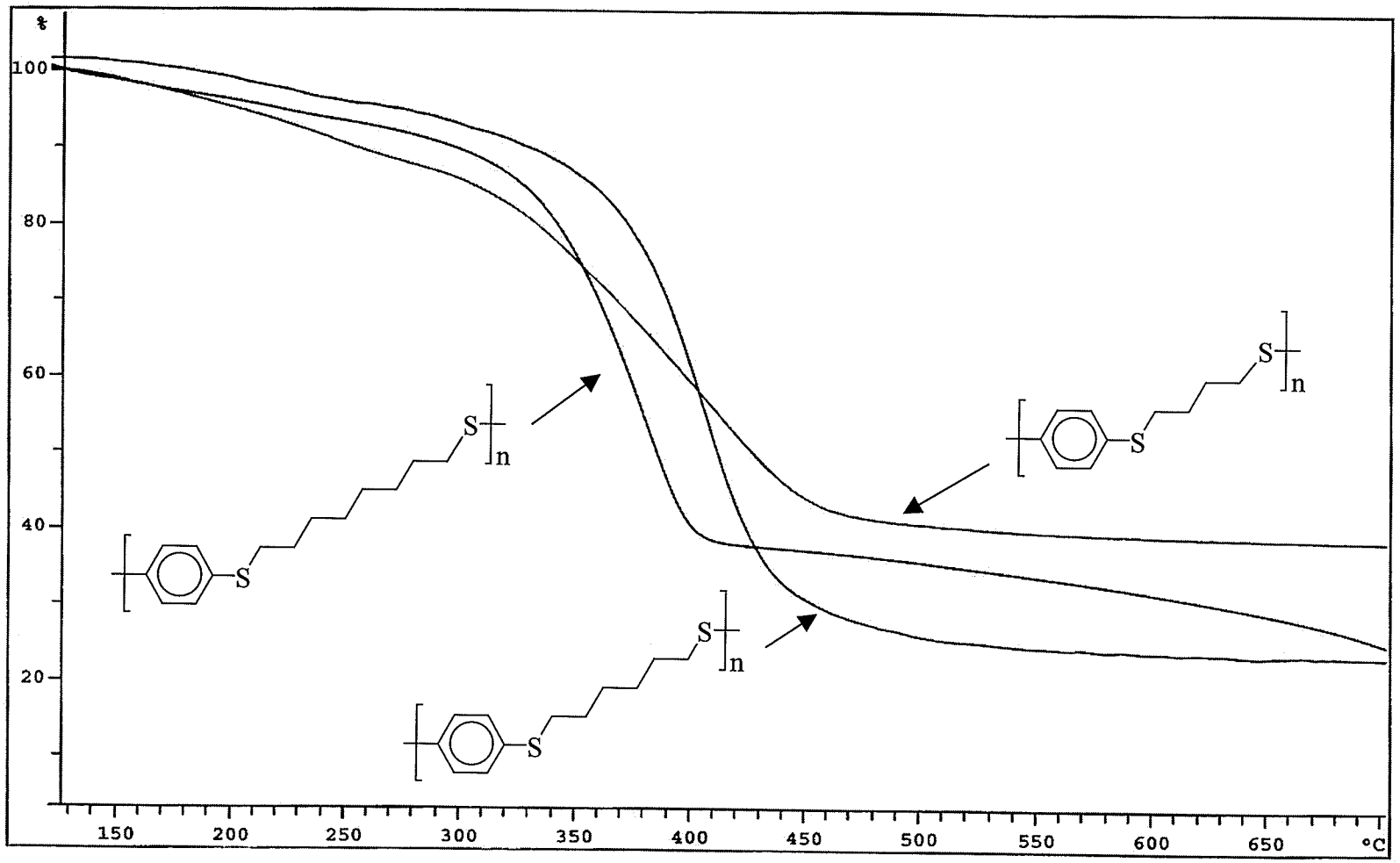

Figure 2.12: TGA thermogram of polymers **2.32-2.34**

Table 2.18: TGA Results for Organometallic Polythioethers **2.29-2.31**

Polymer	Weight loss (%)	T_{onset} (°C)	$T_{midpoint}$ (°C)	T_{endset} (°C)
2.29	17	210	220	229
	46	402	449	498
2.30	24	203	222	240
	41	347	377	412
2.31	25	208	228	248
	44	363	394	427

Table 2.19: TGA Results for Demetallated Polythioethers **2.32-2.34**

Polymer	Weight loss (%)	T_{onset} (°C)	$T_{midpoint}$ (°C)	T_{endset} (°C)
2.32	54	344	369	400
2.33	66	372	397	428
2.34	48	327	380	447

DSC of the organic polythioethers provided the glass transition temperatures of these polymers (Table 2.20). The T_gs of these polymers were approximately 100 °C lower than those observed for the polyaromatic ethers. This is due to both the flexible aliphatic spacers in the polymer backbones and the presence of thioether rather than ether bridges. While all T_gs ranged from of 33 to 37 °C, polymer **2.32** had the highest T_g (and shortest spacer), and polymer **2.34** had the lowest T_g (and longest spacer).

Table 2.20: DSC Results for Demetallated Polythioethers **2.32-2.34**

Polymer	**T_g Onset (°C)**
2.32	37
2.33	34
2.34	33

2.2.3 Synthesis of Polyaromatic Thioethers

2.2.3.1 Synthesis of Polyaromatic Thioethers Coordinated to Cationic Cyclopentadienyliron Moieties

p-Polyphenylene sulfide (PPS) is a well-known engineering thermoplastic that has been the topic of many studies.[41-45] This polymer is usually prepared under very harsh conditions, and its insolubility below 200 °C limits the processability of this material. Reactions of *p*-, *m*-, and *o*-dichlorobenzene complexes (**2.1, 2.35, 2.36**) with 4,4'-thiobisbenzenethiol (**2.37**) gave the corresponding organoiron polyphenylene sulfides (**2.38-2.40**) as yellow solids in very high yields (92-96%) (Scheme 2.5). The synthesis of these cyclopentadienyliron-coordinated polymers occurred very rapidly, and could be readily observed by the viscous nature of the reaction solution within approximately thirty minutes. These organometallic polymers were soluble in polar solvents such as DMAc, DMF and DMSO but displayed very limited solubility in less polar solvents such as acetone, acetonitrile and dichloromethane. The results of the solubility studies of these polymers are given in Table 2.21.

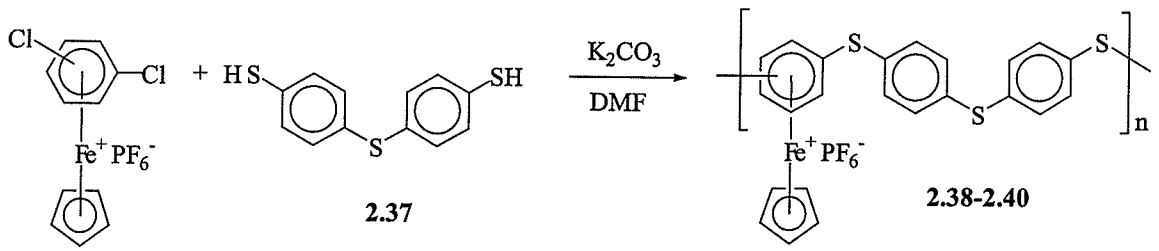

2.1; Cl = *p*-
2.35; Cl = *m*-
2.36; Cl = *o*-

Scheme 2.5

Table 2.21: Solubility of Organoiron Polymers[a]

	Solvent					
Polymer	**CH_2Cl_2**	**Acetone**	**CH_3CN**	**DMAc**	**DMF**	**DMSO**
2.38	I	I	PS	S	S	S
2.39	I	I	PS	PS	PS	S
2.40	I	I	PS	PS	PS	S

[a]Solubility at room temperature: (S), soluble; (PS), partially soluble; (I), insoluble.

In the ^1H NMR spectra of these polyaromatic thioethers, there were singlets corresponding to the cyclopentadienyl resonances appearing from 5.12 to 5.14 ppm. The complexed aromatic protons of the dichloroarene complex **2.1** appeared at 6.99 ppm, and were shifted upfield in polymers **2.38-2.40** to 6.18-6.58 ppm. The spectrum of polymer **2.38** is shown in Figure 2.13. The singlet at 6.32 ppm demonstrates the equivalence of the four complexed aromatic protons, and indicates that both of the chloro groups were successfully displaced by the dinucleophile. In contrast, the spectrum of polymer **2.39** had three signals from 6.18-6.58 ppm, representative of the *m*- substitution pattern expected for this polymer. Similarly, **2.40**, with the *o*-substituted complexed aromatic ring had two signals at 6.19 and 6.31 ppm, which were assigned to the complexed aromatic protons. In the ^{13}C NMR spectra of these polymers, the complexed aromatic resonances of the *p*-, *m*- and *o*-substituted organoiron polyphenylene sulfides (**2.38-2.40**) ranged from 83-87 ppm. In particular, the presence of one Cp resonance from 79-80 ppm indicated successful polymer formation. The ^{13}C NMR spectrum of polymer **2.38** is shown in Figure 2.14. The ^1H and ^{13}C NMR data for polymers **2.38-2.40** are given in Tables 2.22 and 2.23, respectively.

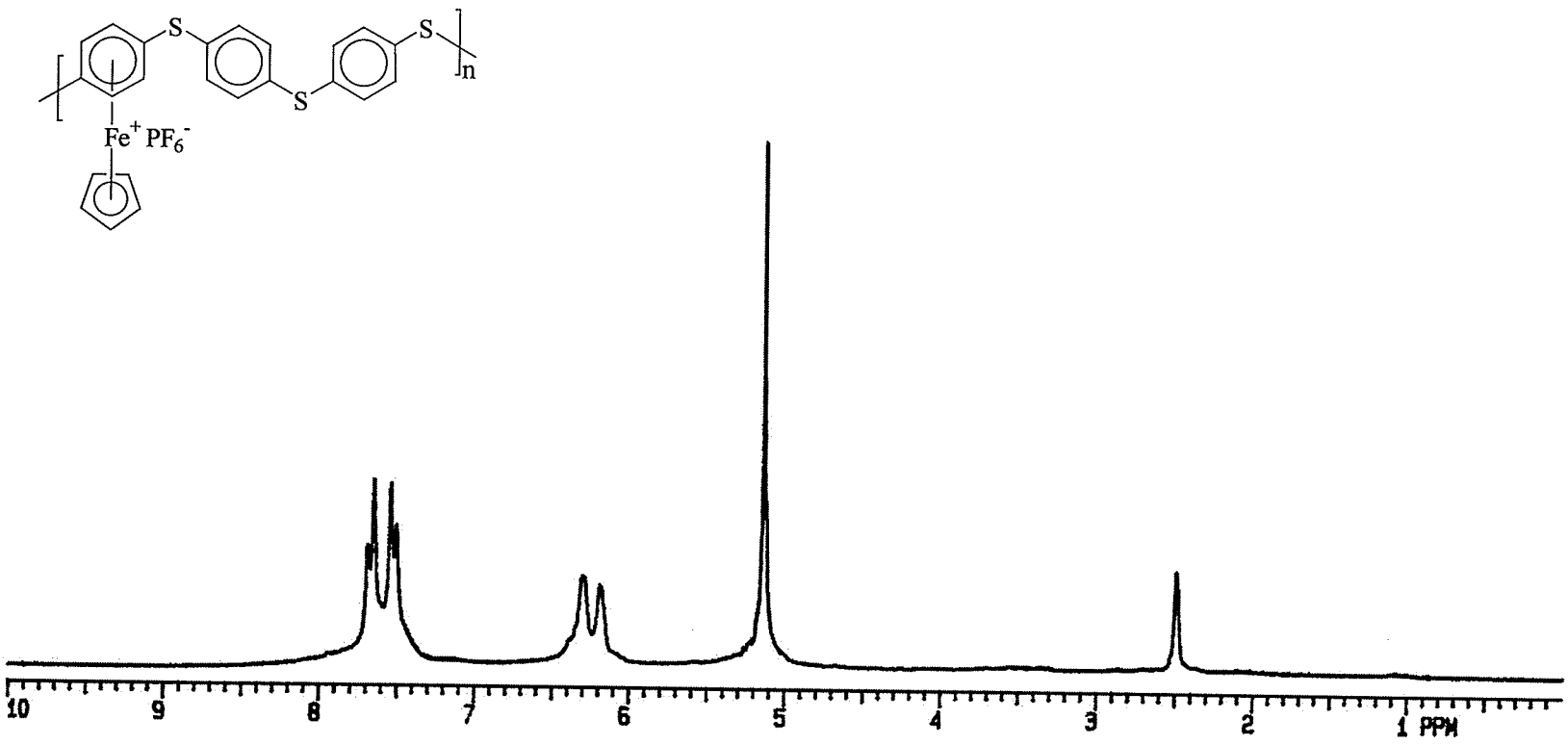

Figure 2.13: ^{1}H NMR spectrum of polymer **2.38** in DMSO-d_6

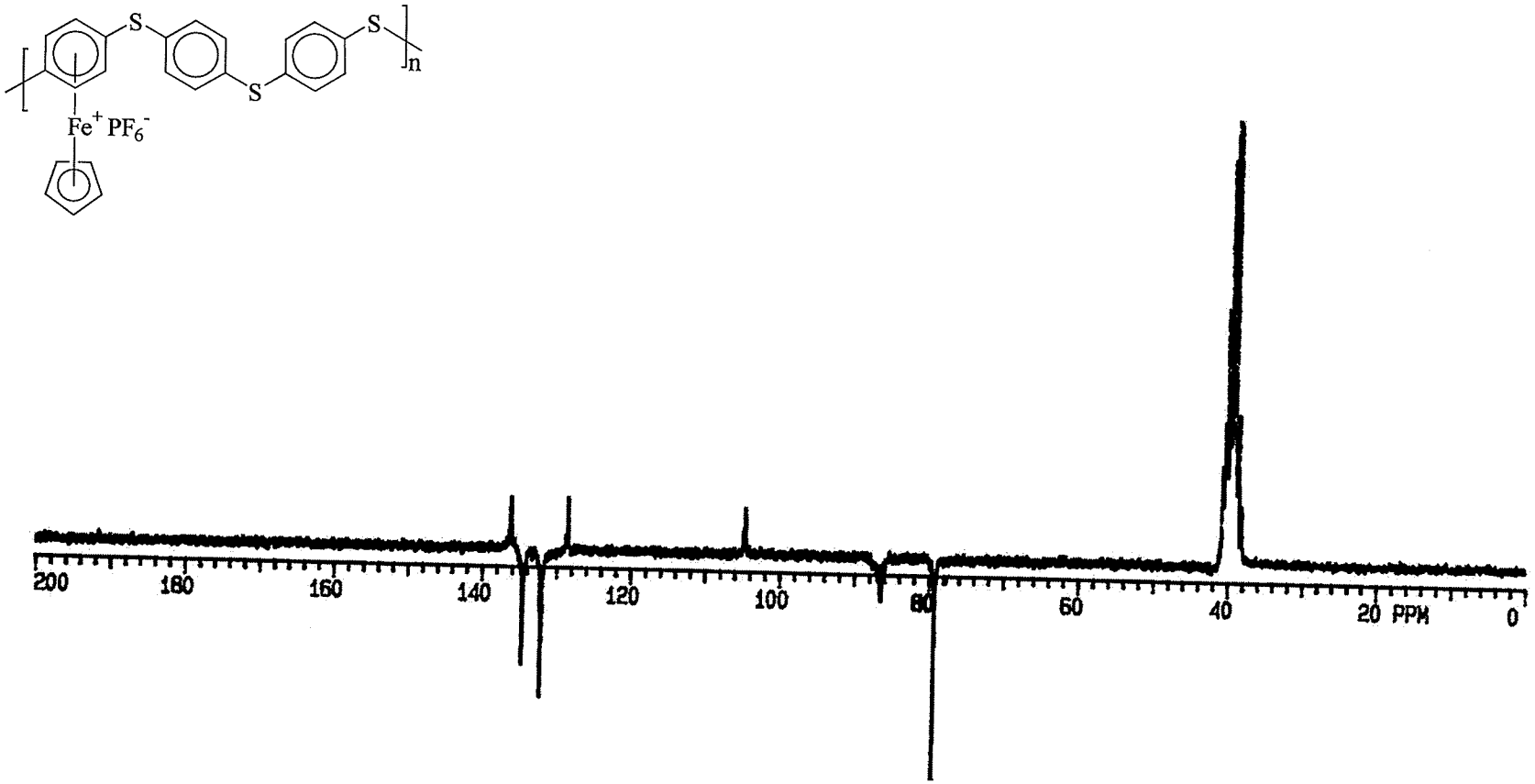

Figure 2.14: ^{13}C NMR spectrum of polymer **2.38** in DMSO-d_6

Table 2.22: % Yield and ^{1}H NMR Analysis of Polymers **2.38-2.40** in DMSO-d_6

Polymer	% Yield	Cp	Complexed Ar	Ar
2.38	96	5.14 (s, 5H)	6.32 (s, 4H)	7.51 (d, *J*=8.26 Hz, 4H), 7.66 (d, *J*=8.26 Hz, 4H)
2.39	96	5.12 (s, 5H)	6.18 (br. s, 1H), 6.38 (br. s, 2H), 6.58 (br. s, 1H)	7.50 (d, *J*=7.77 Hz, 4H), 7.65 (d, *J*=7.77 Hz, 4H)
2.40	92	5.14 (s, 5H)	6.19 (br. s, 2H), 6.31 (br. s, 2H)	7.53 (d, *J*=7.69 Hz, 4H), 7.67 (d, *J*=7.70 Hz, 4H)

Table 2.23: ^{13}C NMR Analysis of Polymers **2.38-2.40** in DMSO-d_6

Polymer	Cp	Complexed Ar	Ar
2.38	79.62	85.32, 106.06*	128.11*, 132.14, 135.41, 136.61*
2.39	79.85	83.11, 83.80, 87.04, 107.59*	127.84*, 132.19, 135.61, 136.91*
2.40	79.23	86.46, 86.90, 104.79*	128.62*, 132.05, 134.53, 136.23*

*Denotes quaternary carbons

2.2.3.2 Isolation of the Organic Polyaromatic Thioethers

Photolytic demetallation of the aromatic polythioethers was achieved in a dimethylformamide solution due to the poor solubility of these polymers (**2.38-2.40**) in acetonitrile and dichloromethane as shown in Scheme 2.6. Upon cleavage of the cyclopentadienyliron cations from the polymer backbones, polymer **2.41** and **2.42** were insoluble in all solvents tested, while polymer **2.43** displayed fair solubility in polar solvents such as chloroform. The reason for the enhanced solubility of polymer **2.43** is because the *ortho*-substituted benzene ring decreases the rigidity of this polymer in comparison to the *para*- and *meta*-substituted polymers.

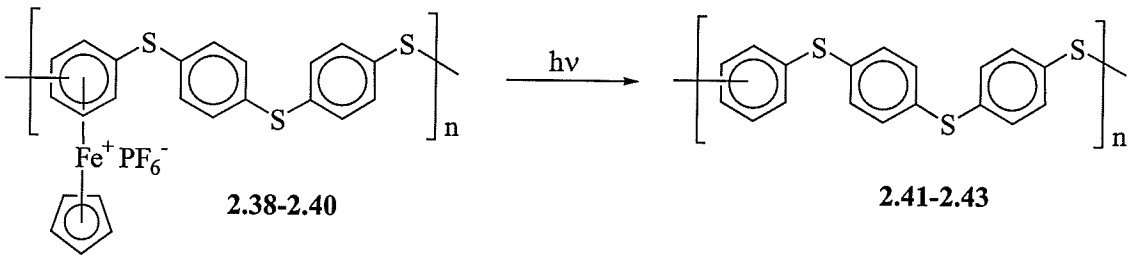

2.38-2.40 **2.41-2.43**

Scheme 2.6

NMR analysis was performed on polymer **2.43** in deuterated chloroform. The ^{1}H and ^{13}C NMR spectra of **2.43** are shown in Figures 2.15 and 2.16 and the data are given in Table 2.24. The ^{1}H NMR spectrum shows two broad singlets at 7.14 and 7.21 ppm, integrating for four and eight protons, respectively. The ^{13}C NMR spectrum shows three CH, and three quaternary aromatic carbon peaks at 128.01, 131.67, 132.00 and 133.87, 134.66 and 137.04 ppm, respectively.

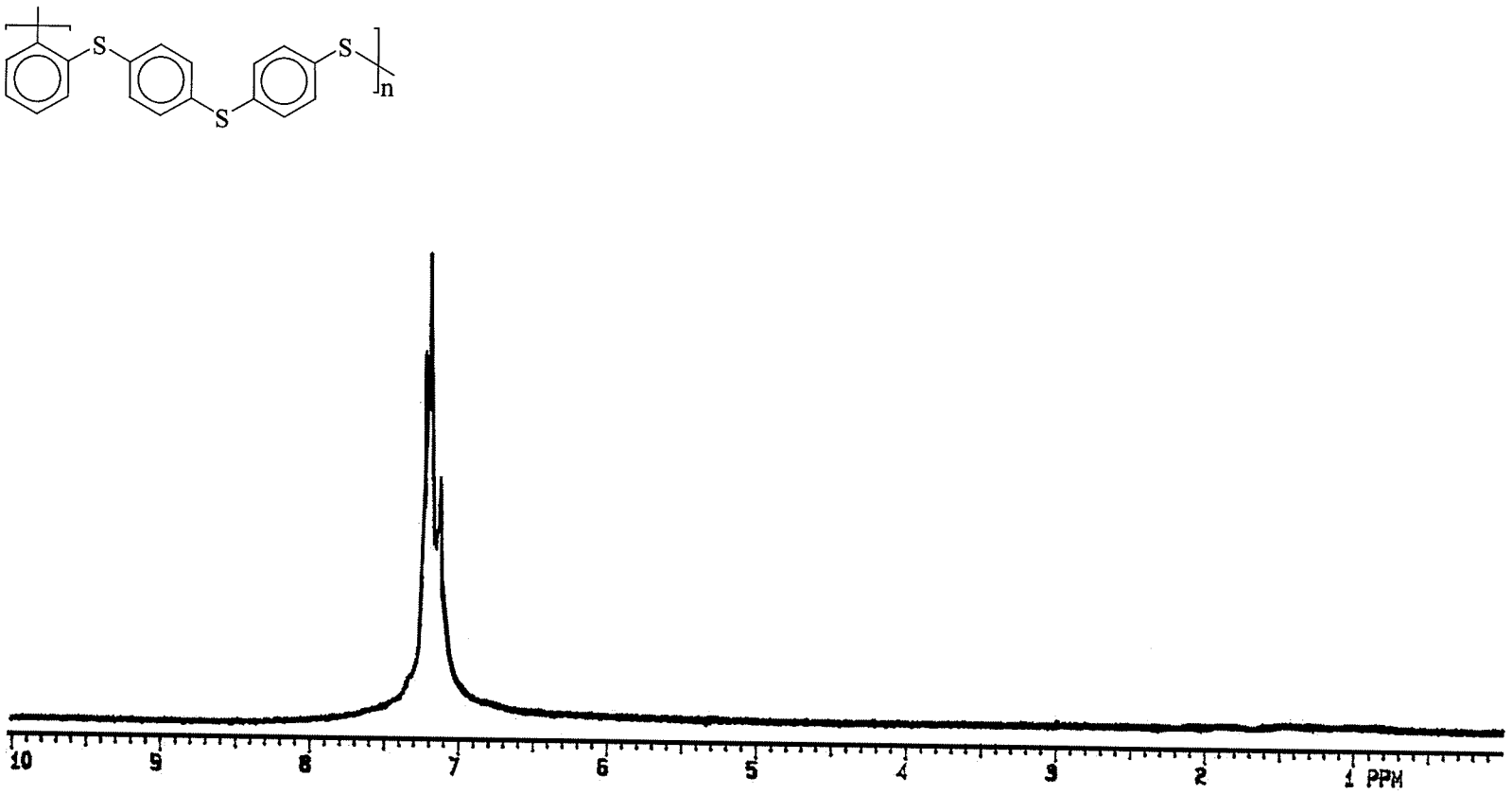

Figure 2.15: ^{1}H NMR spectrum of polymer **2.43** in $CDCl_3$

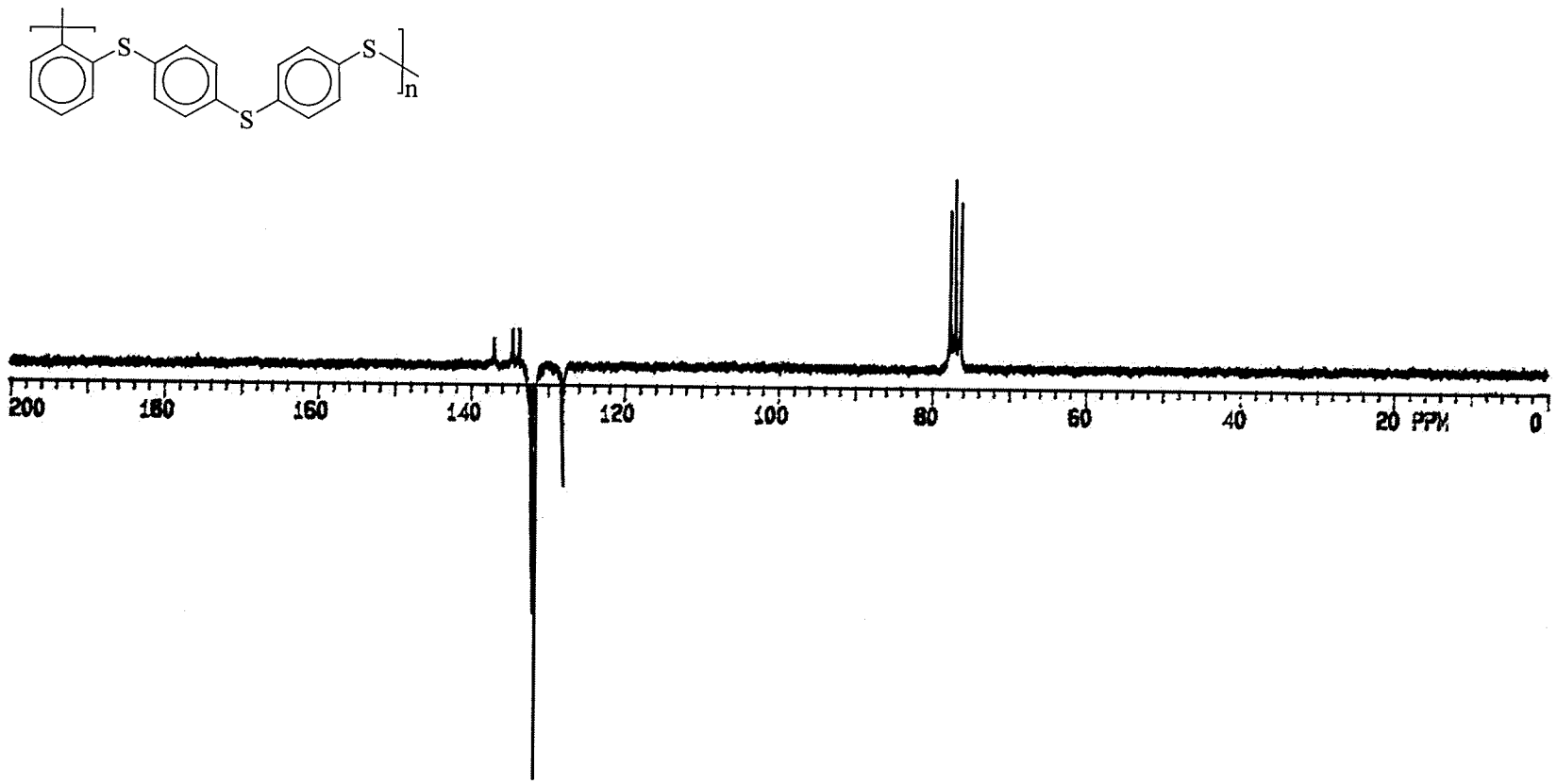

Figure 2.16: ^{13}C NMR spectrum of polymer **2.43** in $CDCl_3$

Table 2.24: % Yield, ^{1}H and ^{13}C NMR Analysis of **2.41-2.43** in $CDCl_3$

Polymer	% Yield	^{1}H NMR	^{13}C NMR
2.41	81		
2.42	78		
2.43	72	7.14 (br. s, 4H, ArH), 7.21 (br. s, 8H, ArH)	128.01, 131.67, 132.00, 133.87*, 134.66*, 137.04*

*Denotes quaternary carbons

The molecular weight of the soluble portion of polymers **2.43** was determined using gel permeation chromatography. The M_w of the *o*-substituted polymer (**2.43**) was found to be 16 200 with a polydispersity index of 3.0. This corresponds to a degree of polymerization of about fifty and a molecular weight for the metallated analogue (**2.40**) of 29 500.

Table 2.25: Molecular Weight Analysis of **2.41-2.43**

Polymer	M_w	M_n	M_w/M_n
2.41	insoluble		
2.42	insoluble		
2.43	16 200	5 400	3.0

2.2.3.3 Thermal Properties of the Organometallic and Organic Polyaromatic Thioethers

The thermal properties of the *p*-, *m*- and *o*-substituted polyphenylene sulfides (**2.41-2.43**) were also examined using TGA and DSC. Figure 2.17 shows the TGA thermograms of the cyclopentadienyliron-coordinated polymers. The TGA results for these materials showed that the thermal stability of these polymers decreased in the order: *p*- > *m*- > *o*-. Figure 2.18 shows a comparison between the metallated and demetallated analogues of the *meta*-substituted polymers **2.39** and **2.42**. It can be seen that the metal moieties are no longer present in the thermogram of **2.42** and that the weight losses corresponding to decomposition of the polymer backbones occur at approximately the same temperature. Although the onsets for the weight losses of the metallated polymers are lower than those of their organic analogues, the midpoints of the weight losses are virtually the same. Tables 2.26 and 2.27 provide the TGA data for the organoiron (**2.38-2.40**) and organic (**2.41-2.43**) polyaromatic thioethers, respectively.

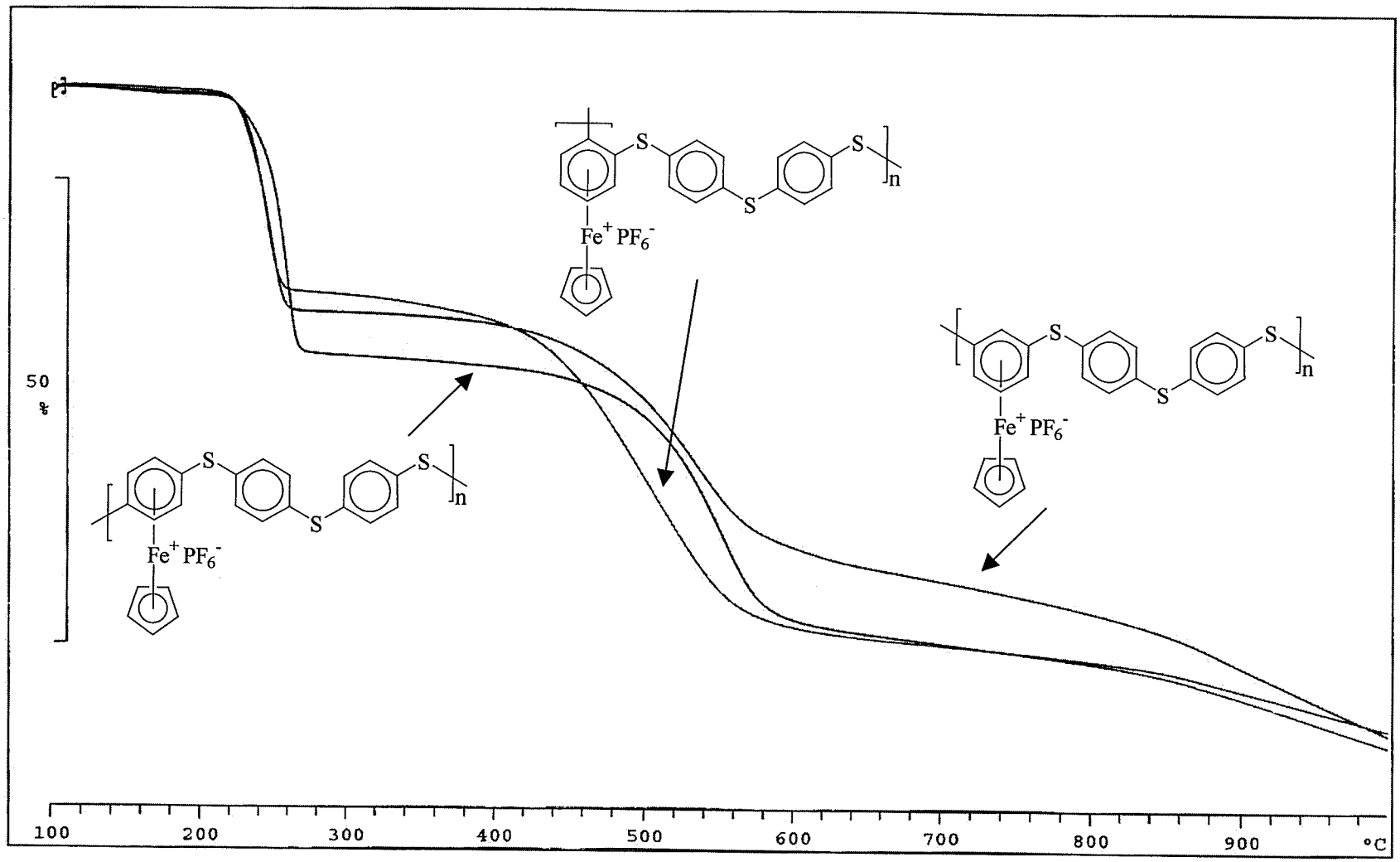

Figure 2.17: TGA thermograms of polymers **2.38-2.40**

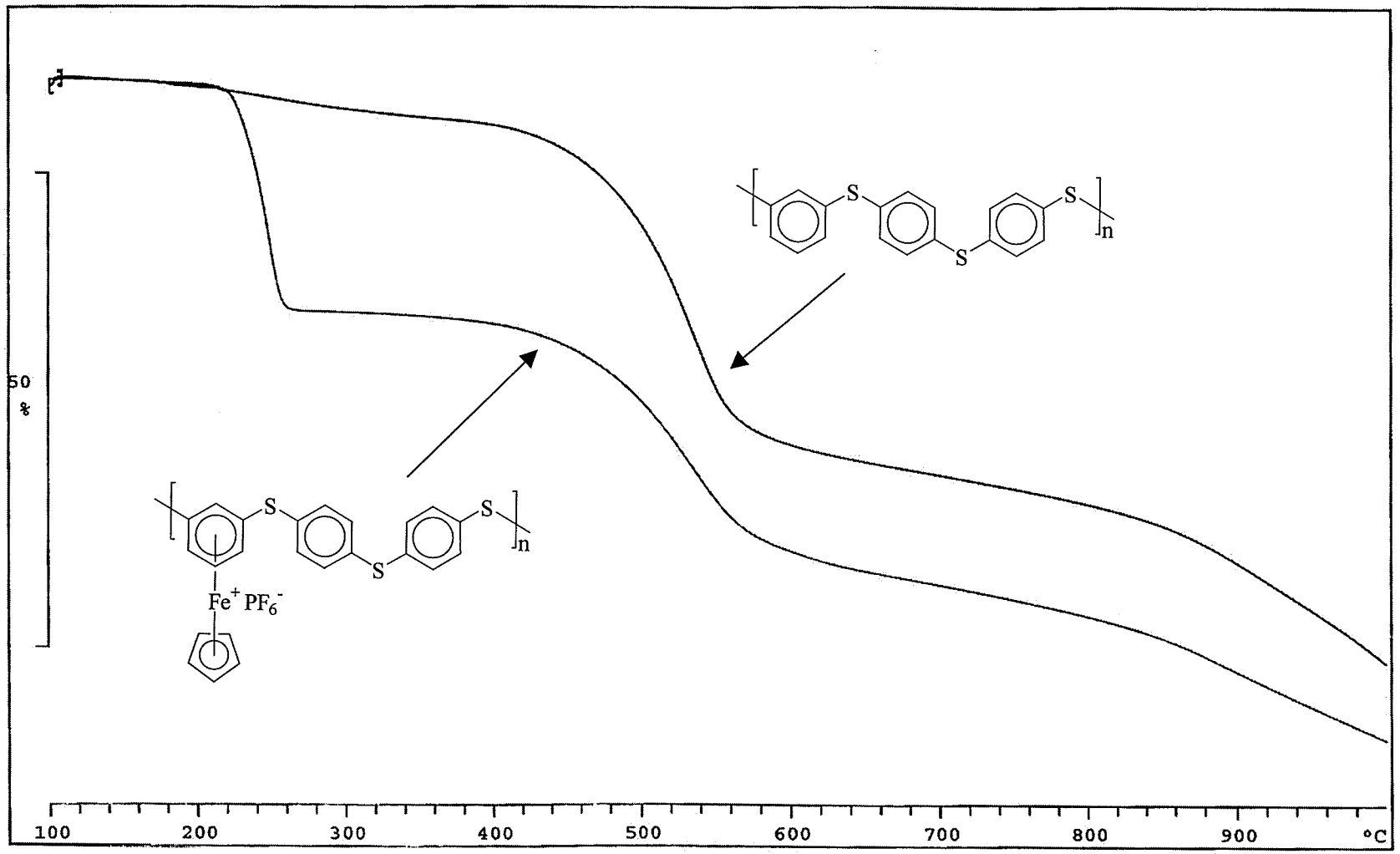

Figure 2.18: TGA thermograms of polymers **2.39** and **2.42**

Table 2.26: TGA Results for Organometallic Polyaromatic Thioethers **2.38-2.40**

Polymer	Weight loss (%)	T_{onset} (°C)	$T_{midpoint}$ (°C)	T_{endset} (°C)
2.38	28	245	255	265
	28	511	544	581
2.39	24	231	243	256
	26	478	527	574
2.40	21	231	241	252
	34	443	500	560

Table 2.27: TGA Results for Organic Polyaromatic Thioethers **2.41-2.43**

Polymer	Weight loss (%)	T_{onset} (°C)	$T_{midpoint}$ (°C)	T_{endset} (°C)
2.41	42	512	538	566
2.42	36	491	529	566
2.43	57	448	497	564

The DSC thermograms of polymers **2.41-2.43** were also obtained. The T_g of the *o*- substituted polymer was 88 °C, followed by the *p*-substituted polymer at 86 °C, while the *m*-substituted polymer's T_g was 72 °C. The DSC trace of the *p*-substituted polyphenylene sulfide is shown in Figure 2.19. This curve shows a glass transition at 86 °C, a crystallization at 140 °C and a melting of the polymer at 278 °C. These values are in agreement with literature T_g and T_m values for *p*-polyphenylene sulfide, which are 85 and 285 °C, respectively.[287] This confirms that the *p*-polyphenylene sulfide prepared in this study has approximately the same molecular weight as the commercially produced PPS. This molecular weight is consistent with the molecular weight obtained for the *m*-substituted polymer reported in this study.

Table 2.28: DSC Results for Organic Polyaromatic Thioethers **2.41-2.43**

Polymer	**T_g Onset (°C)**
2.41	86
2.42	72
2.43	88

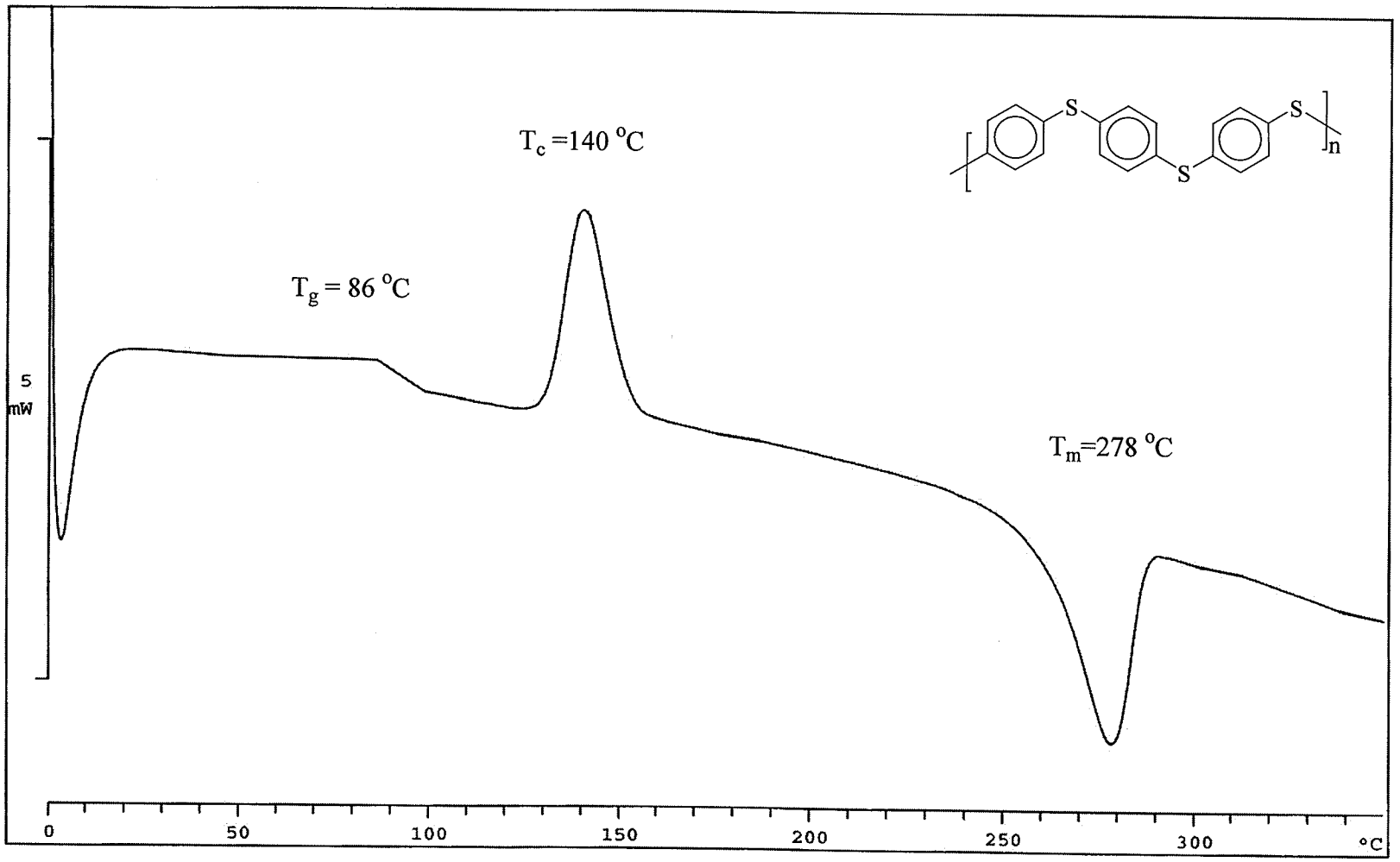

Figure 2.19: DSC trace of polymer **2.41**

2.2.4 Design of Polymers Containing Alternating Ether/thioether and Amine/thioether Bridges

2.2.4.1 Design of Organoiron Polymers Containing Alternating Ether/thioether and Amine/thioether Bridges

In addition to polymers that contained strictly aromatic or aliphatic bridges or ether or thioether linkages, polymers containing alternating systems were also designed. Scheme 2.7 details the synthesis of polymers with alternating ether/thioether bridges. Polymers **2.46** and **2.47** were synthesized by first preparing diiron complex **2.45**, which was subsequently reacted with an aromatic or aliphatic dithiol. Two different dithiols were explored, 4,4'-thiobisbenzenethiol (**2.37**) and 1,8-octanedithiol (**2.28**).

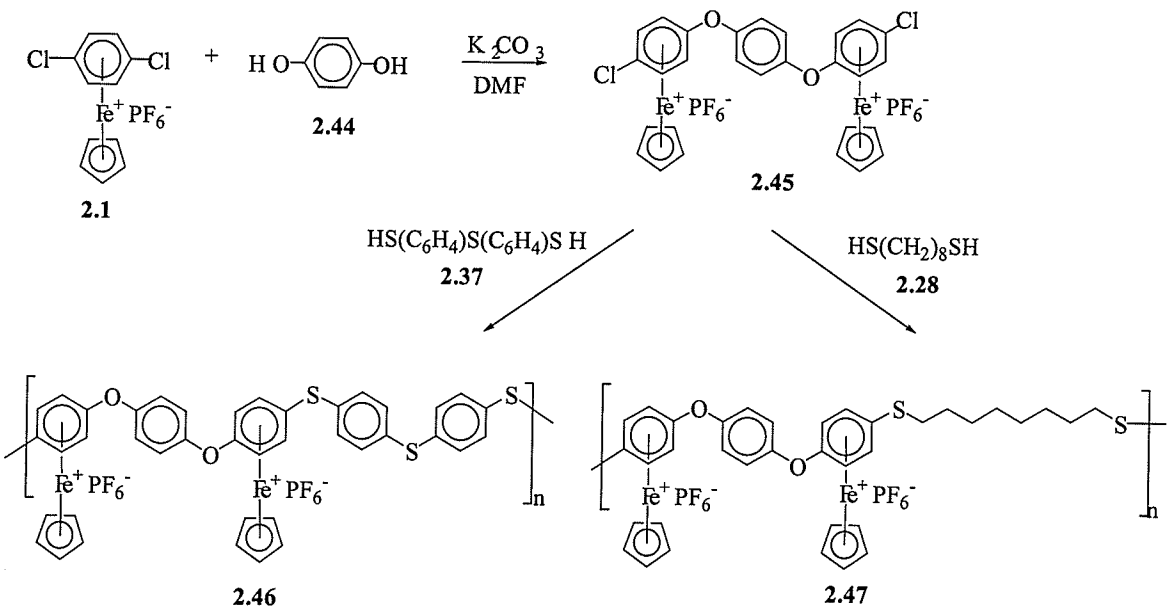

Scheme 2.7

The two resulting polymers (**2.46, 2.47**) had very different solubilities due to their respective aromatic and aliphatic thioether bridges. Although both of these polymers were soluble in polar organic solvents while coordinated to the cyclopentadienyliron moiety, polymer **2.47**, with the aliphatic spacer was much more soluble in organic solvents such as acetone, acetonitrile and dichloromethane than **2.46**. The fully aromatic polymer **2.46** could only be solubilized in very polar solvents such as DMSO and DMF, and often formed a gel. Table 2.29 provides the comparative solubilities of the two organoiron polyether/thioethers.

Table 2.29: Solubility of Organoiron Polymers[a]

	Solvent					
Polymer	**CH_2Cl_2**	**Acetone**	**CH_3CN**	**DMAc**	**DMF**	**DMSO**
2.46	I	I	PS	S	S	S
2.47	PS	PS	S	S	S	S

[a]Solubility at room temperature: (S), soluble; (PS), partially soluble; (I), insoluble.

Polymer **2.46** showed two distinct complexed aromatic resonances in its ^1H NMR spectrum due to its etheric and thioetheric linkages. These signals appeared in the ^1H spectrum of **2.46** at 6.32 and 6.41 ppm, while in the ^1H NMR spectrum of **2.47** the non-equivalent complexed aromatic protons appeared as a broad singlet at 6.42 ppm. The ^{13}C NMR spectra of these two polymers showed two distinct complexed aromatic (CH) resonances at 76.19 and 85.08 for **2.46** and 76.20 and 83.58 ppm for **2.47**. The ^1H and ^{13}C NMR spectra of **2.47** are shown in Figures 2.20 and 2.21.

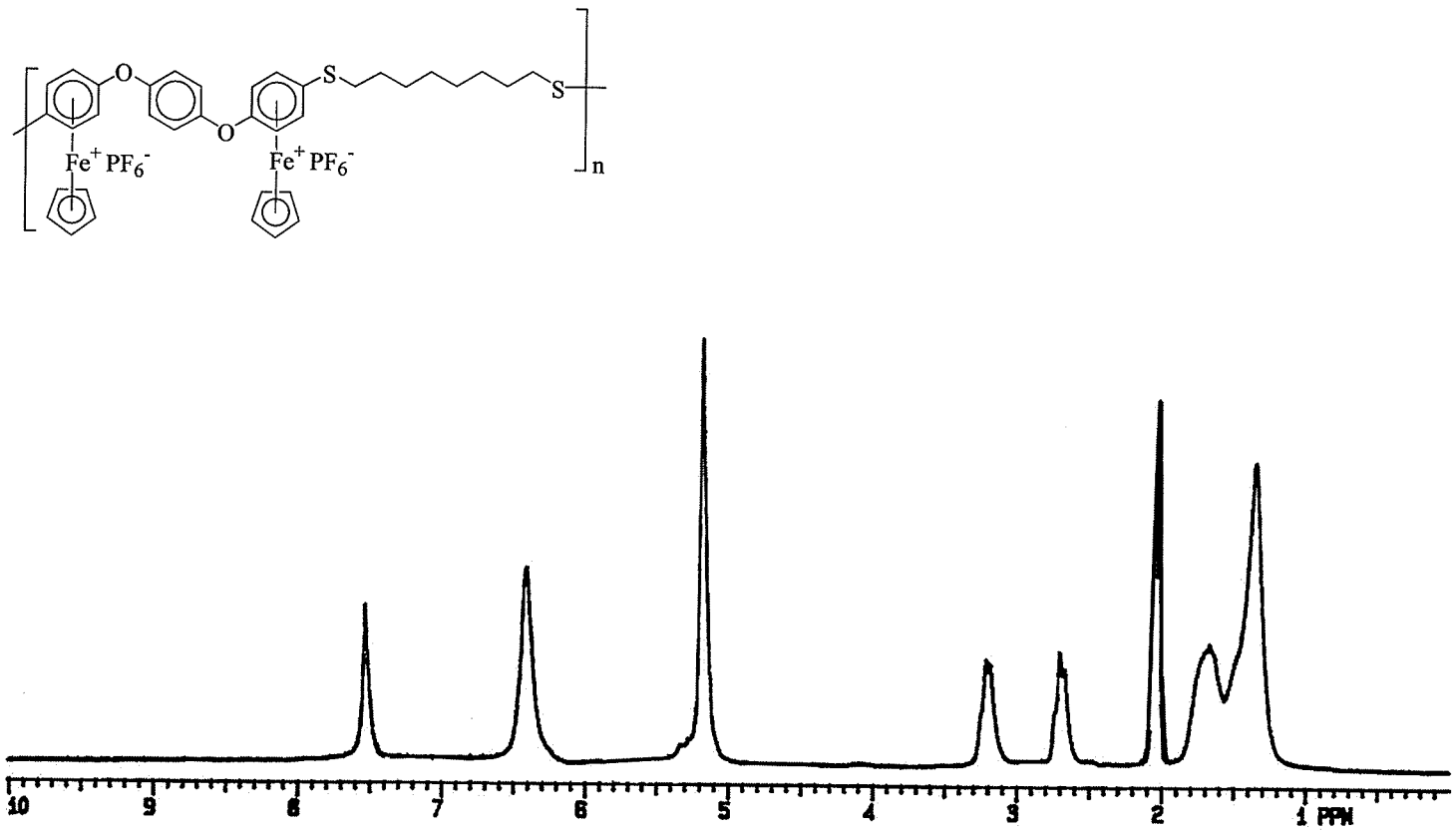

Figure 2.20: ^{1}H NMR spectrum of polymer **2.47** in acetone-d_6

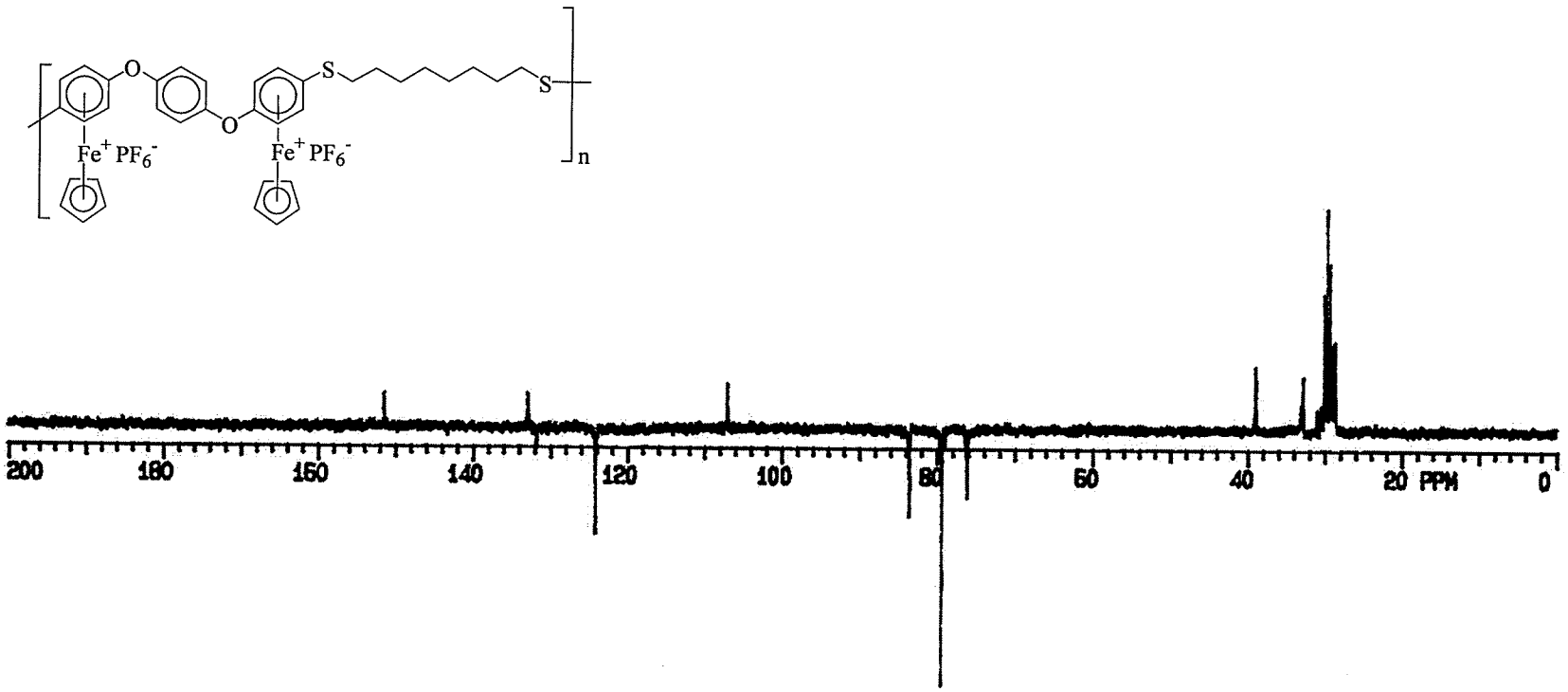

Figure 2.21: ^{13}C NMR spectrum of polymer **2.47** in acetone-d_6

The mixed ether/thioether polymers were isolated as beige or yellow solids in 95 and 97 % yield for polymer **2.46** and **2.47**, respectively. The ^{1}H NMR data for polymers **2.46** and **2.47** are given in Table 2.30, while the ^{13}C NMR data for these polymers are given in Table 2.31.

Table 2.30: ^{1}H NMR Analysis of Polymers **2.46** in DMSO-d_6 and **2.47** in Acetone-d_6

Polymer	% Yield	CH_2	Cp	Complexed Ar	Ar
2.46	97		5.21 (s, 10H)	6.32 (d, *J*=6.60 Hz, 4H), 6.41 (d, *J*=6.60 Hz, 4H)	7.50 (s, 4H), 7.52 (d, *J*=6.60 Hz, 4H), 7.66 (d, *J*=8.26 Hz, 4H)
2.47	95	1.35 (br. s, 4H), 1.67 (br. s, 4H), 2.70 (br. s, 4H), 3.22 (br. s, 4H)	5.19 (s, 10H)	6.42 (br. s, 8H)	7.54 (s, 4H)

Table 2.31: ^{13}C NMR Analysis of Polymers **2.46** in DMSO-d_6 and **2.47** in Acetone-d_6

Polymer	CH_2	Cp	Complexed Ar	Ar
2.46		78.69	76.19, 85.08, 103.27*, 129.09*	123.03, 131.84*, 132.05, 134.78, 136.28*, 150.57*
2.47	29.82, 30.20, 32.90, 39.00	79.39	76.20, 83.58, 107.07*, 132.90*	124.14, 151.56*

*Denotes quaternary carbons

Scheme 2.8 describes the synthesis of diiron complexes containing amine bridges (**2.50, 2.51**). These complexes were synthesized in 74 and 76 % yields, respectively by reaction of two equivalents of complex **2.1** with one equivalent of the diamine compounds (**2.48, 2.49**). The orange precipitates were analyzed using ^{1}H and ^{13}C NMR spectroscopy as well as by CH Analysis as shown in Tables 2.32 and 2.33. Complex **2.51** was also analyzed using HH and CH COSY NMR in order to identify all of the alkyl peaks.

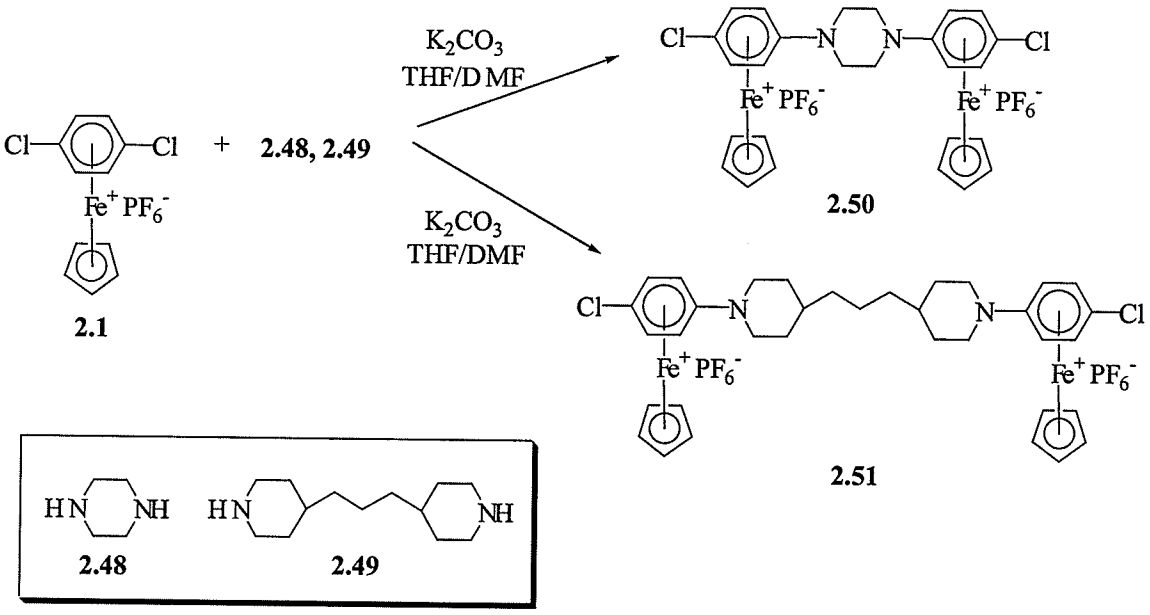

Scheme 2.8

Figures 2.22 and 2.23 show the ^{1}H and ^{13}C NMR spectra of complex **2.51**. The interesting feature of the ^{1}H NMR spectrum of complex **2.51** is that the protons of the methylene groups on the cyclic units (H_a and H_b) appeared as four separate peaks rather than two. Figure 2.22 has a labeled structure that was used to assign the following alkyl

protons. The multiplet at 1.35 ppm corresponds to H_d and H_b', while the broad peak at 1.47 was assigned to H_e. The singlet at 1.64 ppm corresponds to the two H_c protons while the doublet at 1.93 ppm corresponds to H_b". The triplet at 3.05 ppm integrating for four protons is assigned as H_a', while the four protons at 4.01 ppm are assigned to H_a". The singlet integrating for ten protons at 5.14 was assigned to the cyclopentadienyl protons, while two doublets at 6.05 and 6.51 ppm corresponded to the complexed aromatic protons. In contrast to the complexity observed in the ^{1}H NMR spectrum of **2.51**, the spectrum of **2.50** showed only one singlet corresponding to the methylene protons.

The ^{13}C NMR spectrum of complex **2.51** was also quite simple relative to the ^{1}H NMR spectrum. The methylene carbons can be seen in Figure 2.24 at 24.24, 32.13, 36.92 and 47.66 ppm, while the methine carbons appear at 35.41. The cyclopentadienyl carbons are present at 78.00, while the complexed aromatic CH carbons appear at 66.79 and 86.65 ppm and the quaternary complexed aromatics appear at 102.29 and 127.48 ppm.

The yields and ^{1}H NMR analysis of diiron complexes **2.50, 2.51** can be found in Table 2.32 and the CH and ^{13}C NMR data can be found in Table 2.33.

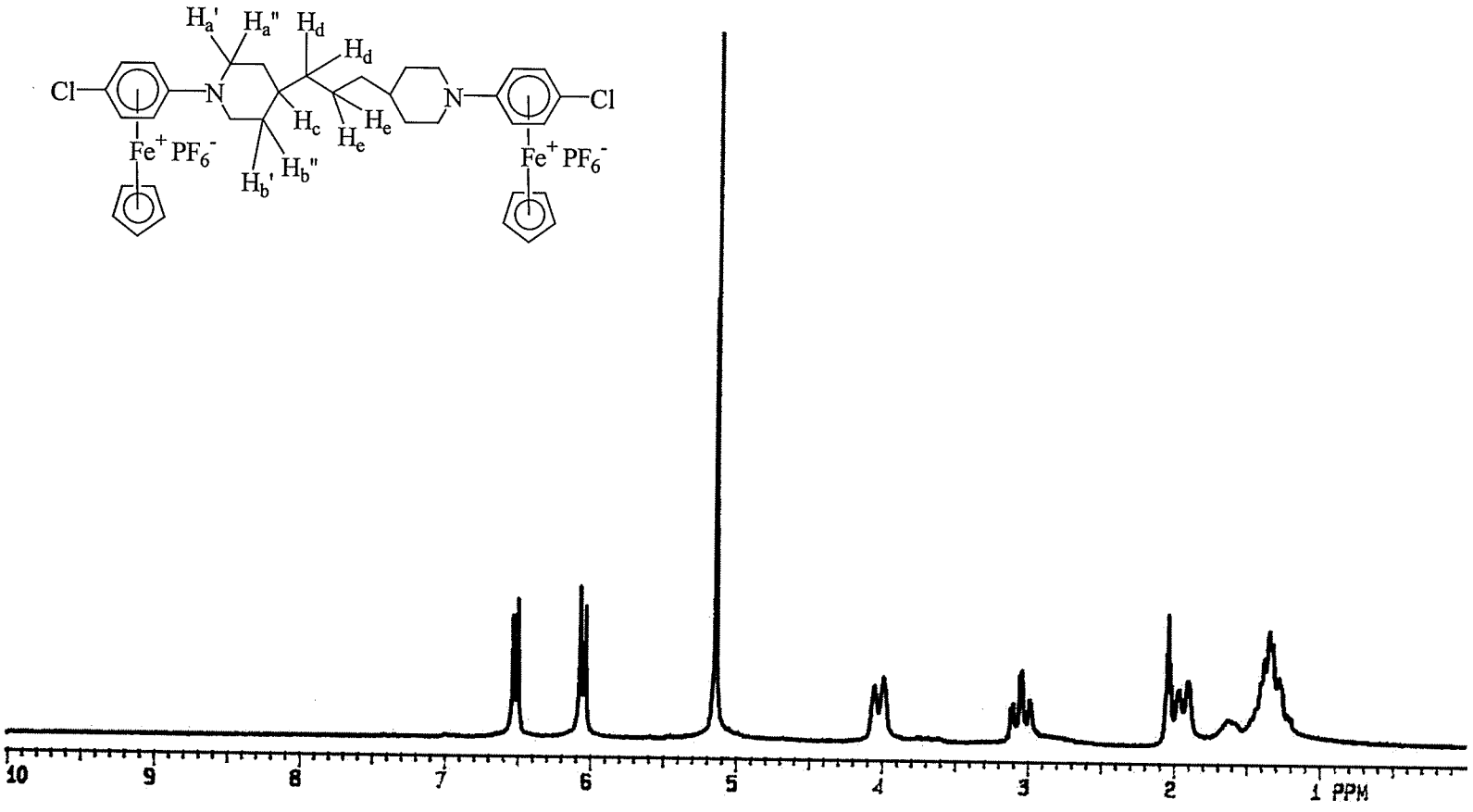

Figure 2.22: ^{1}H NMR spectrum of complex **2.51** in acetone-d_6

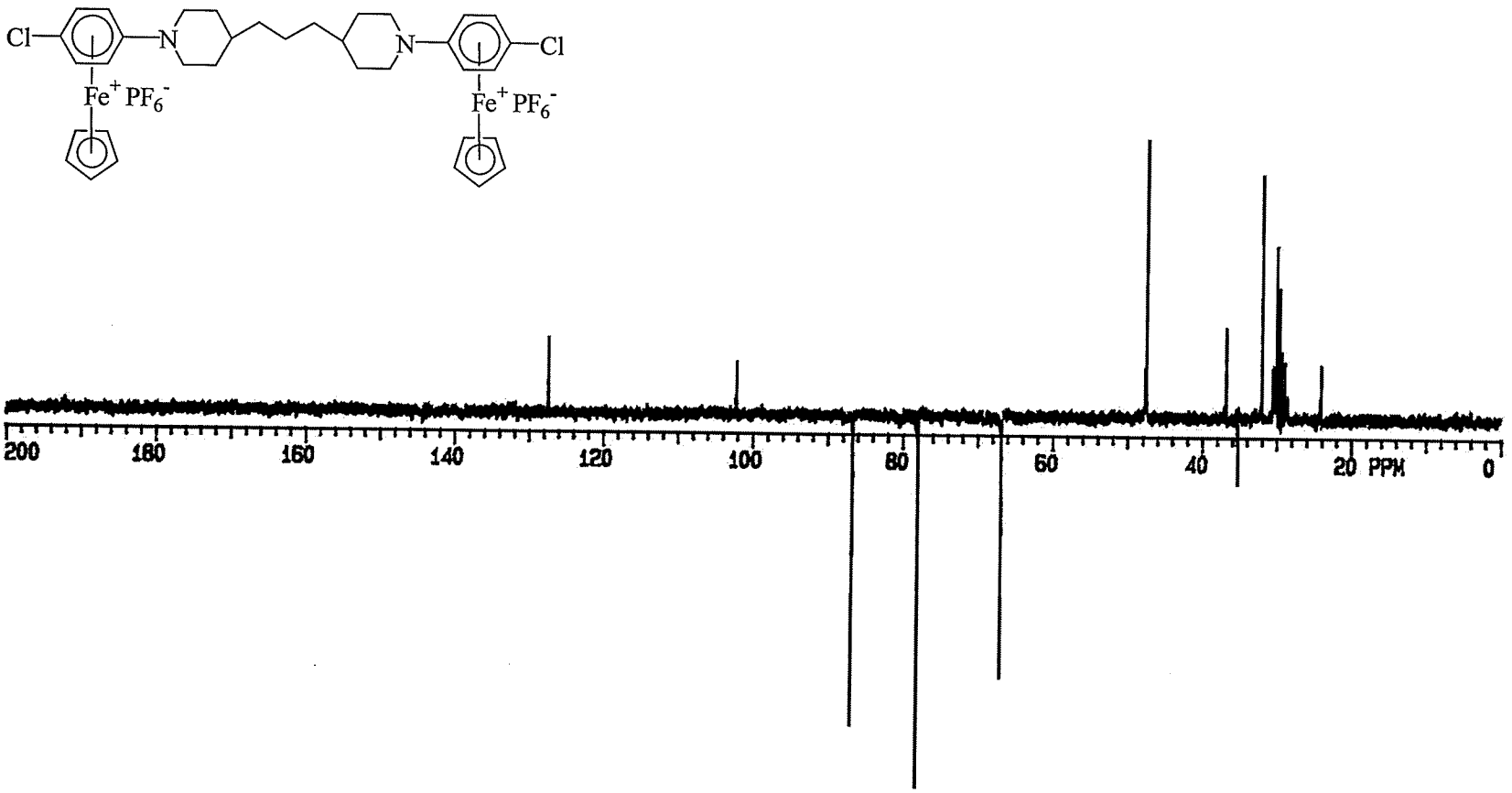

Figure 2.23: ^{13}C NMR spectrum of complex **2.51** in acetone-d_6

Table 2.32: % Yield and ^{1}H NMR Analysis of Diiron Complexes **2.50** and **2.51** in Acetone-d_6

Complex	% Yield	Other	Cp	Complexed Ar
2.50	74	3.83 (s, 8H, CH_2)	5.20 (s, 10H)	6.20 (d, *J*=7.24 Hz, 4H), 6.62 (d, *J*=7.20, 4H)
2.51	76	1.35 (m, 8H, CH_2), 1.47 (br. s, 2H, CH_2), 1.64 (s, 2H, CH), 1.93 (d, *J*=11.92 Hz, 4H, CH_2), 3.05 (t, *J*=11.56 Hz, 4H, CH_2), 4.01 (d, *J*=12.96 Hz, 4H, CH_2)	5.14 (s, 10H)	6.05 (d, *J*=7.12 Hz, 4H), 6.51 (d, *J*=7.04 Hz, 4H)

Table 2.33: CH and ^{13}C NMR Analysis of Diiron Complexes **2.50** and **2.51** in Acetone-d_6

Complex	CH analysis	Other	Cp	Complexed Ar
2.50	$C_{26}H_{26}Cl_2F_{12}Fe_2N_2P_2$: Found: C, 37.01; H, 3.21; N, 3.30 Calculated: C, 37.22; H, 3.12; N, 3.34	46.18 (CH_2)	78.42	68.43, 86.92, 102.79*, 125.91*
2.51	$C_{35}H_{42}Cl_2F_{12}Fe_2N_2P_2$: Found: C, 43.85; H, 4.52; N, 2.78 Calculated: C, 43.64; H, 4.39; N, 2.91	24.24 (CH_2), 32.13 (CH_2), 35.41(CH), 36.92 (CH_2), 47.66 (CH_2)	78.00	66.79, 86.65, 102.29*, 127.48*

*Denotes quaternary carbons

The synthesis of polymers **2.52** and **2.53** are shown in Scheme 2.9. These polymers, with alternating amine/thioether linkages were prepared by reacting the diiron amine complexes **2.50** and **2.51** with 4,4'-thiobisbenzenethiol (**2.37**). These polymers were isolated as orange precipitates in 93 and 98 % yield. The resulting polymers exhibited relatively good solubility in polar organic solvents, however, the solubility of **2.53** was slightly greater than that of polymer **2.52**. The results of solubility tests can be found in Table 2.34.

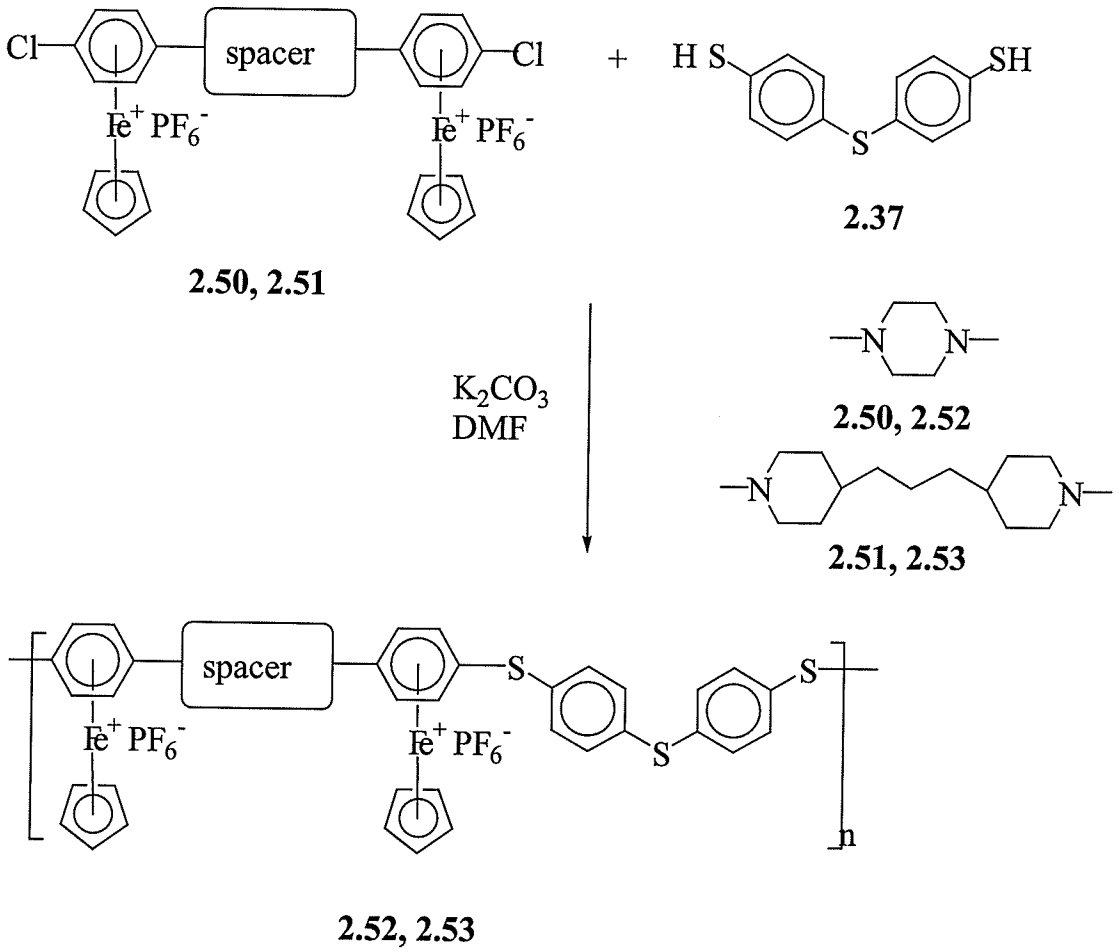

Scheme 2.9

Table 2.34: Solubility of Organoiron Polymers **2.52, 2.53**[a]

	Solvent					
Polymer	**CH_2Cl_2**	**Acetone**	**CH_3CN**	**DMAc**	**DMF**	**DMSO**
2.52	PS	PS	PS	S	S	S
2.53	PS	PS	PS	S	S	S

[a]Solubility at room temperature: (S), soluble; (PS), partially soluble; (I), insoluble.

Polymers **2.52** and **2.53**, with alternating amine/thioether linkages, each had two complexed aromatic (CH) resonances in their ^1H and ^{13}C NMR spectra. Figure 2.24 shows the ^1H NMR spectrum of polymer **2.53**. The aliphatic protons are seen between 1.21 and 3.84 ppm, and the cyclopentadienyl resonance appears at 5.00 ppm as a broad singlet. The complexed aromatic protons appear as two singlets and the uncomplexed aromatic protons also appear as two broad singlets. The peaks corresponding to the complexed and uncomplexed aromatic protons each integrated for four hydrogens.

Figure 2.25 shows the ^{13}C NMR spectrum of polymer **2.53**. There are four CH_2 resonances and one CH resonance, which is consistent with the proposed structure of this polymer. As well, there is one cyclopentadienyl resonance at 75.93 and two complexed aromatic CH carbons at 66.60 and 86.75 ppm. The quaternary complexed aromatic carbons are found at 95.81 and 125.69 ppm. There are two aromatic CH peaks consistent with the incorporation of the thioether bridge at 131.59 and 132.33 ppm and two corresponding quaternary carbon peaks at 131.85 and 134.58 ppm. The full ^1H and ^{13}C NMR data for polymers **2.52** and **2.53** are given in Tables 2.35 and 2.36.

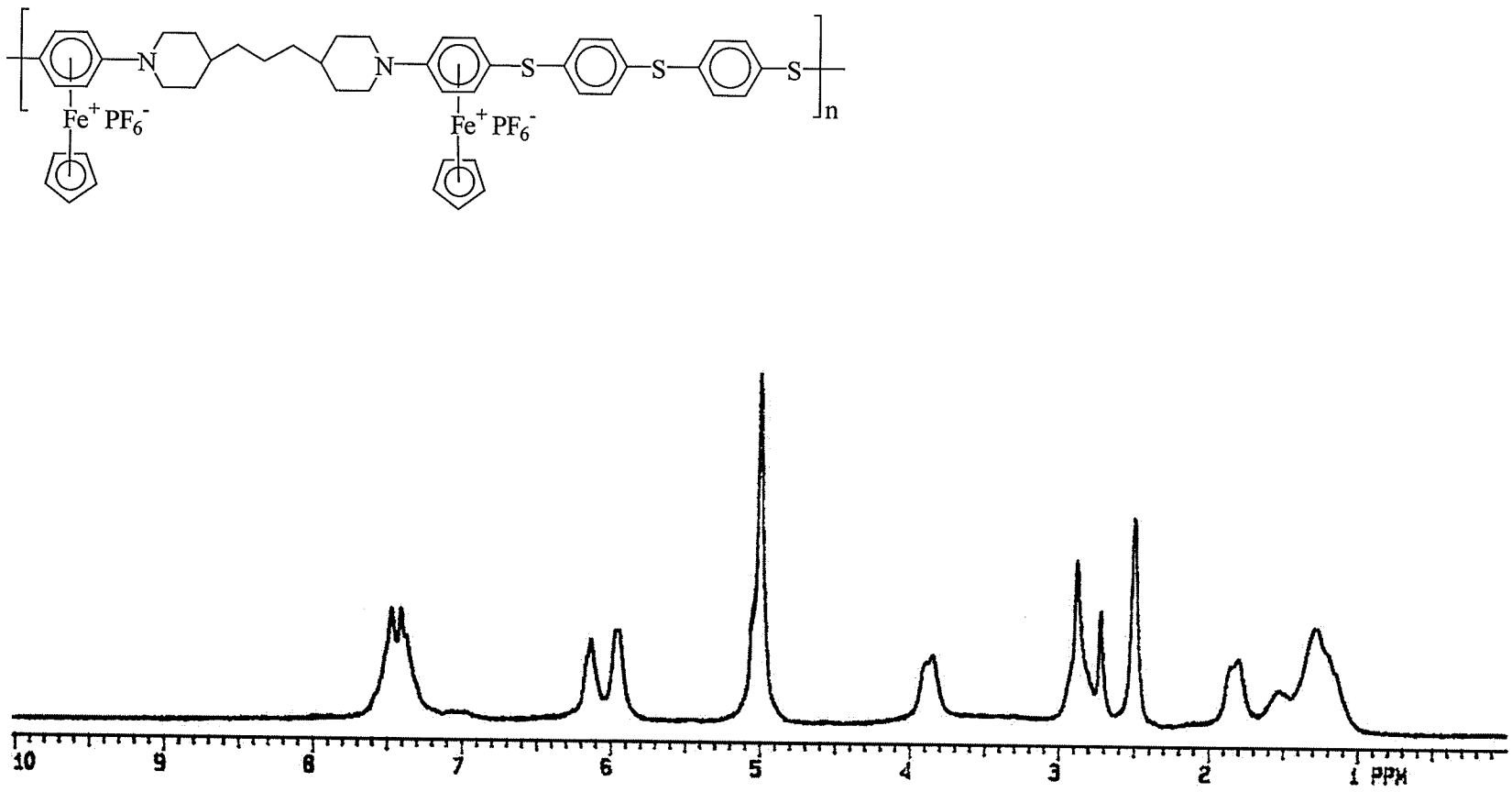

Figure 2.24: ^{1}H NMR spectrum of polymer **2.53** in DMSO-d_6

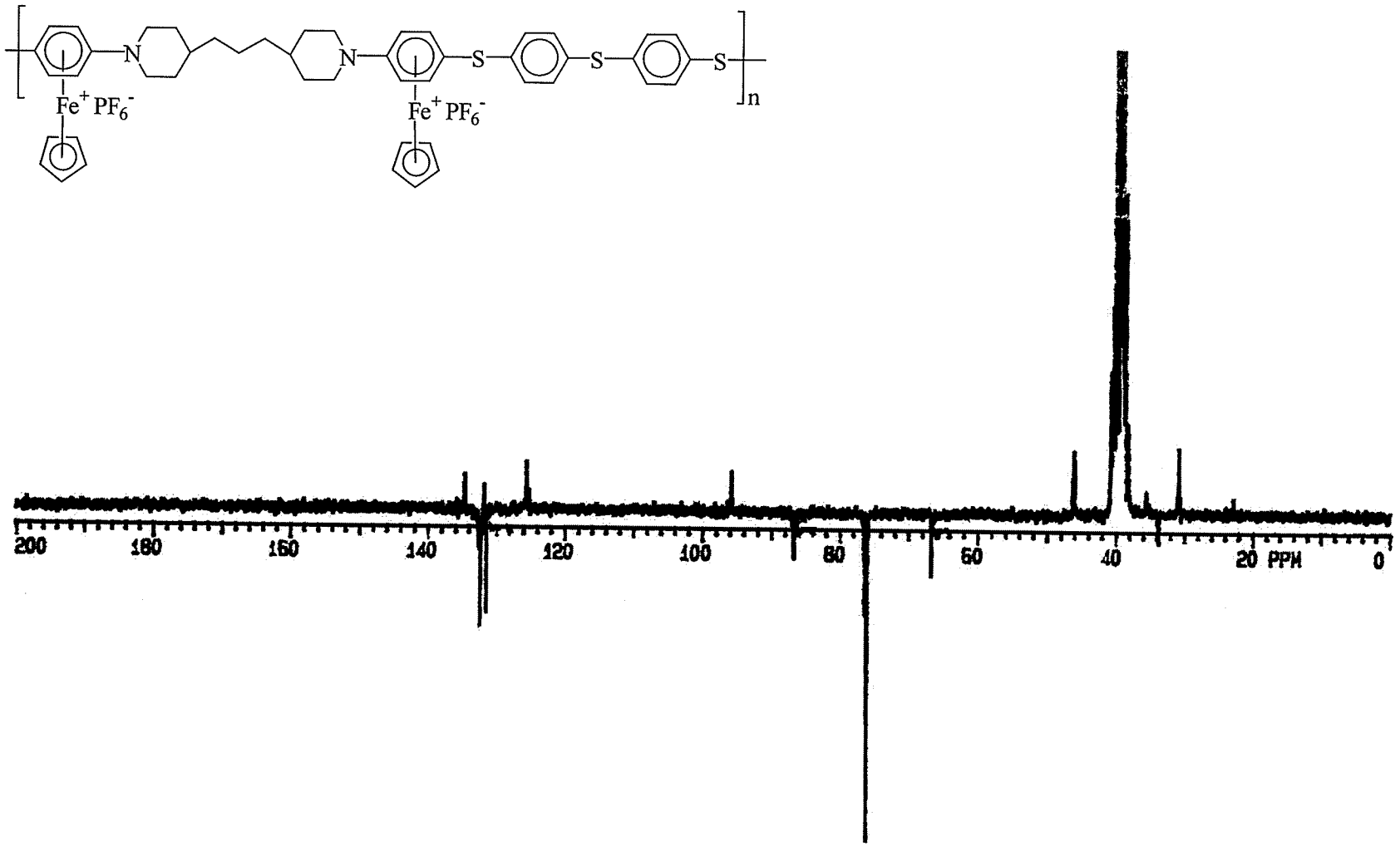

Figure 2.25: ^{13}C NMR spectrum of polymer **2.53** in DMSO-d_6

Table 2.35: % Yield and ^{1}H NMR Analysis of Polymers **2.52** and **2.53** in DMSO-d_6

Polymer	% Yield	Other	Cp	Complexed Ar	Ar
2.52	93	3.57 (s, 8H, CH_2)	5.06 (s, 10H)	6.09 (s, 4H), 6.22 (s, 4H)	7.43 (d, *J*=8.35 Hz, 4H), 7.53 (d, *J*=8.14 Hz, 4H)
2.53	98	1.21-1.61 (m, 12H, CH, CH_2), 1.79 (br. s, 4H, CH_2), 2.88 (s, 4H, CH_2), 3.84 (br. s, 4H, CH_2)	5.00 (s, 10H)	5.94 (s, 4H), 6.13 (s, 4H)	7.41 (br. s, 4H), 7.46 (br. s, 4H)

Table 2.36: ^{13}C NMR Analysis of Polymers **2.52** and **2.53** in DMSO-d_6

Polymer	Other	Cp	Complexed Ar	Ar
2.52	44.83 (CH_2)	76.39	67.99, 86.46, 97.18*, 124.14*	131.43*, 131.79, 132.92, 135.12*
2.53	22.87 (CH_2), 30.84 (CH_2), 33.79 (CH), 35.57 (CH_2), 46.10 (CH_2)	75.93	66.60, 86.75, 95.81*, 125.69*	131.59, 131.85*, 132.33, 134.58*

*Denotes quaternary carbons

2.2.4.2 Isolation of the Organic Polyether/thioethers and Polyamine/thioethers

Scheme 2.10 shows the photolysis of polyaromatic ether/thioethers **2.46** and **2.47** to yield the organic polymers **2.54** and **2.55**. Demetallation of **2.46** resulted in the isolation of the insoluble organic polymer **2.54**, which was obtained as a beige solid in 88% yield. In contrast, polymer **2.55** was isolated in 98% yield, and was soluble in chloroform due to the aliphatic bridges within its backbone.

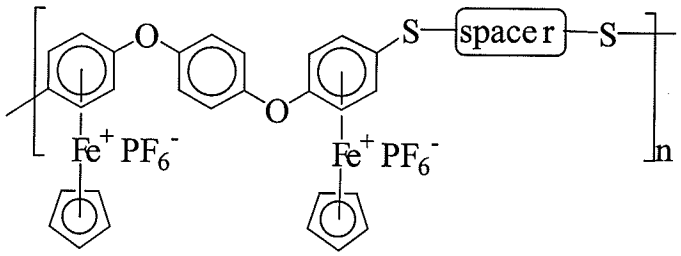

2.46, 2.47

spacer = $C_6H_4SC_6H_4$ **(2.46)**
$(CH_2)_8$ **(2.47)**

hν

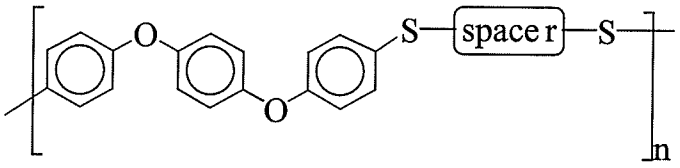

2.54, 2.55

Scheme 2.10

The ^{1}H and ^{13}C NMR spectra of polymer **2.55** are shown in Figures 2.27 and 2.28. The ^{1}H NMR spectrum clearly shows that the cyclopentadienyl resonance is no longer present and that the complexed aromatic peaks present in the organoiron polymer (**2.47**) as a singlet at 6.42 ppm have shifted downfield and now appear as two sets of doublets at 6.90 and 7.30 ppm. The four protons of the inner aryl ether ring appear as a singlet at 6.96 ppm, while previously they appeared as a singlet at 7.54 ppm. There are also four peaks corresponding to the methylene protons in the polymer backbone at 1.29, 1.59, 2.64 and 2.83 ppm. Full ^{1}H NMR analysis of this polymer is given in Table 2.37.

The ^{13}C NMR spectrum of polymer **2.55** shows the four methylene carbons at 28.88, 29.09, 34.98 and 39.07 ppm. The three aromatic CH peaks are visible at 118.76, 120.42 and 131.88 ppm, while the quaternary aromatic carbons are at 130.24, 152.59 and 156.39 ppm. The ^{13}C NMR data for this polymer are given in Table 2.38.

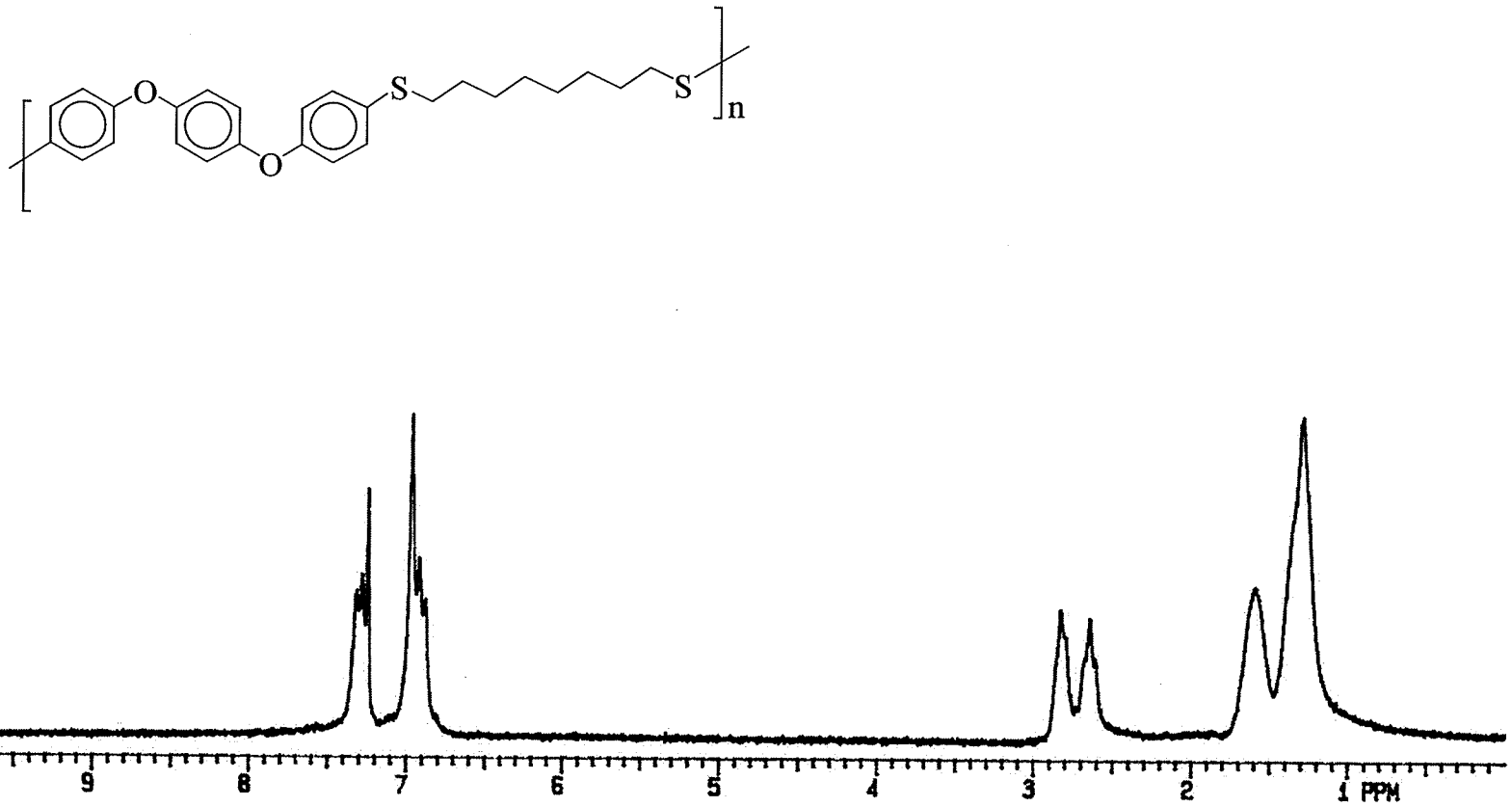

Figure 2.26: ^{1}H NMR spectrum of polymer **2.55** in $CDCl_3$

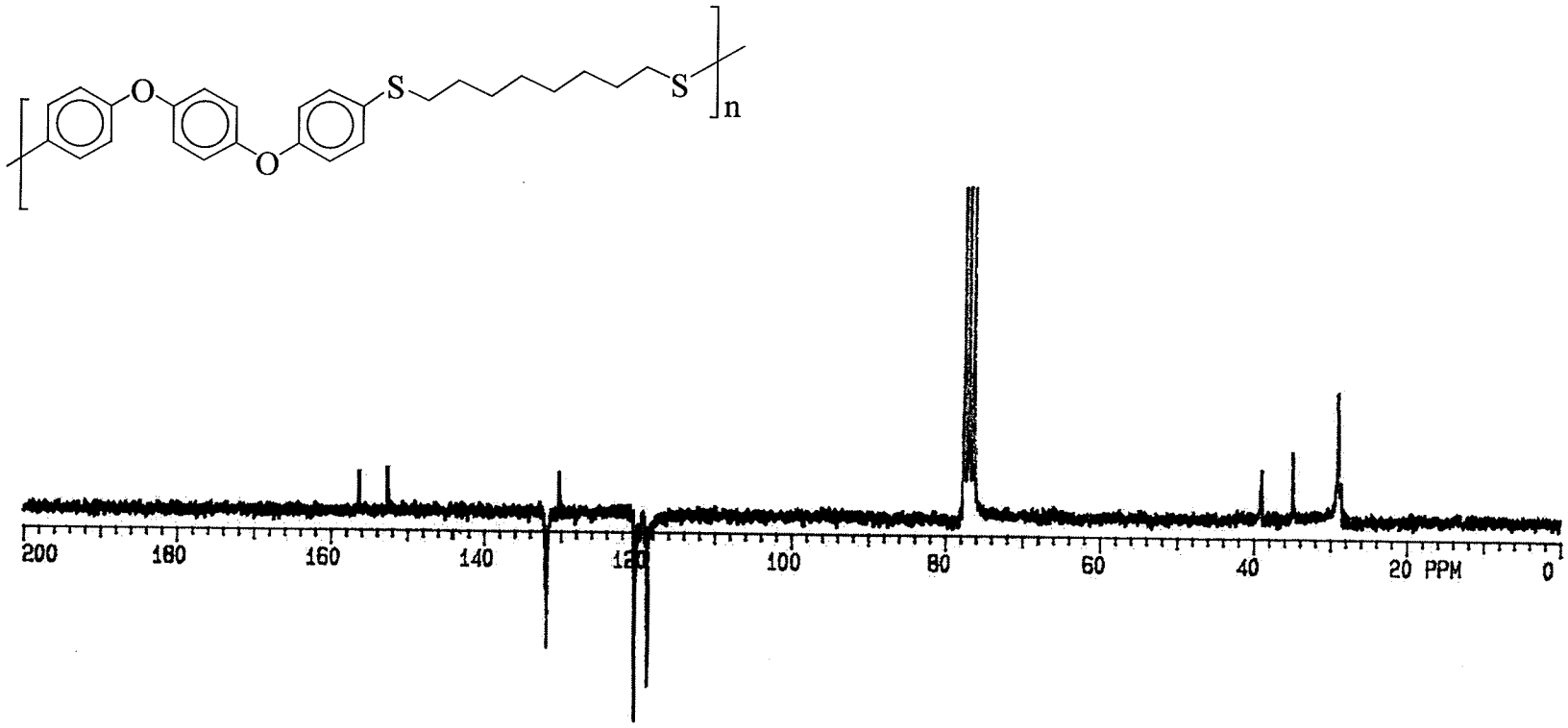

Figure 2.27: ^{13}C NMR spectrum of polymer **2.55** in $CDCl_3$

Scheme 2.11 shows the production of polymers **2.56** and **2.57** in 93 and 78 % yields, respectively, via the photolytic cleavage of the cyclopentadienyliron moieties of polymers **2.52** and **2.53**. The significant difference between the structures of these two polyamine/thioethers (**2.56, 2.57**) is the length of the aliphatic spacers between the complexed arenes. The aliphatic spacer was much longer in polymer **2.57** than in polymer **2.56**, which resulted in increased solubility for polymer **2.53** and its organic analogue **2.57**. While polymer **2.57** was soluble in organic solvents such as chloroform, cleavage of the cyclopentadienyliron moieties from **2.52** allowed for the production of polymer **2.56**, which was completely insoluble.

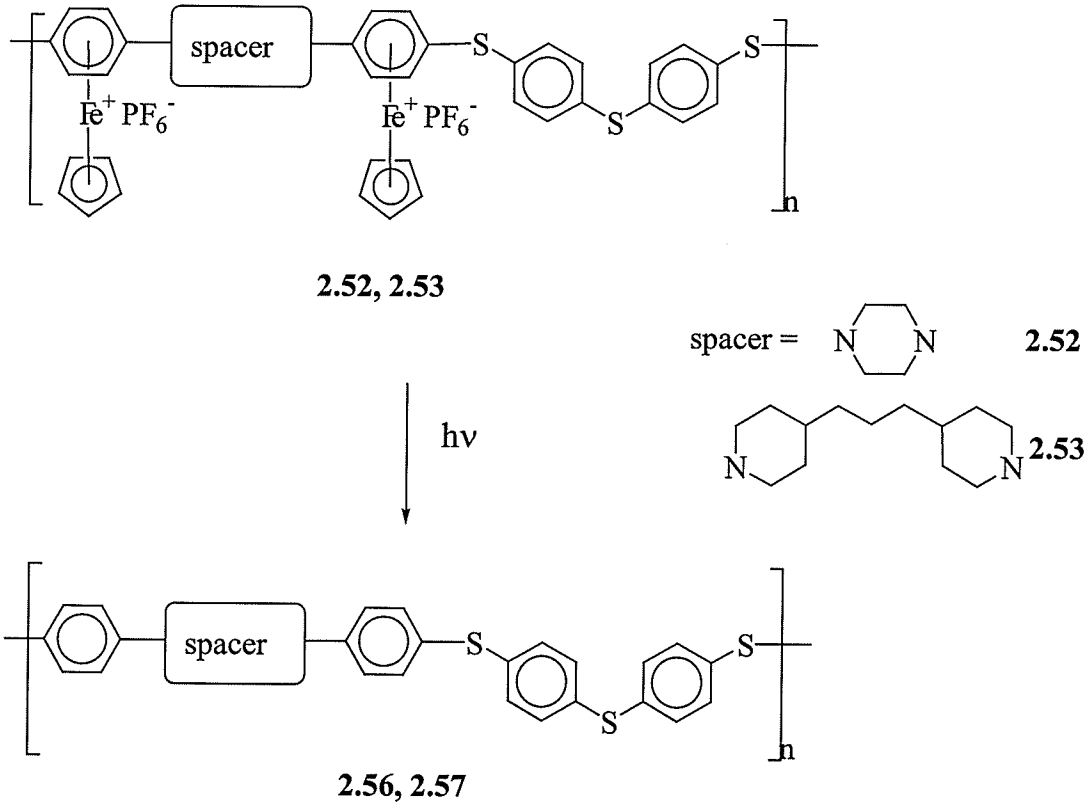

Scheme 2.11

The ^{1}H and ^{13}C NMR spectra of polymer **2.57** are shown in Figures 2.28 and 2.29. The ^{1}H NMR spectrum shows the same pattern observed in the alkyl resonances that was described earlier for the diiron complex **2.51**. For example, the hydrogens alpha to the amines appear as two peaks (each integrating for four protons) at 2.71 and 3.70 ppm. There are four doublets corresponding to the aromatic protons that are observed between 6.88 and 7.32 ppm. Full ^{1}H NMR analysis of this polymer is given in Table 2.37.

The ^{13}C NMR spectrum of polymer **2.57** shows the four methylene carbons at 23.72, 32.01, 36.66 and 49.23 ppm and one methine carbon peak at 35.63. There are four nonequivalent aromatic CH peaks at 116.55, 127.97, 131.39 and 135.56 ppm, while the quaternary aromatic carbons are at 120.19, 132.38, 138.93 and 151.66 ppm. The ^{13}C NMR data for this polymer are given in Table 2.38.

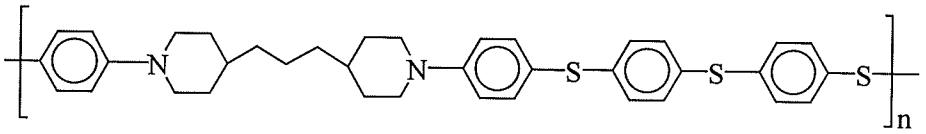

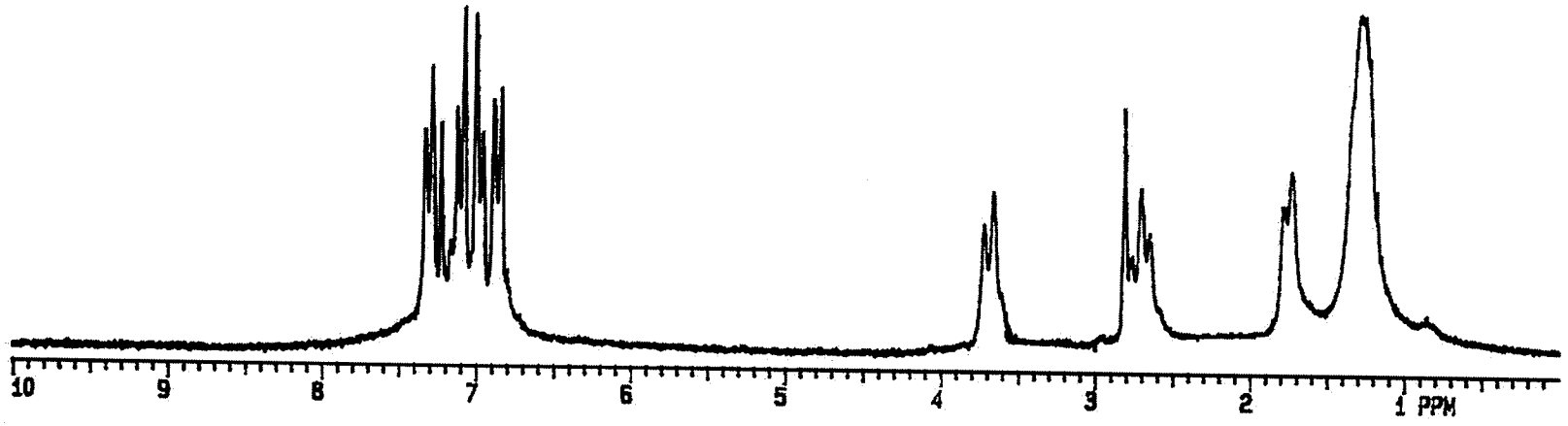

Figure 2.28: ^{1}H NMR spectrum of polymer **2.57** in $CDCl_3$

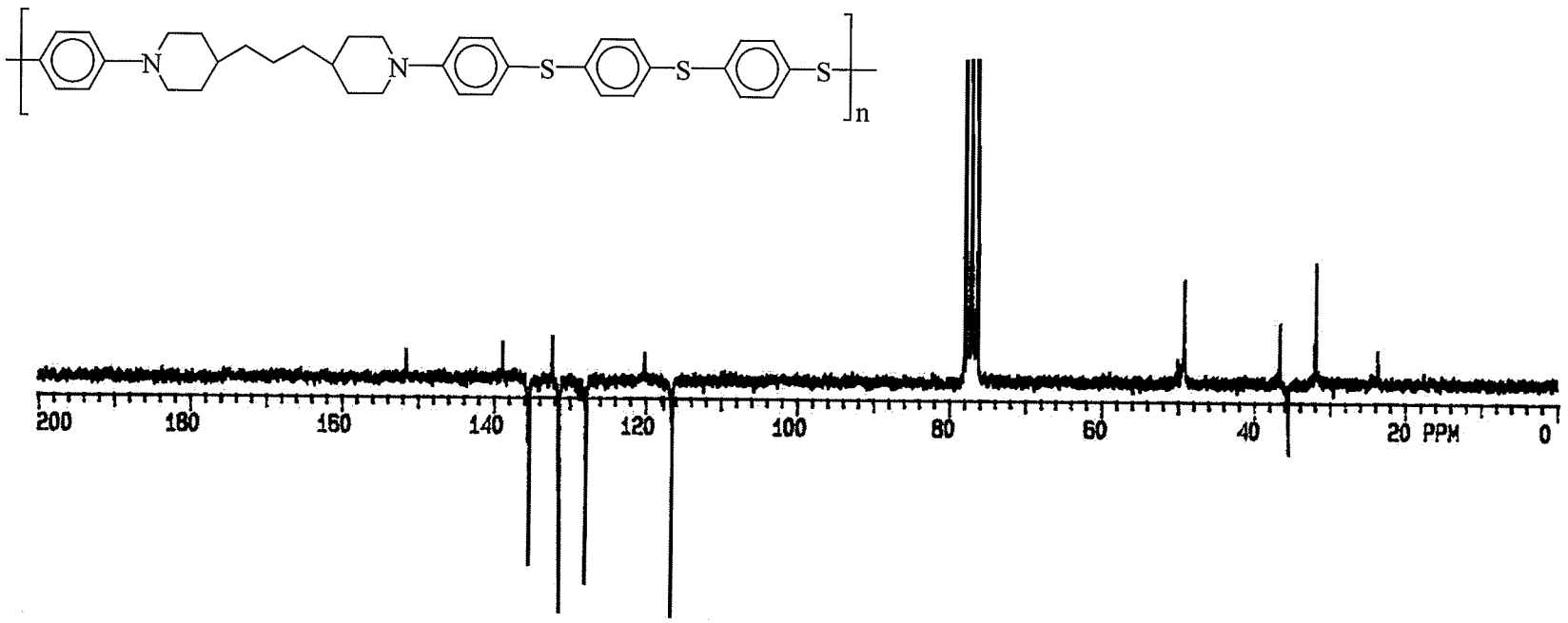

Figure 2.29: ^{13}C NMR spectrum of polymer **2.57** in $CDCl_3$

Table 2.37: % Yield of **2.54-2.57** and ^{1}H NMR Analysis of **2.55** and **2.57** in $CDCl_3$

Polymer	Yield (%)	CH, CH_2	Aromatics
2.54	88	Insoluble	
2.55	98	1.29 (br. s, 4H, CH_2), 1.59 (br. s, 4H, CH_2), 2.64 (br. s, 4H, CH_2), 2.83 (br. s, 4H, CH_2)	6.90 (d, *J*=8.71 Hz, 4H), 6.96 (s, 4H), 7.30 (d, *J*=7.98 Hz, 4H)
2.56	93	Insoluble	
2.57	78	1.30 (br. s, 10H, CH_2), 1.76 (d, *J*=10.46 Hz, 4H, CH_2), 1.90 (m, 2H, CH), 2.71 (t, *J*=10.71 Hz, 4H, CH_2), 3.70 (d, *J*=11.81 Hz, 4H, CH_2)	6.88 (d, *J*=9.08 Hz, 4H), 7.00 (d, *J*=8.42 Hz, 4H), 7.12 (d, *J*=8.35 Hz, 4H), 7.32 (d, *J*=8.42 Hz, 4H)

Table 2.38: ^{13}C NMR Analysis of **2.55** and **2.57** in $CDCl_3$

Polymer	CH, CH_2	Aromatics
2.55	28.88 (CH_2), 29.09 (CH_2), 34.98 (CH_2), 39.07 (CH_2)	118.76, 120.42, 130.24*, 131.88, 152.59*, 156.39*
2.57	23.72 (CH_2), 32.01 (CH_2), 35.63 (CH), 36.66(CH_2), 49.23 (CH_2)	116.55, 120.19*, 127.97, 131.39, 132.38*, 135.56, 138.93*, 151.66*

*Denotes quaternary carbons

Molecular weight analysis of the soluble polyether/thioether (**2.55**) and polyamine/thioether (**2.57**) was accomplished using gel permeation chromatography in chloroform. Table 2.39 provides the molecular weights and molecular weight distributions of these polymers. The factor that determined the solubilities of these organic polymers was the length of their aliphatic chains. While the solubility of **2.55** was quite high due to the octamethylene bridge in its backbone, the purely aromatic polymer **2.54** was insoluble. The weight average molecular weight of polymer **2.55** was 21 700 with a PDI of 2.4. The solubilities of polymers **2.56** and **2.57** with alternating amine/thioether bridges were influenced by the nature of their amine bridges. While polymer **2.56** was completely insoluble, the soluble portion of **2.57** gave a M_w of 9 100 and a PDI of 1.5. From these studies, it was clear that the nature of the backbones of the polymers had a dramatic effect on their solubilities.

Table 2.39: Molecular Weight Analysis of **2.54-2.57**

Polymer	$\mathbf{M_w}$	$\mathbf{M_n}$	$\mathbf{M_w/M_n}$
2.54	Insoluble		
2.55	21 700	9 000	2.4
2.56	Insoluble		
2.57*	9 100	6 100	1.5

* Soluble portion of polymer

2.2.4.3 Thermal Properties of the Organometallic and Organic Polyether/thioethers and Polyamine/thioethers

In the previous sections, it was found that polyaromatic ethers and thioethers had higher thermal stability than aliphatic-bridged polythioethers. It was also noted that the glass transition temperatures of polyaromatic ethers were greater than those of polyaromatic thioethers, which were in turn greater than those of the polythioethers with aliphatic spacers. Therefore, it was of great interest to determine what influence combining different types of spacers into the backbones of these classes of polymers would have on their thermal properties. Figure 2.30 shows the TGA thermograms of polymers **2.46** and **2.54**. It can be seen that the cyclopentadienyliron moieties are no longer present in the thermogram of polymer **2.54**. Figure 2.31 shows the differences in the thermal stabilities of the organic polyether/thioethers **2.54** and **2.55**. These two polymers **2.54** and **2.55** had significantly different thermal stabilities. The completely aromatic-bridged **2.54** had a 38% weight loss at an onset temperature of 523 °C, whereas **2.55** with aliphatic spacers between the aromatic ether bridges displayed a 72% weight loss commencing at 380 °C.

Figure 2.32 shows the thermograms of the metallated and demetallated polyamine/thioethers (**2.52** and **2.56**). Once again, it is clearly visible that polymer **2.56** was successfully demetallated by the lack of weight loss at around 210 °C. Tables 2.40 and 2.41 provide the full TGA results for the organometallic polymers (**2.46, 2.47, 2.52, 2.53**) and organic polymers (**2.54-2.57**), respectively.

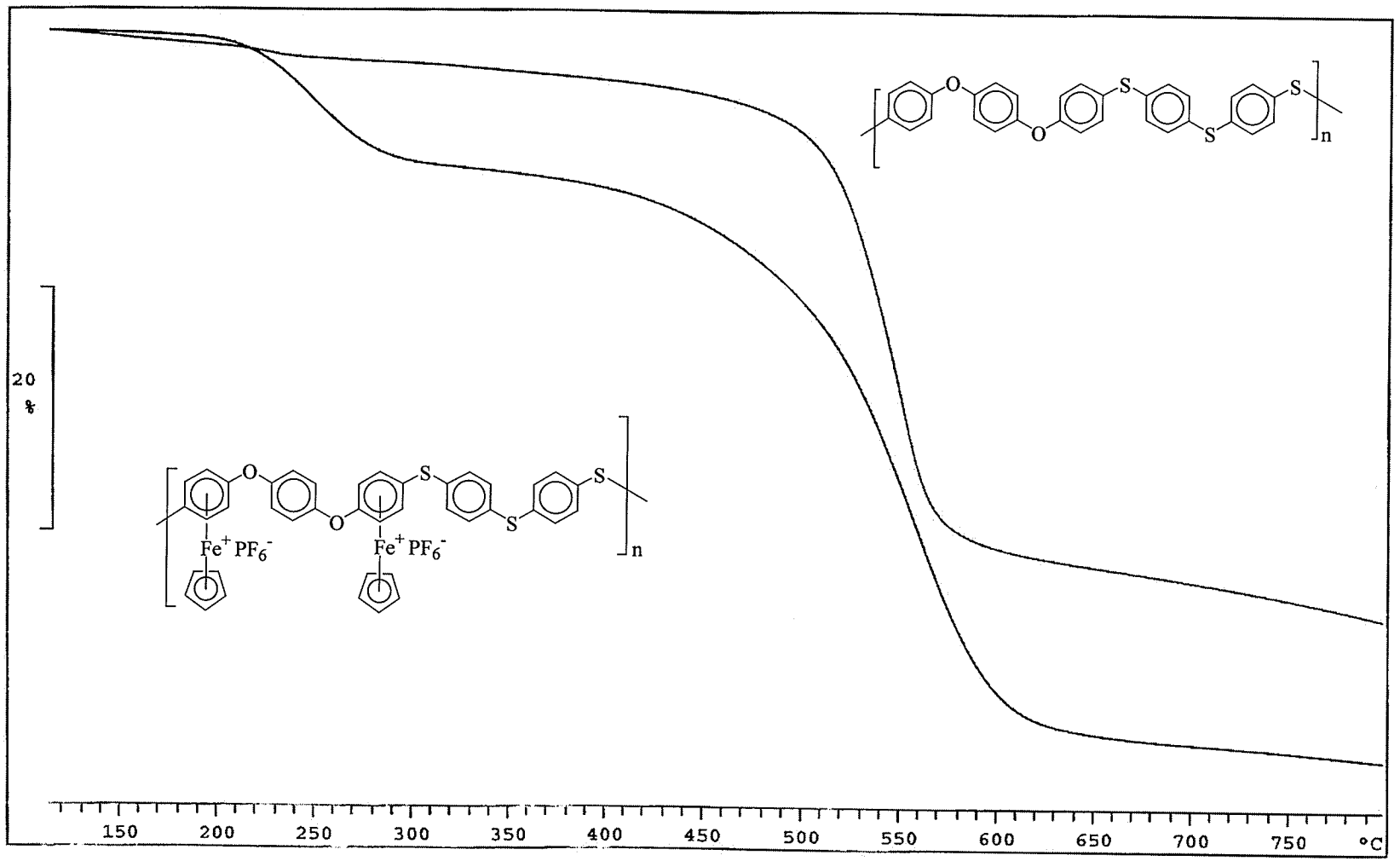

Figure 2.30: TGA thermograms of polymers **2.46** and **2.54**

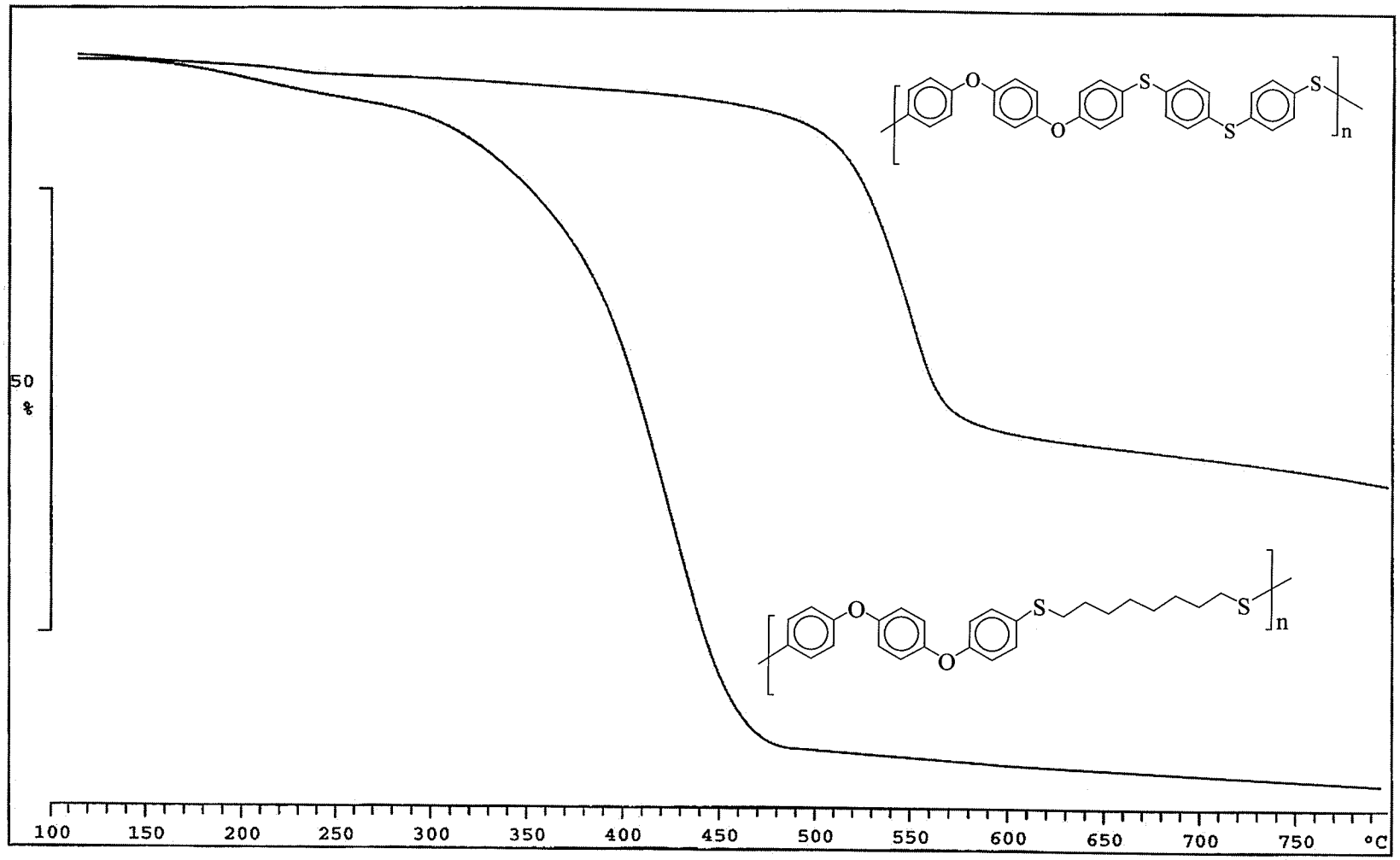

Figure 2.31: TGA thermograms of polymers **2.54** and **2.55**

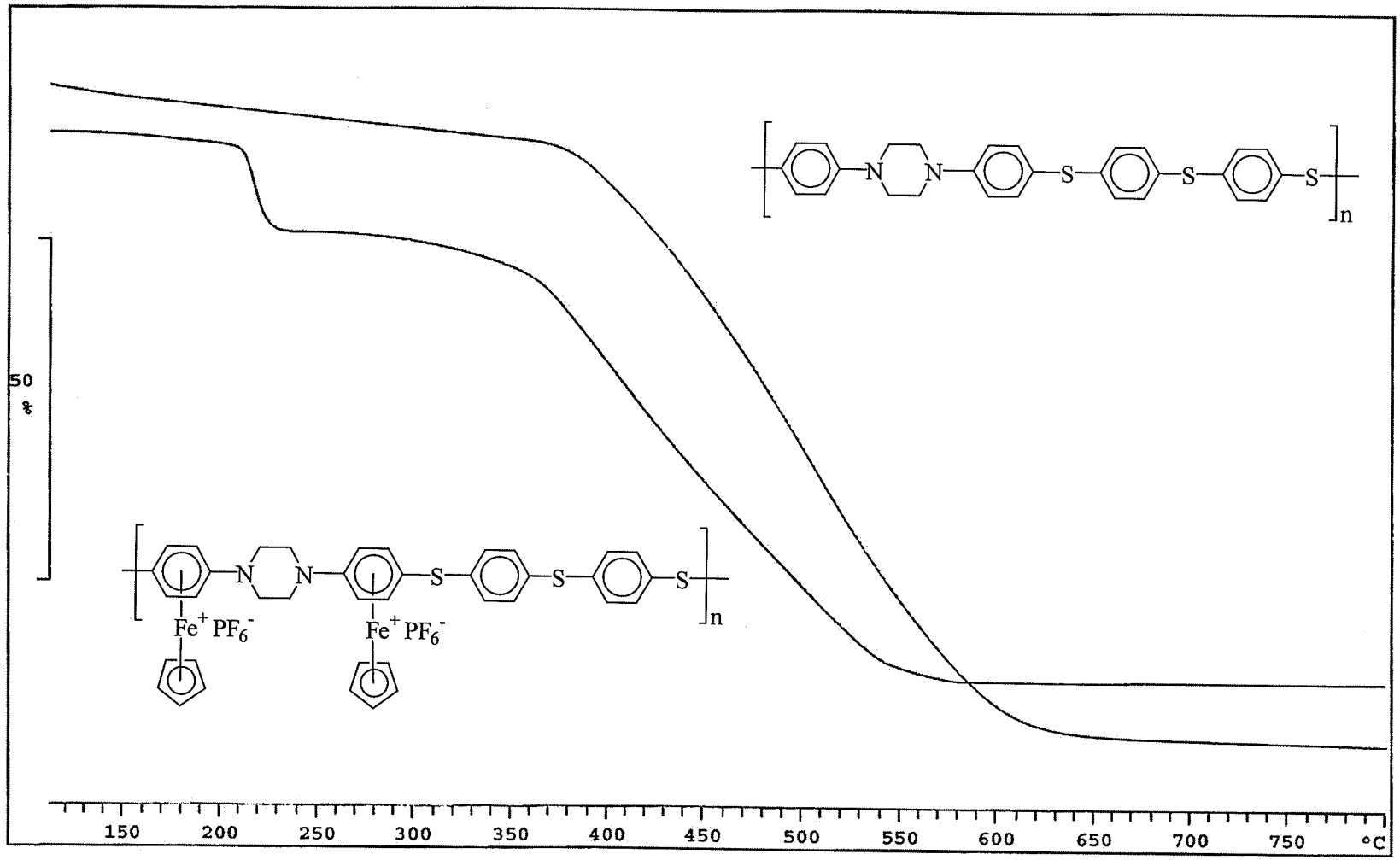

Figure 2.32: TGA thermograms of polymers **2.52** and **2.56**

Table 2.40: TGA Results for Organometallic Polymers **2.46, 2.47, 2.52** and **2.53**

Polymer	Weight loss (%)	T_{onset} (°C)	$T_{midpoint}$ (°C)	T_{endset} (°C)
2.46	22	240	250	260
	22	515	586	590
2.47	24	210	227	242
	59	490	539	625
2.52	14	216	222	228
	62	375	460	533
2.53	26	219	242	258
	28	400	426	461

Table 2.41: TGA Results for Demetallated Polymers **2.54-2.57**

Polymer	Weight loss (%)	T_{onset} (°C)	$T_{midpoint}$ (°C)	T_{endset} (°C)
2.54	38	523	546	570
2.55	72	380	410	443
2.56	83	436	512	589
2.57	51	416	439	465

Differential scanning calorimetry of the organic polymers demonstrated that their glass transition temperatures were strongly influenced by the nature of the spacers in their backbones. For example, polymers **2.54** and **2.55** both had aromatic ether spacers in their backbones, but while **2.54** also had an aromatic thioether linkage, the thioether linkage in **2.55** was aliphatic. The result was that the T_gs of these polymers were very similar to those of polymers **2.41** and **2.34**. The T_g of the *p*-polyphenylenesulfide (**2.41**) was found to be 86 °C, while the T_g of polymer **2.54** was 89 °C. In addition, it was shown earlier that the T_g of polymer **2.34** was 33 °C, and the incorporation of aromatic ether units into polymer **2.55** resulted in a T_g at 38 °C. Since the glass transition temperatures of the polyaromatic ethers described in Section 2.2.1.3 ranged from 113 to 165 °C, it can be concluded that the glass transition temperatures of mixed polyether/thioethers are more highly influenced by the sulfur linkages than the oxygen linkages. It is also notable that the presence of aliphatic spacers had a dominant effect on the T_g of **2.55**, resulting in a decreased glass transition temperature by approximately 60°C. Although the incorporation of arylether linkages did increase the glass transition temperatures of these polymers, it was only by 3 to 5 °C. Figure 2.33 shows the DSC curves of polymers **2.54** and **2.55**. In addition to the glass transition temperature, polymer **2.55** also experienced a melting transition at 113 °C.

Differential scanning calorimetry of polymers **2.56** and **2.57** revealed that these amine/thioether polymers possessed higher glass transition temperatures than their ether/thioether analogues. The T_g of polymer **2.57** was 4 °C lower than that of **2.56**, in light of its longer aliphatic chain. All of the DSC results are provided in Table 2.42.

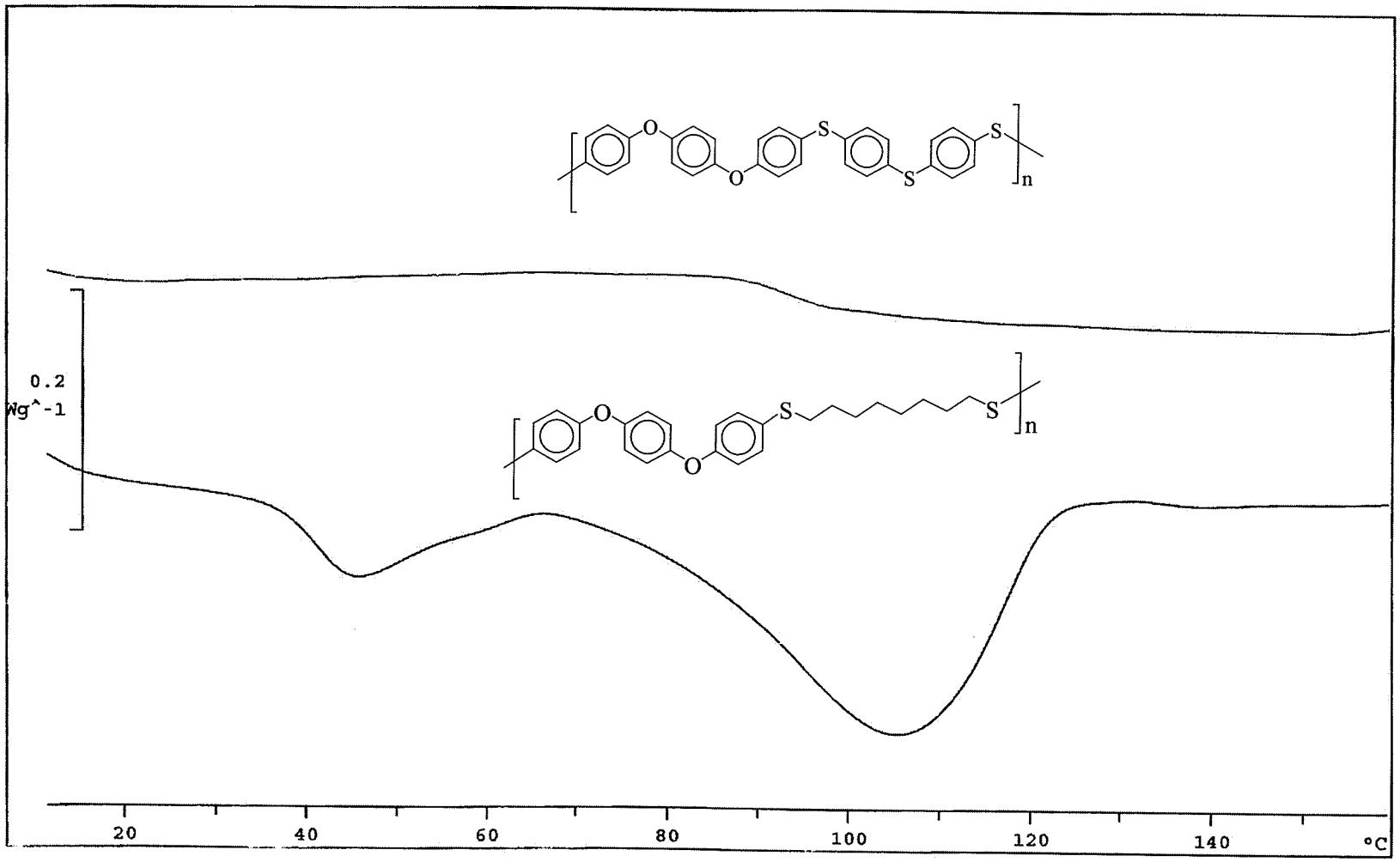

Figure 2.33: DSC traces of polymers **2.54** and **2.55**

Table 2.42: DSC Results for Demetallated Polymers **2.54-2.57**

Polymer	T_g Onset (°C)
2.54	89
2.55	38
2.56	113
2.57	109

2.2.5 Electrochemical Properties of Cyclopentadienyliron-Coordinated Monomers and Polymers

The electrochemical properties of the polyaromatic ethers and thioethers coordinated to cyclopentadienyliron cations were examined using cyclic voltammetry. It has previously been found that the iron centers of this class of complex undergo a one-electron reduction process to give neutral nineteen-electron complexes, which can themselves undergo reduction to give anionic twenty-electron complexes.[49-58] Previous studies on simple aromatic ether and thioether complexes of cyclopentadienyliron have shown that the iron centers do not communicate when they are separated by oxygen bridges. However, a diiron complex containing a thioether bridge demonstrated a small degree of interaction between the iron centers.

This study provides the first examples of the electrochemical properties of high molecular weight polyaromatic ethers and thioethers containing cyclopentadienyliron moieties pendent to their backbones. It was also of interest to prepare model monomeric complexes in order to examine the influence of the polymeric nature of these materials on their electrochemical behaviour. The first compounds that were examined using cyclic voltammetry were the organoiron polyaromatic ethers. Scheme 2.12 describes the synthesis of a monomeric model complex (**2.60**) via reaction of complex **2.1** with the dinucleophile **2.6** in a 2:1 molar ratio to give complex **2.58**, followed by reaction of this diiron complex with phenol (**2.59**). It was important that complex **2.58** be reacted with phenol so that the complexed aromatic rings were substituted by aryl ethers on both sides to give a fair approximation of polymer **2.14**.

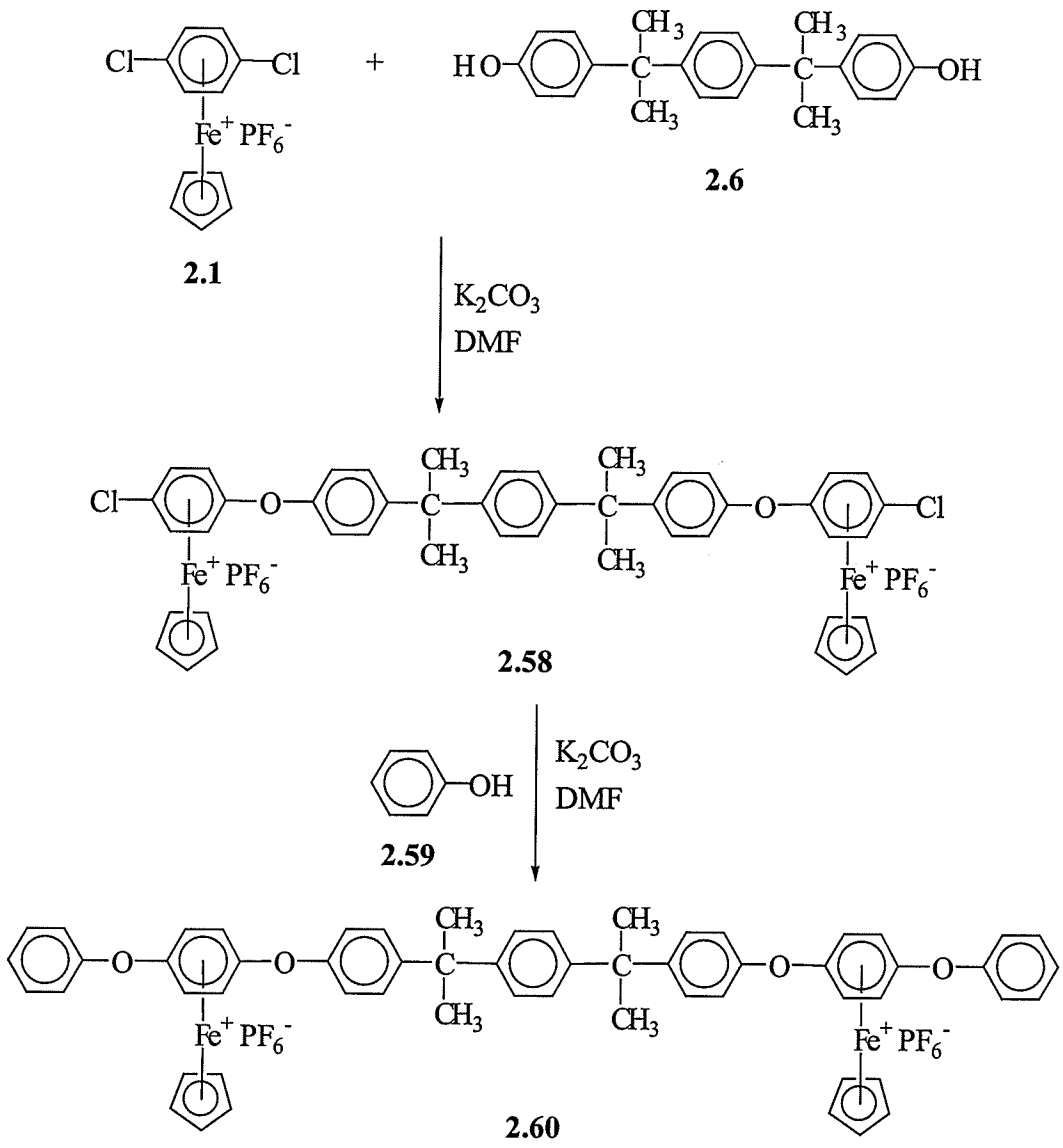

Scheme 2.12

Complexes **2.58** and **2.60** were isolated in 91 and 71 % yields as beige solids. The spectroscopic data for complexes **2.58** and **2.60** were consistent with their structures and are provided in Tables 2.43 and 2.44.

Table 2.43: % Yield and ^{1}H NMR Analysis of Complexes **2.58** and **2.60** in Acetone-d_6

Complex	% Yield	Other	Cp	Complexed Ar	Ar
2.58	91	1.71 (s, 6H, CH_3)	5.36 (s, 10H)	6.47 (d, J = 6.96 Hz, 4H), 6.80 (d, J = 6.96 Hz, 4H)	7.24 (s, 4H), 7.26 (d, J = 8.83 Hz, 4H), 7.45 (d, J = 8.75 Hz, 4H)
2.60	71	1.70 (s, 6H, CH_3)	5.29 (s, 10H)	6.31 (s, 8H)	7.22 (s, 6H), 7.29-7.44 (m, 12H), 7.51-7.59 (m, 4H)

Table 2.44: CH Analysis and ^{13}C NMR Analysis of Complexes **2.58** and **2.60** in Acetone-d_6

Complex	CH Analysis	Other	Cp	Complexed Ar	Ar
2.58		31.06 (CH_3), 42.92 (C)	80.32	76.97, 87.72, 104.69*, 133.81*	120.81, 127.12, 129.84, 148.14*, 149.96*, 151.60*
2.60	($C_{58}H_{52}F_{12}Fe_2O_4P_2$) (1214.65): Calcd. C, 57.35; H, 4.32; Found C, 56.98; 4.35	31.04 (CH_3), 42.77 (C)	78.79	75.77, 75.86, 131.41*, 131.68*	120.65, 121.19, 127.10, 129.71, 131.47, 148.11*, 149.49*, 152.15*, 154.38*

*Denotes quaternary carbons

It was important that the cyclic voltammetric behaviour of this complex be explored in order to understand the electrochemical properties of its macomolecular analogue (polymer **2.14**). The cyclic voltammogram of complex **2.60** is shown in Figure 2.34. The CV was obtained in a DMF solution containing TBAP as the supporting electrolyte at –20 °C with a scan rate of 1 V/s. It was found that the reduction processes for this diiron complex displayed good reversibility and had a cathodic peak potential (E_{pc}) of -1.28 V, and an anodic peak potential (E_{pa}) of -1.08 V. The half-wave potential ($E_{1/2}$) for this reduction process was at -1.18 V.

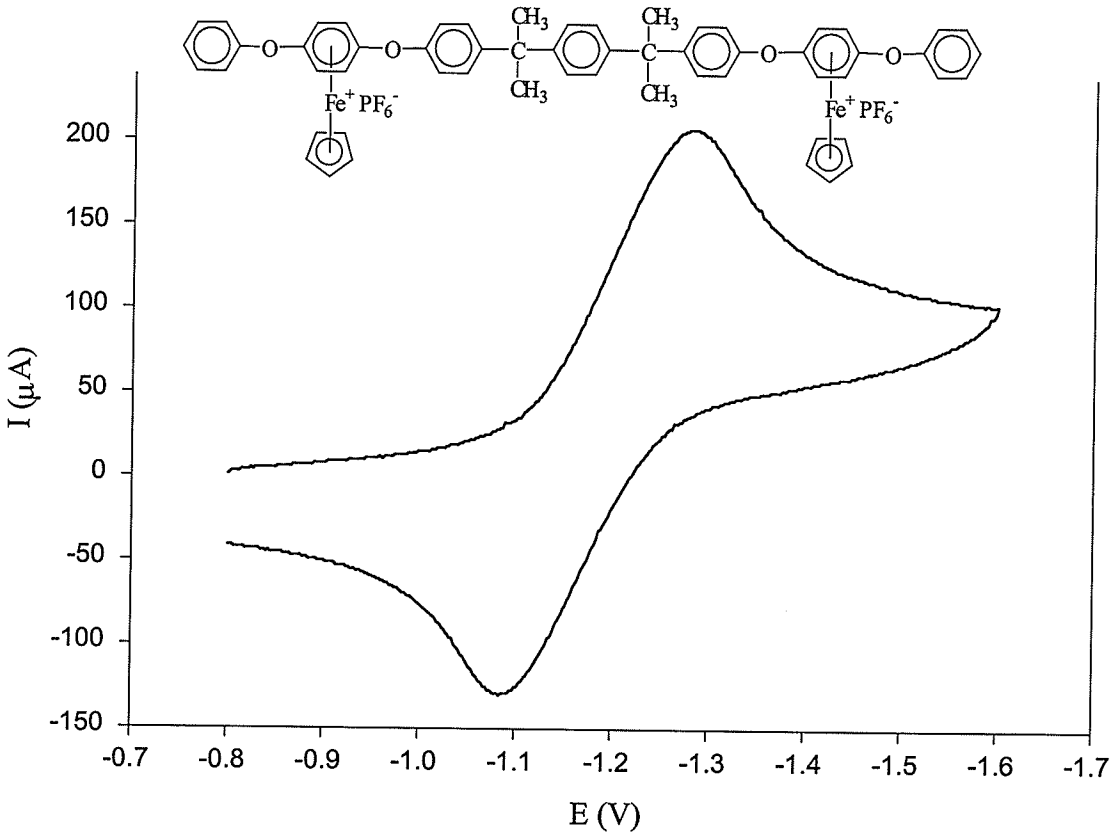

Figure 2.34: Cyclic voltammogram of **2.60**

The cyclic voltammograms of the polymeric analogue, **2.14** showed poorer reversibility relative to complex **2.60**, in particular at low scan rates. The CV of polymer **2.14** shown in Figure 2.35 was obtained under the same conditions as that shown for complex **2.14**. The CV for the polymer is much broader and has an E_{pc} = -1.61 V, E_{pa} = -1.18 V and $E_{1/2}$ = -1.40 V.

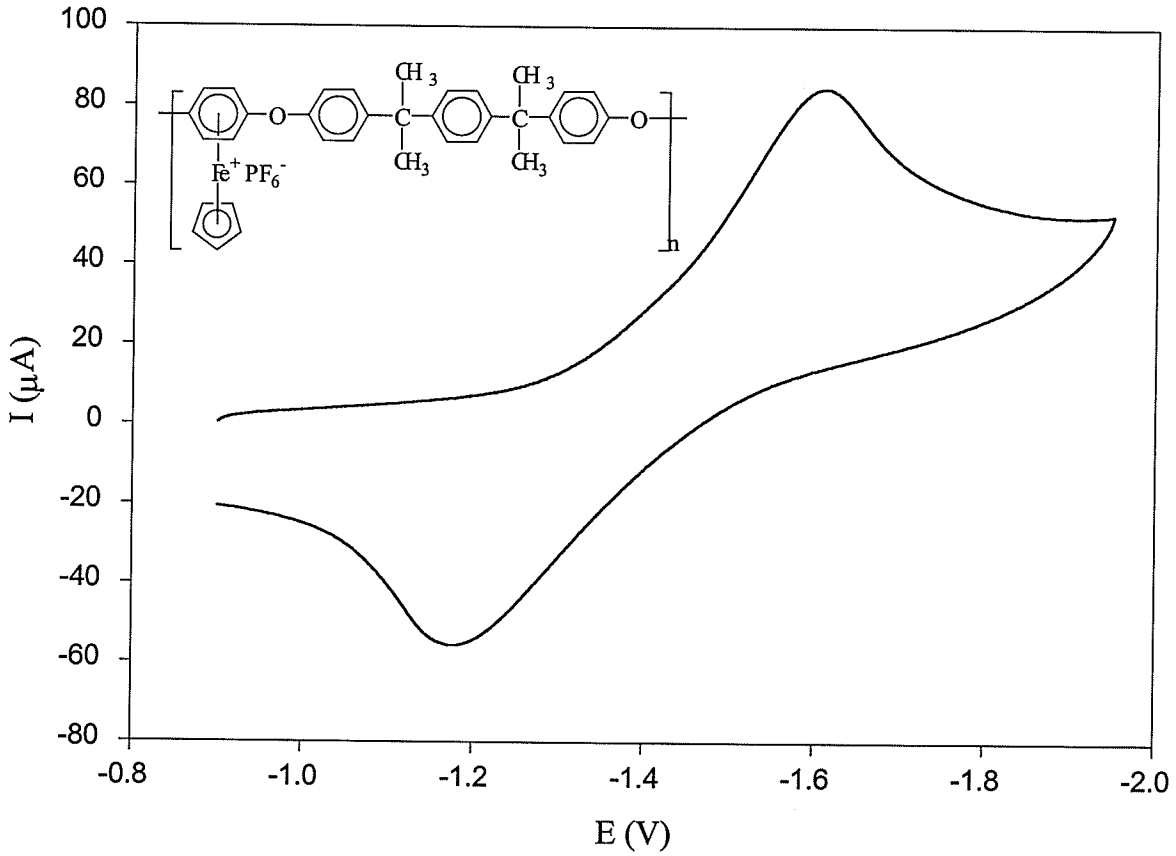

Figure 2.35: Cyclic voltammogram of **2.14**

Many of the cyclopentadienyliron-coordinated polymers also adsorbed onto the working electrode during the cyclic voltammetry experiments, and this phenomenon was most noticeable at low scan rates. The CV's of polymer **2.15** obtained at –30 °C in DMF are shown in Figure 2.36 at scan rates of 0.1, 0.2, 1 and 5 V/s. From these curves, it is quite obvious that the current increases significantly with increased scan rate, while the $E_{1/2}$ values obtained for these curves occurred at –1.03, -1.04, -1.04 and –1.06 V, respectively. In order to visualize more clearly the adsorption of polymer **2.15** at low scan rates, the CVs obtained at 0.1 and 5 V/s are given in Figures 2.37 and 2.38, respectively. The large negative peak in Figure 2.38 is indicative of the adsorption phenomenon, while at a scan rate of 5, the CV appears to be more symmetric.

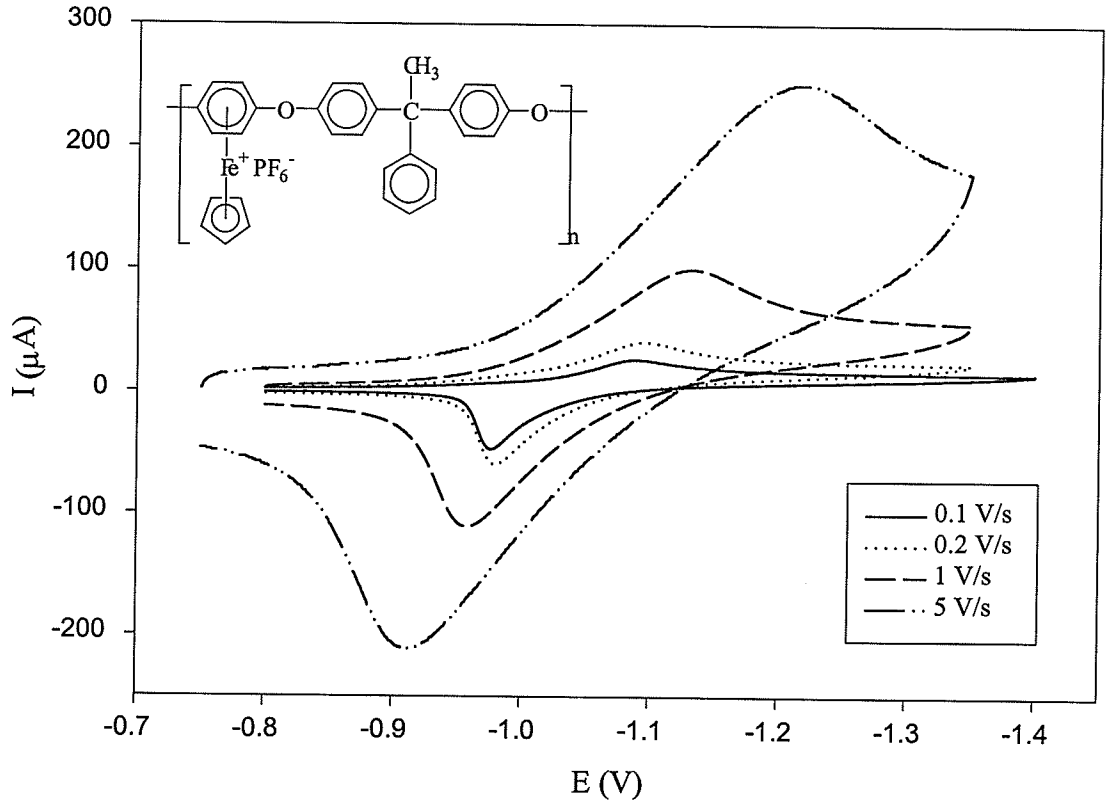

Figure 2.36: Cyclic voltammogram of **2.15** obtained at scan rates of 0.1, 0.2, 1 and 5 V/s

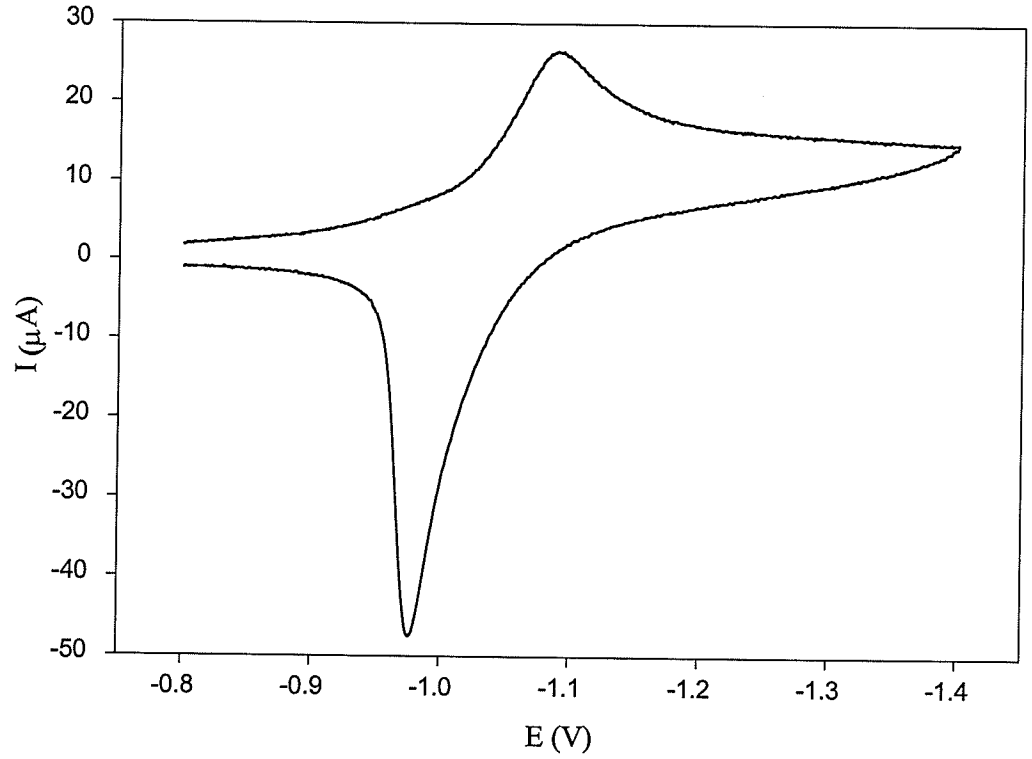

Figure 2.37: Cyclic voltammogram of **2.15** obtained at a scan rate of 0.1 V/s

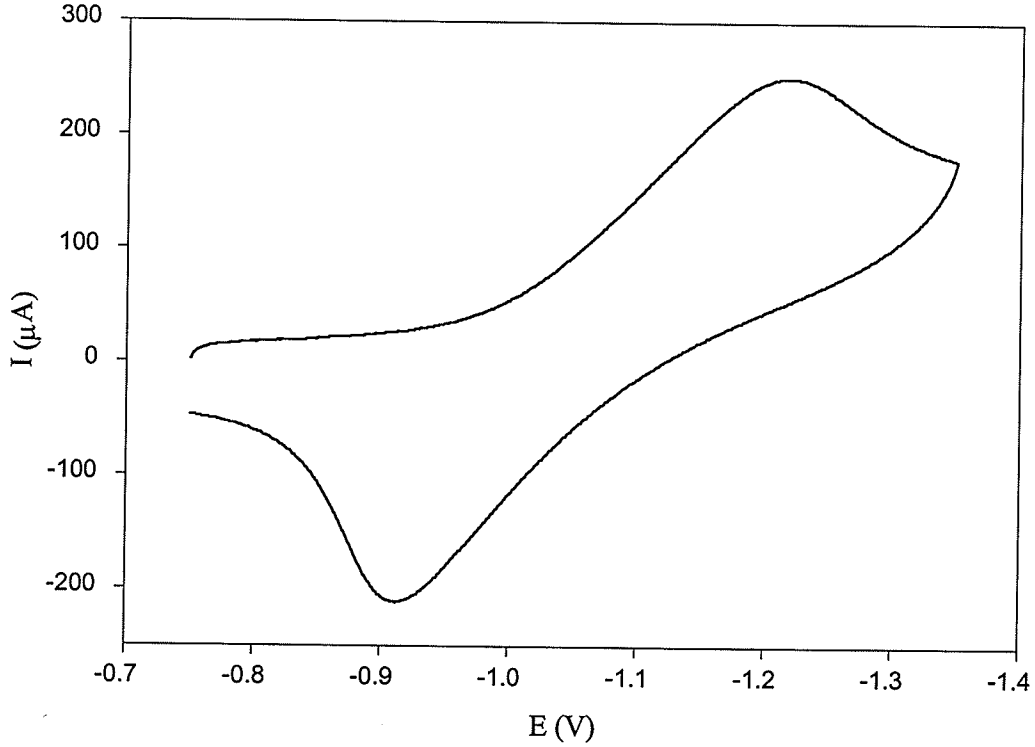

Figure 2.38: Cyclic voltammogram of **2.15** obtained at a scan rate of 5 V/s

While the cyclic voltammetric behaviour of polymers **2.14** and **2.15** were fairly similar, polymer **2.17** displayed very interesting electrochemical properties. This polymer exhibited two redox couples corresponding to two distinct reduction processes. Figure 2.39 shows the CV of this polymer obtained at –40 °C in a DMF solution. This CV was obtained at a scan rate of 0.2 V/s, and the $E_{1/2}$ values for the two redox processes occurred at –0.988 V and –1.11 V.

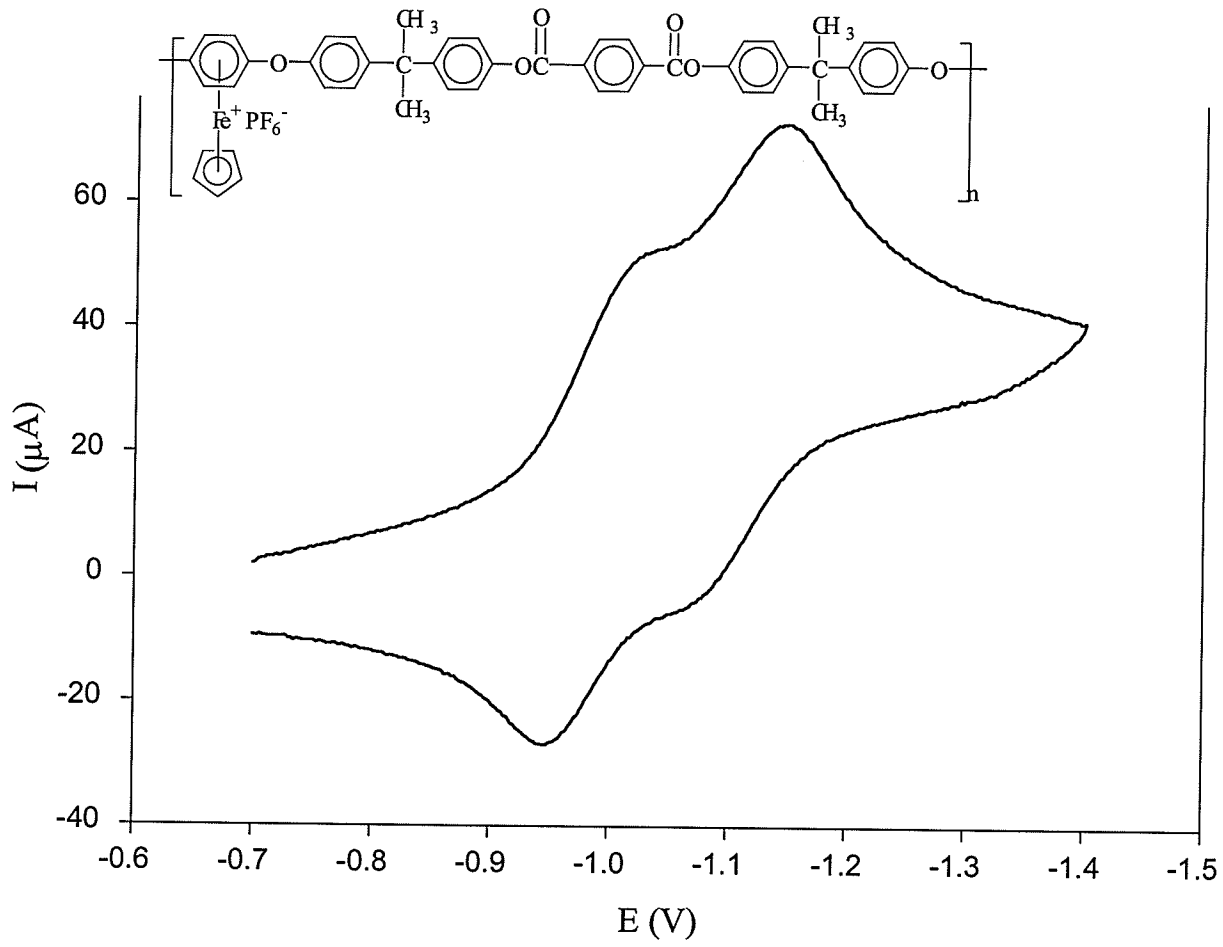

Figure 2.39: Cyclic voltammogram of **2.17** obtained at a scan rate of 0.2 V/s

In order to understand the reason for these two redox waves, a diiron (**2.62**) and monoiron complex (**2.69**) were synthesized as monomeric analogues to polymer **2.17**. The diiron complex was synthesized in order to determine whether or not the two reduction waves were still present, and the monoiron complex was synthesized to ensure that one of the redox waves was not due to the presence of the ester functionality. The syntheses of these complexes are shown in Schemes 2.13 and 2.14.

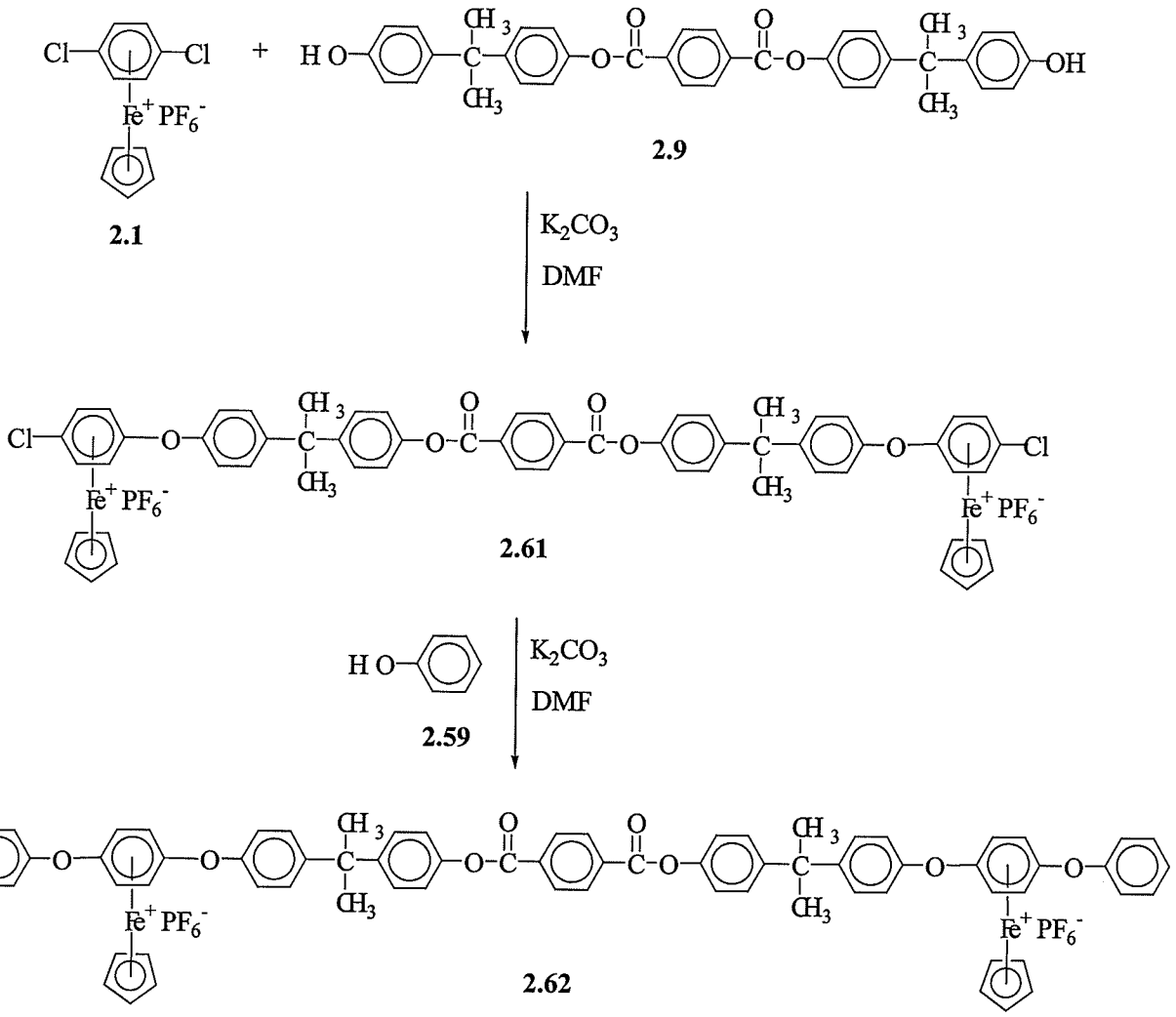

Scheme 2.13

The cyclic voltammogram of complex **2.62** is shown in Figure 2.40. It can be seen that the two redox processes observed in the polymeric analogue are also present in this diiron complex, however the cyclic voltammogram of the diiron complex (**2.62**) is much sharper than the cyclic voltammogram of polymer **2.17**. This CV was obtained at a scan rate of 0.2 V/s, and the $E_{1/2}$ values for the reduction steps occurred at –1.17 V and –1.30 V. The ^{1}H and ^{13}C NMR analysis of complexes **2.61** and **2.62** are given in Tables 2.45 and 2.46.

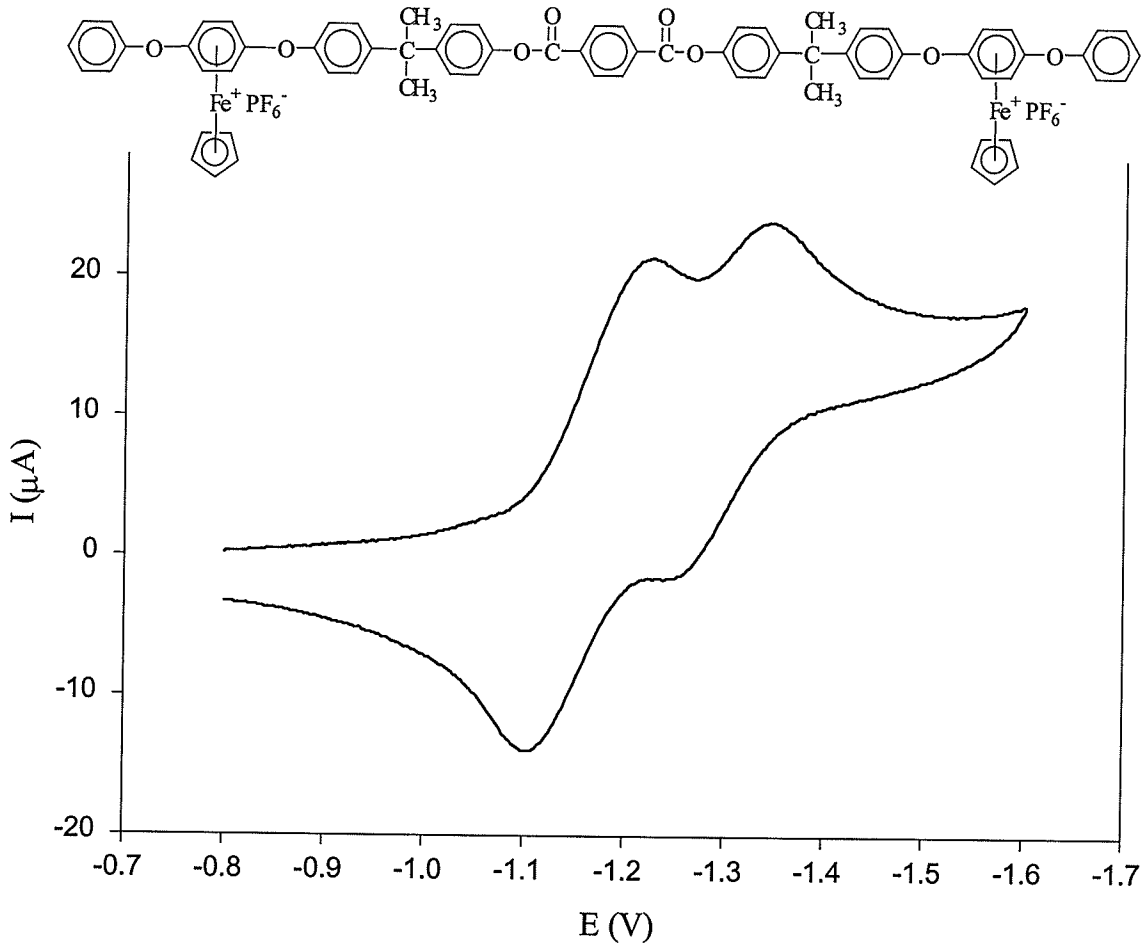

Figure 2.40: Cyclic voltammogram of **2.62** obtained at a scan rate of 0.2 V/s

Table 2.45: % Yield and ^{1}H NMR Analysis of Complexes **2.61** and **2.62** in Acetone-d_6

Complex	% Yield	CH_3	Cp	Complexed Ar	Ar
2.61	95	1.77 (s, 12H)	5.38 (s, 10H)	6.50 (d, J = 6.25 Hz, 4H), 6.82 (d, J = 6.64 Hz, 4H)	7.27 (d, J = 8.98 Hz, 4H), 7.29 (d, J = 8.59 Hz, 4H), 7.42 (d, J = 8.99 Hz, 4H), 7.49 (d, J = 8.59 Hz, 4H), 8.37 (s, 4H)
2.62	98	1.76 (s, 12H)	5.33 (s, 10H)	6.36 (s, 8H)	7.25-7.60 (m, 26H), 8.37 (s, 4H)

Table 2.46: ^{13}C NMR Analysis of Complexes **2.61** and **2.62** in Acetone-d_6

Complex	IR (cm^{-1})	Other	Cp	Complexed Ar	Ar
2.61	1734 (CO)	31.00 (CH_3), 42.95 (C), 164.60 (CO)	80.21	76.83, 87.59, 104.52*, 133.58*	120.86, 121.92, 128.51, 129.74, 130.83, 134.52*, 148.66*, 149.45*, 149.54*, 151.49*
2.62	1735 (CO)	31.08 (CH_3), 42.95 (C), 164.56 (CO)	78.80	75.78, 131.37*, 131.60*	120.78, 121.21, 121.97, 127.05, 128.55, 129.69, 130.86, 131.47, 134.57*, 148.71*, 149.21*, 149.51*, 152.14*, 154.27*

*Denotes quaternary carbons

Scheme 2.14 shows the synthesis of a monoiron complex containing an ester functionality. Complex **2.69** was synthesized in a number of reaction sequences. Initially, compound **2.65** was synthesized in a condensation reaction between 4-hydroxybenzaldehyde (**2.63**) with phenethylamine (**2.64**), allowing for the isolation of the phenolic compound **2.65**. This compound was then reacted with the 4-chlorotoluene complex of cyclopentadienyliron (**2.66**), and the resulting imine complex was decomposed during work-up to give the desired aldehyde complex **2.67**. Oxidation of the aldehyde group with chromium trioxide in the presence of sulfuric acid resulted in the isolation of complex **2.68**. The carboxylic acid was converted to the acid chloride and reacted *in situ* with phenol (**2.59**) to give the monoiron ester complex **2.69**. The ^{1}H NMR spectra of complexes **2.67-2.69** are shown in Figures 2.41-2.43.

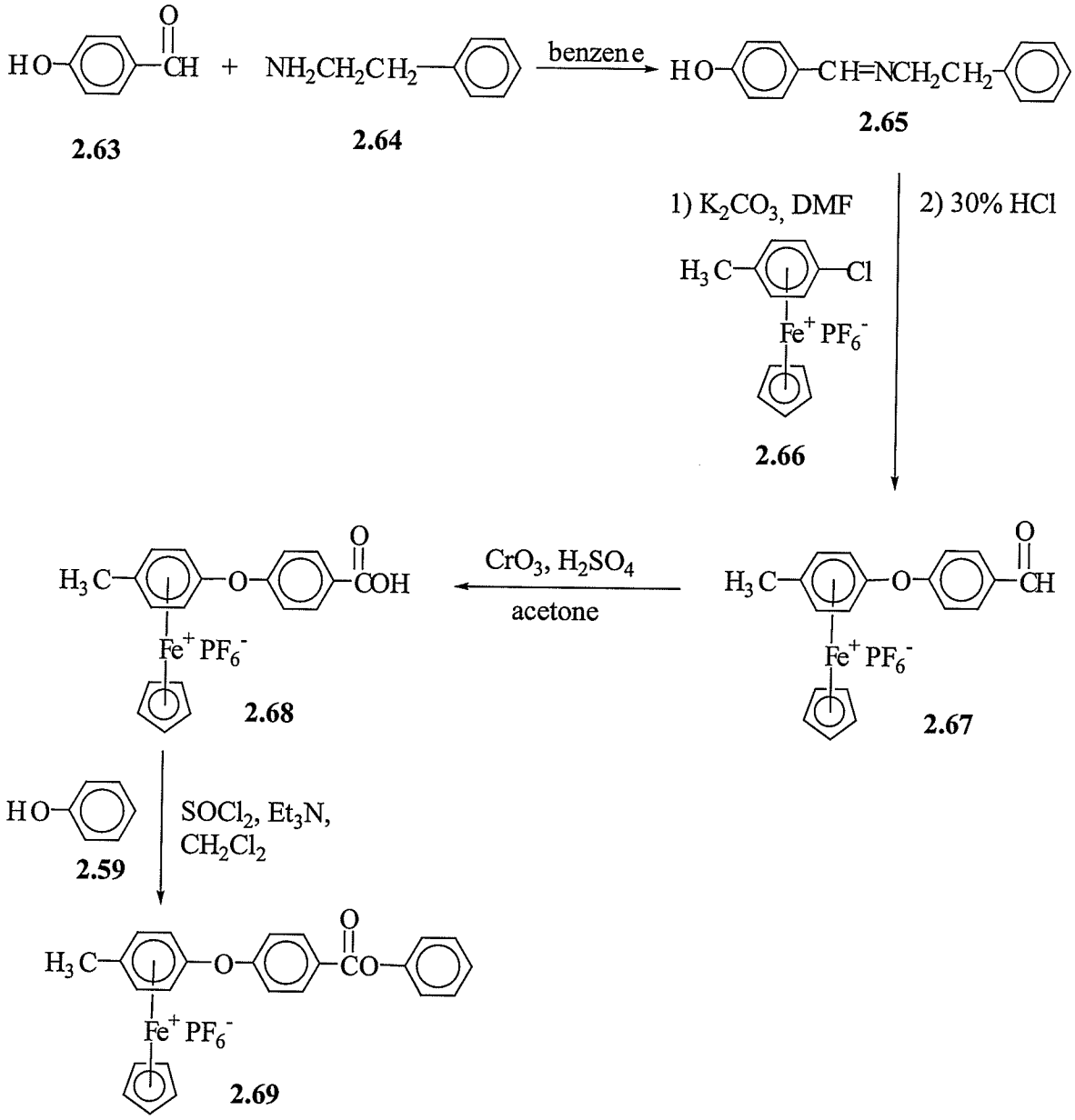
HO
CH
O
+
NH2CH2CH2
benzene
HO
CH=NCH2CH2
2.63
2.64
2.65
1) K2CO3, DMF
2) 30% HCl
H3C
Cl
Fe+ PF6-
2.66
H3C
O
COH
CrO3, H2SO4
acetone
H3C
O
CH
Fe+ PF6-
2.68
2.67
HO
2.59
SOCl2, Et3N,
CH2Cl2
H3C
O
CO
Fe+ PF6-
2.69

Scheme 2.14

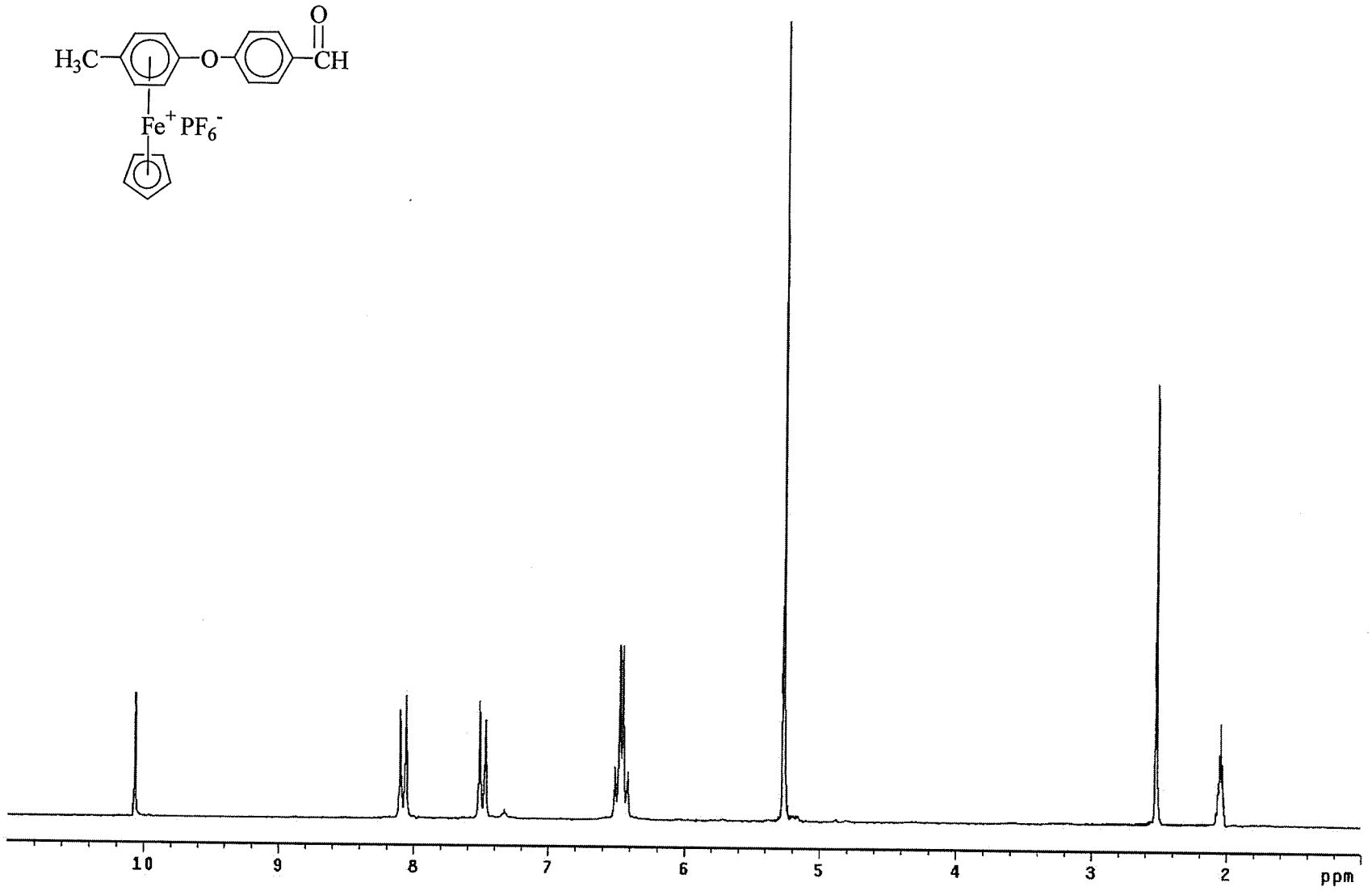

Figure 2.41: ^{1}H NMR spectrum of complex **2.67** in acetone-d_6

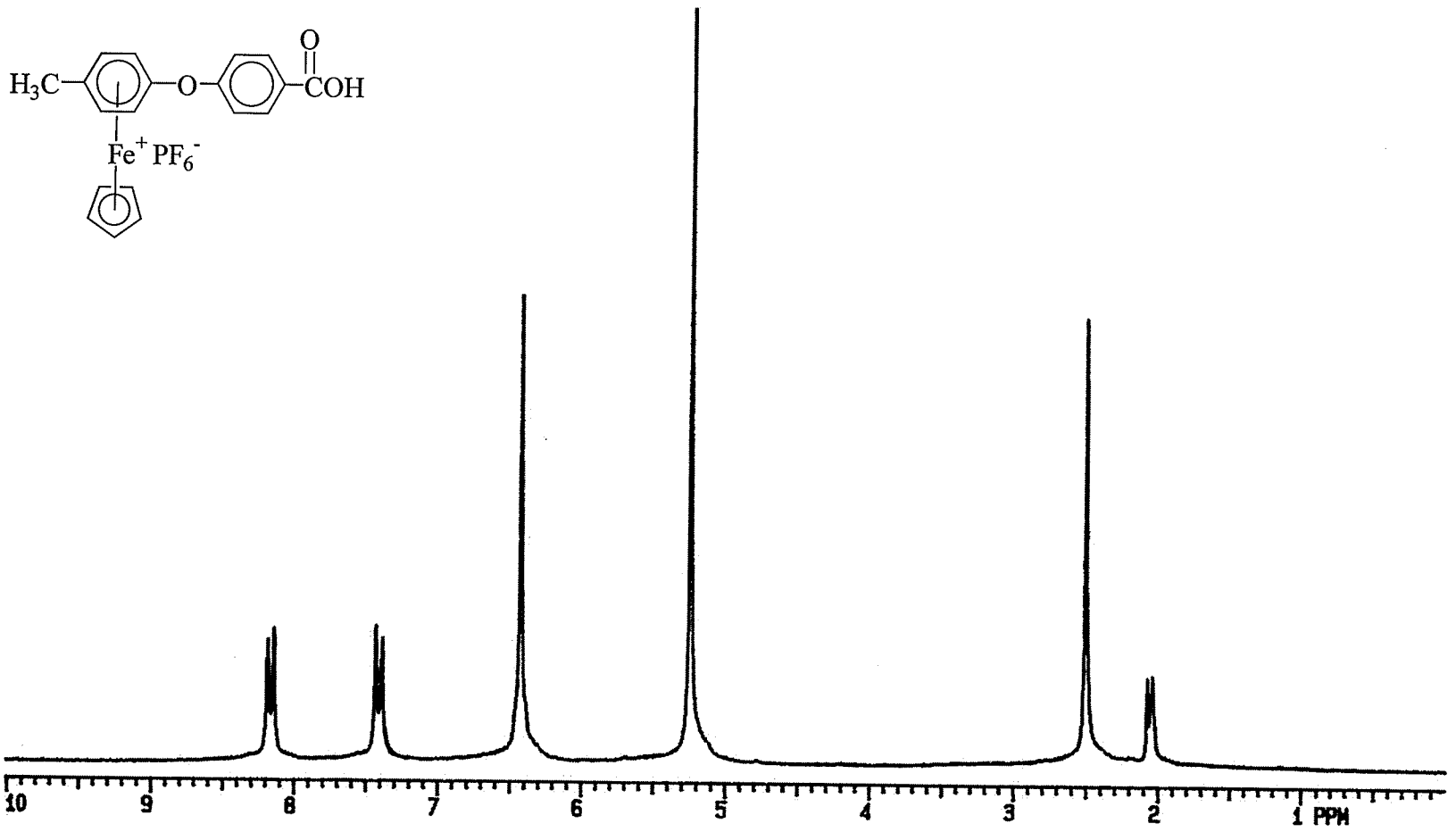

Figure 2.42: ^{1}H NMR spectrum of complex **2.68** in acetone-d_6

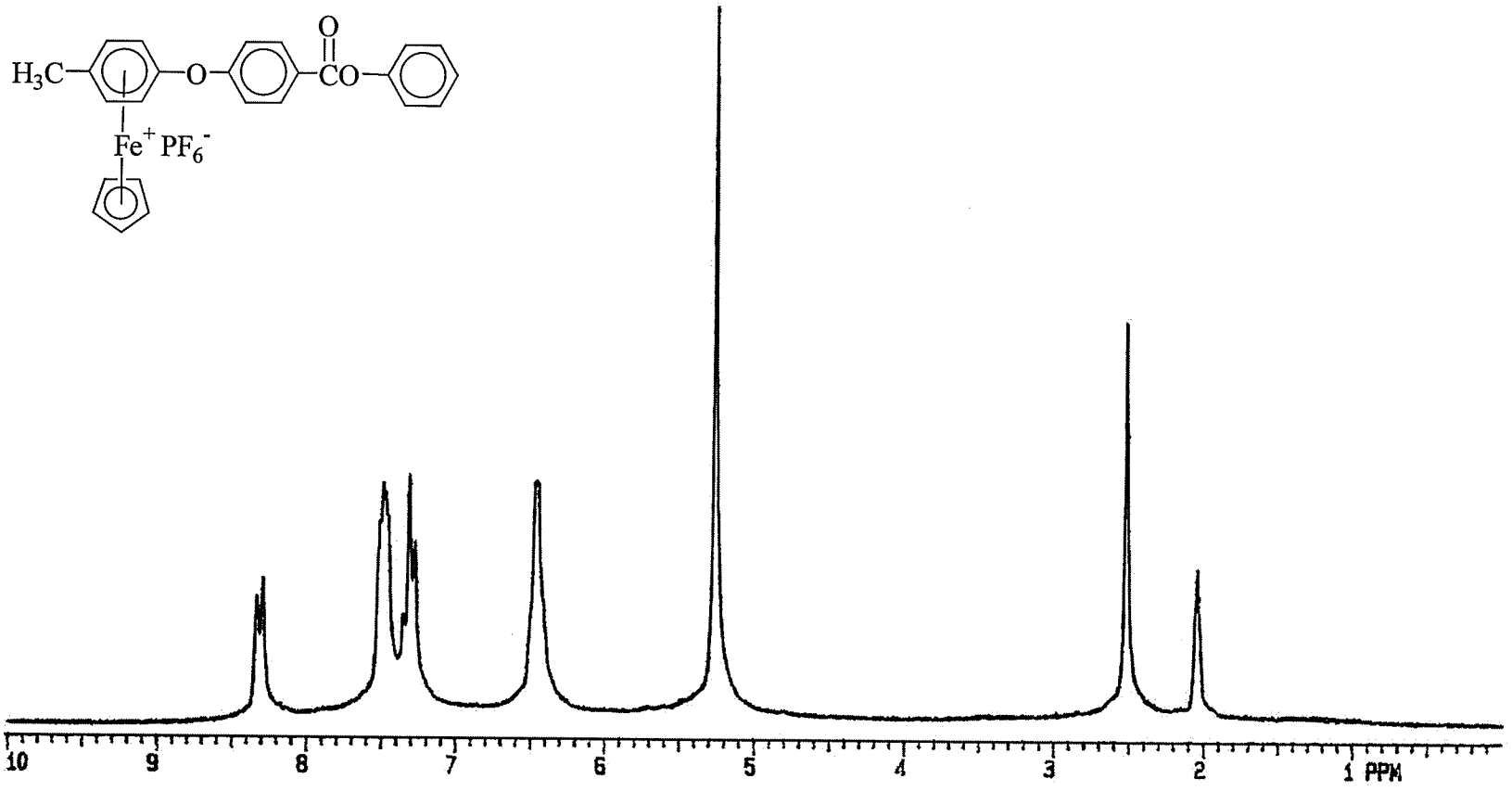

Figure 2.43: ^{1}H NMR spectrum of complex **2.69** in acetone-d_6

The % yields and ^{1}H NMR data corresponding to complexes **2.65** and **2.67-2.69** are provided in Table 2.47. The IR and ^{13}C NMR analysis for these complexes are given in Table 2.48. All data were consistent with successful preparation of the monomeric analogues to polymer **2.17**.

Table 2.47: % Yield and ^{1}H NMR Analysis of Complexes **2.65** and **2.67-2.69** in Acetone-d_6

Complex	% Yield	Other	Cp	Complexed Ar	Ar
2.65	95	2.92 (t, J = 7.23 Hz, 3H, CH_2), 3.76 (t, J = 7.23 Hz, 3H, CH_2), 8.12 (s, 1H, CH=N), 8.77 (s, 1H, OH)			6.86 (d, J = 8.59 Hz, 2H), 7.15-7.26 (m, 5H), 7.60 (d, J = 8.59 Hz, 2H)
2.67	90	2.52 (s, 3H, CH_3), 10.06 (s, 1H, CHO)	5.26 (s, 5H)	6.43 (d, J = 7.03 Hz, 2H), 6.49 (d, J = 7.03 Hz, 2H)	7.49 (d, J = 8.59 Hz, 2H), 8.08 (d, J = 8.98 Hz, 2H)
2.68	68	2.51 (s, 3H, CH_3)	5.25 (s, 5H)	6.43 (s, 4H)	7.42 (d, J = 8.50 Hz, 2H), 8.17 (d, J = 8.50 Hz, 2H)
2.69	61	2.52 (s, 3H, CH_3)	5.27 (s, 5H)	6.48 (br.s, 4H)	7.27-7.36 (m, 3H), 7.45-7.52 (m, 4H), 8.32 (d, J = 8.34 Hz, 2H)

Table 2.48: IR and ^{13}C NMR Analysis of Complexes **2.65** and **2.67-2.69** in Acetone-d_6

Complex	IR (cm^{-1})	Other	Cp	Complexed Ar	Ar
2.65		37.25 (CH_2), 62.03 (CH_2), 160.39 (CH=N)			115.51, 125.91, 127.53*, 128.19, 128.87, 129.64, 140.08*, 159.92*
2.67	1698 (CO)	19.87 (CH_3), 186.10 (CO)	78.83	78.87, 88.04, 102.33*, 131.40*	121.17, 132.90, 134.96*, 159.72*
2.68	1682 (CO)	19.85 (CH_3), 166.68 (CO)	78.74	78.37, 87.97, 102.13*, 131.91*	120.87, 128.87*, 133.16, 158.55*
2.69	1734 (CO)	20.20 (CH_3), 164.42 (CO)	78.95	78.80, 88.22, 102.12*, 131.43*	121.02, 122.53, 126.66, 127.58*, 130.22, 133.45, 151.72*, 159.09*

*Denotes quaternary carbons

It was hoped that the synthesis of complex **2.69** would help to determine whether or not the two reduction waves found in polymer **2.17** and complex **2.62** were a result of communication between the iron centers or due to the presence of the ester functional group. Figure 2.44 shows the cyclic voltammogram of **2.69** run under the same conditions as polymer **2.17** and complex **2.62**. It is clear from this CV that there is only one redox process due to the reversible reduction of the cationic eighteen-electron iron centers to nineteen-electron neutral iron centers.

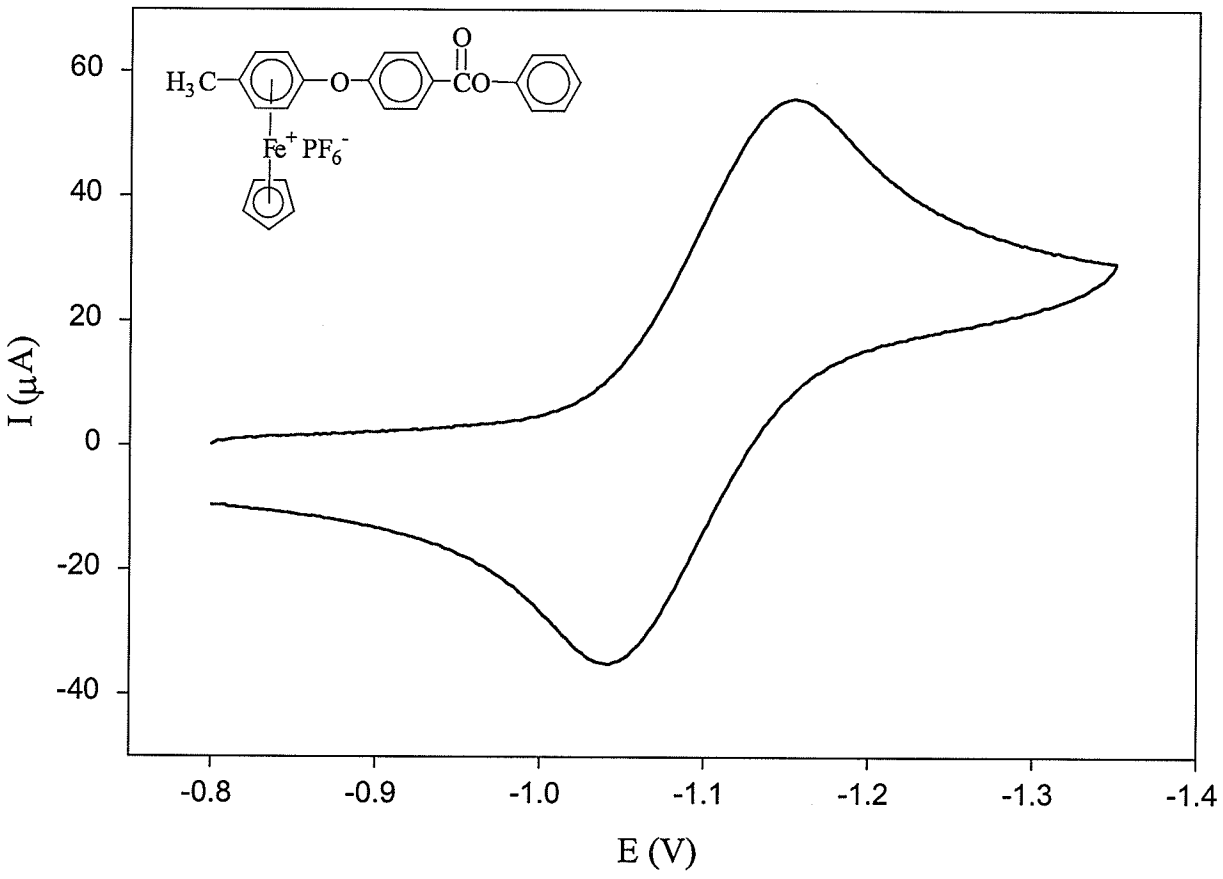

Figure 2.44: Cyclic voltammogram of **2.69** obtained at a scan rate of 0.2 V/s

The electrochemical properties of the organoiron polythioethers were also examined. The CV of polymer **2.31** containing an octamethylene bridge is shown in Figure 2.45. This CV shows two sequential one-electron reduction steps of each of the iron centers pendent to the polymer backbone at a scan rate of 5 V/s. It was found that at low scan rates, the second reduction step was irreversible, however, this reduction step became more reversible at higher scan rates. The $E_{1/2}$ values for the reduction to the neutral nineteen-electron and anionic twenty-electron iron species were found at –1.07 and –1.77 V, respectively.

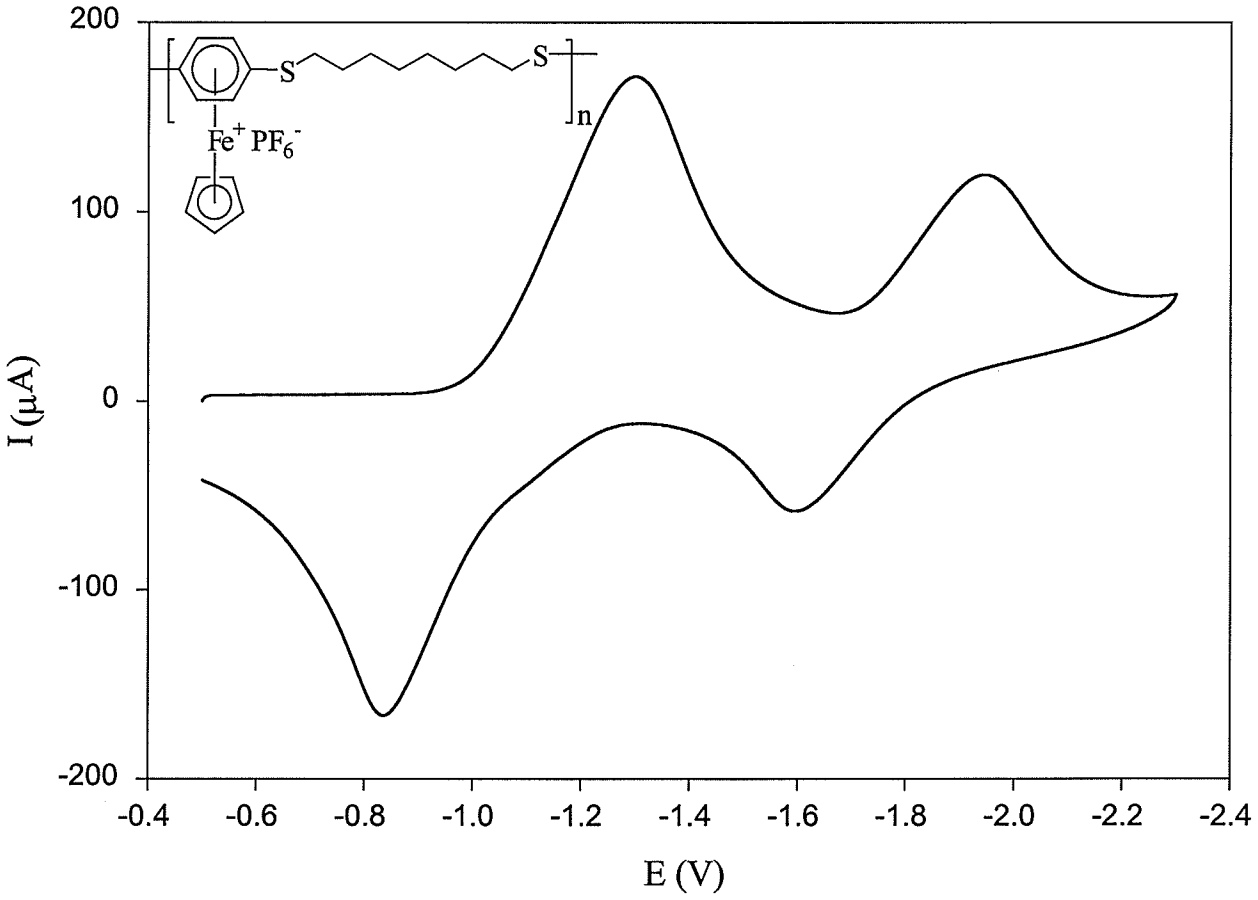

Figure 2.45: Cyclic voltammogram of **2.31** obtained at a scan rate of 5 V/s

The cyclic voltammograms of the cyclopentadienyliron-coordinated polyphenylenesulfide were also examined from scan rates ranging from 0.1 to 5 V/s. At low scan rates, adsorption of the polymer onto the working electrode complicated the cyclic voltammograms. The cyclic voltammograms of this polymer were obtained a number of times, and in each case, there were intense adsorption peaks. Figure 2.46 shows the CV of polymer **2.38** obtained in DMF at –40 °C using a scan rate of 1 V/s. The $E_{1/2}$ for this polymer occurred at –0.87 V versus Ag/AgCl.

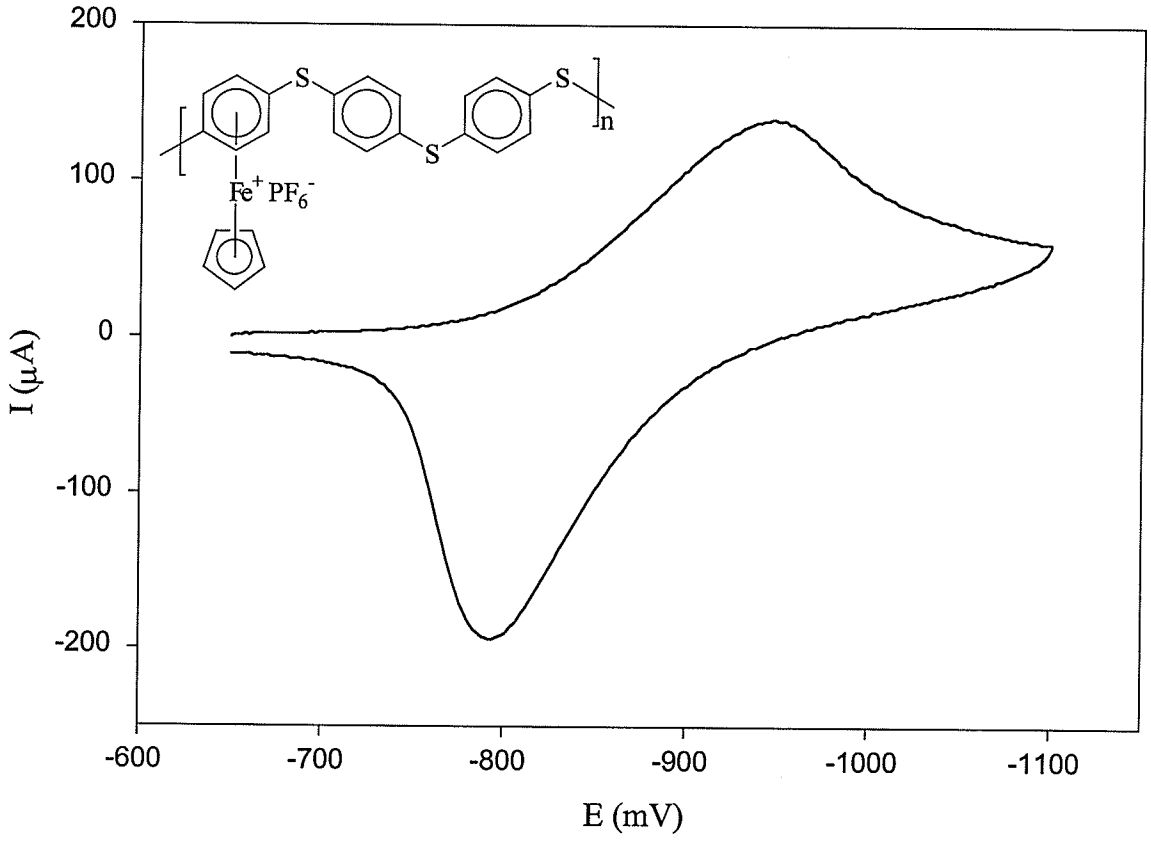

Figure 2.46: Cyclic voltammogram of **2.38** obtained at –40 °C in DMF using a scan rate of 1 V/s

The electrochemical properties of the cyclopentadienyliron-coordinated polyphenylene sulfide were also examined in propylene carbonate in order to investigate the effect of solvent on the electrochemical stability of this polymer. As well, the cyclic voltammograms were obtained from –40 to 0 °C so that the effects of temperature could be determined. Figure 2.47 shows the cyclic voltammogram of polymer **2.38** at –30 °C in DMF obtained with a scan rate of 2 V/s. It is apparent that this polymer is adsorbing to the working electrode and the cyclic voltammogram has an $E_{1/2}$ value of –0.84 V.

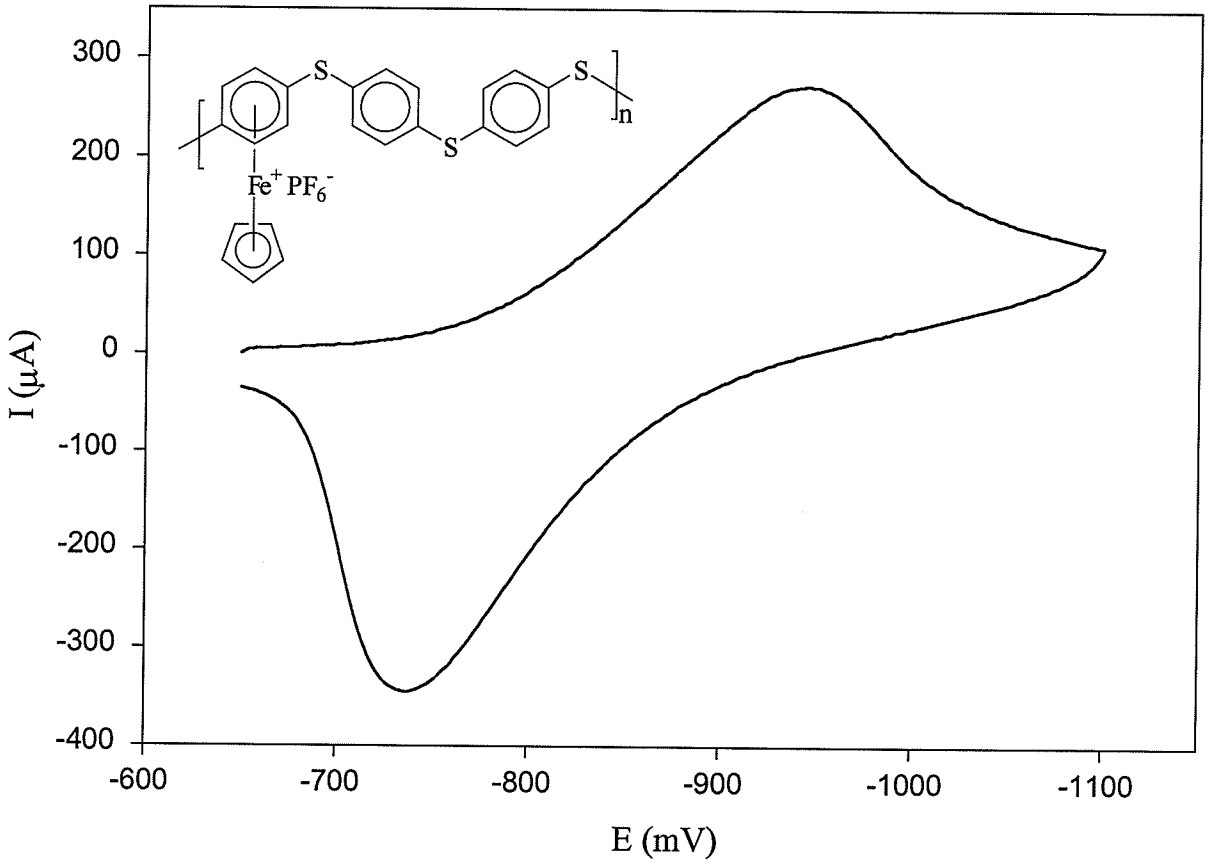

Figure 2.47: Cyclic voltammogram of **2.38** obtained at –30 °C in DMF using a scan rate of 2 V/s

Figure 2.48 shows the cyclic voltammogram of polymer **2.38** obtained at 0 °C with a scan rate of 2 V/s. It can be seen that the redox wave still appears to be reversible, however, the intensity of the oxidation peak is probably still enhanced due to adsorption. It has been reported that adsorption of arene cyclopentadienyliron complexes is more pronounced at low temperatures.[52] It was also reported that complexes containing thioether spacers are more electrochemically stable at high temperatures than complexes containing ether spacers.[50] The $E_{1/2}$ value obtained for this polymer was –0.85 V.

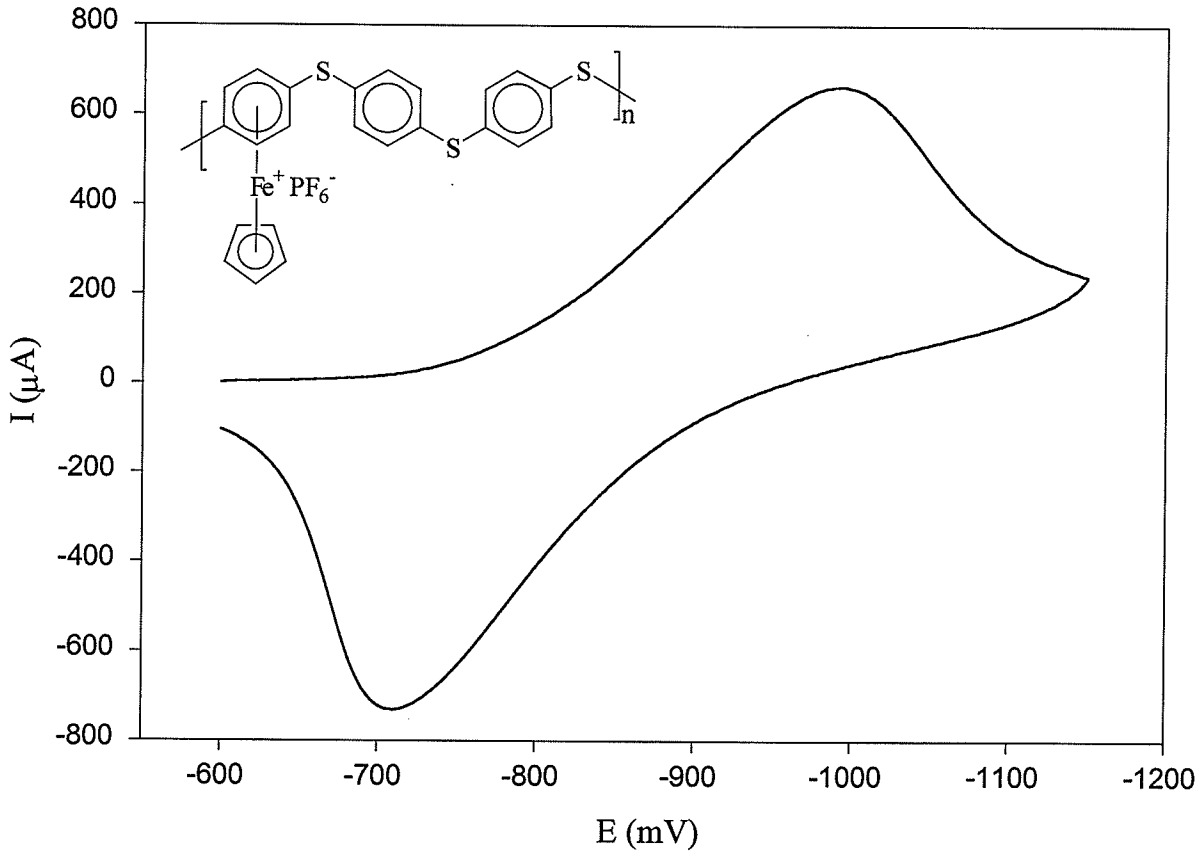

Figure 2.48: Cyclic voltammogram of **2.38** obtained at 0 °C in DMF using a scan rate of 2 V/s

The cyclic voltammograms of the organoiron polyphenylene sulfide were also obtained in propylene carbonate. It has previously been reported that arene complexes of cyclopentadienyliron possess good electrochemical stability in propylene carbonate. The influence of solvents on the reversibility of the redox waves of these complexes is related to their coordinating ability.[50,52] It was found that the cyclic voltammogram of polymer **2.38** did not show the same adsorption peak in propylene carbonate as it did in DMF. The half-wave potential of **2.38** in propylene carbonate at –30 °C was –0.85 V using a scan rate of 2 V/s. This cyclic voltammogram is shown in Figure 2.49.

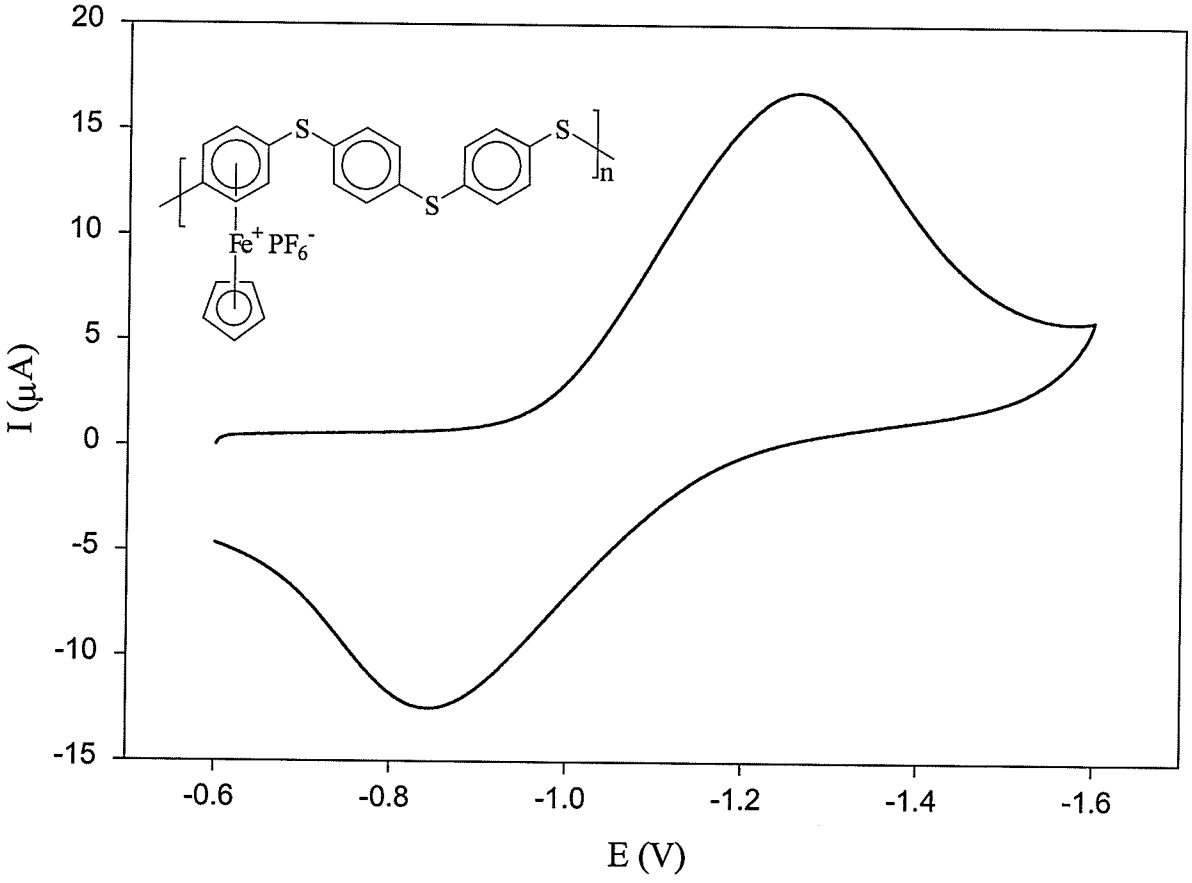

Figure 2.49: Cyclic voltammogram of **2.38** obtained at -30 °C in propylene carbonate with a scan rate of 2 V/s

It was also of interest to study the electrochemical properties of a monomeric analogue of polymer **2.38**. The synthesis of a dithiophenol complex of cyclopentadienyliron is shown in Scheme 2.15. Complex **2.71** was synthesized via reaction of *p*-dichlorobenzene-cyclopentadienyliron hexafluorophosphate with thiophenol (**2.70**). The spectroscopic data for complex **2.71** are found in Tables 2.49 and 2.50. Figures 2.50 and 2.51 show the ^{1}H and ^{13}C NMR spectra of complex **2.71**.

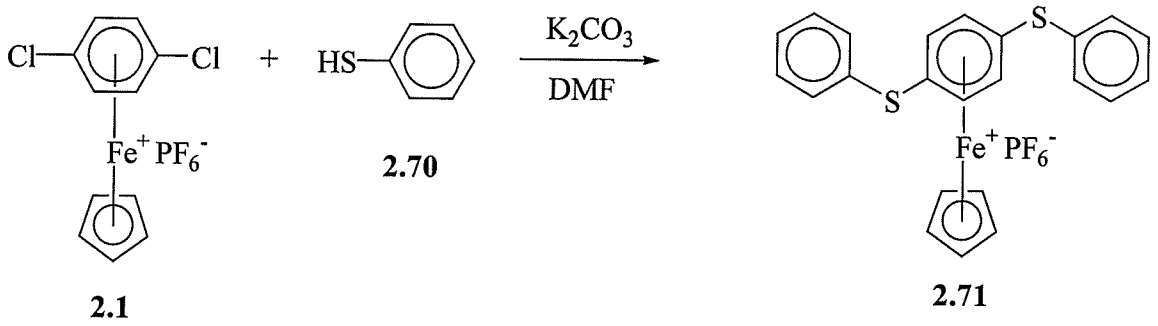

2.1 **2.70** **2.71**

Scheme 2.15

Table 2.49: % Yield and ^{1}H NMR Analysis of Complex **2.71** in Acetone-d_6

Complex	% Yield	Cp	Complexed Ar	Ar
2.71	80	5.20 (s, 5H)	6.32 (s, 4H)	7.58-7.61 (m, 6H), 7.70-7.75 (m, 4H)

Table 2.50: ^{13}C NMR Analysis of Complexes **2.71** in Acetone-d_6

Complex	Cp	Complexed Ar	Ar
2.71	84.50	79.85, 108.30*	128.23*, 130.74, 130.88, 135.39

*Denotes quaternary carbons

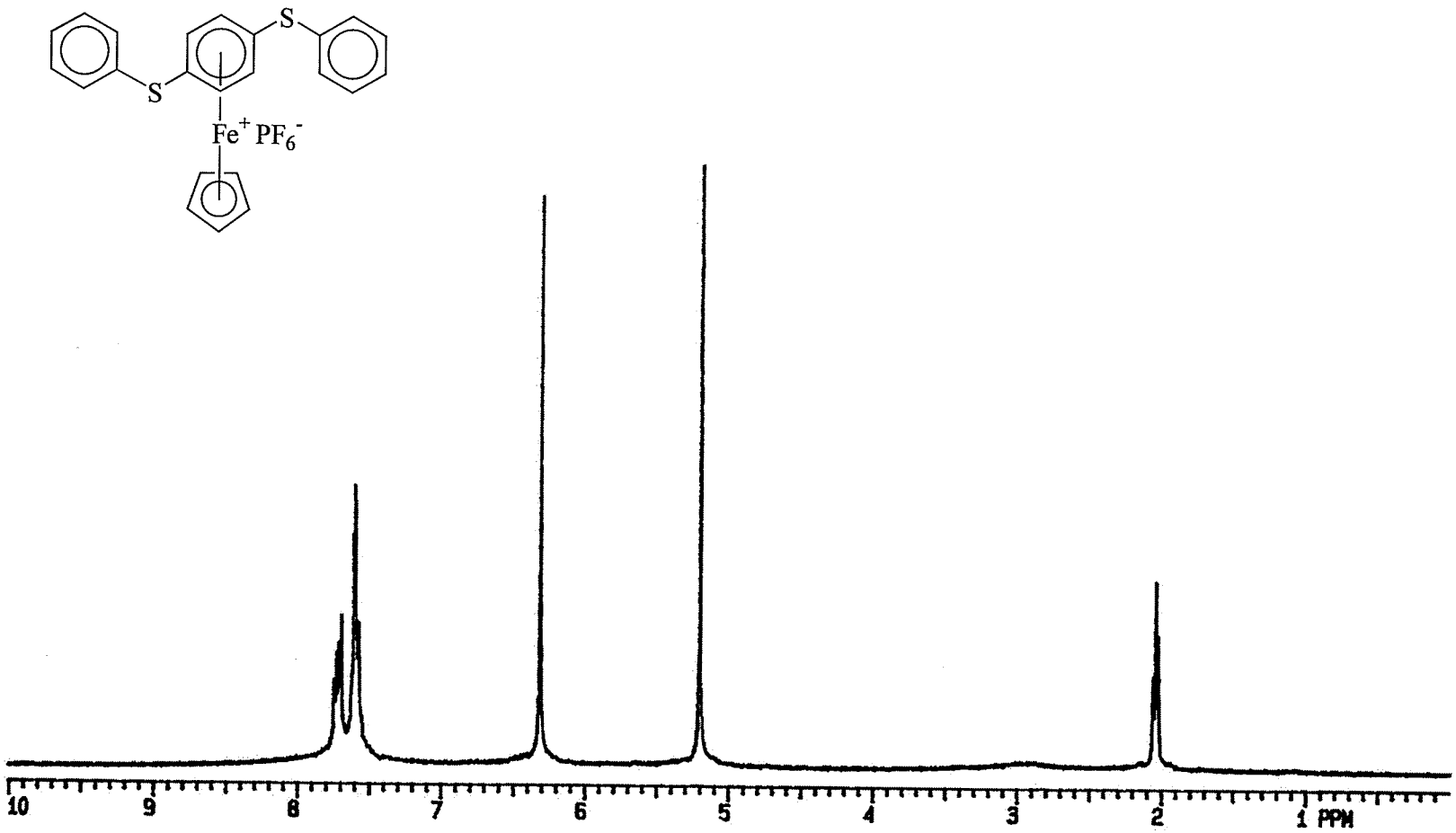

Figure 2.50: ^{1}H NMR spectrum of complex **2.71** in acetone-d_6

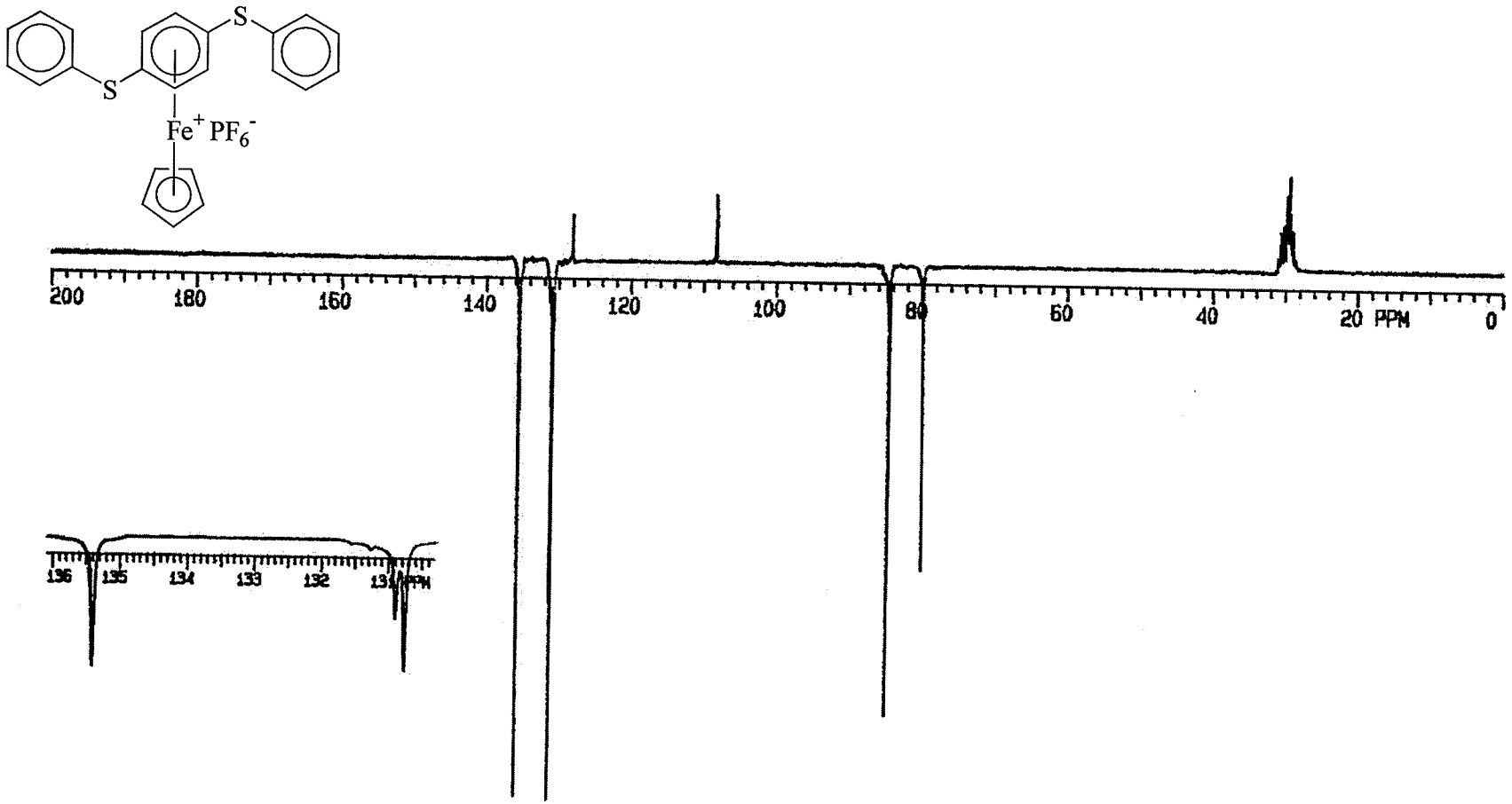

Figure 2.51: ^{13}C NMR spectrum of complex **2.71** in acetone-d_6

The cyclic voltammograms of complex **2.71** showing one and two reduction steps are shown in Figures 2.52 and 2.53. Figure 2.52 shows the one-electron reduction of the iron centers at $E_{1/2}$ = -1.02V. It can be seen that this CV is much more symmetric than its polymeric analogue (**2.38**). As well, there is no adsorption of the monoiron complex onto the working electrode as was observed for the polyphenylenesulfide.

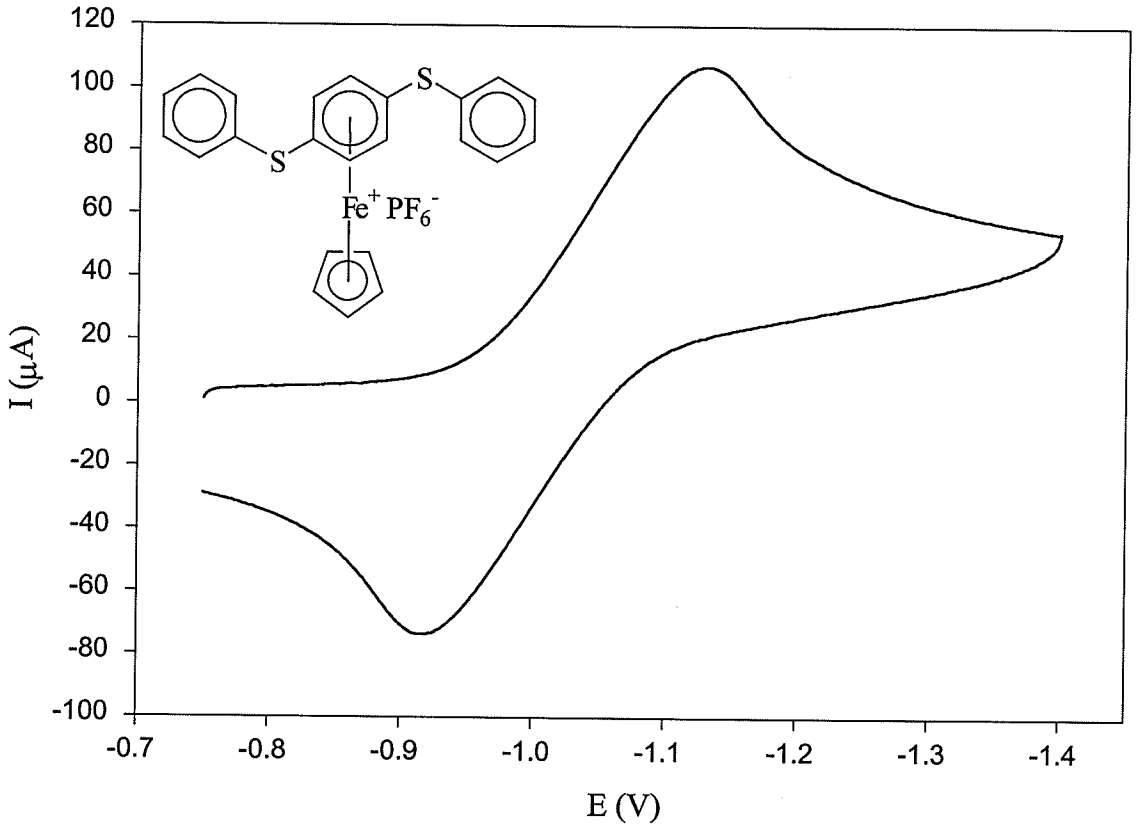

Figure 2.52: Cyclic voltammogram of **2.71** obtained at a scan rate of 1 V/s

Figure 2.53 shows the two sequential one-electron reduction processes of the iron centers in complex **2.71**, something which was not observed in the cyclic voltammograms of the polymer. While the first reduction was reversible at 1 V/s and occurred at $E_{1/2}$ = -1.01V, the second reduction was irreversible and the E_{pc} was observed at –1.84 V.

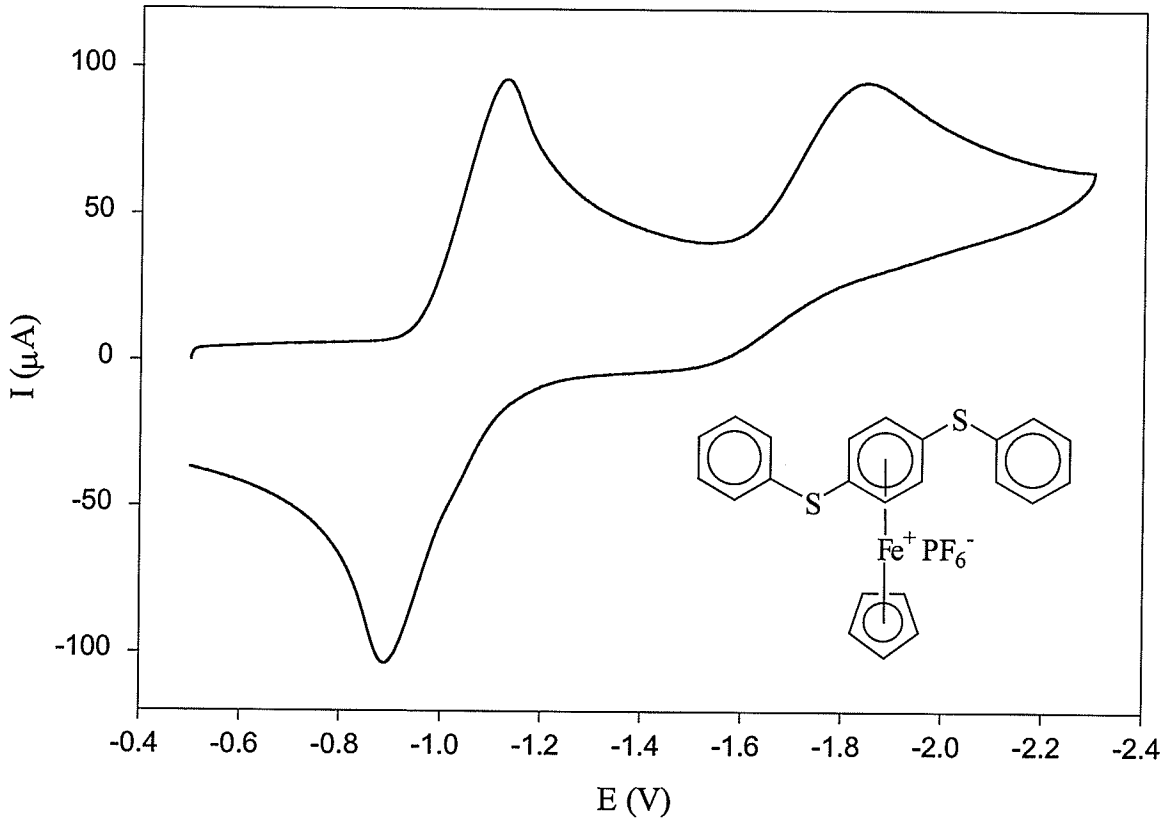

Figure 2.53: Cyclic voltammogram of **2.71** obtained at a scan rate of 1 V/s

In order to complete the electrochemical investigations, the redox properties of the copolymers were also studied. The cyclic voltammogram of polymer **2.46**, containing aromatic ether and thioether bridges was examined. Figure 2.54 shows the CV obtained at –30 °C using a scan rate of 1 V/s. The E_{pc}, E_{pa} and $E_{1/2}$ for this polymer were calculated to be –1.23, -0.955 and –1.09 V, respectively.

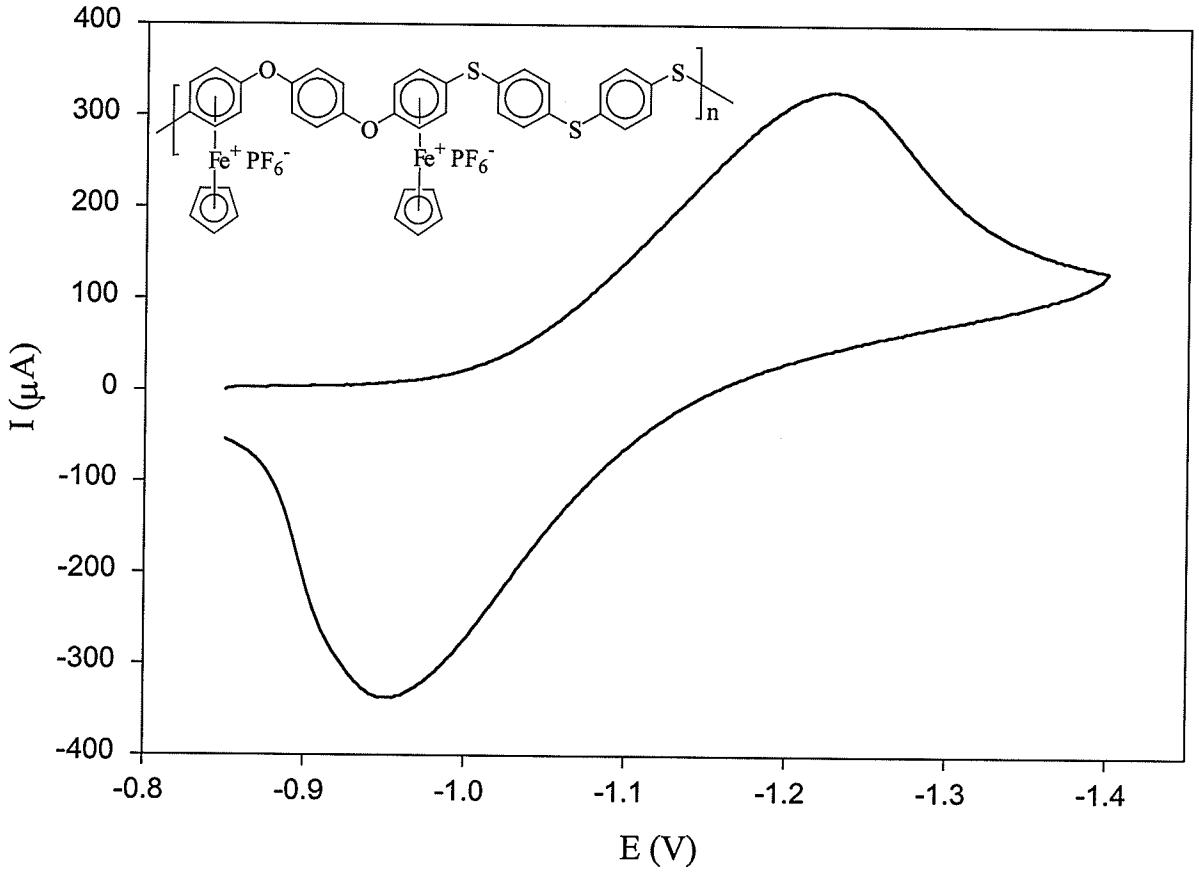

Figure 2.54: Cyclic voltammogram of **2.46** obtained at a scan rate of 1 V/s

A bimetallic complex containing aromatic ether and thioether bridges was also synthesized in order to compare its electrochemical properties to those of polymer **2.46**. The synthesis of this model complex (**2.72**) is shown in Scheme 2.16. Reaction of the diiron complex **2.45** with thiophenol allowed for the isolation of the mixed ether/thioether complex. The spectroscopic data for this complex are given in Tables 2.51 and 2.52.

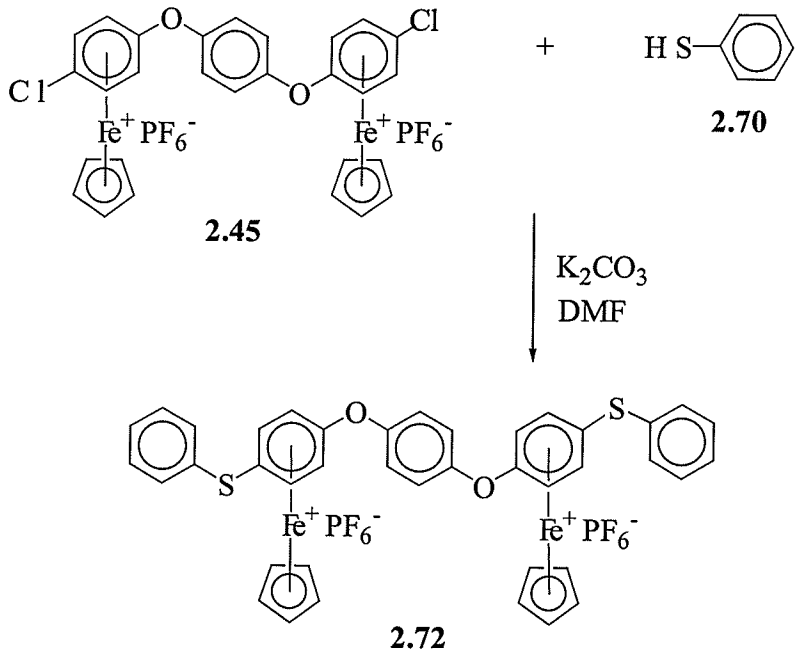

Scheme 2.16

Table 2.51: % Yield and ^{1}H NMR Analysis of Complex **2.72** in Acetone-d_6

Complex	% Yield	Cp	Complexed Ar	Ar
2.72	91	5.25 (s, 5H)	6.30 (br.s, 4H), 6.44 (br.s, 4H)	7.53 (s, 4H), 7.60 (br.s, 6H), 7.71 (br.s, 4H)

Table 2.52: CH Analysis and ^{13}C NMR Analysis of Complexes **2.72** in Acetone-d_6

Complex	CH Analysis	Cp	Complexed Ar	Ar
2.72	($C_{40}H_{32}F_{12}Fe_2O_2P_2S_2$) (1010.43) Calcd. C, 47.55; H, 3.19; Found C, 47.80; H, 3.40	79.54	76.56, 85.11, 106.01*, 133.26*	124.13, 129.74*, 131.06, 131.16, 135.24, 151.49*

*Denotes quaternary carbons

The cyclic voltammogram of complex **2.72** is given in Figure 2.55. The E_{pc}, E_{pa} and $E_{1/2}$ for this bimetallic cyclopentadienyliron complex were found to be –1.21, –1.03 and –1.12 V, respectively. It can be seen that this CV has a much more symmetric shape and the reduction and oxidation peaks are much narrower.

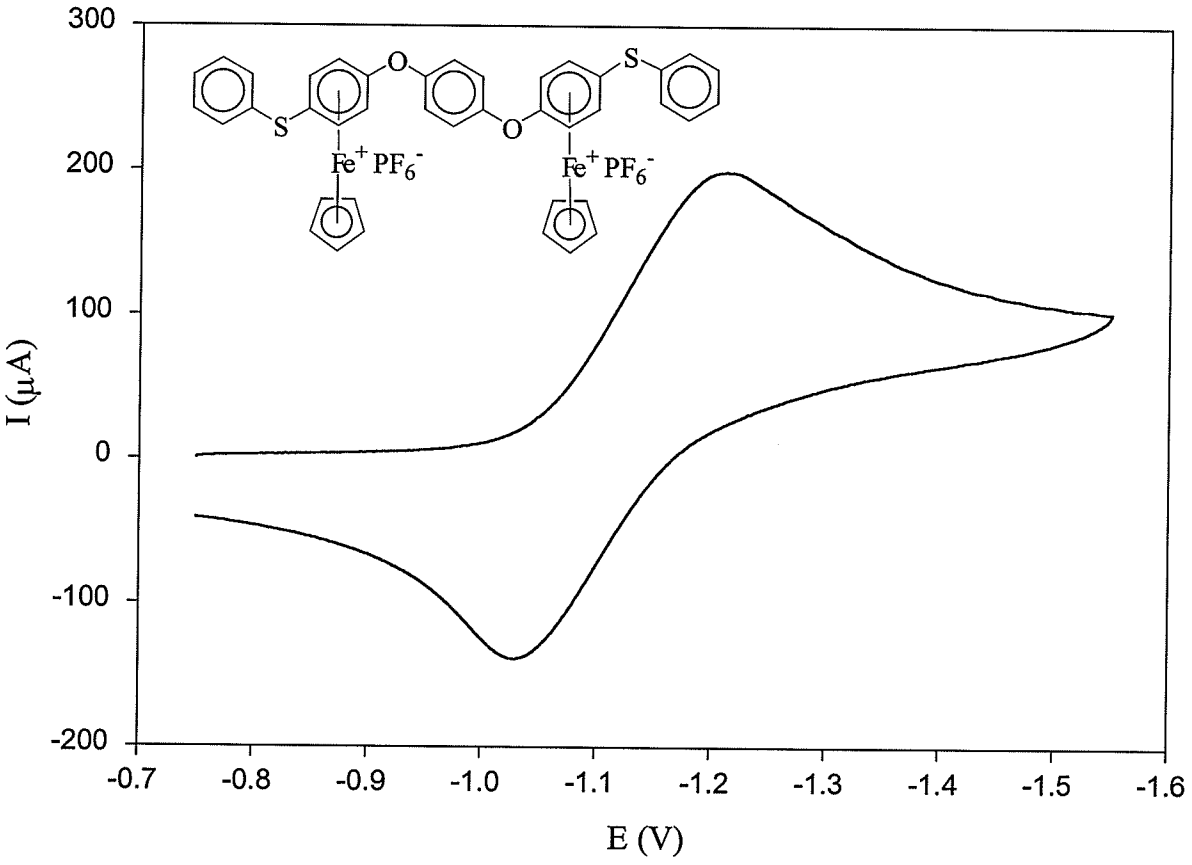

Figure 2.55: Cyclic voltammogram of **2.72** obtained at a scan rate of 1 V/s

2.3 Conclusion

This work presents the synthesis of polyethers, thioethers and amines coordinated to cyclopentadienyliron moieties. The methodology used to prepare these polymers demonstrates the versatility of using dichloroarene complexes of cyclopentadienyliron to prepare soluble organoiron polymers with either aliphatic or aromatic bridges. Demetallation of the organoiron polymers gave rise to the corresponding organic polymers, which exhibited reduced solubility.

The thermal properties of the organoiron and organic polymers were dependent on the nature of the polymeric backbone and the types of heteroatoms present. All of the organometallic polymers exhibited a weight loss starting anywhere from 200 to 270 °C, corresponding to cleavage of the cyclopentadienyliron moieties, however, the second weight loss steps in these polymers were dependent upon the spacers between the complexed aromatic rings. For example, polyaromatic ethers began to lose weight starting from 417 to 518 °C, while the polymers with aliphatic thioether spacers began to decompose from 363 to 402 °C. The polymers with aromatic thioether spacers began to lose weight between 443 and 511 °C. The polyphenylene sulfide with the *o*-substituted rings was the least thermally stable, while the polymer with the *p*-substituted aromatic rings was the most stable of the series. It was also noted that polymers with etheric bridges had higher glass transition temperatures than those with thioetheric bridges.

The organic polyethers had glass transition temperatures between 113 and 165 °C, which is much higher than the 33 to 37 °C measured for the polymers with aliphatic thioether spacers. The polymer with four methylene groups in its spacers had the highest T_g (37 °C), while the polymer with the octamethylene spacers had the lowest T_g (33 °C).

The glass transition temperatures of the aromatic polythioethers occurred at intermediate temperatures ranging from 72 to 88 °C. The *m*-substituted polymer had the highest T_g, while the *o*-substituted polymer had the lowest T_g. The glass transition temperatures of the polymers with ether and thioether spacers in their backbones were very similar to those of the purely thioether analogues. While the T_g values for these materials were slightly higher than their corresponding thioethers, it was apparent that the influence of the sulfur spacers was more important than the influence of the oxygen spacers. Polymers with amine and thioether bridges had glass transition temperatures of 113 and 119 °C, indicating that the amine bridges increased the T_g values of these polymers significantly.

Electrochemical analysis of these polymers demonstrated that the cationic iron centers undergo reduction processes to nineteen- and twenty-electron complexes. Small complexes were also synthesized as model materials for the cyclic voltammetric experiments. While the redox couples of the monomeric and polymeric materials occurred at approximately the same potentials, many of the polymers adsorbed onto the working electrode and had broad cyclic voltammograms. One of the polyaromatic ethers showed two distinct redox processes at –0.988 and –1.11 V, indicating that some communication between the iron centers may be occurring. The same behaviour was observed for its monomeric analogue. The half-wave potentials occurred between –1 and –1.4 V for the polyaromatic ethers, and between –0.8 and –1.1 V for the polythioethers. The second reduction process for an aliphatic polythioether was found to occur at –1.8 V. A polymer with oxygen and sulfur bridges in its backbones had an $E_{1/2}$ value of –1.1 V, which is in between the values obtained for the polyethers and polythioethers.

2.4 Experimental

Materials

The dichloroarene complexes (**2.1, 2.35, 2.36, 2.66**)[21-26,347] and the diiron complex (**2.45**)[106] were prepared according to previously reported procedures. All reagents were commercially available and used without purification, with the exception of hexane and tetrahydrofuran (THF). Hexane was distilled over calcium chloride, and THF was distilled from sodium metal and benzophenone prior to use. All dinucleophiles, with the exception of **2.3** and **2.9**, which were prepared according to the procedures outlined below, were purchased from the Aldrich Chemical Company. All reactions carried out with organometallic complexes were conducted with the flasks covered in aluminum foil to limit contact with light.

Characterization

^{1}H and ^{13}C NMR spectra were recorded at 200 and 50 MHz, respectively, on a Varian Gemini 200 NMR spectrometer, with chemical shifts (ppm) calculated from solvent signals. ^{13}C NMR spectra were obtained using an attached proton test (APT). Infrared spectra were recorded on a Bomem, Hartmann & Braun FT-IR spectrophotometer using KBr pellets. Gel permeation chromatography (GPC) measurements were performed using a Phenomenex BL-gel mixed D column equipped with an Eppendorf CH-30 column heater and a PL-DCU data station (Polymer Laboratories). Molecular weights were calculated relative to polystyrene standards with chloroform as the eluent. Thermogravimetric analysis (TGA) was performed on a Mettler TGA/SDTA851^{e} with a heating rate of 20 °C/min under a nitrogen atmosphere.

Differential scanning calorimetry (DSC) was performed on a Mettler DSC821^e with a heating rate of 20 °C/min under a nitrogen atmosphere. Cyclic voltammetric experiments were performed using an EG&G Princeton Applied Research model 263A potentiostat using a Ag/AgCl reference electrode, a glassy carbon working electrode and a platinum auxiliary electrode.

2.4.1 Synthesis of 2.1

1,4-Dichlorobenzene (40.4 g, 2.75 mol) was melted in a 500 mL, three-neck round bottom flask equipped with a condenser and a thermometer. The solution was stirred as ferrocene (27.9 g, 1.50 mol), anhydrous aluminum chloride (40.0 g, 3.00 mol) and aluminum powder (4.05 g, 1.50 mol) were added. The contents of the flask were stirred at 135 °C under a nitrogen atmosphere for five hours. The solution was cooled to about 85 °C, and then slowly poured into a beaker containing 400 mL of ice. The flask was rinsed with distilled water and this solution was also added to the beaker. The contents of the beaker were stirred for five minutes and then filtered through a Buchner funnel containing sand. The filtrate was poured into a separatory funnel and washed with diethyl ether until the ether was no longer colored. Ammonium hexafluorophosphate (10-12 g) was then added to the aqueous layer, resulting in the formation of a green precipitate. This mixture was then extracted with dichloromethane or a dichloromethane/acetone solution until the aqueous layer was clear. The organic solution was dried over magnesium sulfate and filtered. The solution was concentrated using a rotary evaporator and precipitated upon the addition of diethyl ether. The green-yellow solid was collected in a Buchner funnel, rinsed with ether and then dried.

2.4.2 Synthesis of 2.3

4-Aminophenyl ether (4.01 g, 20 mmol), 4-hydroxybenzoic acid (6.98 g, 5 mmol), triphenyl phosphite (10.5 mL, 40 mmol), 1-methyl-2-pyrolidinone (anhydrous) (20 mL), calcium chloride (1.1 g, 10 mmol) and pyridine (1.72 mL, 20 mmol) were placed in a 100 mL round bottom flask and stirred at 100 °C for 4 hours under a nitrogen atmosphere. The reaction mixture was poured into 20% ethanol, and the product was collected in a sintered glass crucible and dried under reduced pressure.

2.4.3 Synthesis of 2.9

Terephthaloyl chloride (6.06 g, 30 mmol), bisphenol A (16.0 g, 70 mmol) and 70 mL of pyridine were combined in a 100 mL round bottom flask. The reagents were stirred for 24 h at room temperature and were subsequently poured into 50 mL of distilled water. The resulting white precipitate was collected in a sintered glass crucible, washed with water, and dried under reduced pressure.

2.4.4 Synthesis of 2.35 and 2.36

In a 500 mL three-neck round bottom flask equipped with a condenser and a thermometer, 1,2- or 1,3-dichlorobenzene (50 mL) was combined with ferrocene (27.9 g, 1.50 mol), anhydrous aluminum chloride (40.0 g, 3.00 mol) and aluminum powder (4.05 g, 1.50 mol). The contents of the flask were stirred at 135 °C under a N_2 atmosphere for 5 hours. Work-up of these complexes followed the procedure outlined for complex **2.1**.

2.4.5 Synthesis of 2.45

Complex **2.1** (0.826 g, 2.0 mmol) was reacted with **2.44** (0.110 g, 1.0 mmol) and potassium carbonate (0.346 g, 2.5 mmol) in a 50 mL round bottom flask containing 10 mL of DMF. The reagents were stirred at room temperature under a nitrogen atmosphere for 12 h, and then poured into 50 mL of 10% HCl (v:v). Following addition of ammonium hexafluorophosphate (0.326 g, 2.0 mmol), the beige precipitate was collected in a sintered glass crucible, washed with water, followed by ether, and then dried under reduced pressure.

2.4.6 Synthesis of 2.50 and 2.51

Complex **2.1** (1.65 g, 4.0 mmol), dinucleophile **2.48** or **2.49** (2.0 mmol) and potassium carbonate (0.691 g, 5.0 mmol) were combined in a 50 mL round bottom flask containing 7 mL of THF and 7 mL of DMF. The contents of the flask were stirred at 65 ^{o}C for 6 h under a nitrogen atmosphere. Following reaction, the solution was poured into 50 mL of 10% HCl (v:v), and ammonium hexafluorophosphate (0.652 g, 4.0 mmol) was added. The resulting yellow-orange precipitate was collected in a sintered glass crucible, washed with water, dried, then washed with ether.

2.4.7 Synthesis of Organoiron Polymers 2.10-2.17, 2.29-2.31, 2.38-2.40, 2.46, 2.47, 2.52 and 2.53

The organometallic polymers were prepared by placing a dichloroarene complex (**2.1, 2.35, 2.36, 2.45, 2.50** or **2.51**) (2.0 mmol), a dinucleophile (**2.2-2.9, 2.26-2.28** or **2.37**) (2.0 mmol) and potassium carbonate (0.691 g, 5.0 mmol) into a 25 mL round

bottom flask containing 2-3 mL of DMF. The reagents were stirred at 60 °C under a nitrogen atmosphere for 6 h, and then poured into 50 mL of 10% HCl (v:v). Following addition of ammonium hexafluorophosphate, the beige or yellow precipitate was collected in a sintered glass crucible, washed with water, followed by ether, and then dried. If the polymer did not precipitate upon addition of ammonium hexafluorophosphate, the solution was extracted immediately with a dichloromethane/nitromethane mixture, washed with water and dried over magnesium sulfate. After filtration, the solution was concentrated using a rotary evaporator. Following addition of diethyl ether, the precipitated polymer was collected in a sintered glass crucible and dried under reduced pressure.

2.4.8 Isolation of Organic Polymers 2.18-2.25, 2.32-2.34, 2.41-2.43 and 2.54-2.57

The organometallic polymer (**2.10-2.17, 2.29-2.31, 2.38-2.40, 2.46, 2.47, 2.52** or **2.53**) (1 mmol) was placed in a 50 mL Pyrex tube containing 20 mL of dichloromethane and 20 mL of acetonitrile. If the polymer was not completely soluble in this solvent system, DMF was added to the mixture, and the solution stirred for a few hours. The polymer solution was flushed with nitrogen and then placed in a Rayonet Mini-Reactor containing RMR-2537A° lamps, and irradiated for 8 h. The solvents were removed under reduced pressure, and the resulting material was extracted with chloroform or a chloroform/nitromethane mixture. The organic layer was washed with water repeatedly, and then dried over magnesium sulfate. The polymer solution was filtered and concentrated by rotary evaporation. The organic polymer (**2.18-2.25, 2.32-2.34, 2.41-**

2.43 or **2.54-2.57**) precipitated upon addition of hexane, and the resulting off white material was collected in a sintered glass crucible and dried.

2.4.9 Synthesis of 2.58 and 2.61

Complex **2.1** (0.826 g, 2.0 mmol) was reacted with **2.6** or **2.9** (1.0 mmol) and potassium carbonate (0.346 g, 2.5 mmol) in a 50 mL round bottom flask containing 10 mL of DMF. The reagents were stirred at room temperature under a nitrogen atmosphere for 12 h, and then poured into 50 mL of 10% HCl (v:v). Following addition of ammonium hexafluorophosphate (0.326 g, 2.0 mmol), the beige precipitate was collected in a sintered glass crucible, washed with water, followed by ether, and then dried under reduced pressure.

2.4.10 Synthesis of 2.60 and 2.62

Complex **2.58** or **2.61** (1.0 mmol) was reacted with phenol (**2.59**) (0.471 g, 5.0 mmol) and potassium carbonate (0.346 g, 2.5 mmol) in a 50 mL round bottom flask containing 10 mL of DMF. The reagents were stirred at room temperature under a nitrogen atmosphere for 12 h, and then poured into 50 mL of 10% HCl (v:v). Following addition of ammonium hexafluorophosphate (0.326 g, 2.0 mmol), the beige precipitate was collected in a sintered glass crucible, washed with water, followed by ether, and then dried under reduced pressure.

2.4.11 Synthesis of 2.65

4-Hydroxybenzaldehyde (**2.63**) (7.33 g, 60 mmol) and phenethylamine (**2.64**) (8 mL, 64 mmol) and 60 mL of benzene were placed in a 250 mL round bottom flask equipped with a condenser and Dean-Stark trap. The solution was refluxed with stirring for 1 h and then cooled. The off-white solid was collected in a Buchner funnel and dried under reduced pressure.

2.4.12 Synthesis of 2.66

4-Chlorotoluene (50 mL) was combined with ferrocene (27.9 g, 1.50 mol), anhydrous aluminum chloride (40.0 g, 3.00 mol) and aluminum powder (4.05 g, 1.50 mol) in a 500 mL, three-neck round bottom flask equipped with a condenser and a thermometer. The contents of the flask were stirred at 135 °C under a nitrogen atmosphere for five hours. Work-up of this complex followed the procedure outlined for complex **2.1**.

2.4.13 Synthesis of 2.67

Complex **2.66** (3.14 g, 8.0 mmol) was reacted with **2.65** (2.25 g, 10.0 mmol) and potassium carbonate (1.66 g, 12.0 mmol) in a 50 mL round bottom flask containing 15 mL of DMF. The reagents were stirred at room temperature under a nitrogen atmosphere for 12 h, and then poured into 250 mL of 30% HCl (v:v). Following addition of ammonium hexafluorophosphate (1.30 g, 8.0 mmol), the beige precipitate was stored in the refrigerator for 24 h. Complex **2.67** was collected in a sintered glass crucible, washed with water, followed by ether, and then dried under reduced pressure. If necessary, the

complex was redissolved in acetone or DMF and added dropwise to a new solution of 30 % HCl in order to ensure that all of the imine groups were decomposed to aldehydes.

2.4.14 Synthesis of 2.68

Complex **2.67** (3.83 g, 8.0 mmol) was dissolved in 100 mL of acetone and placed in a 250 mL round bottom flask containing a stir bar. In a small flask, chromium trioxide (2.40 g, 24.0 mmol), 5 mL of sulfuric acid and 8 mL of water were combined. This solution was slowly added to complex **2.67**, and an additional 2 mL of water was added if necessary to dissolve the chromium trioxide. This solution was stirred for an additional hour and then poured into 200 mL of water. Following addition of ammonium hexafluorophosphate (1.30 g, 8.0 mmol), the carboxylic acid complex was extracted with dichloromethane and then washed with water until the solution is no longer green. The organic layer was dried over magnesium sulfate, filtered, and the solution was concentrated using a rotary evaporator. Following addition of diethyl ether, the yellow solid was collected in a sintered glass crucible and dried under reduced pressure.

2.4.15 Synthesis of 2.69

Complex **2.68** (0.988 g, 2.0 mmol) was dissolved in 3 mL of thionyl chloride and stirred at 60 °C under a nitrogen atmosphere for 2 h. The solution was dried under reduced pressure, and phenol (0.235 g, 2.5 mmol), triethylamine (0.35 mL, 2.5 mmol) and 7 mL of dichloromethane were added. This solution was stirred at room temperature under a nitrogen atmosphere for 7 h. The solution was poured into 50 mL of 10% HCl (v:v), and then ammonium hexafluorophosphate (0.326 g, 2.0 mmol) was added. The

ester complex was extracted with dichloromethane and then washed with water until the solution is no longer green. The organic layer was dried over magnesium sulfate, filtered, and the solution was concentrated using a rotary evaporator. Following addition of diethyl ether, the yellow solid was collected in a sintered glass crucible and dried under reduced pressure.

2.4.16 Synthesis of 2.71

Complex **2.1** (0.826 g, 2.0 mmol) was reacted with thiophenol (**2.70**) (0.51 mL, 5.0 mmol) and potassium carbonate (0.691 g, 5.0 mmol) in a 50 mL round bottom flask containing 5 mL of DMF. The reagents were stirred at room temperature under a nitrogen atmosphere for 12 h, and then poured into 50 mL of 10% HCl (v:v). Following addition of ammonium hexafluorophosphate (0.326 g, 2.0 mmol), the yellow precipitate was collected in a sintered glass crucible, washed with water, followed by ether, and then dried under reduced pressure.

2.4.17 Synthesis of 2.72

Complex **2.45** (0.863 g, 1.0 mmol) was reacted with thiophenol (**2.70**) (0.26 mL, 2.5 mmol) and potassium carbonate (0.346 g, 2.5 mmol) in a 50 mL round bottom flask containing 10 mL of DMF. The reagents were stirred at room temperature under a nitrogen atmosphere for 12 h, and then poured into 50 mL of 10% HCl (v:v). Following addition of ammonium hexafluorophosphate (0.163 g, 1.0 mmol), the beige precipitate was collected in a sintered glass crucible, washed with water, followed by ether, and then dried under reduced pressure.

3.0 Star Polymers Coordinated to Cyclopentadienyliron Moieties

3.1 Introduction

Recently, dendrimers and star polymers containing redox active sites have been utilized in the design of new types of catalysts, sensors and molecular batteries.[264-274] These materials have also displayed properties similar to those of enzymes, and have the potential to be used in bio-electronic devices.[66]

Highly branched polymers containing arenes coordinated to organometallic moieties have been prepared with chromium tricarbonyl, cyclopentadienyliron and pentamethylcyclopentadienylruthenium moieties.[91-100,277-280] Astruc has used this class of complex to design polyfunctional cores, which were subsequently used to prepare dendritic materials containing various organic and organometallic moieties within their structures.[91-100] However, none of these examples possessed the organometallic moieties as a repeating unit along the branches of the polymers. Rather, the cyclopentadienyliron-coordinated arenes were present at the core and/or the termini of the branches.

As an extension of the research describing the synthesis of linear polyaromatic ethers in the previous chapter, this work describes the first examples of aromatic ether star complexes of cyclopentadienyliron. These complexes were prepared via sequential nucleophilic aromatic substitution reactions of complexed chloroarenes with di- and tri-phenolic reagents. A star-shaped complex containing neutral and cationic cyclopentadienyliron complexes within its structure was also synthesized. The electrochemical properties of these branched materials were examined using cyclic voltammetry.

3.2 Results and Discussion

3.2.1 Synthesis and Properties of Trimetallic Star-Shaped Complexes

Synthesis of the star-shaped aromatic ether complexes was accomplished via the displacement of the chloro groups of chlorobenzene complexes with di- and tri-nucleophilic reagents. Reaction of phloroglucinol (**3.1**) with complexes **2.1** and **2.66** resulted in the isolation of trimetallic complexes **3.2** and **3.3** in 78-90% yield as yellow and beige solids, respectively (Scheme 3.1). While complex **3.2** could be synthesized at room temperature in a DMF solution, complex **3.2** was more difficult to isolate. Due to the lower reactivity of complex **2.66** relative to **2.1**, complex **3.3** was prepared by reaction of **2.66** with **3.1** at 60 °C. This trimetallic complex containing terminal methyl groups was also isolated in much lower yield.

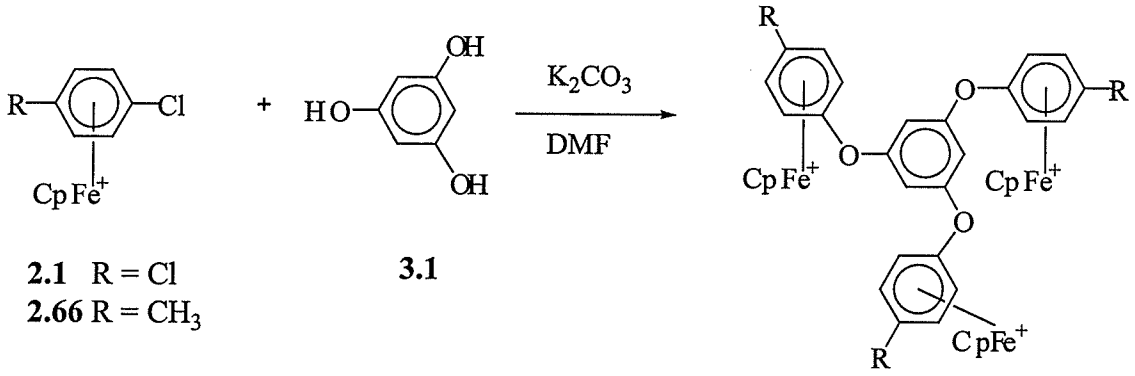

2.1 R = Cl
2.66 R = CH_3

3.1

3.2 R = Cl
3.3 R = CH_3

Scheme 3.1

It is important to note that only one chloro group of the *p*-dichlorobenzene complex (**2.1**) was displaced during the initial reaction, which was confirmed by ^{1}H and ^{13}C NMR as well as elemental analysis. Figure 3.1 shows the ^{1}H NMR spectrum of complex **3.2** in acetone-d_6. The ^{1}H NMR spectrum of **3.2** shows that only one cyclopentadienyl resonance integrating for 15 protons was present at 5.37 ppm, while the metal-coordinated arene protons appeared as two sets of doublets at 6.73 and 6.81 ppm. The three protons on the trisubstituted central aromatic ring appeared as a singlet at 7.49 ppm.

The ^{13}C NMR spectrum of the trimetallic complex **3.2** shown in Figure 3.2 was also valuable in the structural characterization of this complex. In this spectrum, the cyclopentadienyl resonance appeared at 80.31 ppm, while the complexed aromatic CH carbons resonated at 78.11 and 87.83 ppm, and the quaternary complexed aromatic carbons were observed at 105.39 and 133.59 ppm, respectively. The uncomplexed aromatic CH carbons were observed at 111.85 ppm, while the three equivalent quaternary aromatic carbons were found at 157.35 ppm.

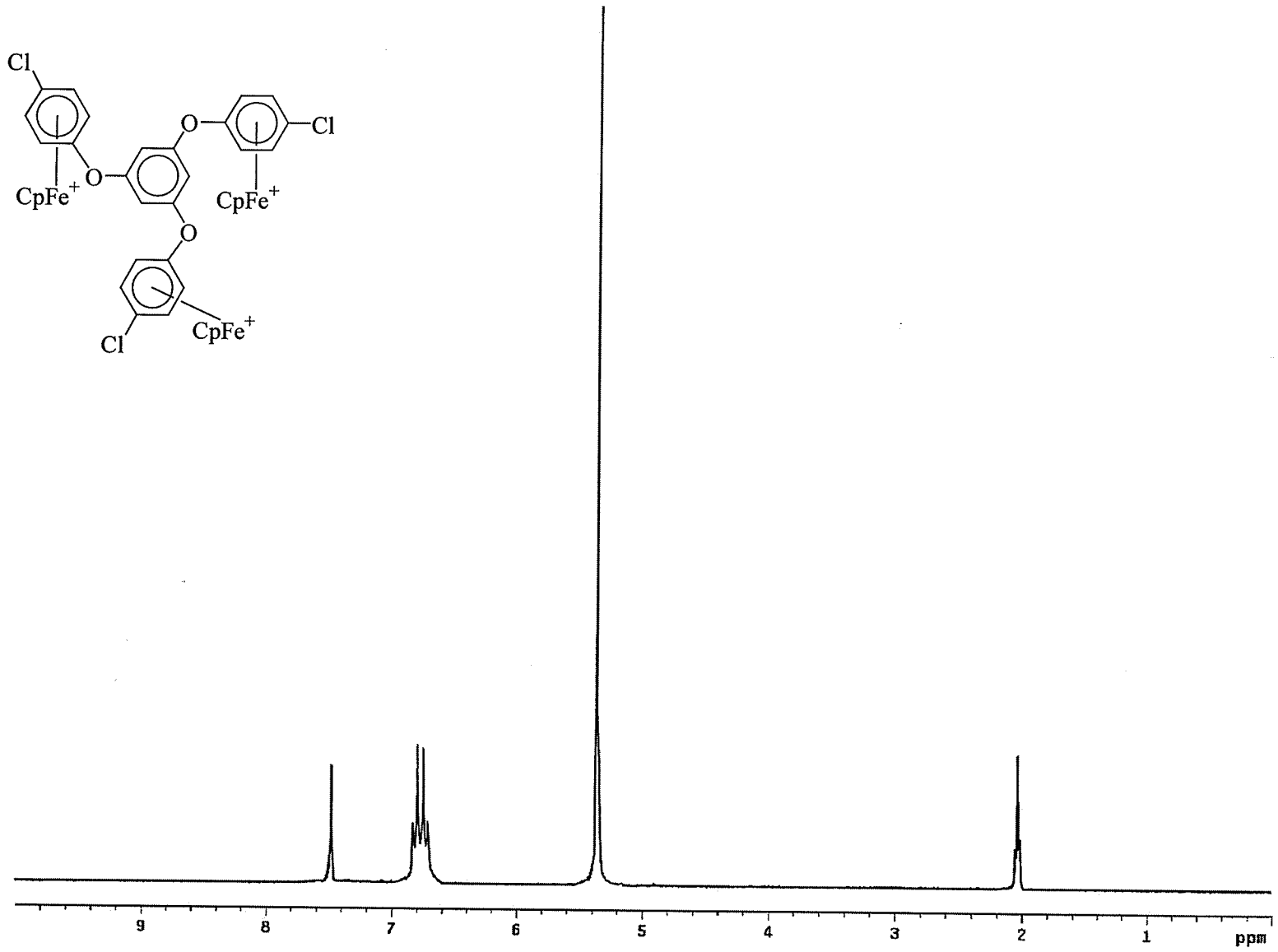

Figure 3.1: ^{1}H NMR spectrum of complex **3.2** in acetone-d_6

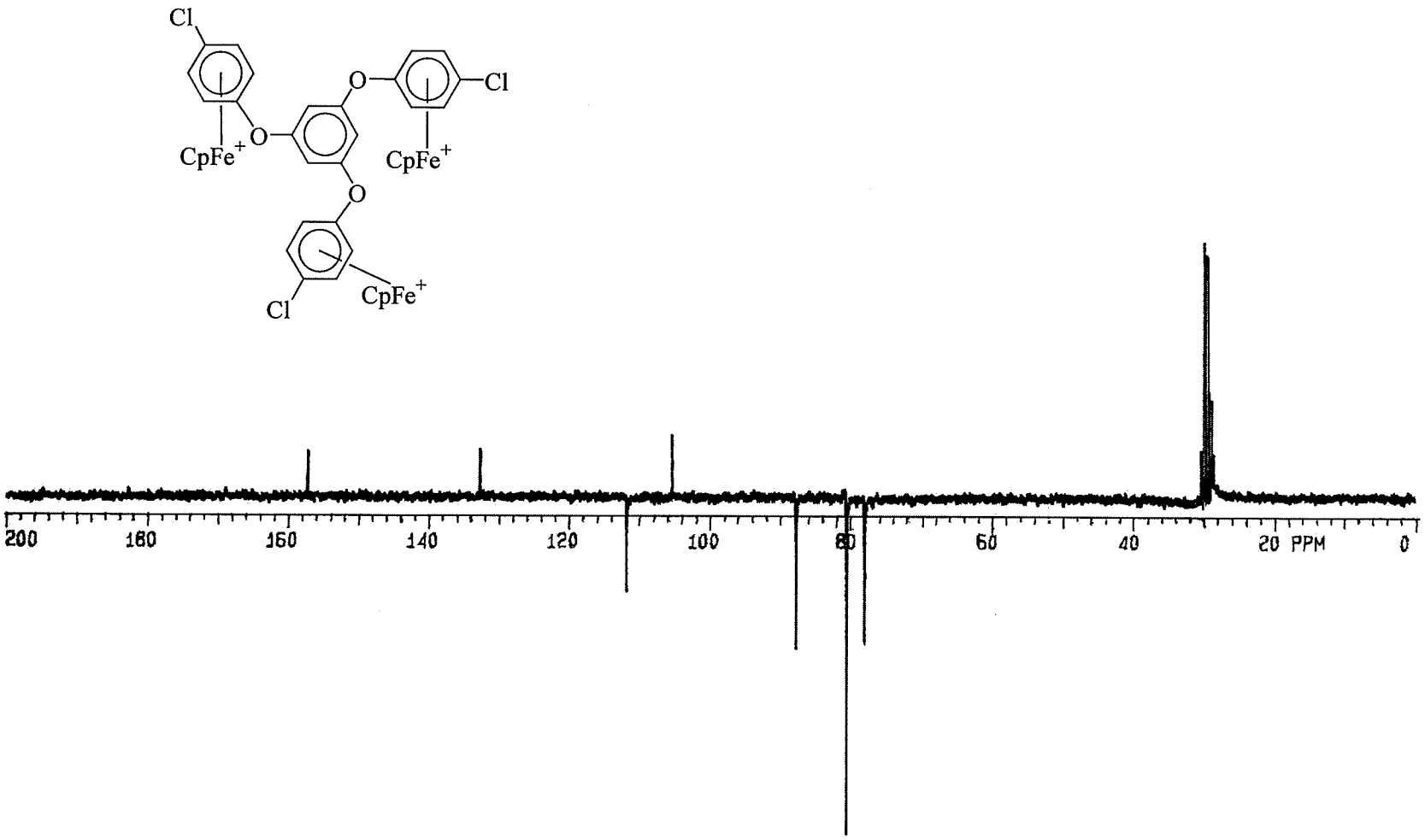

Figure 3.2: ^{13}C NMR spectrum of complex **3.2** in acetone-d_6

Table 3.1: % Yield and ^{1}H NMR Analysis of Complexes **3.2** and **3.3** in Acetone-d_6

Complex	% Yield	CH_3	Cp	Complexed Aromatic	Aromatic
3.2	90		5.37 (s, 15H)	6.73 (d, *J*=7.0 Hz, 6H), 6.81 (d, *J*=7.0 Hz, 6H)	7.49 (s, 3H)
3.3	78	2.49 (s, 3H)	5.20 (s, 15H)	6.36 (d, *J*=7.0 Hz, 6H), 6.45 (d, *J*=6.6 Hz, 6H)	6.76 (s, 3H)

Table 3.2: CH Analysis and ^{13}C NMR Analysis of Complexes **3.2** and **3.3** in Acetone-d_6

Complex	CH Analysis	CH_3	Cp	Complexed Aromatic	Aromatic
3.2	($C_{39}H_{30}O_3Cl_3F_{18}Fe_3P_3$) (1255.4): Calcd. C 37.31, H 2.41; Found C 37.02, H 2.25		80.31	78.11, 87.83, 105.39*, 133.59*	111.85, 157.35*
3.3		19.82	78.56	77.60, 87.83, 101.87*, 132.72*	106.55, 156.66*

* Denotes quaternary carbons

The electrochemical properties of the cyclopentadienyliron-coordinated star-shaped trimetallic complexes (**3.2, 3.3**) were examined using cyclic voltammetry. Figure 3.3 shows the cyclic voltammograms of these two complexes. All of these complexes were found to undergo chemically reversible reduction processes, which is characteristic of arene cyclopentadienyliron complexes.[14,17] The cyclic voltammetric studies were carried out in DMF from –40 to +20 °C at sweep rates of 0.1 to 5 V/s. The $E_{1/2}$ value corresponding to reduction of complex **3.2**, containing terminal chloro groups was found to be –0.99 V, while the $E_{1/2}$ value corresponding to reduction of complex **3.3** was –1.41

V at –40 °C, ν = 0.1 V/s. This indicates that electron-withdrawing groups attached to the complexed arenes results in less negative redox couples. The presence of only one redox wave corresponding to conversion from eighteen to nineteen-electron iron centers in the voltammograms of complexes **3.2** and **3.3** indicated that the iron moieties behaved as isolated redox centers.

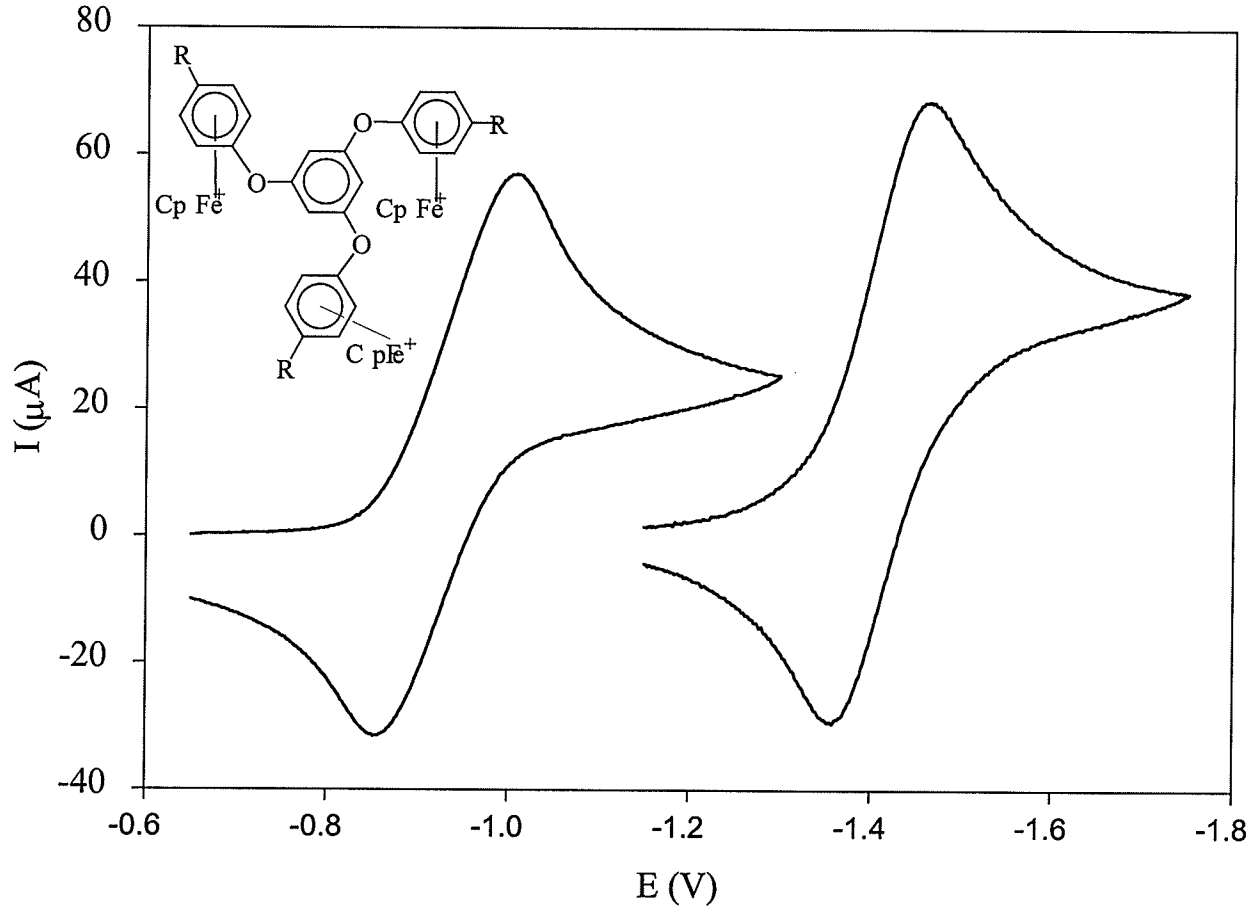

Figure 3.3: Cyclic voltammograms of complexes **3.2** (left, R=Cl) and **3.3** (right, R=CH_3)

Scheme 3.2 shows the synthesis of complex **3.4**, containing three phenolic groups. This complex was synthesized by displacing the terminal chloro groups of complex **3.2** with an excess of hydroquinone in the presence of potassium carbonate.

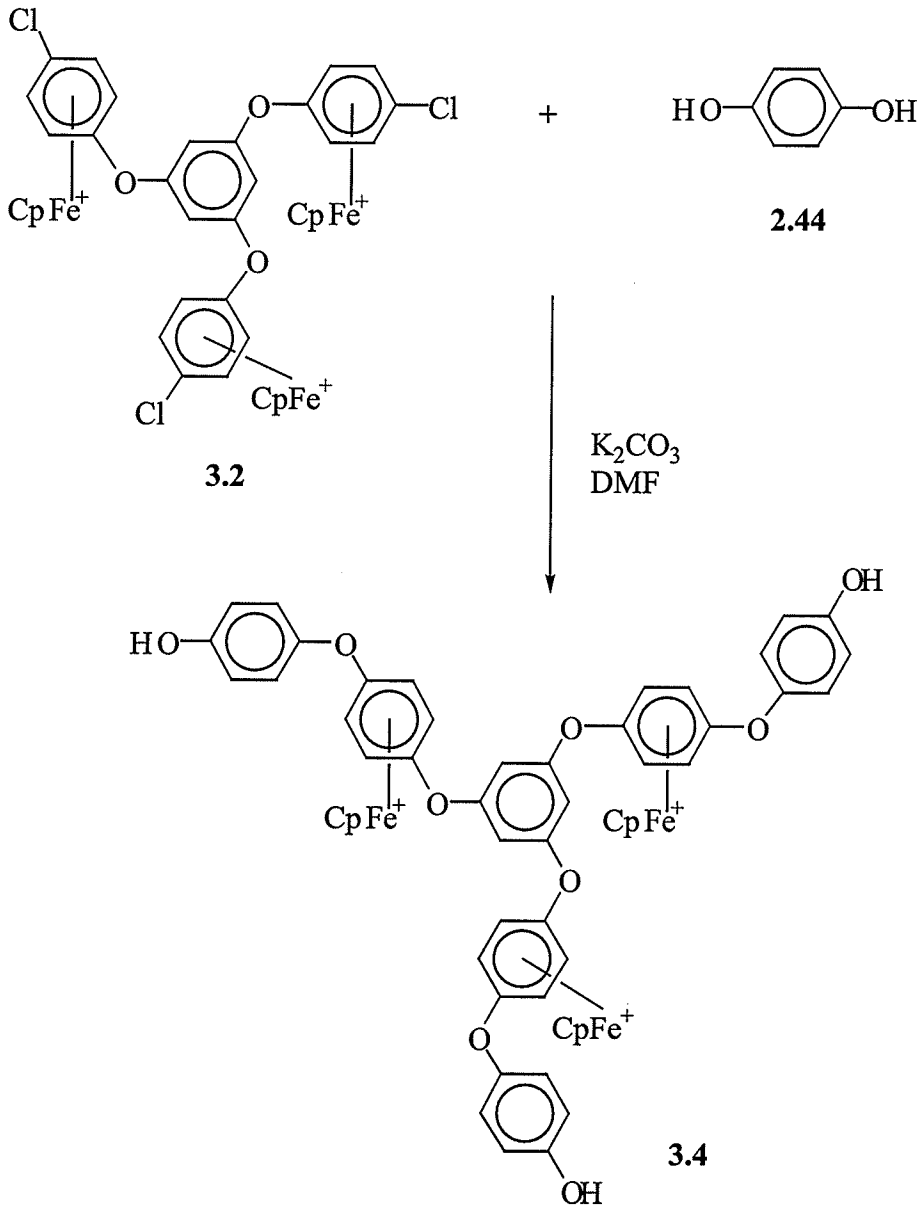

Scheme 3.2

The synthesis of complex **3.4** is important because it provides another star-shaped trimetallic complex to be used in the design of cyclopentadienyliron-coordinated star polymers. For example, reaction of **3.4** with linear complexes containing terminal complexed chloroarenes could be carried out. The ^{1}H and ^{13}C NMR data for complex **3.4** are given in Tables 3.3 and 3.4, respectively.

The ^{1}H NMR spectrum of **3.4** in deuterated dimethyl sulfoxide is shown in Figure 3.4. This spectrum shows that the Cp resonance shifted from 5.37 in complex **3.2** to 5.22 ppm, while the complexed aromatic protons shifted from 6.73 and 6.81 ppm to 6.17 and 6.56 ppm, respectively. As well, two new sets of resonances corresponding to the terminal arene protons appeared at 6.90 and 7.11 ppm. The three equivalent inner protons resonated as a singlet at 7.31 ppm, while the phenolic protons appeared at 9.78 ppm.

The ^{13}C NMR spectrum of this complex was also consistent with the proposed structure of complex **3.4**. The spectrum shown in Figure 3.5 shows the presence of only one cyclopentadienyl resonance at 77.79 ppm. The complexed aromatic CH carbons appear at 73.62 and 75.85 ppm, while the quaternary complexed aromatic carbons appear at 128.99 and 131.89 ppm. The carbons (CH) corresponding to the central aromatic ring resonate at 110.12 ppm, while the carbons of the three terminal arenes resonate at 116.85 for the carbons alpha to the OH and 122.00 ppm for the carbons alpha to the ether linkage. The quaternary carbons of the uncomplexed aromatic rings appear at 144.63, 155.78 and 156.36 ppm.

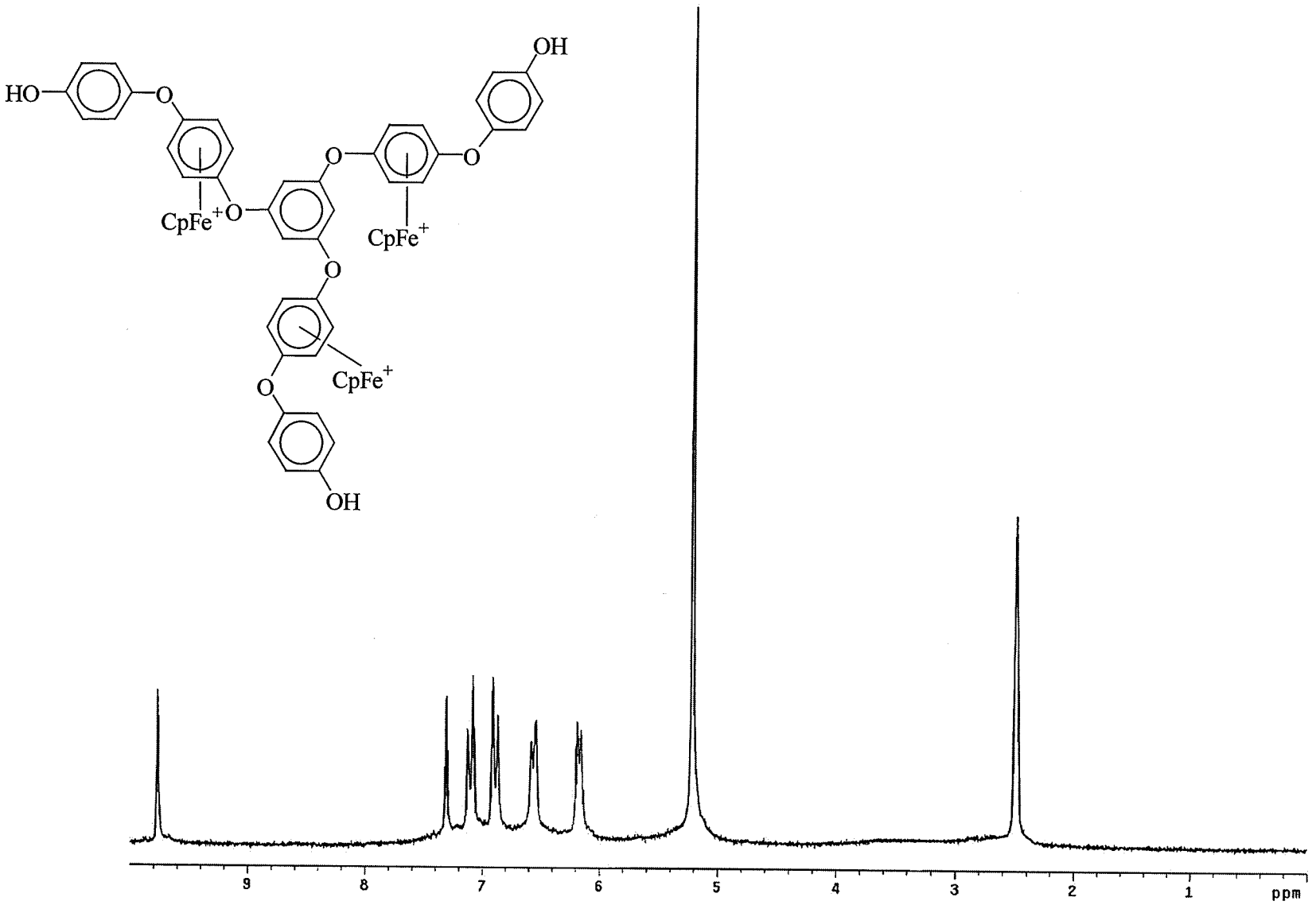

Figure 3.4: ^{1}H NMR spectrum of complex **3.4** in DMSO-d_6

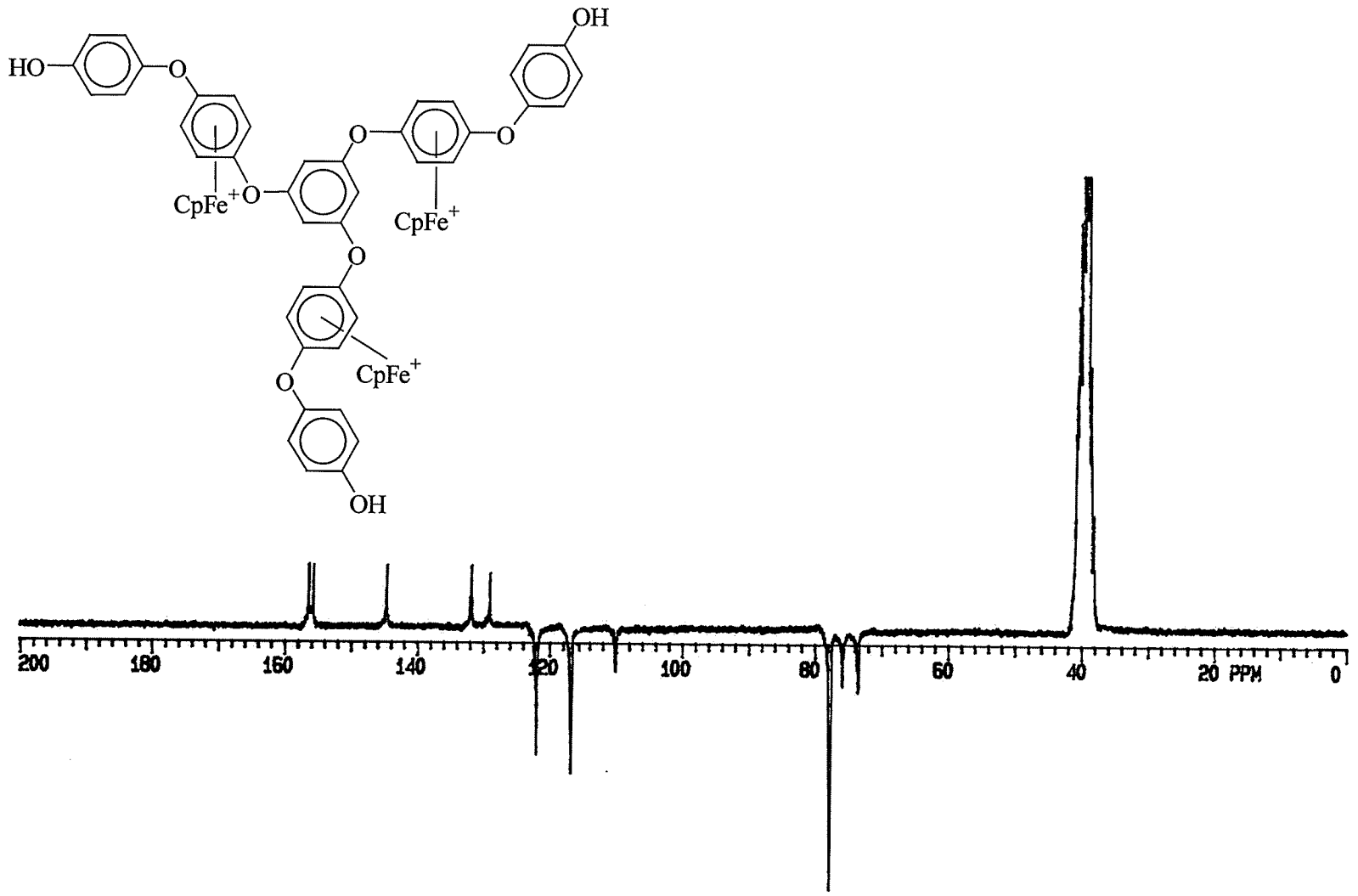

Figure 3.5: ^{13}C NMR spectrum of complex **3.4** in DMSO-d_6

Table 3.3: % Yield and ^{1}H NMR Analysis of Complex **3.4** in DMSO-d_6

Complex	% Yield	Other	Cp	Complexed Aromatic	Aromatic
3.4	83	9.78 (s, 3H, OH)	5.22 (s, 15H)	6.17 (d, *J*=6.22 Hz, 6H), 6.56 (d, *J*=6.23 Hz, 6H)	6.90 (d, *J*=8.42 Hz, 6H), 7.11 (d, *J*=8.26 Hz, 6H), 7.31 (s, 3H)

Table 3.4: IR, CH and ^{13}C NMR Analysis of Complex **3.4** in DMSO-d_6

Complex	IR (cm^{-1})	CH Analysis	Cp	Complexed Aromatic	Aromatic
3.4	3539 (OH)	($C_{57}H_{45}O_9F_{18}Fe_3P_3$) (1476.4): Calcd. C 46.37, H 3.07 Found C 45.97, H 3.29	77.79	73.62, 75.85, 128.99*, 131.89*	110.12, 116.85, 122.00, 144.63*, 155.78*, 156.36*

* Denotes quaternary carbons

3.2.2 Synthesis and Properties of Hexametallic Star-Shaped Complexes

The synthesis of complexes **3.6-3.9** containing terminal phenolic groups is described in Scheme 3.3. Reaction of the *p*-chlorotoluene complex of cyclopentadienyliron (**2.66**) with an excess of dinucleophiles **2.44, 2.6, 3.5** and **2.4** gave the phenolic organoiron complexes (**3.6-3.9**) in yields ranging from 77 to 96%.

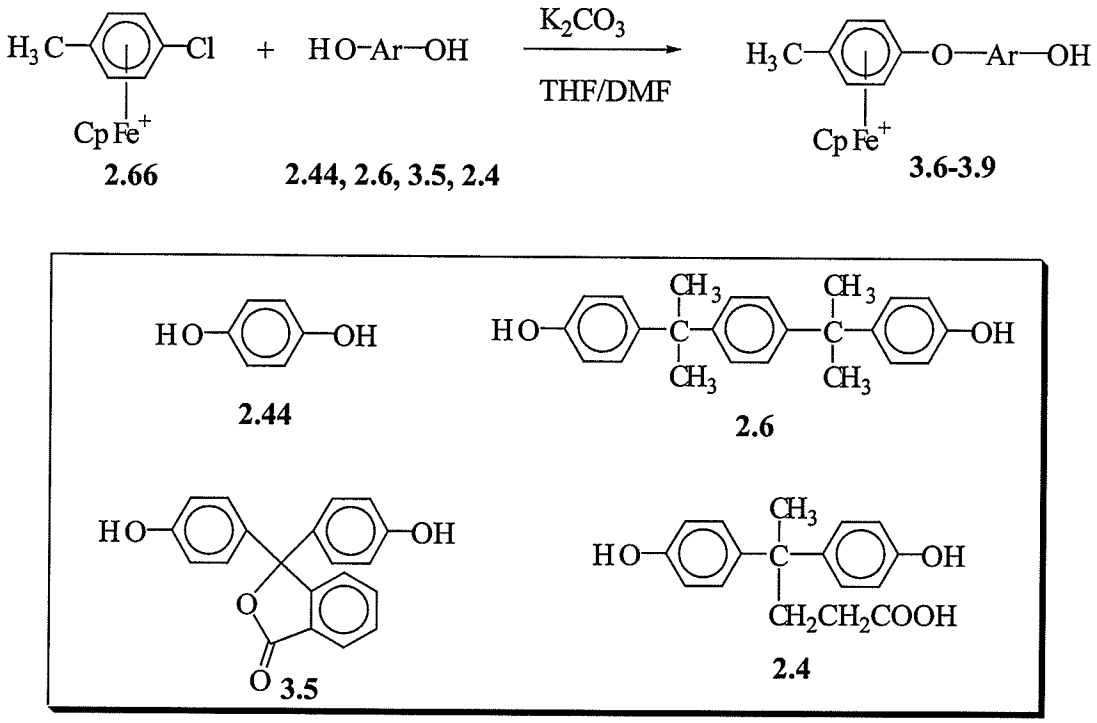

Scheme 3.3

The nature of the diphenolic nucleophiles was varied in order to impart different properties and reactivities into the star-shaped complexes. As an example, complex **3.7**, which contains isopropylidene units in its backbone, displays higher solubility than its purely aromatic analogues, while complex **3.9**, with the pendent carboxylic acid group could be coupled to a variety of organic and organometallic reagents. The synthesis of complexes **3.6-3.8** was accomplished by refluxing the organoiron complex with an excess

of the dinucleophile in a solution of 1:1 DMF:THF, however reaction of **2.66** with **2.4** in this solvent system resulted in the isolation of mostly starting materials due to the low solubility of **2.4** in this solvent system. Thus, a solution containing an excess of DMF was utilized, and if there was any starting material in the resulting product, it could be dissolved in a NaOH solution and precipitated into 10 % HCl. Only the desired phenolic compound was isolated after purification.

The ^{1}H NMR spectrum of complex **3.7** (Figure 3.6) shows two methyl groups at 1.62 and 1.67 ppm corresponding to the isopropylidene groups and the methyl on the complexed aromatic ring at 2.48 ppm. There is one cyclopentadienyl resonance at 5.20 ppm and the complexed aromatic protons are seen as two sets of doublets at 6.29 and 7.22 ppm. The protons on the uncomplexed aromatic rings resonate as four sets of doublets at 6.73, 7.07, 7.22 and 7.71 ppm and a singlet at 7.17 ppm.

The ^{13}C NMR spectrum of complex **3.7** (Figure 3.7) shows the two methyl groups of the isopropylidene groups at 30.56 and 31.12 ppm, while the methyl group on the complexed aromatic ring appeared more upfield at 19.65 ppm. The quaternary carbons of the isopropylidene groups appeared at 42.13 and 42.72 ppm. There is one cyclopentadienyl resonance at 78.22 ppm, while the complexed aromatic CH carbons appear at 76.71 and 87.54 ppm. The quaternary carbons of the complexed aromatic ring appear at 101.15 ppm for the carbon *ipso* to the methyl group, and at 133.17 ppm for the carbon *ipso* to the ether bond. As anticipated, there are six aromatic CH carbons ranging from 115.37 to 129.63 ppm, and six quaternary aromatic carbons resonating from 142.01 to 155.71 ppm. The full ^{1}H and ^{13}C NMR data for complexes **3.7-3.9** are given in Tables 3.5 and 3.6, respectively. The synthesis of complex **3.6** has been reported previously.[106]

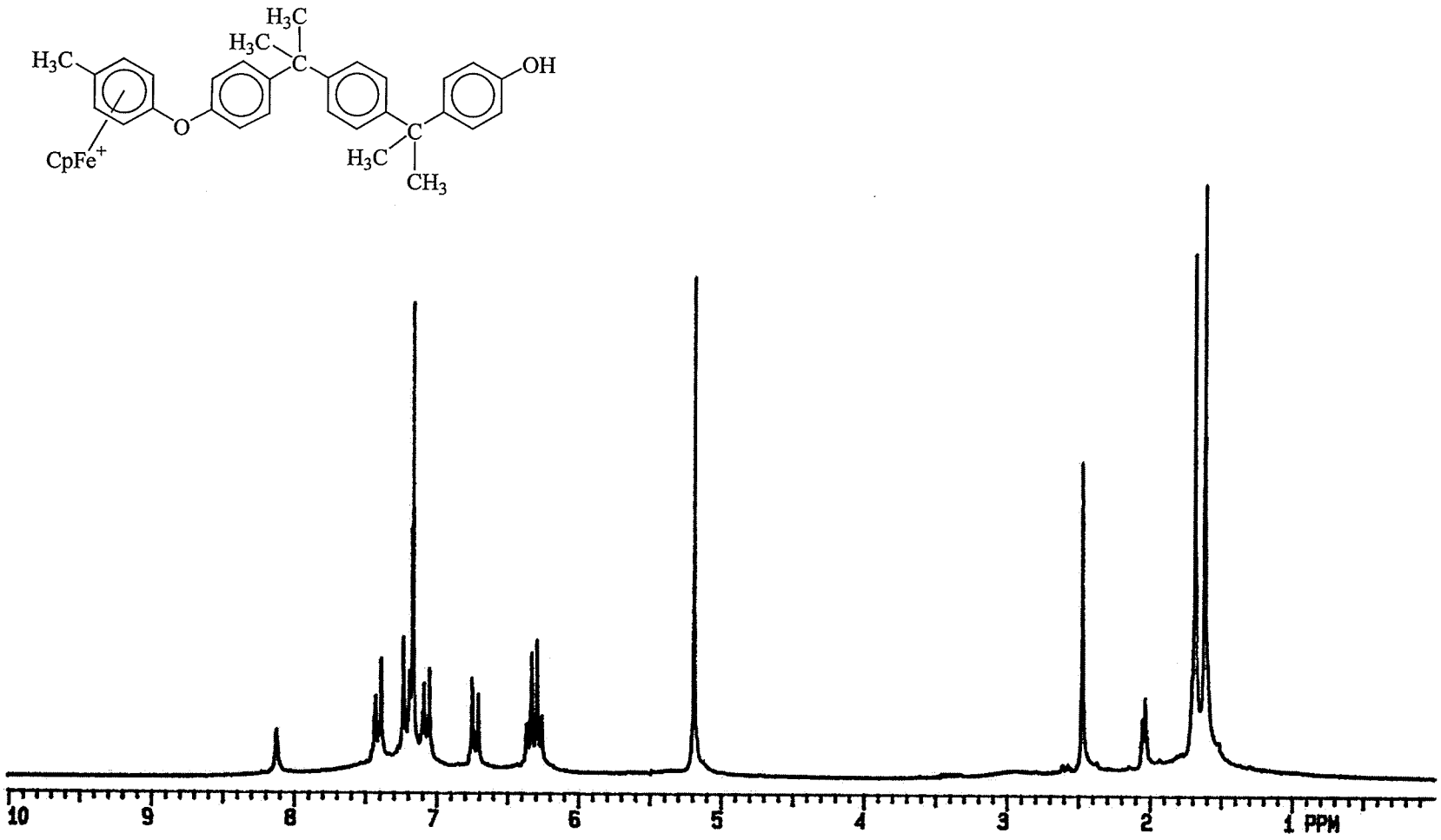

Figure 3.6: ^{1}H NMR spectrum of complex **3.7** in acetone-d_6

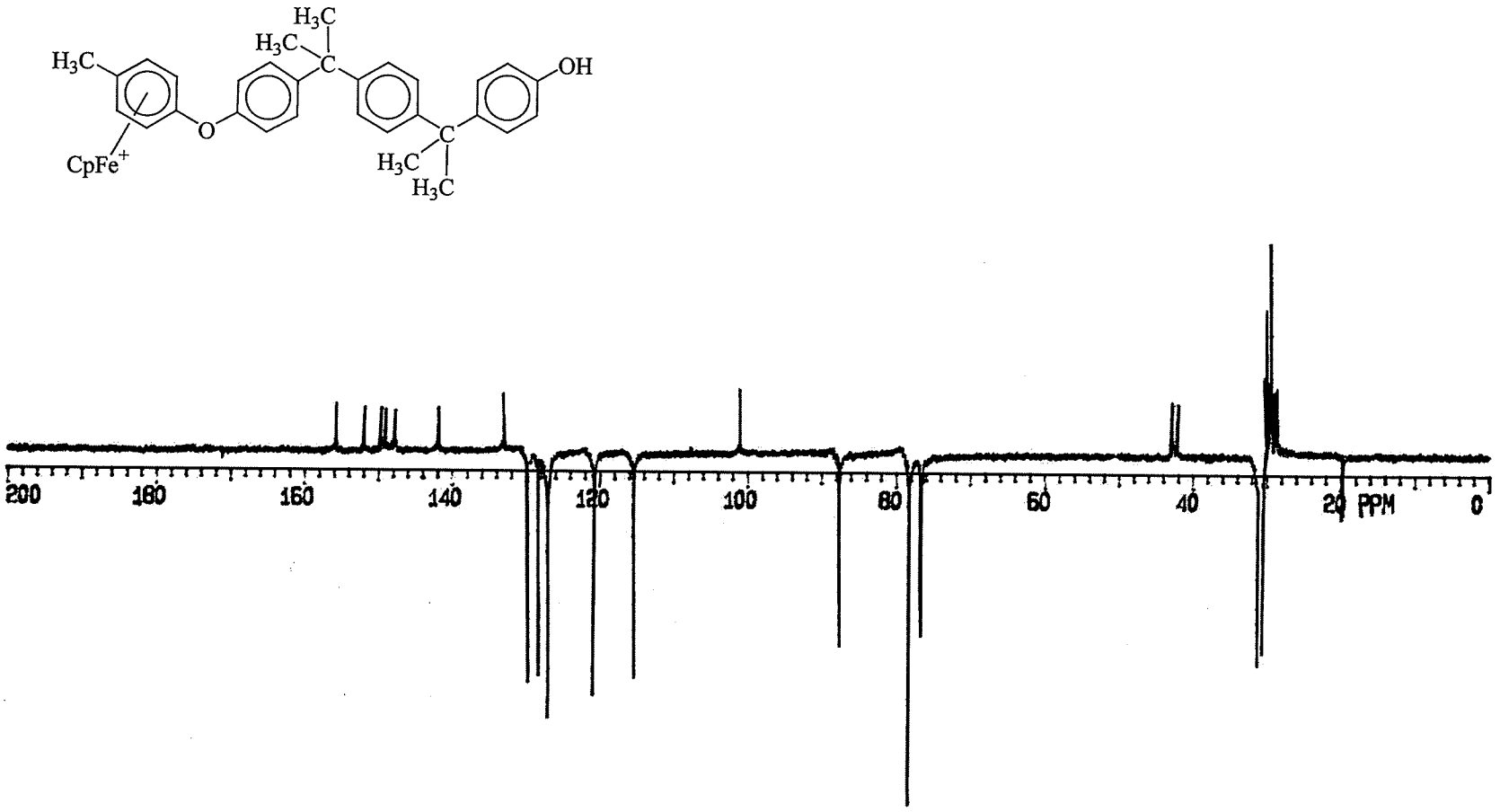

Figure 3.7: ^{13}C NMR spectrum of complex **3.7** in acetone-d_6

Table 3.5: % Yield, IR and CH Analysis of Complexes **3.7-3.9**

Complex	% Yield	IR (cm^{-1})	CH Analysis
3.7	84	3245 (OH)	($C_{36}H_{37}O_2F_6FeP$) (702.5): Calcd. C 61.55, H 5.31; Found C 61.82, H 5.38
3.8	61	1763 (CO), 3529 (OH)	
3.9	93	1713 (CO), 3093 (OH)	

Table 3.6: ^{1}H NMR Analysis of Complexes **3.7-3.9** in Acetone-d_6

Complex	Other	Cp	Complexed Aromatic	Aromatic
3.7	1.62 (s, 6H, CH_3), 1.67 (s, 6H, CH_3), 2.48 (s, 3H, CH_3), 8.12 (s, 1H, OH)	5.20 (s, 5H)	6.29 (d, *J*=7.0 Hz, 2H), 6.36 (d, *J*=7.0 Hz, 2H)	6.73 (d, *J*=8.6 Hz, 2H), 7.07 (d, *J*=8.6 Hz, 2H), 7.17 (s, 4H), 7.22 (d, *J*=8.6 Hz, 2H), 7.71 (d, *J*=9.0 Hz, 2H)
3.8	2.47 (s, 3H, CH_3), 8.65 (s, 1H, OH)	5.19 (s, 5H)	6.34 (s, 4H)	6.85 (d, *J*=6.3 Hz, 2H), 7.18 (d, *J*=7.0 Hz, 2H), 7.34 (d, *J*=6.6 Hz, 2H), 7.56 (d, *J*=8.2 Hz, 2H), 7.72 (d, *J*=6.6 Hz, 2H), 7.85-7.96 (m, 4H)
3.9	1.65 (s, 3H, CH_3), 2.16 (m, 2H, CH_2), 2.44 (m, 2H, CH_2), 2.48 (s, 3H, CH_3), 8.13 (s, 1H, OH)	5.20 (s, 5H)	6.30 (d, *J*=7.0 Hz, 2H), 6.36 (d, *J*=7.0 Hz, 2H)	6.79 (d, *J*=8.6 Hz, 2H), 7.10 (d, *J*=8.6 Hz, 2H), 7.24 (d, *J*=8.6 Hz, 2H), 7.41 (d, *J*=9.0 Hz, 2H)

Table 3.7: ^{13}C NMR Analysis of Complexes **3.7-3.9** in Acetone-d_6

Complex	Other	Cp	Complexed Aromatic	Aromatic
3.7	19.65 (CH_3), 30.56 (CH_3), 31.12 (CH_3), 42.13 (C), 42.74 (C)	78.22	76.71, 87.54, 101.15*, 133.17*	115.37, 120.69, 126.80, 126.98, 128.29, 129.63, 142.01*, 147.67*, 149.08*, 149.57*, 151.79*, 155.71*
3.8	19.78 (CH_3), 91.55 (C), 169.57 (CO)	78.42	77.25, 87.66, 101.43*, 130.53*	116.11, 121.29, 125.28, 126.21, 129.38, 129.97, 132.29*, 132.58* 135.56, 140.14*, 152.77*, 154.16*, 158.39*
3.9	19.79 (CH_3), 28.65 (CH_2), 37.34 (CH_2), 27.76 (CH_3), 45.56 (C), 174.94 (CO)	78.41	76.97, 87.78, 101.37*, 133.41*	115.79, 120.89, 129.02, 130.41, 139.68*, 148.85*, 152.05*, 156.33*

* Denotes quaternary carbons

Complexes **3.6-3.9** were subsequently reacted with the trimetallic complex containing terminal chloro groups (**3.2**) to give the hexametallic stars **3.10-3.13** as shown in Scheme 3.4. This cyclopentadienyliron-mediated methodology enabled the synthesis of fully aromatic ether complexes such as **3.10** under relatively mild reaction conditions.

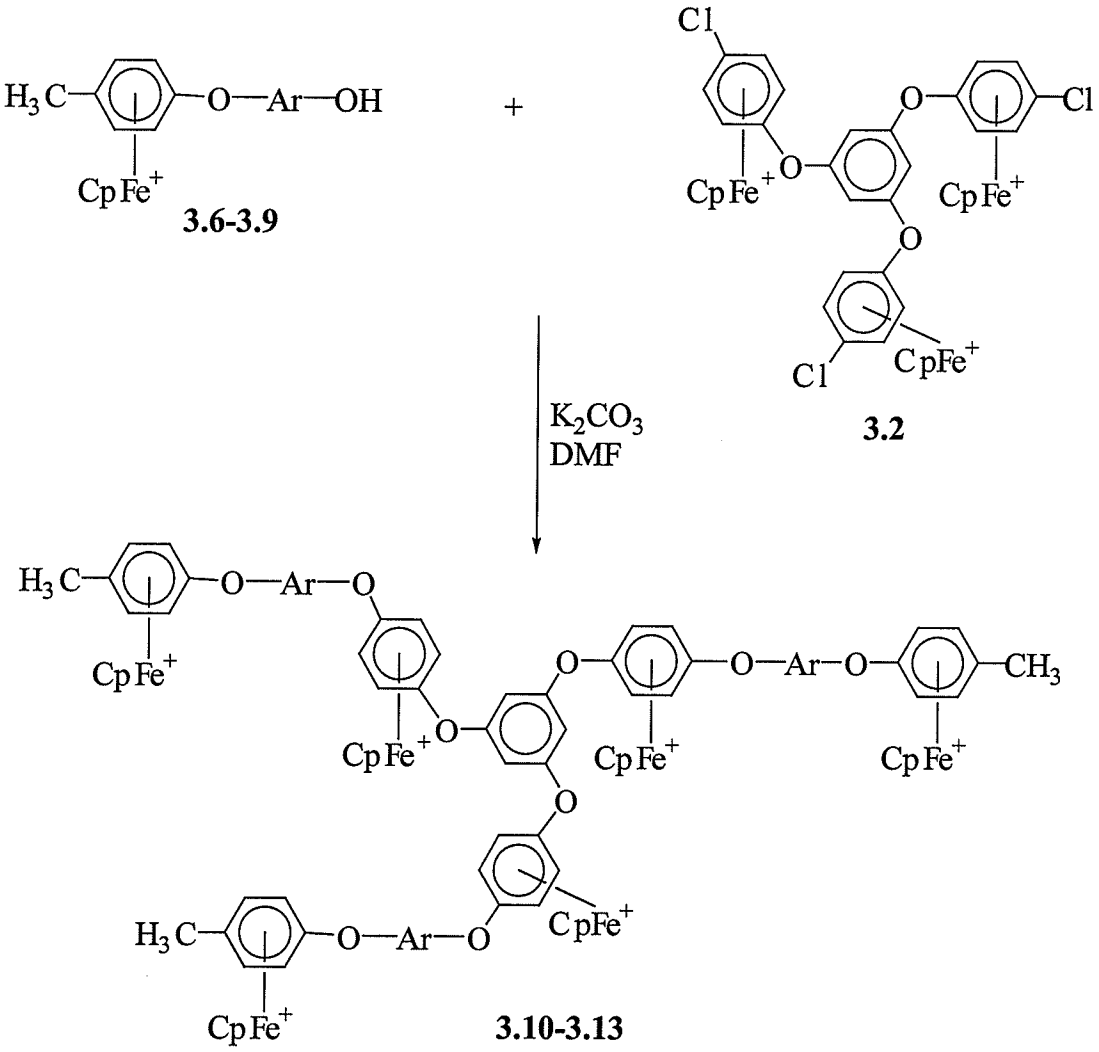

Scheme 3.4

The hexametallic star complexes were isolated in yields ranging from 88-94 %. Spectroscopic and chemical data for complexes **3.10-3.13** are provided in Table 3.8. The ^{1}H and ^{13}C NMR analysis of these complexes are provided in Tables 3.9 and 3.10, respectively. The NMR analysis of these star-shaped hexametallic complexes clearly showed that there were no peaks corresponding to either of the organoiron-complexed starting materials in their spectra. The ^{1}H NMR spectra showed the absence of resonances in the range of 6.7-6.9 ppm, which correspond to the aromatic protons on the carbons alpha to the OH groups in complexes **3.6-3.9**. As well, the complexed aromatic protons of complex **3.2** are shifted upfield in these hexametallic complexes as a result of substituting the chloro groups with ether linkages. Each complex showed two cyclopentadienyl resonances corresponding to the non-equivalent Cp rings.

The ^{1}H NMR spectrum of complex **3.11** is shown in Figure 3.8. The methyls of the isopropylidene groups appear at 1.68 and 1.70 ppm, while the methyls of the complexed toluene ring resonate as a singlet at 2.47 ppm. The protons of the two non-equivalent cyclopentadienyl rings appear at 5.19 and 5.28 ppm, while the complexed aromatic protons appear at 6.29 and 6.53 ppm as broad peaks. The uncomplexed aromatic protons appear as two broad peaks at 7.21 ppm and 7.31-7.45 ppm.

The ^{13}C NMR spectrum of complex **3.11** is shown in Figure 3.9. The notable features of this spectrum are the absence of a peak at 116.11 ppm, which was present in the spectrum of the alcohol complex **3.8** and the presence of a peak at 111.14 ppm, corresponding to the central aromatic ring of this branched complex. As well, there are two cyclopentadienyl carbon peaks in the spectrum at 78.49 and 79.11 ppm.

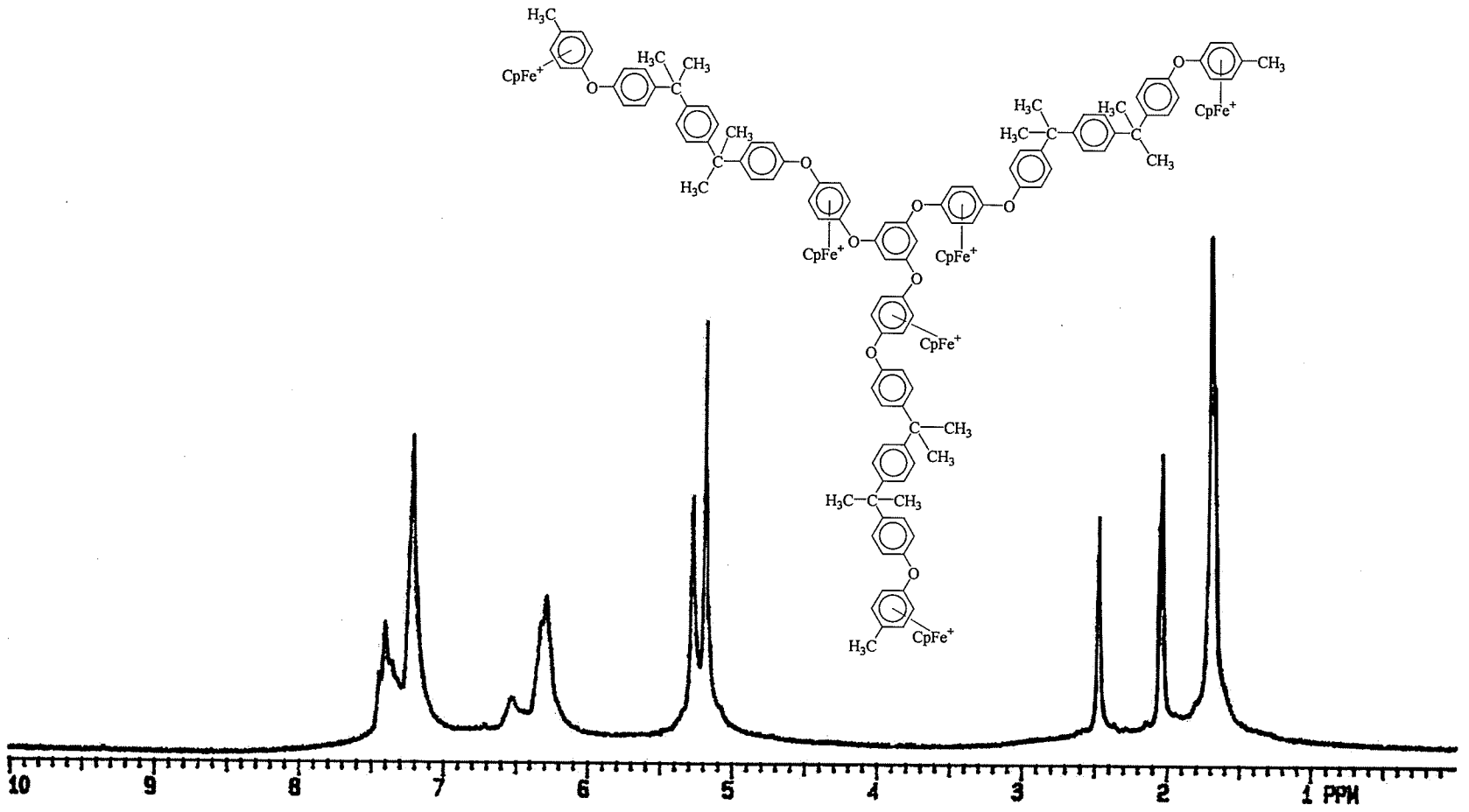

Figure 3.8: ^{1}H NMR spectrum of complex **3.11** in acetone-d_6

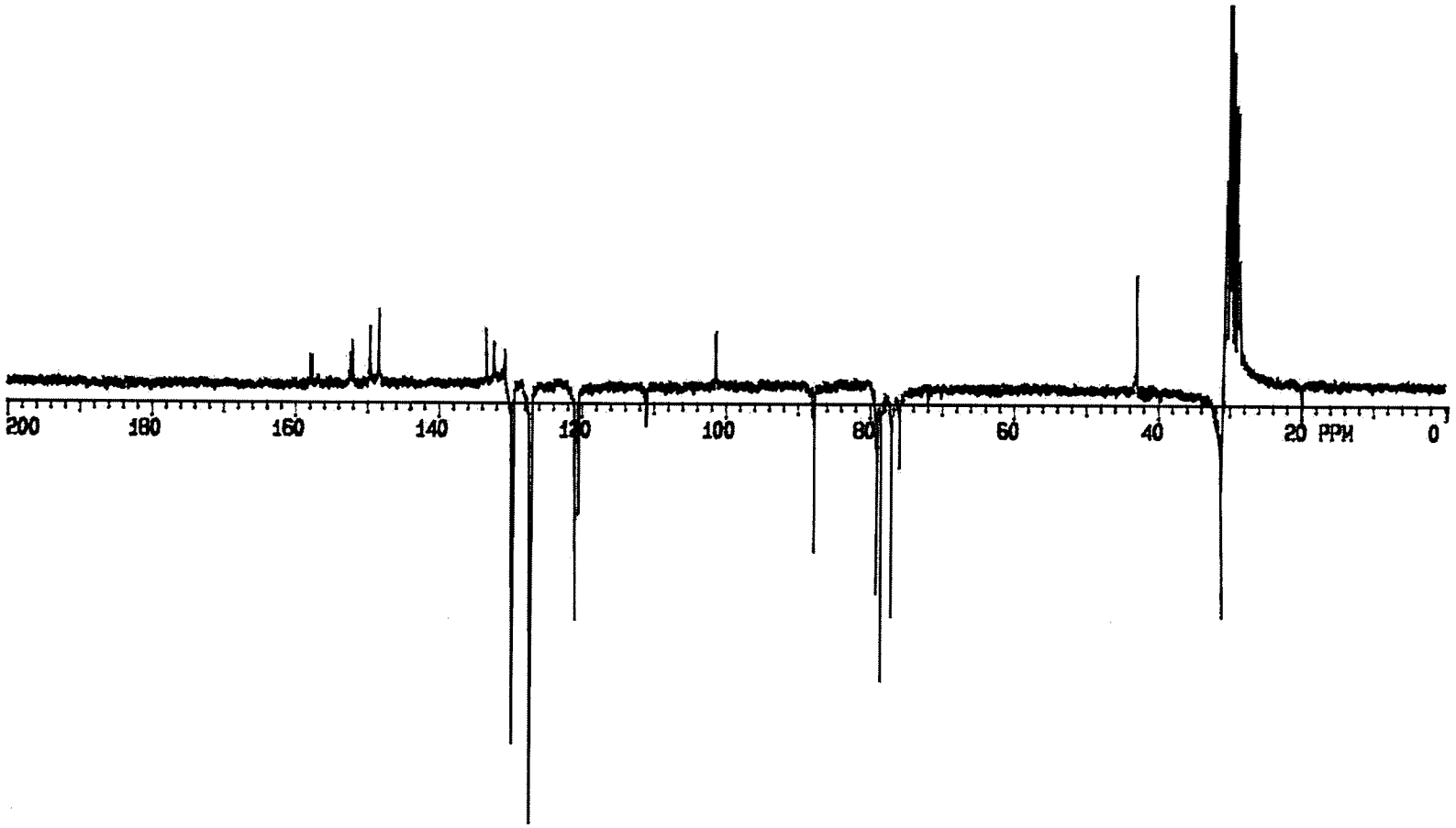

Figure 3.9: ^{13}C NMR spectrum of complex **3.11** in acetone-d_6

Table 3.8: % Yield, IR and CH Analysis of Complexes **3.10-3.13**

Complex	% Yield	IR (cm^{-1})	CH Analysis
3.10	94		
3.11	88		($C_{147}H_{138}F_{36}Fe_6O_9P_6$) (3253.5): Calcd. C 54.27, H 4.28; Found C 54.04, H 4.11
3.12	93	1770 (CO)	
3.13	94	1725 (CO), 3440 (OH)	

Table 3.9: ^{1}H NMR Analysis of Complexes **3.10-3.13** in Acetone-d_6

Complex	Other	Cp	Complexed Aromatic	Aromatic
3.10[#]	2.37 (s, 9H, CH_3)	5.13 (s, 15H), 5.26 (s, 15H)	6.28 (s, 12H), 6.39 (d, *J*= 6.3 Hz, 6H), 6.53 (d, *J*= 6.7 Hz, 6H)	7.31 (s, 3H), 7.46 (br.s, 12H)
3.11	1.68 (s, 18H, CH_3), 1.70 (s, 18H, CH_3), 2.47 (s, 9H, CH_3)	5.19 (s, 15H), 5.28 (s, 15H)	6.29 (br.s, 18H), 6.53 (br.s, 6H)	7.21 (br.s, 24H), 7.31-7.45 (m, 15H)
3.12	2.49 (s, 9H, CH_3)	5.19 (s, 15H), 5.27 (s, 15H)	6.33 (s, 12H), 6.35 (s, 6H), 6.52 (d, *J*= 7.0 Hz, 6H)	7.32 (d, *J*=6.6 Hz, 12H), 7.38 (s, 3H), 7.50 (s, 3H), 7.58 (d, *J*=6.6 Hz, 12H), 7.77 (d, *J*=8.2 Hz, 3H), 7.89 (br.s, 3H), 7.99 (d, *J*=7.4 Hz, 3H)
3.13	1.71 (s, 9H, CH_3), 2.18 (br.s, 6H, CH_2), 2.47 (s, 15H, CH_2, CH_3)	5.18 (s, 15H), 5.28 (s, 15H)	6.32 (br.s, 18H), 6.66 (br.s, 6H)	7.11 (br.s, 12H), 7.42 (br.s, 15H)

[#]Analysis in DMSO-d_6

Table 3.10: ^{13}C NMR Analysis of Complexes **3.10-3.13** in Acetone-d_6

Complex	Other	Cp	Complexed Aromatic	Aromatic
3.10[#]	19.10 (CH_3)	77.24, 77.92	74.82, 75.86, 86.50, 100.25*, 128.89*, 130.41*, 131.36*	109.43, 122.53, 122.85, 150.60*, 150.70*, 156.31*
3.11	19.92 (CH_3), 31.14 (CH_3), 42.97 (C)	78.49, 79.11	75.96, 77.02, 87.85, 101.38*, 130.83*, 132.34*, 133.45*	111.14, 120.69, 120.95, 127.25, 129.85, 148.34*, 149.66*, 149.74*, 152.06*, 152.49*, 157.79*
3.12	19.76 (CH_3), 90.98 (C), 169.35 (CO)	78.45, 79.06	76.37, 76.76, 77.23, 87.69, 101.54*, 131.02*, 131.52*, 132.69*	111.01, 121.19, 121.60, 125.36, 125.69*, 126.54, 130.31, 130.97, 135.93, 139.44*, 139.58*, 152.17*, 154.41*, 155.01*, 157.69*
3.13	19.95 (CH_3), 27.83 (CH_3), 38.88 (CH_2), 46.18 (C), 174.33 (CO)	78.49, 79.09	76.00, 76.98, 87.83, 101.31*, 131.08*, 132.24*, 133.34*	111.56, 120.97, 121.27, 130.57, 147.50*, 147.72*, 152.17*, 152.76*, 157.72*

*Denotes quaternary carbons, [#]Analysis in DMSO-d_6

The cyclic voltammogram of complex **3.10** is shown in Figure 3.10. While the CV's of complexes **3.2** and **3.3** showed single redox processes corresponding to three concurrent one-electron reductions, the CV's of complex **3.10** showed that two distinct redox processes are occurring. These two processes can be attributed to the inner three and outer three iron centers. The $E_{1/2}$ values for these two redox processes occurred at –1.20 and –1.30 V, respectively. This cyclic voltammogram was obtained in DMF at –40 ^{o}C at a sweep rate of 0.1 V/s.

The dependence of the electrochemical potentials of the iron centers on the substituents on the complexed arenes also allowed for some conclusions to be drawn about the purity of the star-shaped complexes. For example, electrochemical analysis showed there was no peak corresponding to the reduction of the iron centers in complex **3.2**, since this redox process occurred at $E_{1/2} = -0.99$ V. In addition, the two redox waves that were present had very similar currents, which signifies that the same number of iron atoms were being reduced.

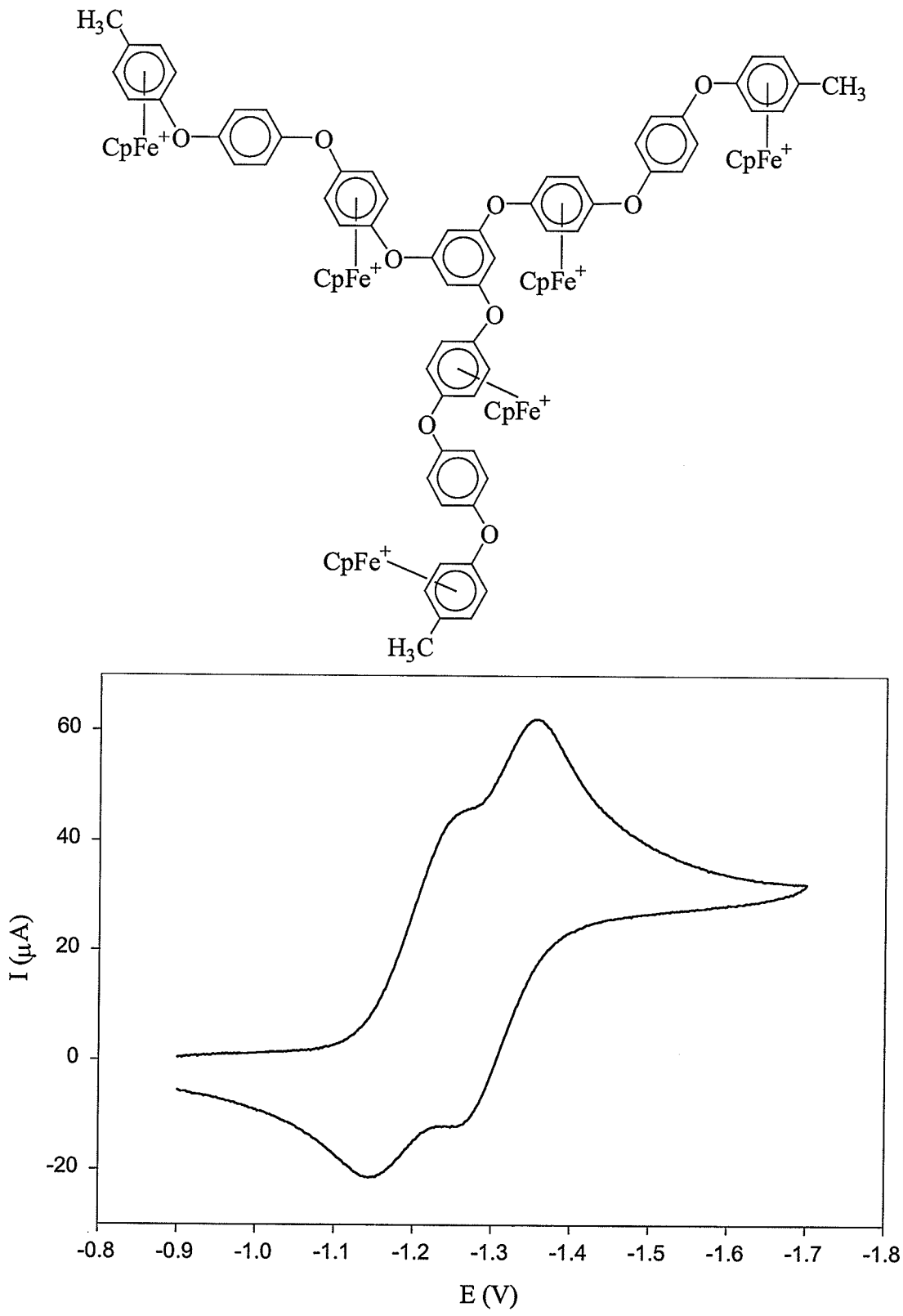

Figure 3.10: Cyclic voltammogram of complex **3.10**

3.2.3 Synthesis and Properties of Star-Shaped Aryl Ethers Containing Nine Cationic Organoiron Moieties

Scheme 3.5 describes the synthesis of linear bimetallic complexes containing one terminal chloro group. These complexes (**3.14-3.17**) were synthesized to serve as branches for complex **3.4**, in the design of higher molecular weight star polymers. Complexes **3.14-3.17** were isolated in 85 to 92 % yields as yellow complexes by reaction of complexes **3.6-3.9** with one molar equivalent of complex **2.1**.

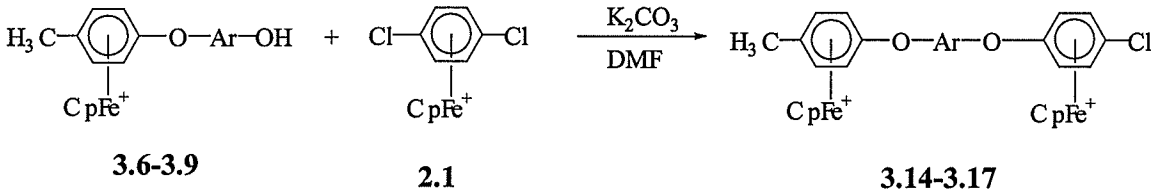

3.6-3.9 **2.1** **3.14-3.17**

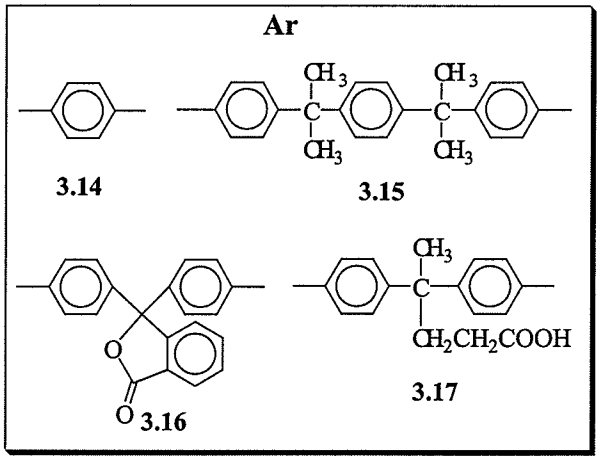

Scheme 3.5

NMR analysis of complexes **3.14-3.17** provided good evidence that the reactions outlined in Scheme 3.5 were successful. It was possible to identify the products using ^{1}H NMR spectroscopy due to the large differences in the chemical shifts in the complexed and uncomplexed aromatic protons of the terminal aromatic rings of **3.14-3.17** and **3.6-3.9**, respectively. For example, in the ^{1}H NMR spectra of complexes **3.14-3.17**, two sets of doublets between 6.5 and 6.8 ppm correspond to the complexed aromatic protons of the newly introduced chloroarene. Figure 3.11 shows the ^{1}H NMR spectrum of complex **3.14**. The singlet at 2.52 ppm corresponds to the methyl group of the complexed aromatic ring. The two cyclopentadienyl resonances appear at 5.22 and 5.38 ppm, and they each integrate for five protons. There are four sets of doublets corresponding to the complexed aromatic protons, which appear at 6.34, 6.40, 6.57 and 6.78 ppm. Finally, the singlet at 7.57 ppm corresponds to the four protons of the uncomplexed aromatic ring.

The ^{13}C NMR spectrum of complex **3.14** is shown in Figure 3.12. The peak at 19.82 ppm is assigned as the methyl carbon, while the cyclopentadienyl resonances appear at 78.48 and 80.46 ppm. The complexed aromatic CH carbons appear at 76.84, 76.99 and 87.74 ppm, while the quaternary complexed aromatic carbons appear at 101.49, 104.96, 133.45 and 133.97 ppm. The uncomplexed aromatic carbons are inequivalent in the ^{13}C spectrum and appear at 124.22 and 124.32 ppm, with the quaternary aromatic peaks at 151.53 and 152.11 ppm. The full analytical and spectroscopic analysis of **3.14-3.17** are provided in Tables 3.11 and 3.12.

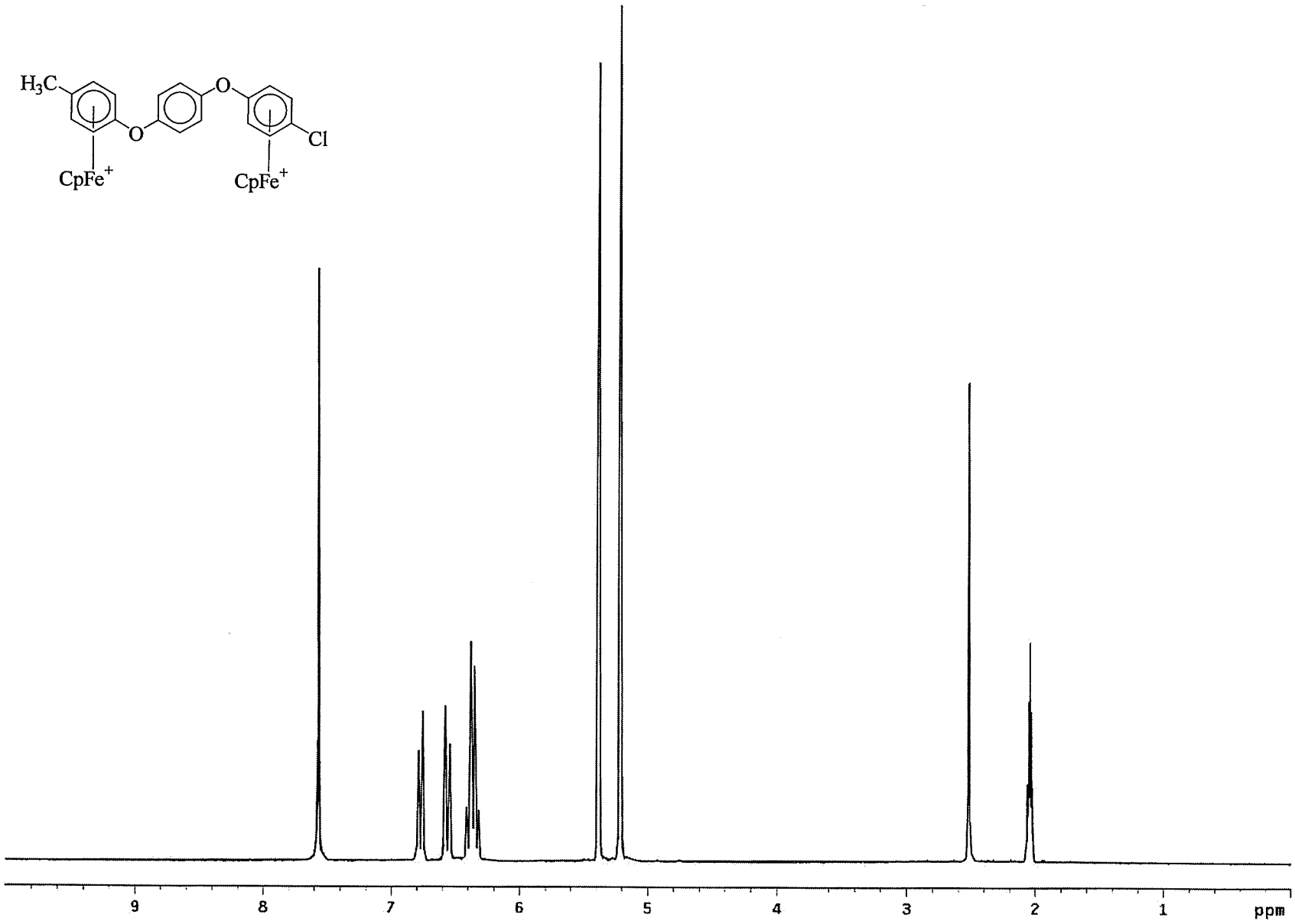

Figure 3.11: ^{1}H NMR spectrum of complex **3.14** in acetone-d_6

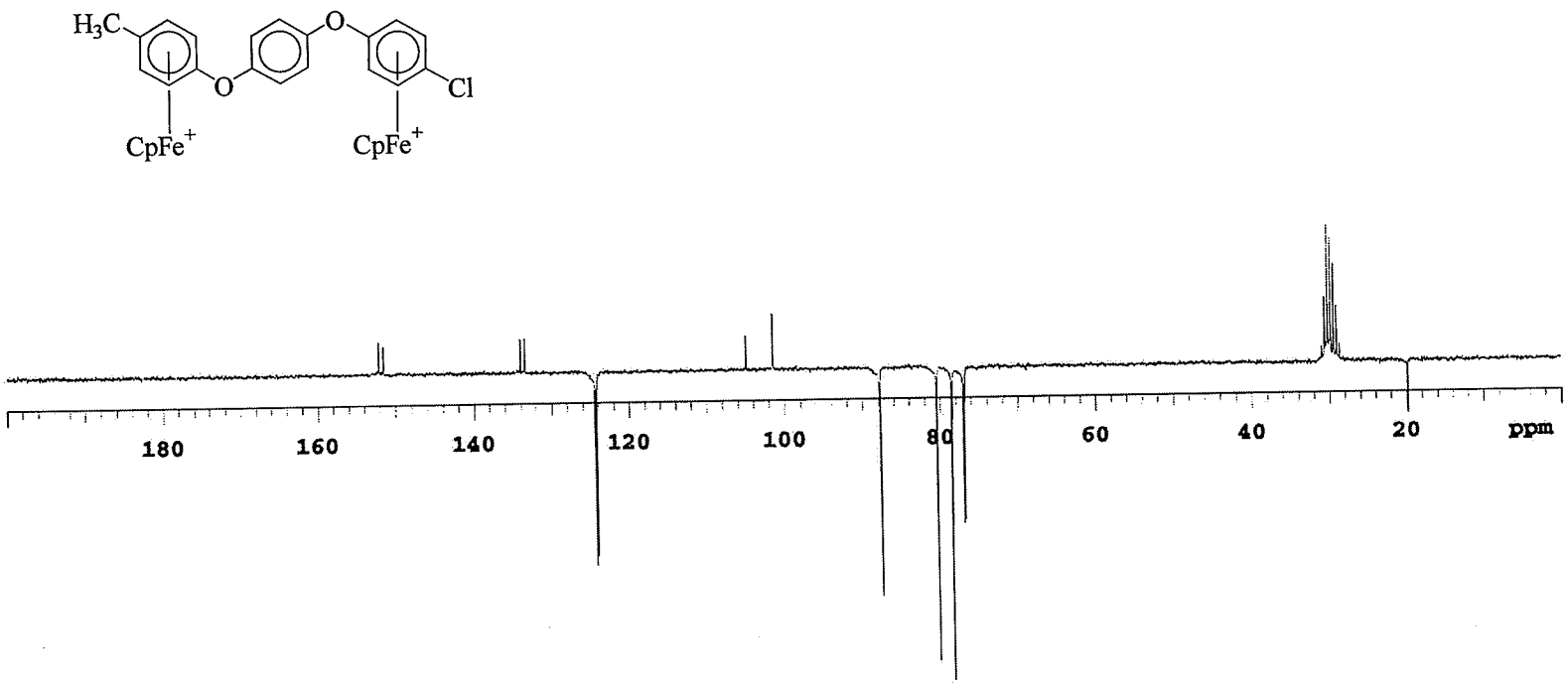

Figure 3.12: ^{13}C NMR spectrum of complex **3.14** in acetone-d_6

Table 3.11: % Yield and ^{1}H NMR Analysis of Complexes **3.14-3.17** in Acetone-d_6

Complex	% Yield	Other	Cp	Complexed Aromatic	Aromatic
3.14	85	2.52 (s, 3H, CH_3)	5.22 (s, 5H), 5.38 (s, 5H)	6.34 (d, *J*=7.03 Hz, 2H), 6.40 (d, *J*=7.03 Hz, 2H), 6.57 (d, *J*=6.57 Hz, 2H), 6.78 (d, *J*=6.77 Hz, 2H)	7.57 (s, 4H)
3.15	88	1.71 (s, 12H, CH_3), 2.48 (s, 3H, CH_3)	5.20 (s, 5H), 5.36 (s, 5H)	6.28 (d, *J*=6.64 Hz, 2H), 6.36 (d, *J*=6.25 Hz, 2H), 6.47 (d, *J*=6.64 Hz, 2H), 6.80 (d, *J*=6.25 Hz, 2H)	7.23 (s, 8H), 7.44 d, *J*=7.03 Hz, 4H)
3.16	92	2.49 (s, 3H, CH_3)	5.20 (s, 5H), 5.37 (s, 5H)	6.36 (s, 4H) 6.53 (d, *J*=5.86 Hz, 2H), 6.81 (d, *J*=5.86 Hz, 2H)	7.40-7.43 (m, 4H), 7.57-7.80 (m, 5H), 7.94-8.03 (m, 3H)
3.17	85	1.75 (s, 3H, CH_3), 2.17 (br.t, 2H, CH_2), 2.48 (s, 3H, CH_3), 2.49 (br.t, 2H, CH_2)	5.20 (s, 5H), 5.36 (s, 5H)	6.34 (s, 4H), 6.50 (d, *J*=6.64 Hz, 2H), 6.80 (d, *J*=6.64 Hz, 2H)	7.32 (br.d, 4H), 7.46 (br.d, 4H)

Table 3.12: IR and ^{13}C NMR Analysis of Complexes **3.14-3.17** in Acetone-d_6

Complex	IR (cm^{-1})	Other	Cp	Complexed Aromatic	Aromatic
3.14		19.82 (CH_3)	78.48, 80.46	76.84, 76.99, 87.74, 101.49*, 104.96*, 133.45*, 133.97*	124.22, 124.32, 151.53*, 152.11*
3.15		19.78 (CH_3), 31.04 (CH_3), 42.84 (C)	78.35, 80.34	76.84, 76.99, 87.70, 101.28*, 104.69*, 133.30*, 133.80*	120.84, 127.14, 129.73, 129.85, 148.14*, 148.21*, 149.56*, 149.71*, 151.63*, 151.89*
3.16	1770 (CO)	19.75 (CH_3), 90.83 (C), 169.23 (CO)	78.36, 80.34	77.14, 87.60, 101.36*, 104.72*, 132.48*, 133.05*	121.51, 121.61, 125.29, 125.40*, 126.40, 130.29, 130.88, 139.33*, 139.79*, 151.98*, 153.86*, 154.23*
3.17	1725 (CO), 3446 (OH)	19.74 (CH_3), 27.72 (CH_2), 31.20 (CH_3), 37.03 (CH_2), 46.01 (C), 174.64 (CO)	78.27, 80.25	76.73, 76.85, 87.59, 101.12*, 104.58*, 133.12*, 133.65*	121.10, 130.30, 147.38*, 147.83*, 151.72*, 152.02*

*Denotes quaternary carbons

Scheme 3.6 shows the reaction of complex **3.4** with diiron complexes **3.14-3.17**, resulting in the formation of star polymers **3.18-3.21**.

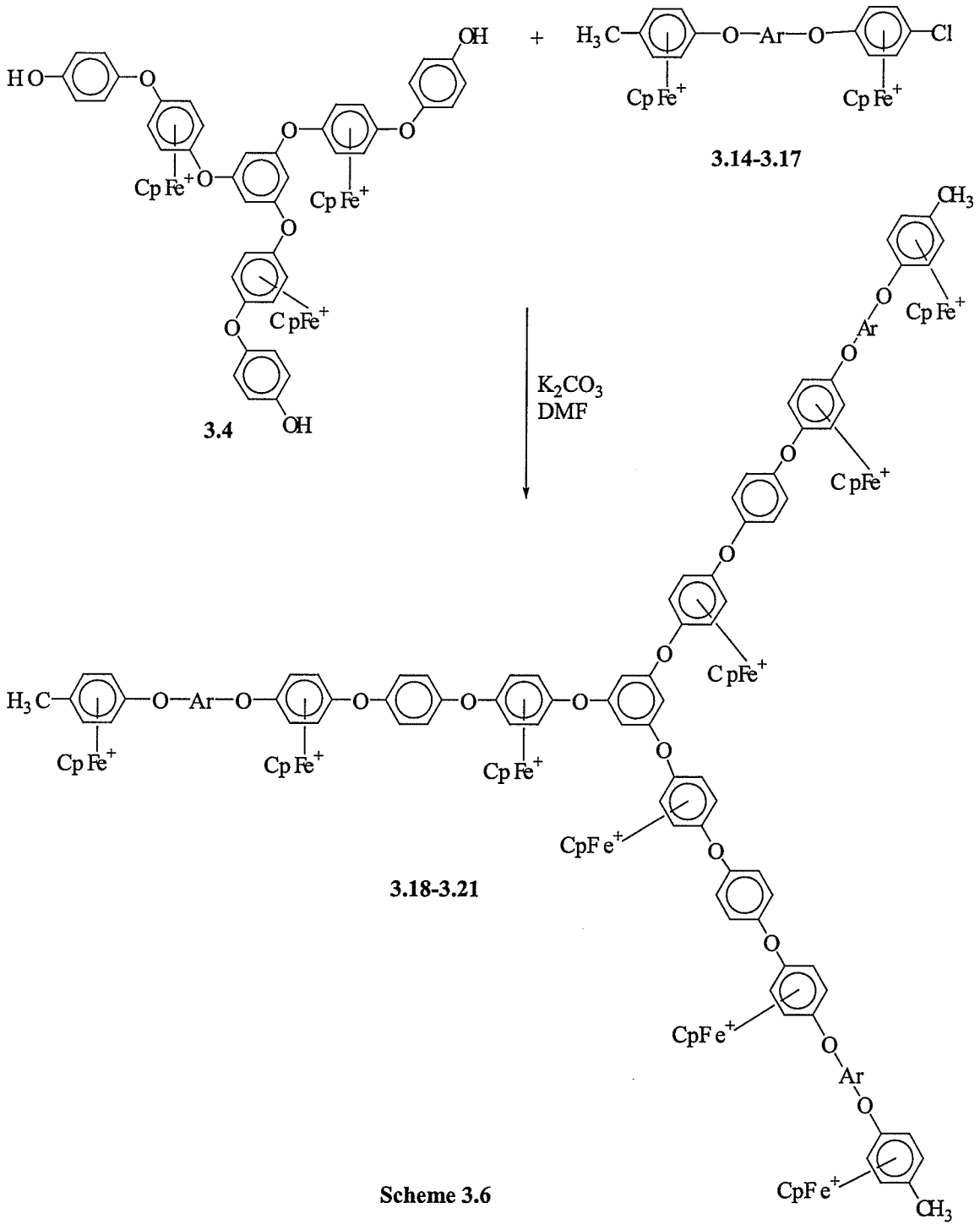

Scheme 3.6

It was also possible to follow the progress of these reactions using NMR spectroscopy. Figures 3.13 and 3.14 show the ^{1}H and ^{13}C NMR spectra of complex **3.18**. The proposed structure of this complex shows that there are three cyclopentadienyliron cations pendent to each of the three branches of the star. In the ^{1}H NMR spectrum of **3.18**, the three methyl groups appear as a singlet at 2.37 ppm and integrate for nine protons. There are two cyclopentadienyl resonances at 5.14 and 5.27 ppm. The peak at 5.14 ppm integrated for fifteen protons, while the peak at 5.27 ppm integrated for thirty protons. There are two broad singlets at 6.29 and 6.35 ppm corresponding to twelve and eighteen complexed aromatic protons respectively, and a doublet at 6.53 ppm corresponding to the remaining six complexed aromatic protons. The full ^{1}H NMR analysis for complexes **3.18-3.21** is given in Table 3.14.

The ^{13}C NMR spectrum of the star complex **3.18** shows the methyl carbons at 19.21 ppm, and three cyclopentadienyl resonances at 77.37, 77.88 and 78.03 ppm. The complexed aromatic (CH) carbons appeared at 74.81 and 75.85 ppm for the carbon atoms alpha to the etheric linkages and at 86.58 ppm for the carbons alpha to the methyl groups. The complexed aromatic carbon ipso to the methyl group resonates at 100.31 ppm, while the carbons ipso to the oxygen linkages appear at 129.01, 130.25, 130.62 and 131.63 ppm. The peak at 109.88 ppm corresponded to the three aromatic carbons of the central arene unit, while the peaks at 122.81 and 123.03 corresponded to the aromatic carbons in the star branches. The quaternary aromatic carbons resonated at 150.61, 150.77, 150.93 and 156.43 ppm. The full ^{13}C NMR analysis for complexes **3.18-3.21** is given in Table 3.15.

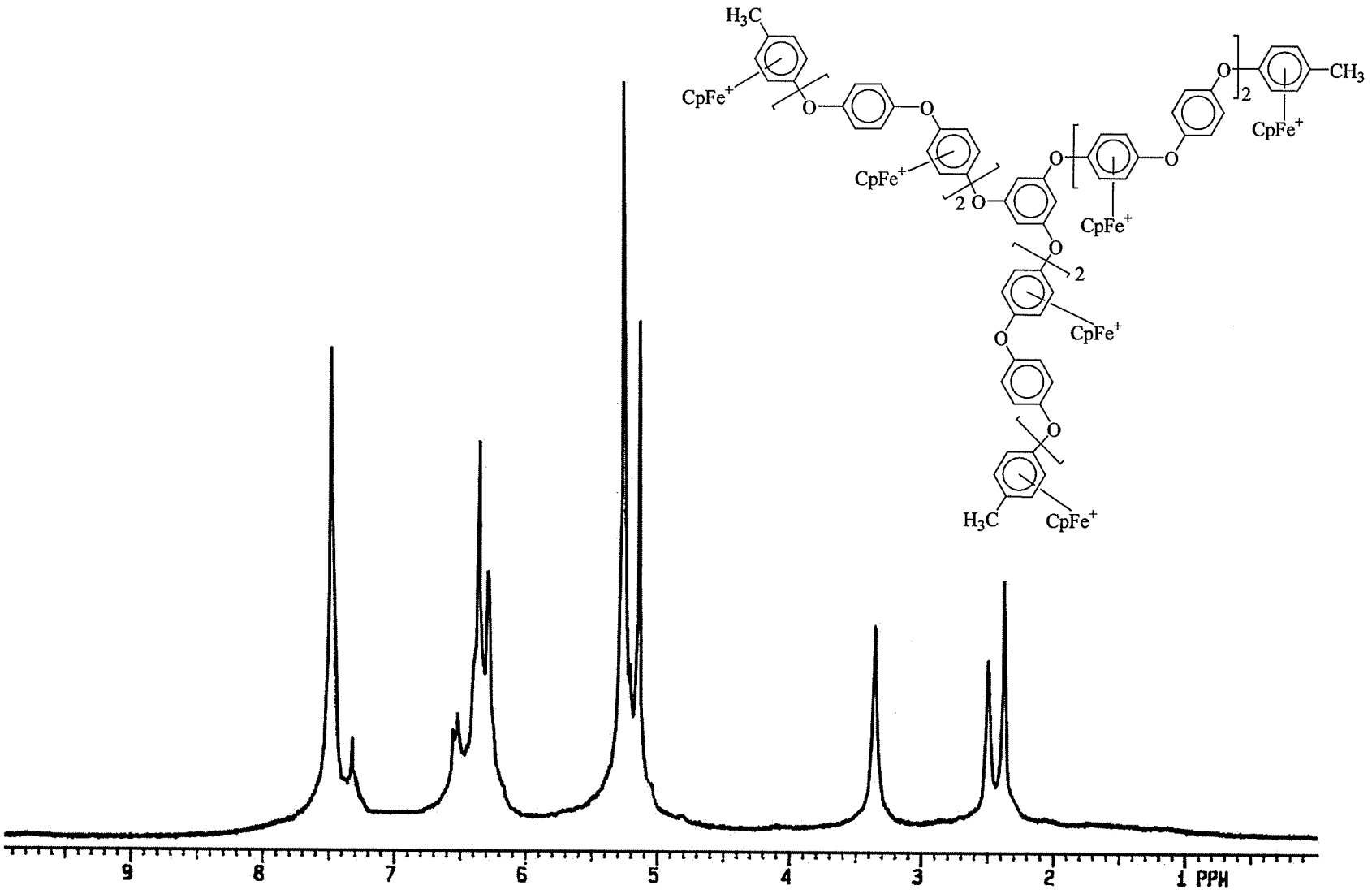

Figure 3.13: ^{1}H NMR spectrum of complex **3.18** in DMSO-d_6

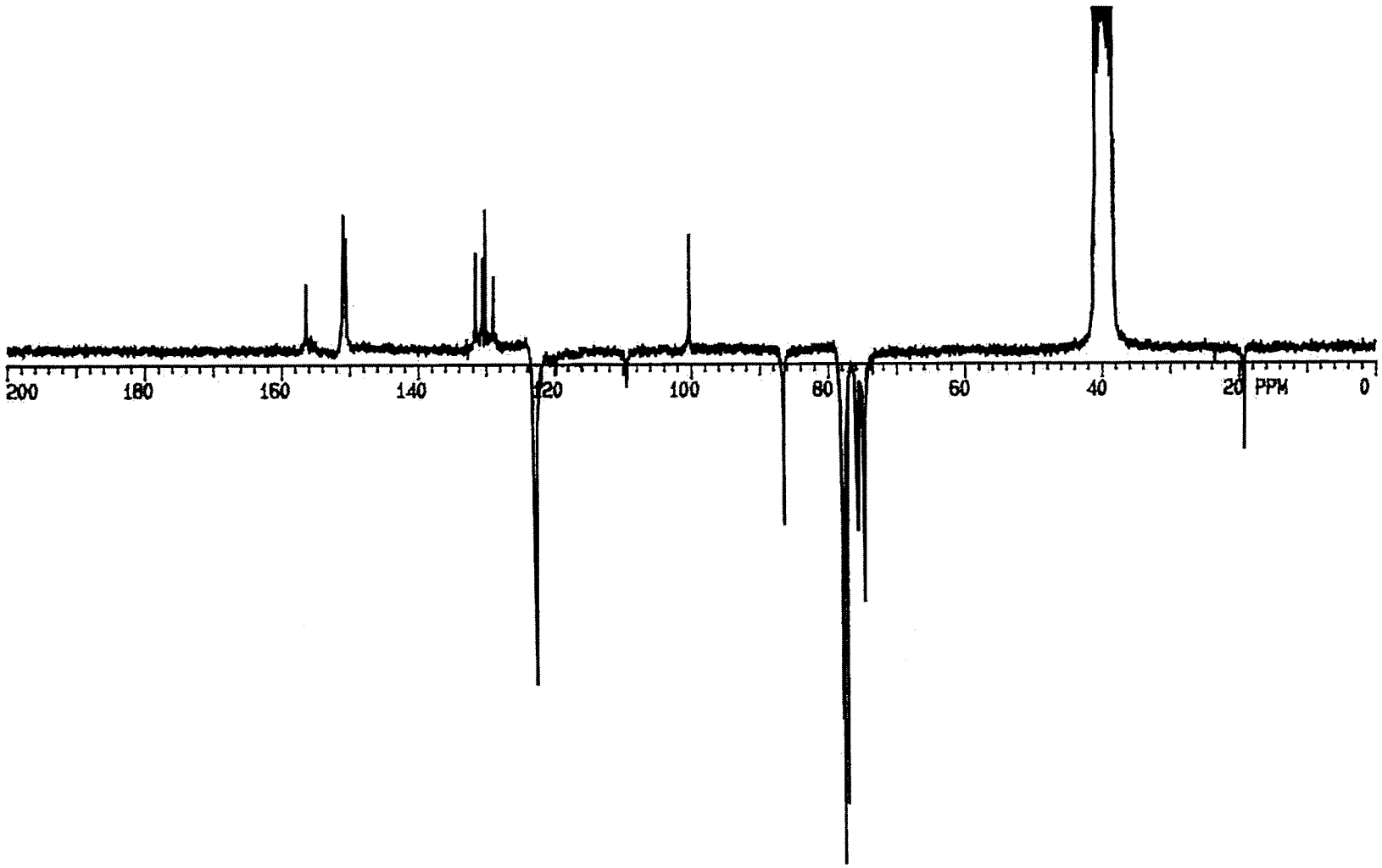

Figure 3.14: ^{13}C NMR spectrum of complex **3.18** in DMSO-d_6

Table 3.13: % Yield, IR and CH Analysis of Complexes **3.18-3.21**

Complex	% Yield	IR (cm^{-1})	CH Analysis
3.18	90		($C_{144}H_{117}O_{15}F_{54}Fe_9P_9$) (3894.8): Calcd. C 44.41, H 3.03; Found C 44.73, H 2.84
3.19	94		
3.20	76	1771 (CO)	
3.21	81	1733 (CO), 3433 (OH)	

Table 3.14: ^{1}H NMR Analysis of Complexes **3.18-3.21** in DMSO-d_6

Complex	Other	Cp	Complexed Aromatic	Aromatic
3.18	2.37 (s, 9H, CH_3)	5.14 (s, 15H), 5.27 (s, 30H)	6.29 (s, 12H), 6.35 (br.s, 18H), 6.53 (d, *J*=6.6 Hz, 6H)	7.32 (s, 3H), 7.49 (s, 24H)
3.19[#]	1.70 (s, 36H, CH_3), 2.46 (s, 9H, CH_3)	5.18 (s, 15H), 5.28 (s, 30H)	6.31 (br.s, 30H), 6.43 (br.s, 6H)	7.22 (s, 24H), 7.33 (s, 3H), 7.40-7.50 (m, 24H)
3.20	2.34 (s, 9H, CH_3)	5.11 (s, 15H), 5.23 (s, 30H)	6.27-6.52 (m, 36H)	7.37 (br.d, 15H), 7.45 (br.d, 12H), 7.73 (m, 3H), 7.98 (m, 9H)
3.21	1.66 (s, 9H, CH_3), 2.07 (br.s, 6H, CH_2), 2.35 (s, 9H, CH_3), 2.45 (br.s, 6H, CH_2)	5.18 (s, 15H), 5.24 (s, 15H), 5.27 (s, 15H)	6.25 (s, 12H), 6.31-6.36 (m, 18H), 6.56 (br.d, 6H)	7.24 (d, *J*=8.42 Hz, 12H), 7.38 (m, 15H), 7.47 (s, 12H)

[#]Analysis in Acetone-d_6

Table 3.15: ^{13}C NMR Analysis of Complexes **3.18-3.21** in DMSO-d_6

Complex	Other	Cp	Complexed Aromatic	Aromatic
3.18	19.21 (CH_3)	77.37, 77.88, 78.03	74.81, 75.85, 86.58, 100.31*, 129.01*, 130.25*, 130.62*, 131.63*	109.88, 122.81, 123.03, 150.61*, 150.77*, 150.93*, 156.43*
3.19[#]	19.82 (CH_3), 31.03 (CH_3), 42.71 (C)	78.29, 78.76, 78.99	75.44, 75.58, 76.74, 87.62, 101.08*, 130.54*, 131.67*, 132.20*, 133.13*	110.85, 120.77, 123.96, 127.04, 129.64, 148.06*, 149.45*, 151.74*, 152.03*, 157.56*
3.20	19.25 (CH_3), 90.00 (C), 168.53 (CO)	77.47, 77.99, 78.07	74.97, 76.48, 86.73 100.50*, 129.61*, 130.19*, 130.91*, 131.96*	109.46, 120.47, 120.63, 122.79, 124.26*, 124.65, 125.83, 129.13, 130.37, 144.64*, 151.06*, 153.54*, 153.79* 155.77*, 156.44*
3.21	19.28 (CH_3), 26.99 (CH_3), 30.22 (CH_2), 36.50 (CH_2), 45.03 (C), 174.64 (CO)	77.39, 77.91, 78.09	74.98, 76.12, 86.73, 100.25*, 129.07*, 130.08*, 130.23*, 130.62*, 131.48*	109.52, 119.83, 120.05, 122.85, 129.23, 146.26*, 150.83*, 151.07*, 151.26*, 151.51*, 156.48*

*Denotes quaternary carbons, [#]Analysis in Acetone-d_6

The electrochemical properties of the star-shaped complexes were examined using cyclic voltammetry. It is important to note that increasing the size of the oligomers resulted in broader redox waves, due to overlapping reduction processes. For example, while the CV of complex **3.10** (containing six organoiron units) showed two distinct redox waves at a scan rate of 0.1 V/s, the CV of complex **3.18** (containing nine organoiron units) showed only one broad reduction wave at a scan rate of 0.1 V/s (Figure 3.17). The $E_{1/2}$ of this reduction process occurred at –1.30 V.

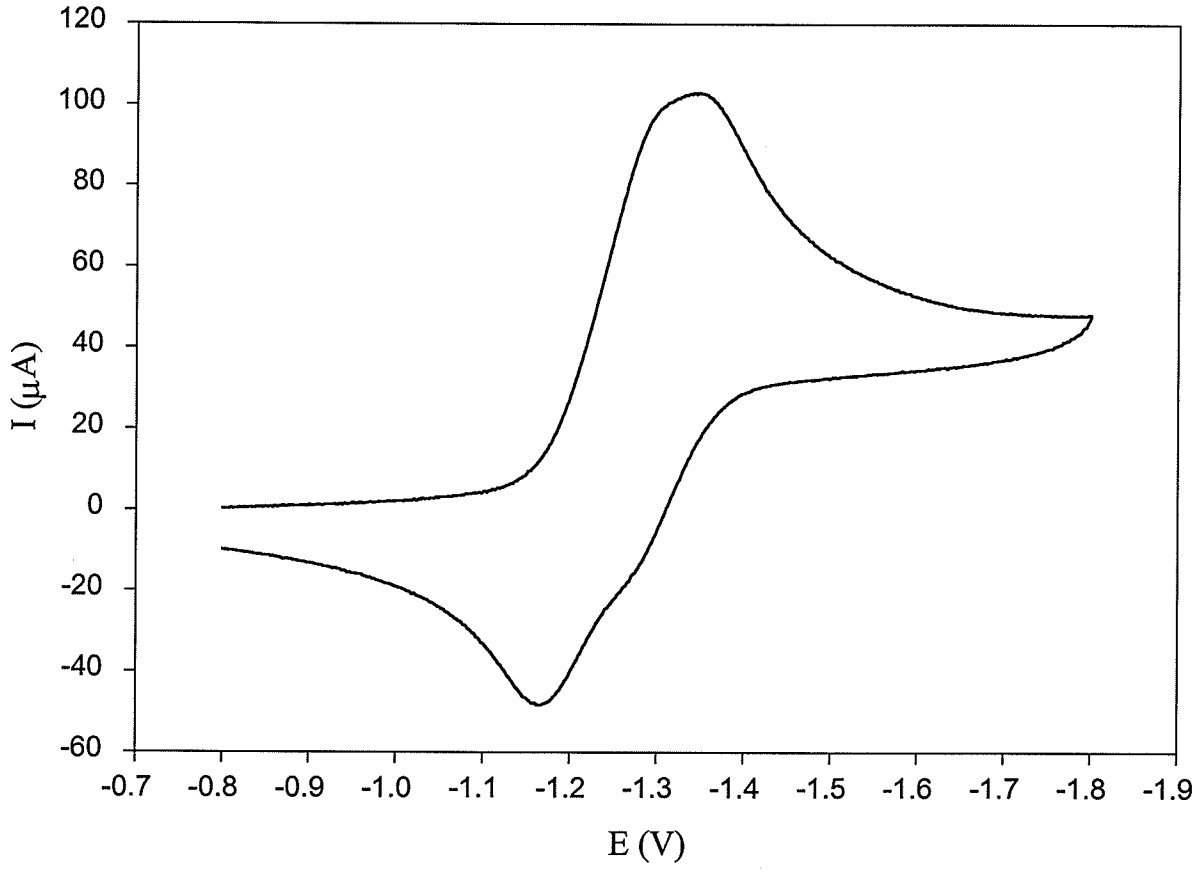

Figure 3.15: Cyclic voltammogram at glassy carbon of 0.001 M **3.19** in 0.1 M TBAP in DMF, $\nu = 0.1$ V/s at –40 °C

By decreasing the scan rate to 0.05 V/s, it was possible to distinguish two separate redox processes as shown in Figure 3.18. It was not possible, however, to distinguish three separate redox waves due to the similar redox potentials of the inner six iron centers. The E_{pc} and E_{pa} values of the first wave were at –1.32 and –1.21 V, respectively, leading to an $E_{1/2}$ value of –1.27 V. The cathodic and anodic potentials of the second wave occurred at –1.38 and –1.31 V, respectively, giving an $E_{1/2}$ value of –1.35 V.

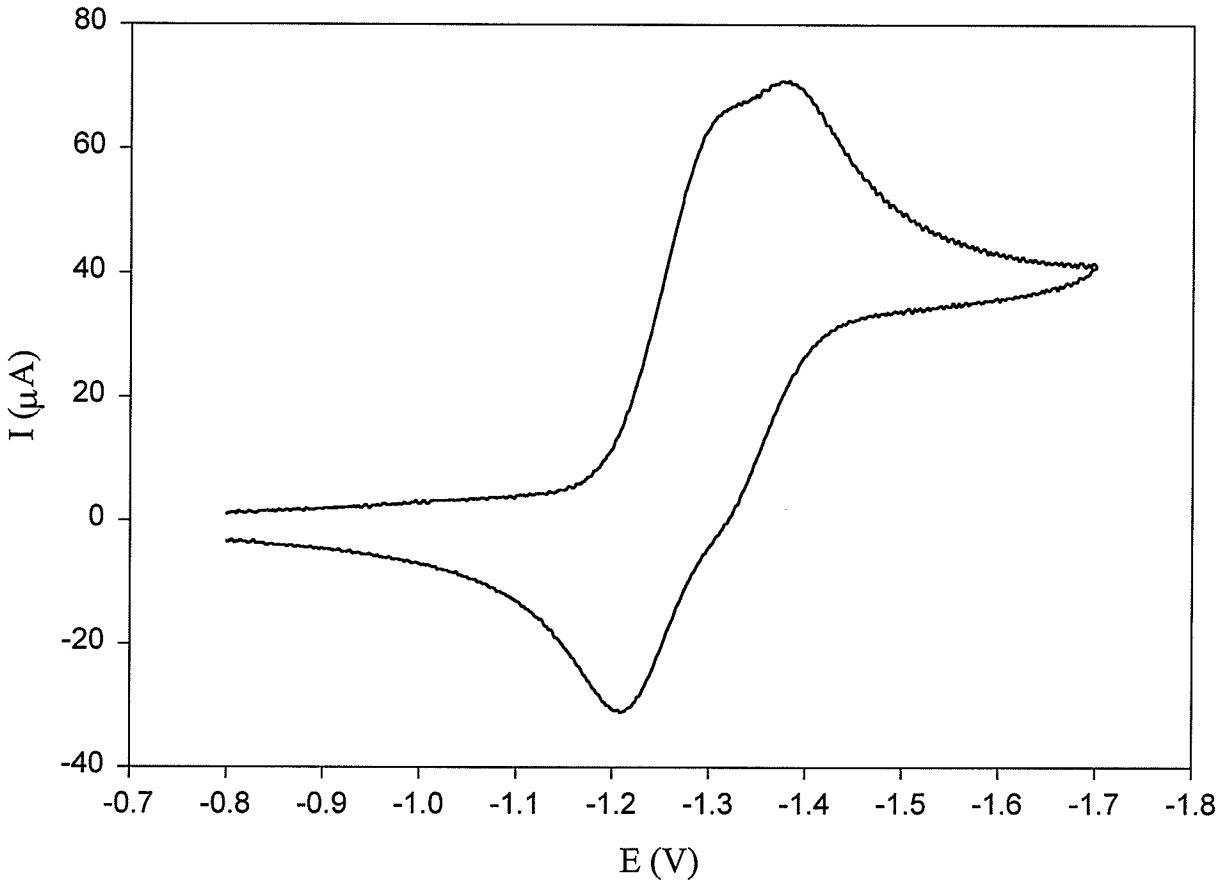

Figure 3.16: Cyclic voltammogram at glassy carbon of 0.001 M **3.19** in 0.1 M TBAP in DMF, ν = 0.05 V/s at –40 °C

3.2.4 Synthesis and Properties of Star-Shaped Aryl Ethers Containing Twelve and Fifteen Cationic Organoiron Moieties

The synthesis of higher molecular weight materials was also accomplished using the hydroquinone-based system. The synthesis of linear aromatic ether complexes containing three and four cyclopentadienyliron cations pendent to their structures is shown in Scheme 3.7. Reaction of complexes **3.21** and **3.23** with an excess of hydroquinone resulted in the isolation of the aryl ether oligomers **3.22** and **3.24**. These complexes contain terminal phenolic groups that can be further reacted with chloroarene complexes. Complexes **3.22** and **3.24** were isolated as beige powders in 87 and 94 % yields, respectively. Reaction of complexes **3.22** and **3.24** with one molar equivalent of the *p*-dichlorobenzene complex (**2.1**) resulted in the isolation of complexes **3.23** and **3.25**. These complexes each contain one terminal chloroarene complex that can be reacted with the triphenolic star complex **3.4** to produce larger star polymers. Complexes **3.23** and **3.25** were isolated as yellow solids in 93 and 90 % yields, respectively.

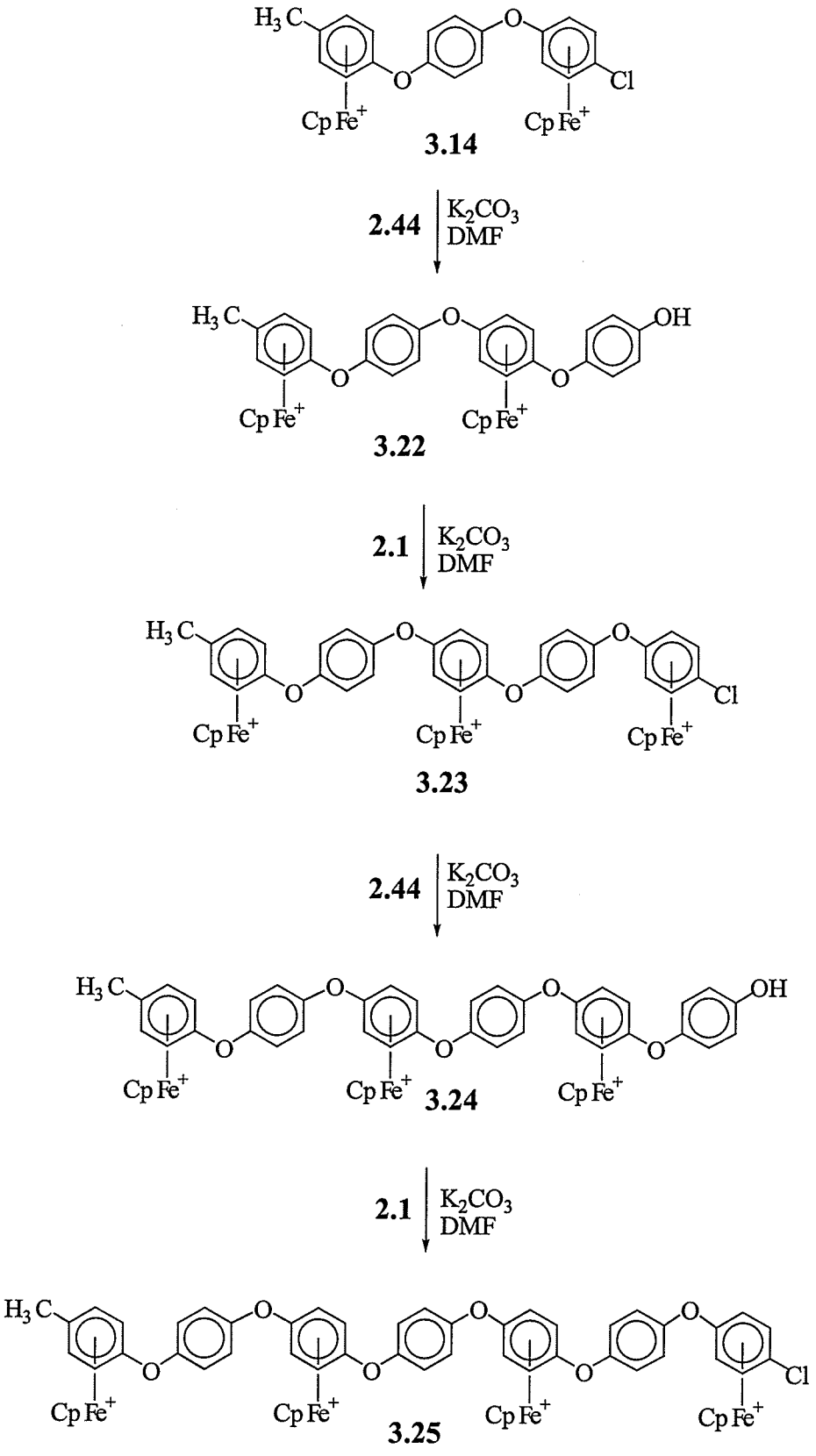
H3C
O
O
Cl
Cp Fe+
Cp Fe+
3.14
2.44
K2CO3
DMF
H3C
O
O
OH
Cp Fe+
Cp Fe+
3.22
2.1
K2CO3
DMF
H3C
O
O
O
O
Cl
Cp Fe+
Cp Fe+
Cp Fe+
3.23
2.44
K2CO3
DMF
H3C
O
O
O
O
OH
Cp Fe+
Cp Fe+
Cp Fe+
3.24
2.1
K2CO3
DMF
H3C
O
O
O
O
Cl
Cp Fe+
Cp Fe+
Cp Fe+
Cp Fe+
3.25

Scheme 3.7

Complexes **3.22** and **3.24** were analyzed using IR and NMR spectroscopy. Infrared spectroscopy confirmed the presence of OH groups around 3545 cm^{-1}, and the OH resonances were also apparent in the ^{1}H NMR spectra between 9.71 and 9.74 ppm. The ^{1}H NMR spectrum of complex **3.22** is shown in Figure 3.17. Upon reaction of complex **3.14** with hydroquinone, the complexed aromatic protons of the complexed chloroarene shifted upfield to 6.28 ppm. The complexed aromatic protons alpha to the methyl groups appeared as a doublet at 6.16 ppm. Two new sets of doublets appeared at 6.90 and 7.15 ppm in the spectrum of **3.22**. These peaks were assigned to the newly introduced phenolic ether arene protons. The singlet at 7.46 ppm was identified as the peak corresponding to the four protons of the inner uncomplexed aromatic ring.

The ^{13}C NMR spectrum of complex **3.22** is shown in Figure 3.18. The methyl carbon appears as a downward peak at 19.23 ppm. The two sets of cyclopentadienyl carbons appear at 77.38 and 77.65 ppm. The complexed aromatic CH carbons appear at 73.56, 74.86, 75.89 and 86.61 ppm, while the quaternary complexed carbons resonate at 100.34, 129.83, 131.59 and 131.67 ppm. The peaks at 116.83, 122.03, 122.72 and 123.00 correspond to the uncomplexed aromatic (CH) carbons, while the peaks at 144.75, 150.55, 151.07 and 155.70 ppm correspond to the quaternary uncomplexed aromatic carbons. Tables 3.16 and 3.17 provide the full spectroscopic data for complexes **3.22** and **3.24**.

Tables 3.18 and 3.19 provide the full spectroscopic data for complexes **3.23** and **3.25**. The patterns observed in the spectra of these complexes follow the description given for complex **3.14**.

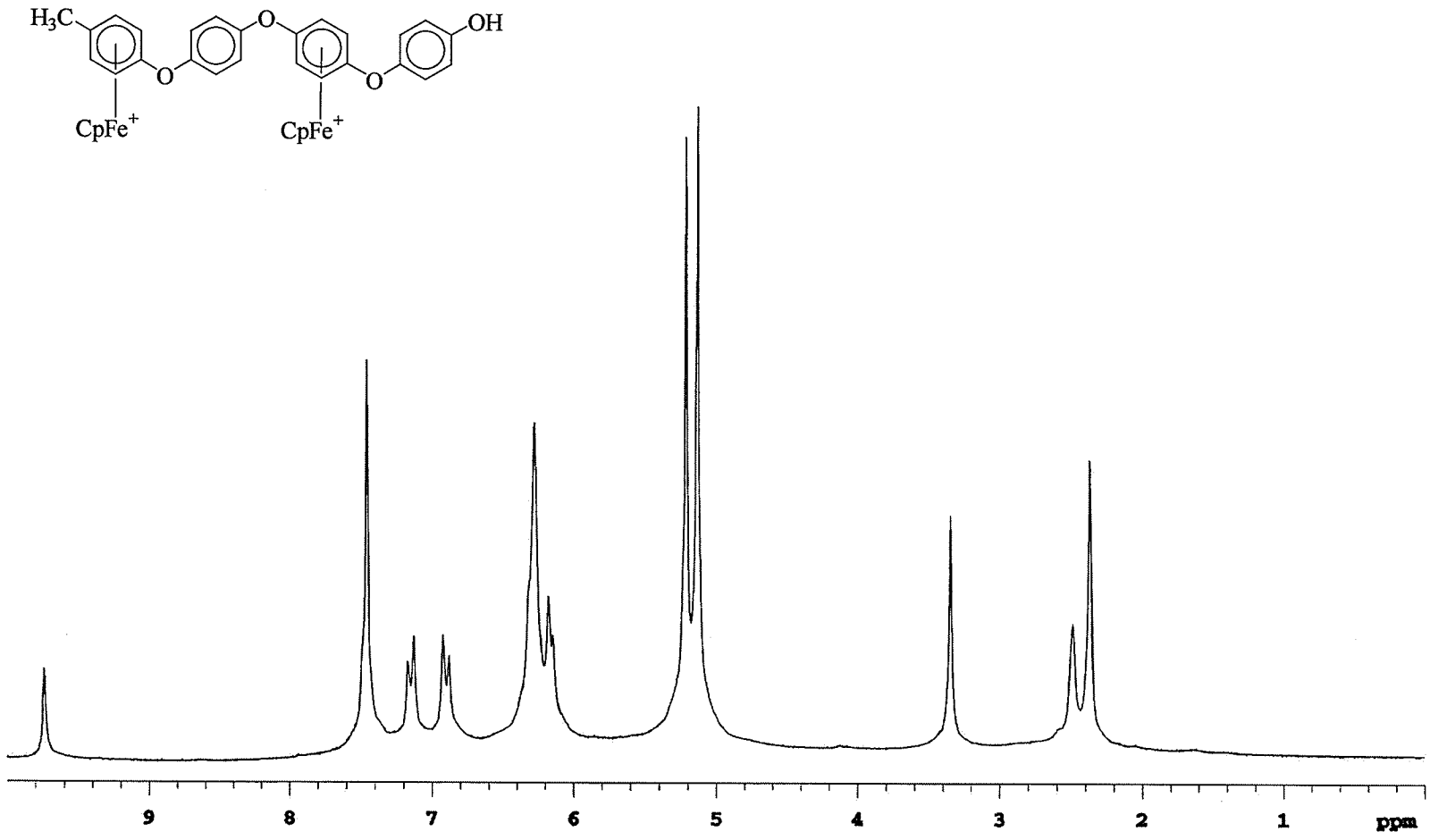

Figure 3.17: ^{1}H NMR spectrum of complex **3.22** in DMSO-d_6

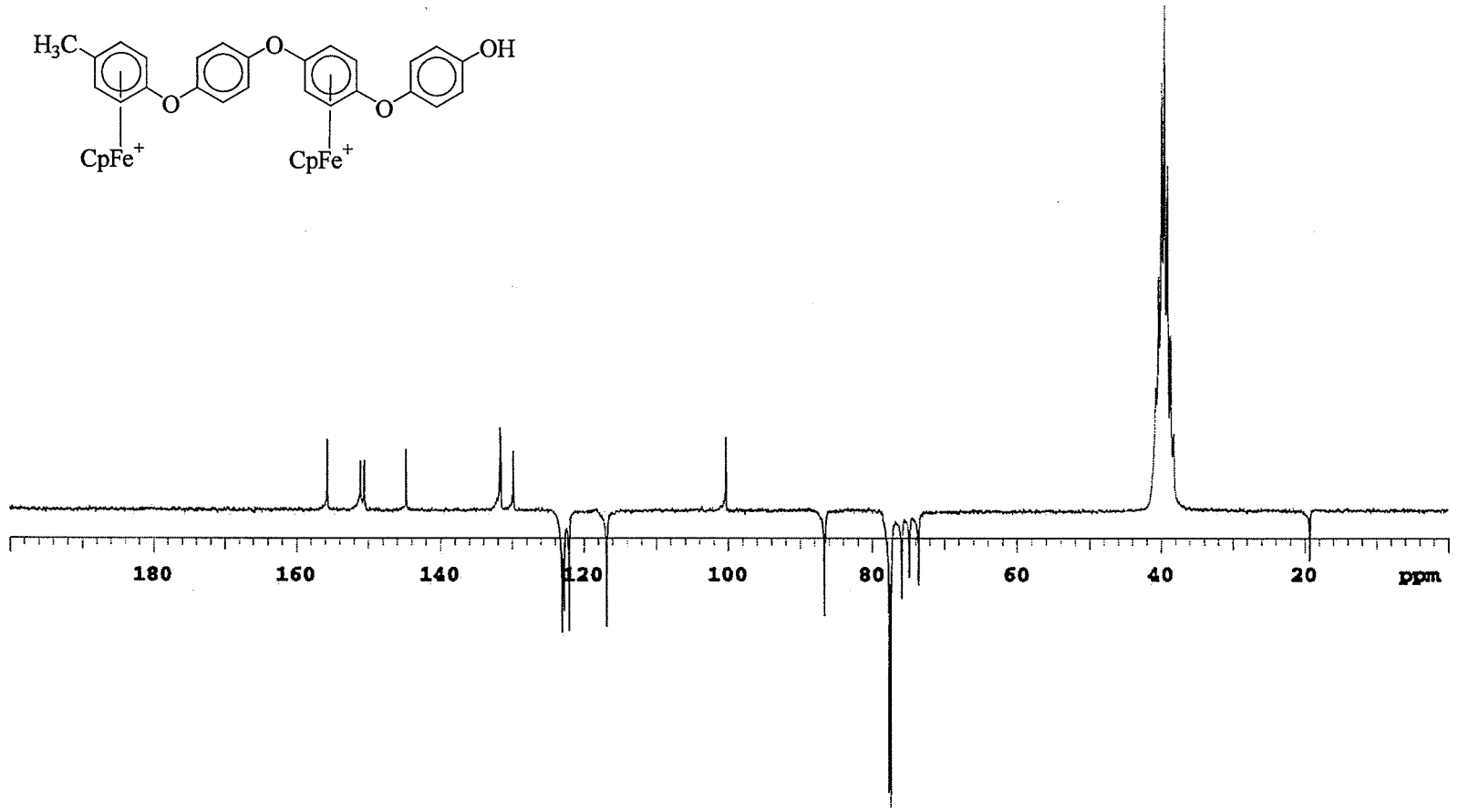

Figure 3.18: ^{13}C NMR spectrum of complex **3.22** in DMSO-d_6

Table 3.16: % Yield and ^{1}H NMR Analysis of Complexes **3.22** and **3.24** in DMSO-d_6

Complex	% Yield	Other	Cp	Complexed Aromatic	Aromatic
3.22	87	2.37 (s, 3H, CH_3), 9.74 (s, 1H, OH	5.14 (s, 5H), 5.22 (s, 5H)	6.16 (d, J = 6.25 Hz, 2H), 6.28 (s, 6H)	6.90 (d, J = 8.55 Hz, 2H), 7.15 (d, J = 8.55 Hz, 2H), 7.46 (s, 4H)
3.24	94	2.38 (s, 3H, CH_3), 9.71 (s, 1H, OH	5.14 (s, 5H), 5.22 (s, 5H), 5.27 (s, 5H)	6.17 (br.s, 2H), 6.30-6.54 (m, 8H)	6.93 (d, J = 7.65 Hz, 2H), 7.14 (d, J = 7.10 Hz, 2H), 7.48 (s, 8H)

Table 3.17: IR and ^{13}C NMR Analysis of Complexes **3.22** and **3.24** in DMSO-d_6

Complex	IR (cm^{-1})	CH_3	Cp	Complexed Aromatic	Aromatic
3.22	3544 (OH)	19.23	77.38, 77.65	73.56, 74.86, 75.89, 86.61, 100.34*, 129.83*, 131.59*, 131.67*	116.83, 122.03, 122.72, 123.00, 144.75*, 150.55*, 151.07*, 155.70*
3.24	3545 (OH)	19.34	77.42, 77.68, 77.96	73.56, 75.00, 76.01, 76.14, 86.67, 100.38*, 130.20*, 131.57*, 131.62*, 131.66*	116.80, 122.04, 122.74, 122.97, 144.70*, 150.96*, 151.01*, 151.13*, 155.74*

*Denotes quaternary carbons

Table 3.18: % Yield and ^{1}H NMR Analysis of Complexes **3.23** and **3.25** in Acetone-d_6

Complex	% Yield	CH_3	Cp	Complexed Aromatic	Aromatic
3.23	93	2.52	5.22 (s, 5H), 5.34 (s, 5H), 5.39 (s, 5H)	6.35 (s, 4H), 6.38 (s, 4H), 6.52 (d, *J*=6.88 Hz, 2H), 6.77 (d, *J*=6.43 Hz, 2H)	7.58 (s, 4H), 7.61 (s, 4H)
3.25	90	2.51	5.21 (s, 5H), 5.34 (s, 10H), 5.38 (s, 5H)	6.35-6.37 (m, 16H), 6.52 (d, *J*=6.80 Hz, 2H), 6.66 (d, *J*=6.80 Hz, 2H)	7.57 (s, 4H), 7.59 (s, 8H)

Table 3.19: CH and ^{13}C NMR Analysis of Complexes **3.23** and **3.25** in Acetone-d_6

Complex	CH Analysis	CH_3	Cp	Complexed Aromatic	Aromatic
3.23	($C_{46}H_{38}ClF_{18}Fe_3O_4P_3$) (1292.68) Calcd. C, 42.74; H, 2.96 Found C, 42.26; H, 2.93	19.88	78.49, 78.95, 80.49	75.42, 76.72, 76.85, 87.77, 101.52*, 104.94*, 132.23*, 133.63*, 134.12*	124.32, 124.41, 124.48, 151.60*, 151.90*, 152.06*, 152.34*
3.25		19.89		75.40, 75.60, 76.80, 76.94, 87.81, 101.57*, 105.00*, 132.12*, 132.32*, 133.72* 134.11*	124.41, 151.64*, 151.95*, 152.92*

*Denotes quaternary carbons

Complex **3.4** was subsequently reacted with the chloroarene complexes **3.23** and **3.25** resulting in the isolation of star polymers **3.26** and **3.27** containing twelve and fifteen metallic moieties pendent to their backbones, respectively. The synthesis of these polymetallic stars is shown in Scheme 3.8. It was found that the solubility of the polymers decreased with increasing molecular weight, however all polymers could be solubilized in polar aprotic solvents such as DMF and DMSO. This is consistent with our previous work, which found that the solubility of aromatic ether polymers is enhanced via coordination to cationic cyclopentadienyliron moieties. These star-shaped polymers were isolated in yields ranging from 91 to 93% as beige solids.

The organoiron-mediated methodology allowed for the facile synthesis of aromatic ether star polymers using mild reaction conditions. Controlled design of aromatic ether oligomers is often difficult to accomplish using organic synthetic methodologies since they require much harsher reaction conditions. These complexes are the first examples of star polymers containing cyclopentadienyliron-coordinated arenes on alternating aromatic rings.

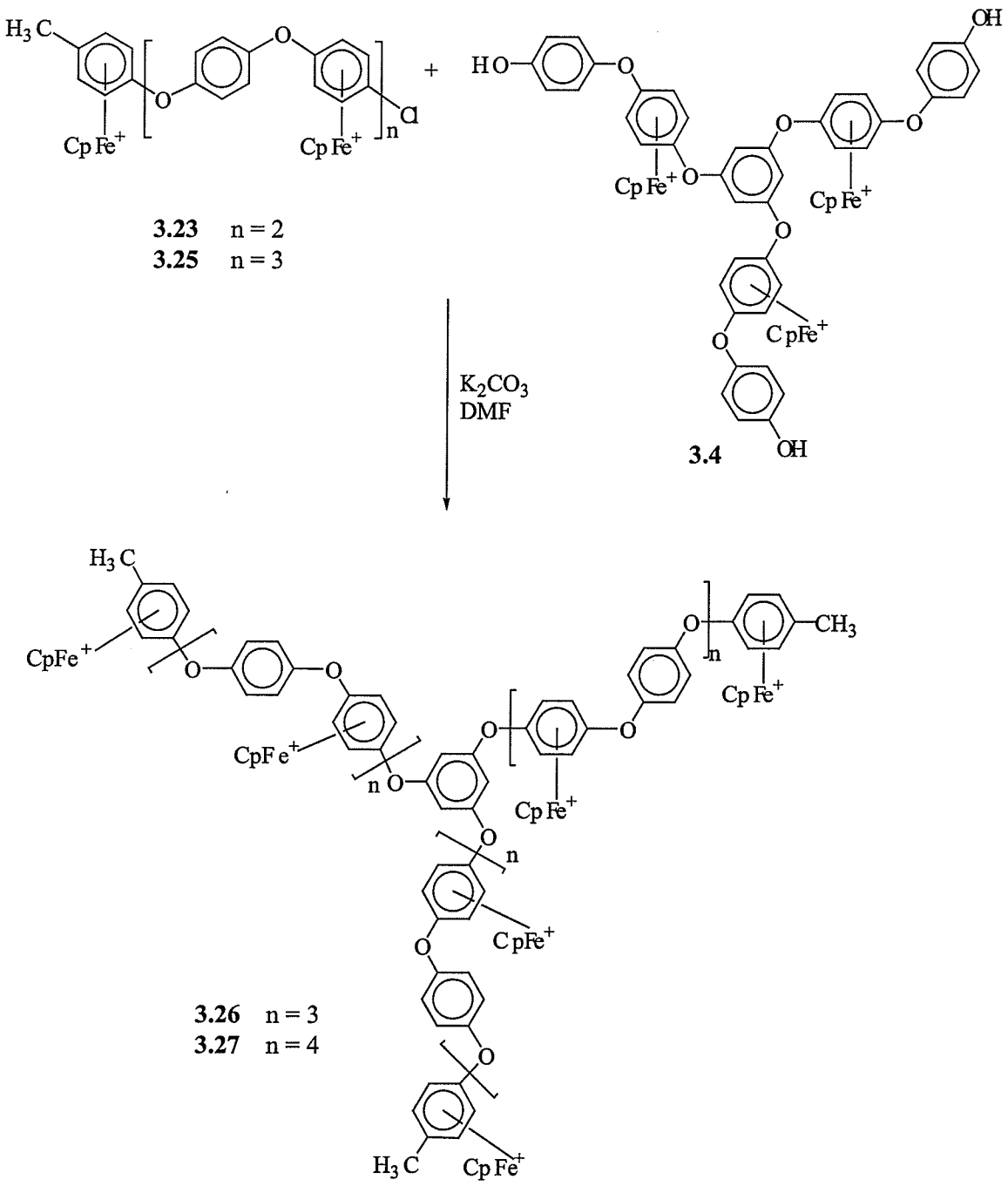

3.23 n = 2
3.25 n = 3

3.4

3.26 n = 3
3.27 n = 4

Scheme 3.8

Complexes **3.26** and **3.27** were analyzed using ^{1}H and ^{13}C NMR spectroscopy and the characterization of these complexes is given in Tables 3.20 and 3.21. Figure 3.19 shows the ^{1}H NMR spectrum of the star-shaped complex containing twelve cyclopentadienyliron cations within its structure (**3.26**). The spectrum shows the nine methyl protons at 2.38 ppm and the cyclopentadienyl protons at 5.15 and 5.27 ppm. The peak at 5.15 ppm corresponds to the cyclopentadienyl protons of the outer three complexes, while the peak at 5.27 ppm corresponds to the proton resonances of the nine inner cyclopentadienyl rings. The complexed aromatic protons appear as two peaks at 6.29 and 6.36 ppm. The uncomplexed aromatic protons of the central arene appear as a singlet at 7.34 ppm and those of the linear branches appear at 7.49 ppm.

Figure 3.20 shows the ^{13}C NMR spectrum of complex **3.26**. As expected, there are four cyclopentadienyl peaks between 77.41 and 78.01 ppm, three complexed aromatic (CH) peaks and five quaternary complexed aromatic peaks. The aromatic CH peak corresponding to the central arene appears at 109.90 ppm, and the other aromatic carbons appear at 122.82 and 123.05 ppm. The four quaternary aromatic carbon peaks appear between 150.67 and 156.50 ppm. The NMR spectrum of the complex containing fifteen metallic moieties (**3.27**) is actually simpler than that of complex **3.26**, with twelve organoiron units. For example, there were only two cyclopentadienyl resonances, and fewer complexed aromatic carbon peaks due to overlapping of peaks.

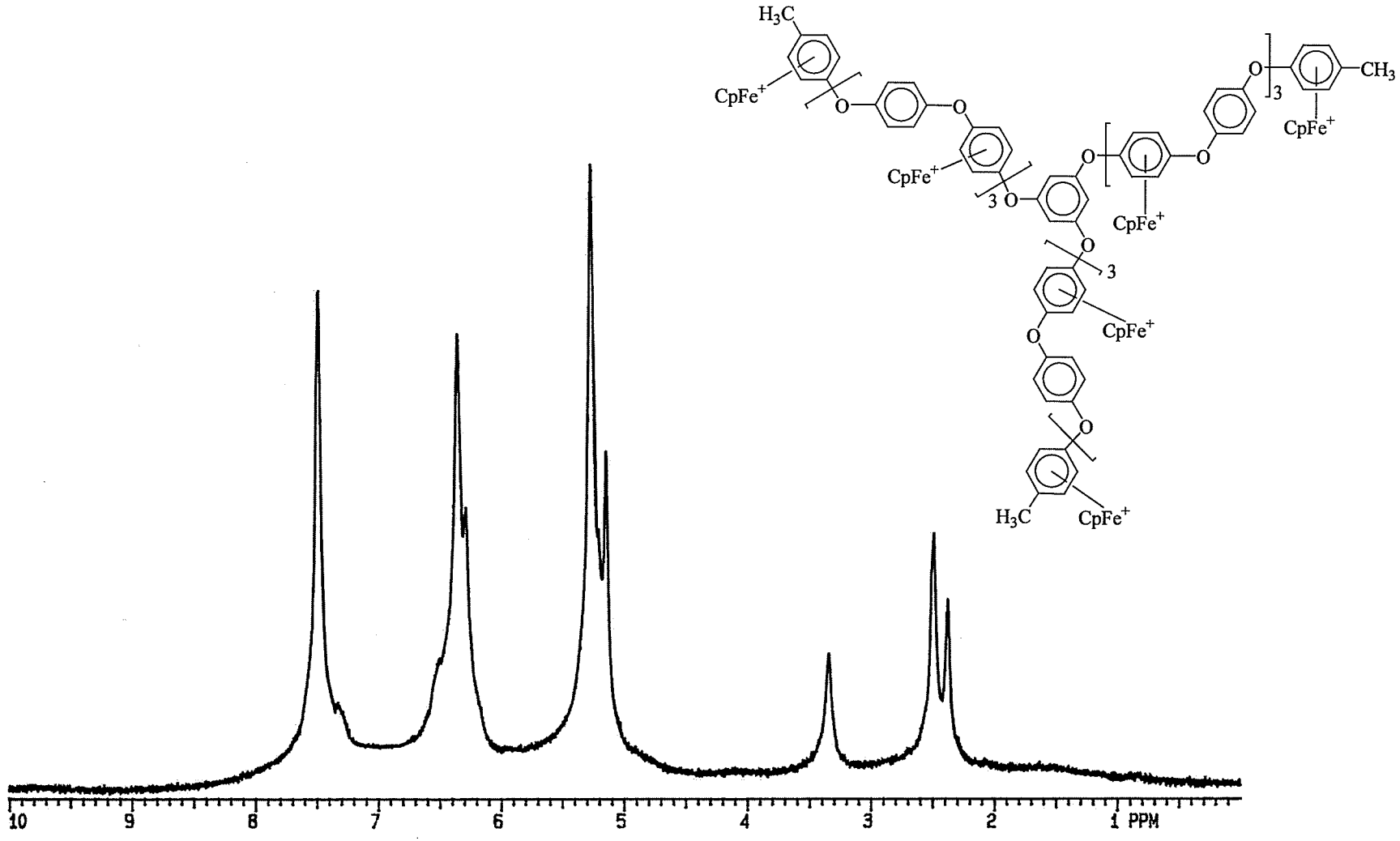

Figure 3.19: ^{1}H NMR spectrum of complex **3.26** in DMSO-d_6

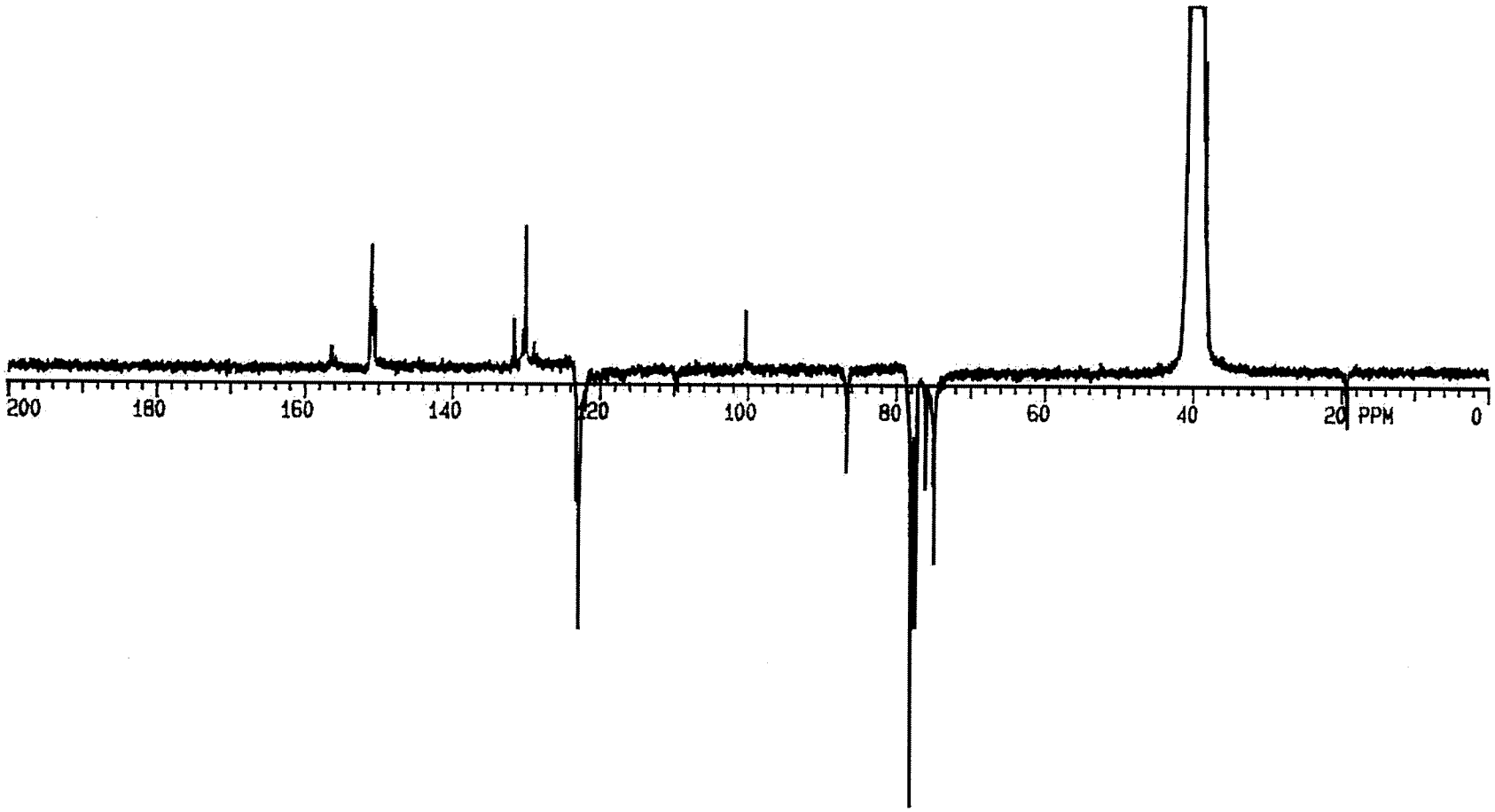

Figure 3.20: ^{13}C NMR spectrum of complex **3.26** in DMSO-d_6

Table 3.20: % Yield and ^{1}H NMR Analysis of Complexes **3.26** and **3.27** in DMSO-d_6

Complex	% Yield	CH_3	Cp	Complexed Aromatic	Aromatic
3.26	91	2.38 (s, 9H)	5.15 (s, 15H), 5.27 (s, 45H)	6.29 (s, 12H), 6.36 (br.s, 36H)	7.34 (s, 3H), 7.49 (s, 36H)
3.27	93	2.38 (s, 9H)	5.15 (s, 15H), 5.27 (s, 60H)	6.29 (s, 12H), 6.36 (br.s, 48H)	7.35 (s, 3H), 7.49 (s, 48H)

Table 3.21: CH and ^{13}C NMR Analysis of Complexes **3.26** and **3.27** in DMSO-d_6

Complex	CH Analysis	CH_3	Cp	Complexed Aromatic	Aromatic
3.26	($C_{195}H_{156}O_{21}F_{72}Fe_{12}P_{12}$) (5245.1): Calcd. C 44.65, H 3.00; Found C 44.79, H 2.87	19.27	77.41, 77.83, 77.94, 78.01	74.91, 75.94, 86.64, 100.37*, 130.07*, 130.24*, 130.59*, 131.62*	109.90, 122.82, 123.05, 150.67*, 150.81*, 150.99*, 156.50*
3.27	($C_{246}H_{195}O_{27}F_{90}Fe_{15}P_{15}$) (6595.4): Calcd. C 44.80, H 2.98; Found C 44.58, H 3.12	19.24	77.41, 77.95	74.93, 75.96, 86.65, 100.36*, 130.27*, 131.64*	109.88, 122.83, 122.90, 150.67*, 150.74*, 150.99*, 156.57*

*Denotes quaternary carbons

The electrochemical properties of the star-shaped complexes (**3.26, 3.27**) were examined using cyclic voltammetry. The cyclic voltammogram of the star-shaped complex containing twelve metallic moieties in its structure (**3.26**) is shown in Figure 3.21. The reduction wave is very broad due to overlapping redox processes, however, the reduction peaks for this complex became narrower at higher scan rates. The $E_{1/2}$ value corresponding to reduction of the iron centers in this complex was –1.25 V at a scan rate of 0.1 V/s.

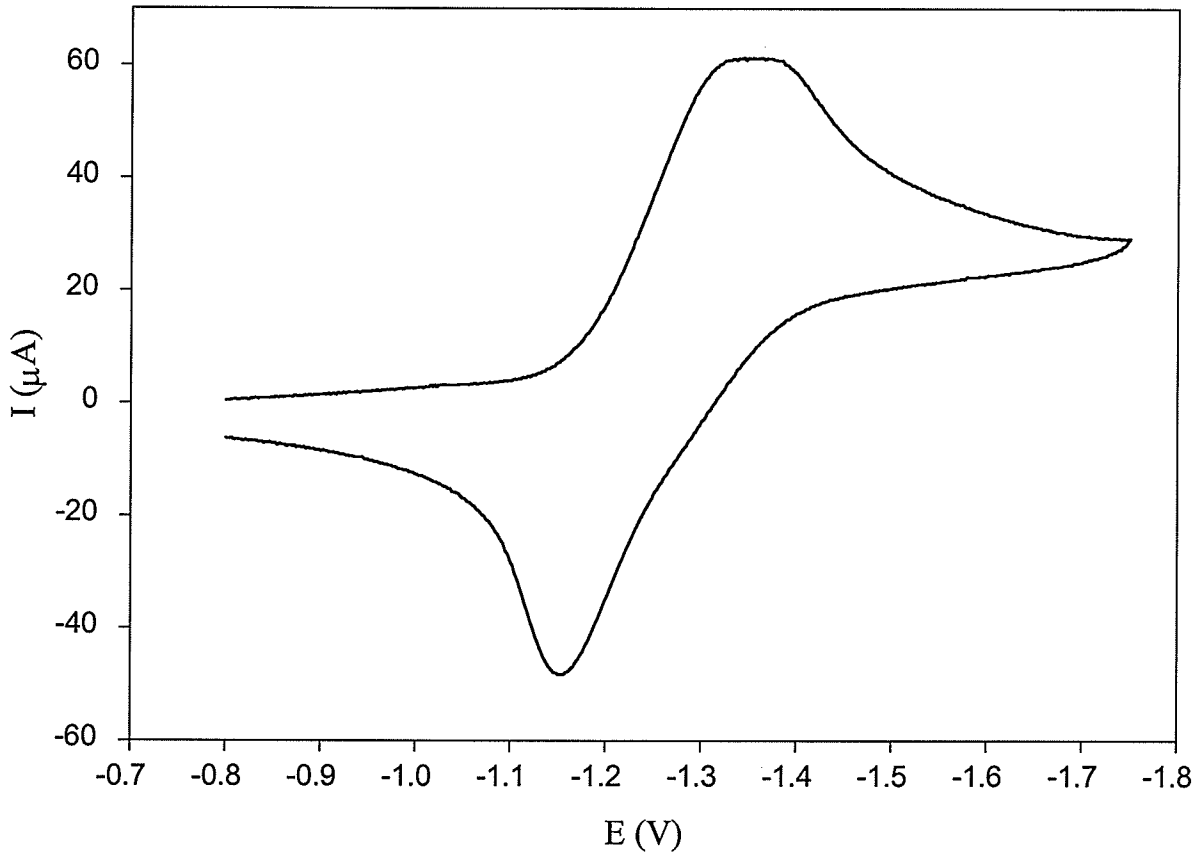

Figure 3.21: Cyclic voltammogram at glassy carbon of 0.001 M **3.26** in 0.1 M TBAP in DMF, $\nu = 0.1$ V/s at –40 °C

The redox wave of complex **3.27**, containing fifteen pendent metallic moieties is shown in Figure 3.22. In contrast to the CV of **3.26**, the cyclic voltammogram of complex **3.27** appears to be much narrower. This fairly broad redox wave at $E_{1/2} = -1.34$ V, corresponds to one-electron reductions of each of the fifteen metal centers. The reason why this CV appears to be narrower is that there are more iron centers that are equivalent (or quasi-equivalent) due to the larger number of complexed aromatic rings containing diarylether linkages. Due to the greater number of these complexes relative to the terminal toluene complexes, these redox waves seem to predominate.

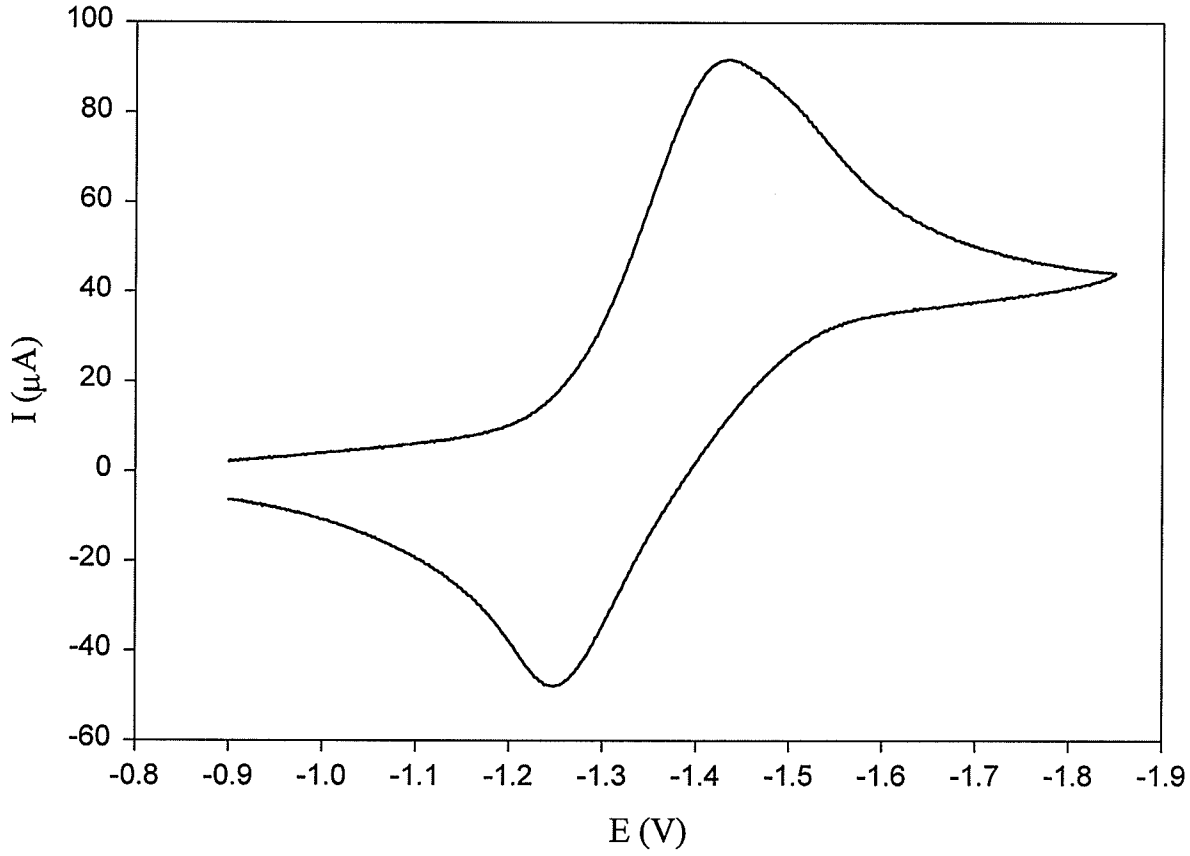

Figure 3.22: Cyclic voltammogram at glassy carbon of 0.001 M **3.27** in 0.1 M TBAP in DMF, $\nu = 0.1$ V/s at –40 °C

3.2.5 Thermal Properties of Star-Shaped Aryl Ethers

The thermal stability of the star-shaped complexes was studied using thermogravimetric analysis. The loss of the cyclopentadienyliron moieties from the backbones of these materials occurred between 210 and 284 °C, which is consistent with our previous studies of organoiron-coordinated polyaromatic ethers. The thermal stability of the trimetallic complex **3.2** had a second weight loss accounting for 29% of its weight beginning at 445 °C, and a third weight loss accounting for 14% of its weight beginning at 565 °C. The hexametallic (**3.10**) and nonametallic (**3.18**) complexes also had third weight losses starting around 750-775 °C. The larger star complexes possessed slightly higher thermal stability, and only exhibited two weight losses. Following loss of the metallic moieties, they were thermally stable until around 450 °C. Table 3.22 provides the percent weight losses, onset and endset temperatures corresponding to the star shaped complexes containing three, six, nine, twelve and fifteen metallic moieties.

Table 3.22: TGA Results for Star Complexes **3.2, 3.10, 3.18, 3.26** and **3.27**

Complex	Weight loss (%)	T_{onset} (°C)	T_{endset} (°C)	Weight loss (%)	T_{onset} (°C)	T_{endset} (°C)	Weight loss (%)	T_{onset} (°C)	T_{endset} (°C)
3.2	36	224	284	29	445	483	14	565	657
3.10	28	239	279	29	480	599	33	750	859
3.18	21	243	273	17	486	509	35	774	883
3.26	17	207	237	22	472	560			
3.27	33	250	278	21	450	502			

3.2.6 Synthesis of a Star Shaped Complex Containing Neutral and Cationic Cyclopentadienyliron Cations

It was also of interest to prepare star-shaped complexes containing two different redox active groups. While it has been established that cyclopentadienyliron cations coordinated to arenes undergo reversible reduction processes, it has been well-established that ferrocene and its derivatives undergo highly reversible oxidation processes. The synthesis of a hexametallic complex containing neutral and cationic cyclopentadienyliron moieties in their structure is shown in Scheme 3.9. Complex **3.29** was prepared via reaction of the trimetallic star complex **3.4** with ferrocene carboxylic acid (**3.28**). A slight excess of complex **3.28** was utilized in the reaction in order to ensure complete coupling of the carboxylic acid to the phenolic groups. In order to remove the excess starting materials from the reaction, complex **3.29** was passed through two alumina columns and isolated as an orange solid in 49 % yield.

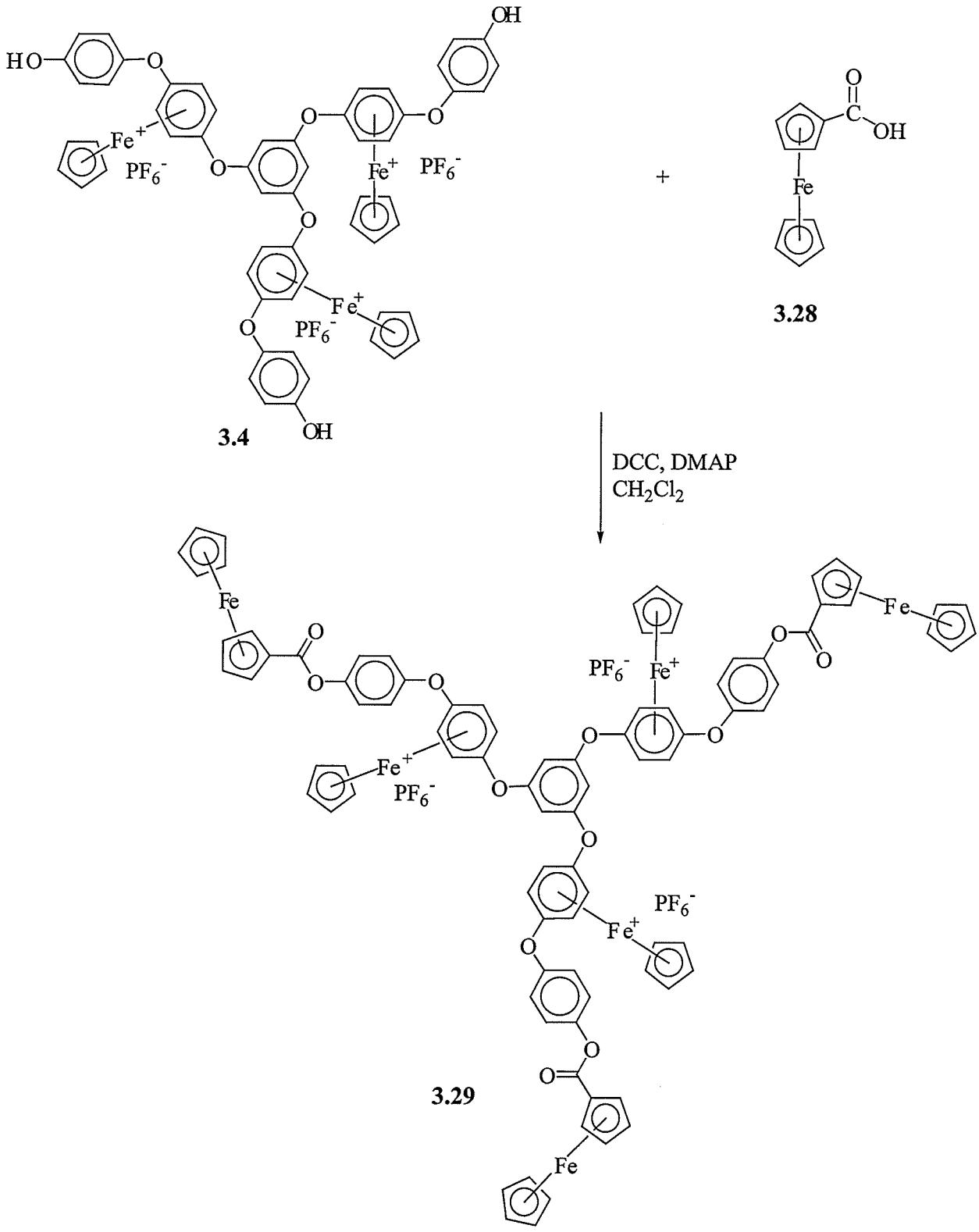
HO
OH
Fe+
PF6-
Fe+
PF6-
Fe+
PF6-
OH
3.4
+
O
C
OH
Fe
3.28
DCC, DMAP
CH2Cl2
Fe
Fe
PF6-
Fe+
Fe+
PF6-
PF6-
Fe+
Fe
3.29

Scheme 3.9

Complex **3.29** was analyzed using ^{1}H, ^{13}C NMR and IR spectroscopy. The results of this analysis are given in Tables 3.23 and 3.24. Figure 3.23 shows the ^{1}H NMR spectrum of complex **3.29** is shown in Figure 3.21. The cyclopentadienyl protons of the unsubstituted ferrocenyl groups appear as a singlet at 4.33 ppm, while the protons of the substituted cyclopentadienyl ring appear as two sets of triplets at 4.40 and 4.94 ppm. The protons of the cyclopentadienyl ring coordinated to the cationic iron center appear as a singlet at 5.35 ppm. The complexed aromatic protons appear as two sets of doublets at 6.41 and 6.63 ppm, which is consistent with the proposed structure. The protons of the central aromatic ring appear as a singlet at 7.35 ppm, while the protons of the three aromatic rings bonded to the ferrocene groups appear as a singlet at 7.38 ppm.

The ^{13}C NMR spectrum shown in Figure 3.24 shows the cyclopentadienyl carbons (CH) of the neutral organoiron unit at 70.68, 71.23 and 72.95 ppm, while the quaternary carbon appears at 70.46 ppm. The cyclopentadienyl resonance of the ring coordinated to the cationic iron center appears at 78.99 ppm. The complexed aromatic carbons (CH) appear at 75.84 and 76.87 ppm, while the quaternary complexed aromatic carbons resonate at 130.70 and 131.94 ppm. The carbons alpha to the ether linkages in the central arene and the branches appear at 110.71 ppm and 122.17 and 124.84 ppm, respectively. The three quaternary aromatic carbons appeared at 149.57, 151.70 and 157.62 ppm. The peak at 170.35 ppm corresponds to the carbonyl carbons of the ester functionalities.

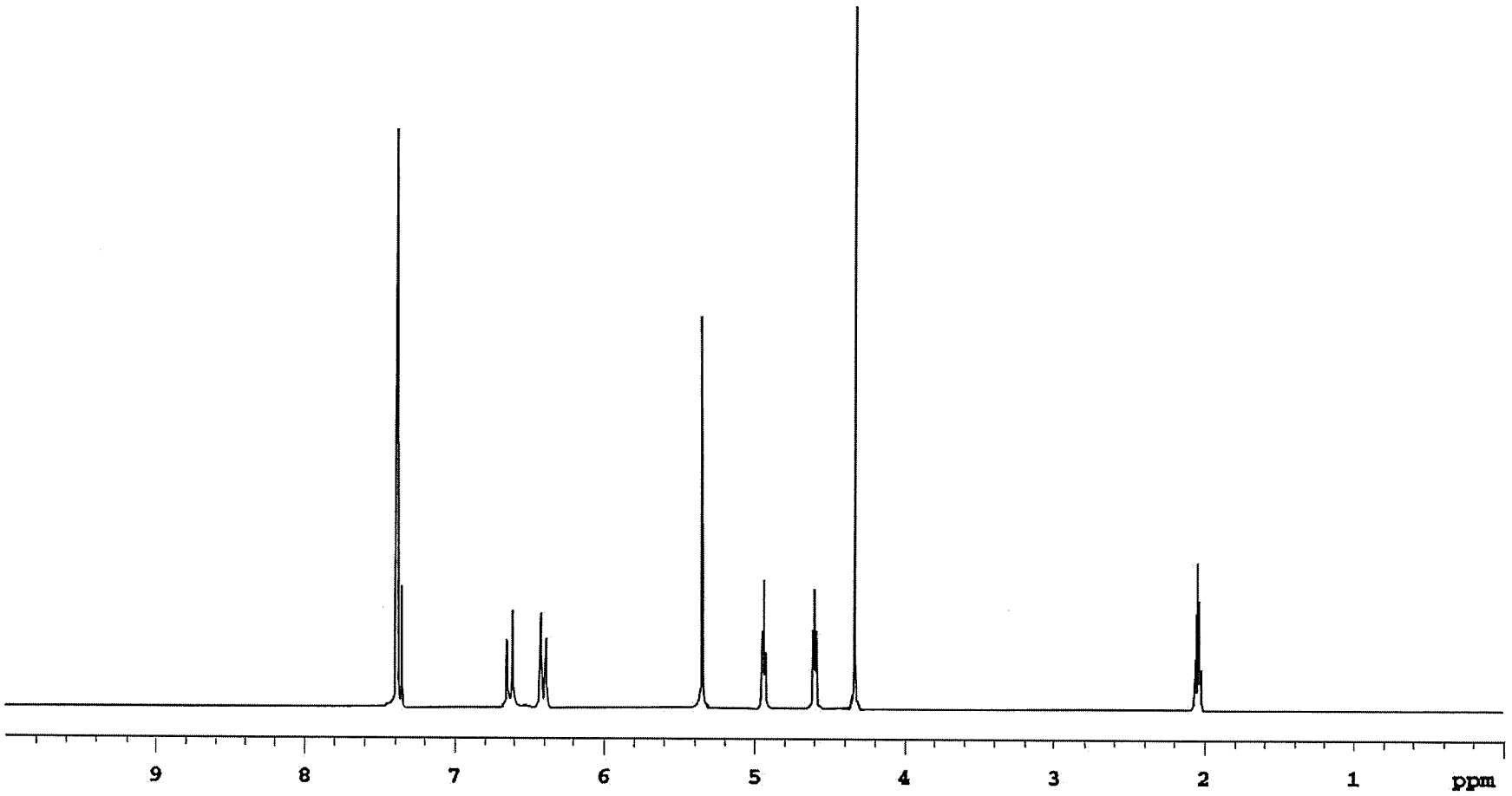

Figure 3.23: ^{1}H NMR spectrum of complex **3.29** in acetone-d_6

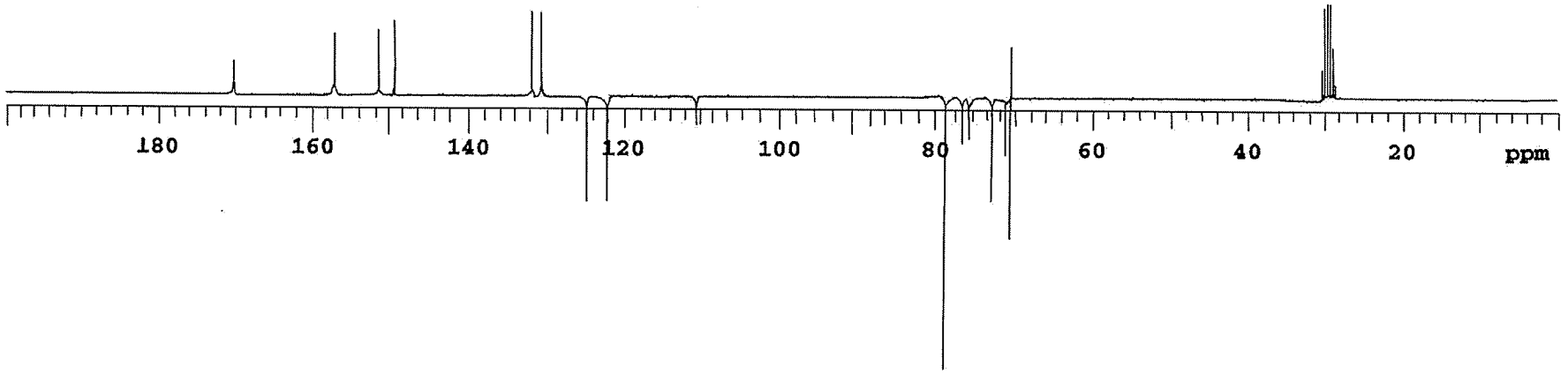

Figure 3.24: ^{13}C NMR spectrum of complex **3.29** in acetone-d_6

Table 3.23: % Yield and ^{1}H NMR Analysis of Complex **3.29** in Acetone-d_6

Complex	% Yield	CpFe	$CpFe^{+}$	Complexed Aromatic	Aromatic
3.29	49	4.33 (s, 15H), 4.60 (t, J = 1.95 Hz, 6H), 4.94 (t, J = 1.95 Hz, 6H)	5.35 (s, 15 H)	6.41 (d, J = 7.03 Hz, 6H), 6.63 (d, J = 7.03 Hz, 6H)	7.35 (s, 3H), 7.38 (s, 12H)

Table 3.24: IR and ^{13}C NMR Analysis of Complex **3.29** in Acetone-d_6

Complex	IR (cm^{-1})	CO	CpFe	$CpFe^{+}$	Complexed Aromatic	Aromatic
3.29	1725 (CO)	170.35	70.46*, 70.68, 71.23, 72.95,	78.99	75.84, 76.78, 130.70*, 131.94*	110.71, 122.17, 124.84, 149.57*, 151.70*, 157.62*

*Denotes quaternary carbons

The electrochemical properties of complex **3.29** were examined in order to determine the redox potentials of the two distinct iron centers within its structure. These cyclic voltammograms were obtained in propylene carbonate rather than DMF, because the oxidation of the neutral iron moieties occurred in a region not readily accessible in DMF. Another advantage to using propylene carbonate as the solvent was that the redox processes were much more reversible and stable at higher temperatures. The redox waves were measured from –30 to +10 °C and were reversible during this region. The cyclic voltammogram in Figure 3.25 shows the oxidation of neutral iron centers at $E_{1/2}$ = 0.694 V and reduction of the cationic iron centers at $E_{1/2}$ = –1.29 V.

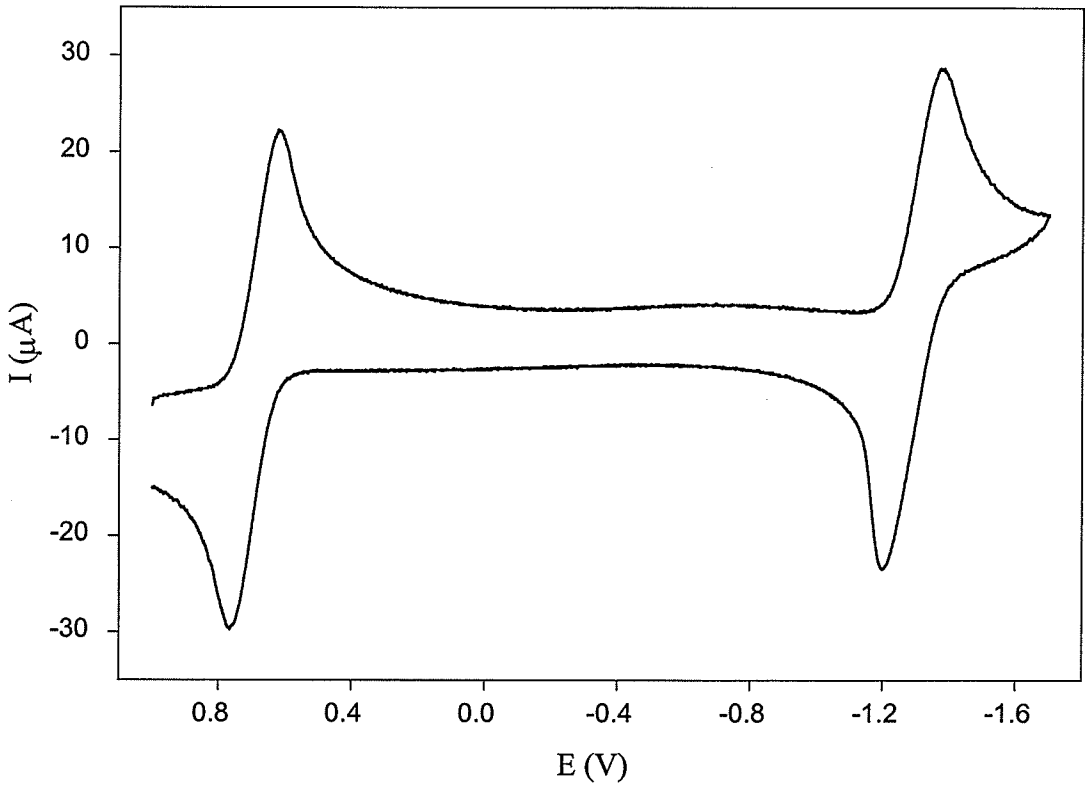

Figure 3.25: Cyclic voltammogram at glassy carbon of 0.001 M **3.29** in 0.1 M TBAP in propylene carbonate, ν = 0.2 V/s at –30 °C

3.3 Conclusions

This work illustrates the controlled design of star-shaped aromatic ethers with pendent cyclopentadienyliron moieties. A trimetallic core was prepared by reacting phloroglucinol with chloroarene cyclopentadienyliron complexes. This core molecule was then reacted with a number of oligomeric ether complexes to give star-shaped polymers with six, nine, twelve and fifteen pendent cationic cyclopentadienyliron moieties. These new classes of star-shaped aromatic ether organoiron complexes were synthesized using cyclopentadienyliron-mediated nucleophilic displacement reactions. Cyclic voltammetric studies of these complexes showed that the eighteen-electron iron centers were reduced between –0.99 and –1.41 V, and that the iron moieties behaved as isolated redox centers. Thermogravimetric analysis showed that loss of the metallic moieties occurred between 210 and 284 °C, while decomposition of the aryl ether backbones began between 445 and 486 °C. A star-shaped complex containing three neutral and three cationic cyclopentadienyliron complexes was also synthesized. Electrochemical analysis of this complex showed that the neutral eighteen-electron iron centers were reversibly oxidized to seventeen-electron species and that the cationic eighteen-electron iron centers were reversibly reduced to nineteen-electron species.

3.4 Experimental

Materials

Phloroglucinol (Fluka), hydroquinone, phenolphthalein, 4,4'-(1,4-phenylenediisopropylene)bisphenol and 4,4-bis(4-hydroxyphenyl)valeric acid (Aldrich Chemical Co.) were used as received without purification. Solvents were HPLC grade and used without further purification, with the exception of THF, which was distilled over benzophenone/sodium prior to use. Acetylferrocene and ferrocene carboxylic acid were prepared according to established methodologies.[348-350]

Characterization

^{1}H and ^{13}C NMR spectra were recorded at 200 and 50 MHz, respectively, on a Gemini 200 NMR spectrometer, with chemical shifts calculated in ppm, referenced to solvent residues. ^{13}C NMR spectra were obtained using an attached proton test (APT). Cyclic voltammetric experiments were performed using an EG&G Princeton Applied Research model 263A potentiostat using an Ag/AgCl reference electrode, a glassy carbon working electrode and a platinum auxiliary electrode. Thermogravimetric analysis of the complexes was performed on a Mettler TGA/SDTA851^{e} using a heating rate of 20 ^{o}C/min under a flow of nitrogen.

3.4.1 Synthesis of Complex 3.2

Complex **2.1** (1.24 g, 3 mmol), phloroglucinol (**3.1**) (0.126 g, 1 mmol) and K_2CO_3 (0.415 g, 3 mmol) were stirred in 10 mL of DMF in a 50 mL round bottom flask under a nitrogen atmosphere for 16 h. This solution was poured into 50 mL of a 10% HCl

solution and ammonium hexafluorophosphate (0.489 g, 3 mmol) was added. The resulting precipitate was collected in a sintered glass crucible and washed with water. The complex was then washed with diethyl ether and dried under reduced pressure.

3.4.2 Synthesis of Complex 3.3

Complex **2.66** (1.18 g, 3 mmol), phloroglucinol (**3.1**) (0.126 g, 1 mmol) and K_2CO_3 (0.415 g, 3 mmol) were stirred in 5 mL of DMF and 5 mL of THF at 60 °C in a 50 mL round bottom flask under a nitrogen atmosphere for 16 h. The THF was removed, and the solution was poured into 50 mL of a 10% HCl solution and ammonium hexafluorophosphate (0.489 g, 3 mmol) was added. The resulting precipitate was collected in a sintered glass crucible and washed with water. The complex was then washed with diethyl ether and dried under reduced pressure. Purification of the complex was achieved by passing the complex through an alumina column in dichloromethane or acetone.

3.4.3 Synthesis of Complexes 3.4

Complex **3.2** (0.628 g, 0.5 mmol), hydroquinone (**2.44**) (0.826 g, 7.5 mmol), K_2CO_3 (0.691 g, 5 mmol) and 12 mL of DMF were combined in a 50 mL RBF and stirred under a N_2 atmosphere for 16 h. The solution was poured into 50 mL of a 10% HCl solution and NH_4PF_6 (0.245 g, 1.5 mmol) was added. The beige precipitate was collected in a sintered glass crucible and washed with water and ether.

3.4.4 Synthesis of Complexes 3.6-3.8

Complex **2.66** (1.18 g, 3 mmol), **2.44, 2.6, 3.5** (12 mmol) and K_2CO_3 (1.24 g, 9 mmol) were placed in a 50 mL round bottom flask containing 16 mL of 1:1 THF:DMF. The solution was stirred at 60 °C for 16 hours under a nitrogen atmosphere, and then poured into 50 mL of a 10% HCl solution. Upon addition of NH_4PF_6 (0.489 g, 3 mmol), the product was extracted with dichloromethane and washed 5 times with water. The solution was dried over $MgSO_4$, filtered and concentrated by rotary evaporation. The residue was redissolved in dichloromethane, and diethyl ether was added to promote precipitation of the complex.

3.4.5 Synthesis of Complex 3.9

Complex **2.66** (1.18 g, 3 mmol), **2.4** (3.27 g, 12 mmol) and K_2CO_3 (1.24 g, 9 mmol) were placed in a 50 mL round bottom flask containing 12 mL of DMF and 4 mL of THF. The solution was stirred at 60 °C for 16 hours under a nitrogen atmosphere, and then poured into 50 mL of a 10% HCl solution. Ammonium haxafluorophosphate (0.489 g, 3 mmol) was added to the solution and the complex was extracted with dichloromethane and washed with water three to five times. The solution was dried over magnesium sulfate, filtered, and dried under reduced pressure. A sodium hydroxide solution was added to the flask, resulting in dissolution of the complex. A 10 % HCl solution was then added to the basic solution causing the complex to precipitate.

3.4.6 Synthesis of Complexes 3.10-3.13

Complex **3.6-3.9** (0.9 mmol), complex **3.2** (0.376 g, 0.3 mmol) and K_2CO_3 (3-6 mmol) were placed in a 25 mL round bottom flask containing 5 mL of DMF. The reagents were stirred at room temperature for 16 h under a nitrogen atmosphere. This solution was poured into 50 mL of a 10% HCl solution and ammonium hexafluorophosphate (0.293 g, 1.8 mmol) was added. Work-up of these complexes followed the procedure outlined for complexes **3.3**.

3.4.7 Synthesis of Complexes 3.14-3.17

Complex **3.6-3.9** (3 mmol), complex **2.1** (1.24 g, 3 mmol) and K_2CO_3 (0.553 g, 4 mmol) were stirred in 15 mL of DMF in a 50 mL round bottom flask under a nitrogen atmosphere for 16 h. This solution was poured into 50 mL of a 10% HCl solution and ammonium hexafluorophosphate (0.489 g, 3 mmol) was added. Work-up of these complexes followed the procedure outlined for complexes **3.2**.

3.4.8 Synthesis of Complexes 3.18-3.21

Complex **3.14-3.17** (0.9 mmol), complex **3.4** (0.443 g, 0.3 mmol) and K_2CO_3 (0.276g, 2 mmol) were placed in a 25 mL round bottom flask containing 10 mL of DMF. The reagents were stirred at room temperature for 16 h under a nitrogen atmosphere. This solution was poured into 50 mL of a 10% HCl solution and ammonium hexafluorophosphate (0.440 g, 2.7 mmol) was added. Work-up of these complexes followed the procedure outlined for complexes **3.3**.

3.4.9 Synthesis of Complexes 3.22 and 3.24

Complex **3.14, 3.23** (1 mmol), hydroquinone (**2.44**) (0.551 g, 5 mmol), K_2CO_3 (0.691 g, 5 mmol) and 12 mL of DMF were combined in a 50 mL RBF and stirred under a N_2 atmosphere for 16 h. The solution was poured into 50 mL of a 10% HCl solution and NH_4PF_6 (0.326 g, 2 mmol) was added. The beige precipitate was collected in a sintered glass crucible and washed with water and ether.

3.4.10 Synthesis of Complexes 3.23 and 3.25

These complexes were synthesized by reacting complexes **3.22** and **3.24** with an excess of hydroquinone (**2.44**) using the procedure outlined for complexes **3.14-3.17**.

3.4.11 Synthesis of Complexes 3.26 and 3.27

These complexes were synthesized using the procedure outlined for complexes **3.18-3.21** by reacting complexes **3.23** and **3.25** with complex **3.4**.

3.4.12 Synthesis of Complex 3.28

Ferrocene (10 g, 54 mmol), acetic anhydride (27 mL, 286 mmol) and 2.2 mL of 85 % phosphoric acid were combined in a 100 mL round bottom flask and stirred at 100 °C for 15 minutes under a nitrogen atmosphere. The solution was poured into a flask of ice-water and sodium carbonate (about 22 g) was added to the stirring solution. The resulting solid was collected in a Buchner funnel, washed with water, and then dried under reduced pressure. The acetylferrocene was isolated by column chromatography

using a silica gel column made in hexanes. Ferrocene was first eluted with hexanes, and the acetylferrocene eluted with diethyl ether.

Acetylferrocene (1.0 g, 4.4 mmol), iodine (1.1 g, 4.4 mmol) and 2 mL of pyridine were combined in a 100 mL round bottom flask and stirred at room temperature for 12 hours. The solution was then heated to 100 °C for 90 minutes and then diluted with 30 mL of 0.6 M NaOH. The solution was then stirred at room temperature for 24 hours and then for an additional hour at 100 °C. The solution was cooled, filtered and acidified with glacial acetic acid. The resulting precipitate (**3.28**) was collected via filtration and dried under reduced pressure.

3.4.13 Synthesis of Complex 3.29

Complex **3.4** (0.369g, 0.25 mmol), complex **3.28** (0.184 g, 0.80 mmol), DMAP (0.098 g, 0.8 mmol), 14 mL of DMSO and 6 mL of dichloromethane were combined in a 50 mL round bottom flask and stirred under a N_2 atmosphere for 10 minutes. To this solution DCC (0.165g, 0.8 mmol) was added, and the solution was stirred under a nitrogen atmosphere for an additional 12 h. The solution was poured into a solution of 10% HCl and ammonium hexafluorophosphate (0.122g, 0.75 mmol) was added. The star complex was extracted with dichloromethane and washed with water 5 times. The solution was dried over magnesium sulfate and filtered. The solution was concentrated and then passed through a short alumina column using acetone. The solution was added to ether and the resulting golden orange precipitate was collected in a crucible and dried under reduced pressure. If there was any starting material left over in the product, the complex was again passed through an alumina column and precipitated into ether.